Calmodulin during photopolarisation of *Fucus serratus* zygotes

John Love

Doctor of Philosophy

The University of Edinburgh

1994

" The *morphological* "polarity" is accompanied by, and is but the outward expression (or part of it) of a true *dynamical* polarity, or distribution of forces... "

D'Arcy Wentworth Thompson, 1917.

Preface

There are many people to whom I would like to express my thanks and I apologise to those I omit to mention. In particular I wish to thank Tony Trewavas for his constant interest, encouragement and guidance throughout this project. Thanks also to the members of his research group with whom it has been a pleasure to work, and especially to Kevin Fallon, Billy Sinclair, Marc and Heather Knight, Andrew Allan, Jason Shepard and Arnold van der Luit for their help and friendship. I am extremely grateful to Ian Oliver who so patiently gave me his advice and time during the molecular phase of the project, and to Ann Haley for her critical reading of the manuscript and helpful comments.

I am also indebted to Colin Brownlee and the members of the Plymouth Marine Laboratory for their welcome and assistance during my visits there.

Finally, I declare that the work described here is my own and has not been submitted in any form for any other degree at this or any other university.

Contents

Abbreviations

A: Alanine

Abs_{280}: Spectrophotometric absorbance with the analytical wavelength indicated in subscript.

AF: After fertilization.

AMPS: Ammonium persulfate.

ASW: Artificial sea water.

ATP: Adenosine triphosphate.

bp: Base pairs.

Br_2 BAPTA: Bromo-1,2 bis (2 aminophenoxy) ethane-N,N,N',N' tetraacetic acid.

BSA: Bovine serum albumin.

C: Cysteine

Ca^{2+}-CaM: Calcium-calmodulin complex or active calmodulin.

$[Ca^{2+}]_{cyt}$: Concentration of cytosolic free calcium.

CCD: Closed circuit display.

cDNA: Complementary deoxyribonucleic acid.

CHAPS: 3-[(3-cholamidopropyl)-dimethyl ammonio]-1 propane sulfonate.

CICR: Ca^{2+} induced Ca^{2+} release.

CTAB: Hexadecyltrimethylammonium bromide.

CTC: Chlorotetracycline.

D: Aspartic acid.

Da: Daltons.

DASW: Ca^{2+} depleted artificial sea water.

dATP: Deoxyadenosine triphosphate.

dCTP: Deoxycytosine triphosphate.

DEPC: Diethylpyrocarbonate.

dGTP: Deoxyguanosine triphosphate.

DMSO: Dimethylsulfoxide.

DNA: Deoxyribonucleic acid.

dNTP: Deoxynucleoside triphosphate.

dTTP: Doexythimidine triphosphate.

DTE: Dithioerythritol.

DTT: Dithiothreitol.

DU: Developmental unit.

E: Glutamic acid.

EDTA: Ethylenediamine tetraacetic acid.

e.g.: *Exempli gratia* (for example).

EGTA: Ethylene glycol-bis (β-aminoethyl ether) N,N,N',N'-tetraacetic acid.

EMBL: European molecular biology laboratory

et al.: *Et alii* (and others).

EtBr: Ethidium bromide.

F: Phenylalanine.

F-actin: Filamentous actin.

G: Glycine.

H: Histidine.

H-cDNA: cDNA synthesised using a random hexamer as reaction primer.

I: Isoleucine.

i.e.: *Id est* (that is).

IP_3: Inositol 1,4,5-triphosphate.

IPTG: Isopropyl β-D-thiogalactoside.

K: Lysine.

K-Ac: Potassium acetate.

kb: Kilobase pairs.

kDa: Kilodaltons.

L: Leucine

λ: Wavelength of electromagnetic radiation, when associated with a numerical value.

LB: Luria-Bertani

M: Methionine.

M: Molar ($mol \cdot l^{-1}$), when associated with a numerical value.

MCS: Multiple cloning site.

MOPS: 3-[N-morpholino] propanesulfonic acid.

N: Asparagine.

Na-Ac: Sodium acetate.

Oligo-dT: Thymidine oligonucleotide.

P: Proline.

PAGE: Polyacrylamide gel electrophoresis.

PCR: Polymerase chain reaction.

^{32}P-dCTP: ^{32}P labelled deoxycytidine triphosphate.

PEG: Polyethylene glycol.

pers. comm.: Personal communication.

pfu: Plaque forming units.

PIPES: Piperazine-N-N'-bis[2-ethansulfonic acid].

PSP_{cell}: Photosensitive period of a single Fucoid zygote.

PSP_{pop}: Photosensitive period of a population of Fucoid zygotes.

PVP-40: Polyvinylpyrrolidone (molecular weight 40,000).

PVPP: Polyvinylpolypyrrolidone.

Q: Glutamine.

R: Arginine.

RNA: Ribonucleic acid.

r.p.m.: Revolutions per minute.

S: Serine.

^{35}S-dATP: ^{35}S labelled deoxyadenosine triphosphate.

SDS: Sodium dodecyl sulfate.

T: Threonine

T-cDNA: cDNA synthesised using oligo-dT as reaction primer.

TEMED: N,N,N',N'-tetramethylethylenediamine.

TFP: Trifluoperazine.

TMB-8: (8-N,N-diethylamino) octyl-3,4,5-trimethoxybenzoate.

U: Units

U.V.: Ultra violet.

V: Valine.

v/v: Volume per volume.

W: Tryptophan.

W7: N-(6-aminohexyl)-5-chloro-1-naphthalenesulfonamide.

w/v: Weight per volume.

x: Magnification when associated with a numerical value.

X-Gal: 5-bromo-4-chloro-3-indolyl-β-D-galactopyranoside.

Y: Tyrosine.

Abstract

Zygotes of the Fucales (Phaeophyceae) have been widely used as a model system to study plant cell polarity. Zygotes in the early stages of development are apolar. During the first cell cycle, a gradual cytoplasmic re-organisation, oriented by numerous environmental stimuli, replaces the initial spherical symmetry by a highly polarised morphology. Gradients of cytoplasmic free Ca^{2+} and of the Ca^{2+} binding protein, calmodulin, have been observed in the growing tips of polarised plant cells such as root hairs and pollen tubes. Moreover, calmodulin is essential for budding in *Saccharomyces cerevisiae*, and localises to the future bud site where it is thought to guide microfilament concentration. Both Ca^{2+} and microfilament localisations have been linked to polarity in Fucoid zygotes, but data regarding the role of calmodulin has been lacking.

Fucus serratus zygotes were treated with various inhibitors of cytoplasmic Ca^{2+} mobilisation and of calmodulin activity from 10 to 13 hours after fertilisation, when zygotes are polarised by light. Following treatment, photopolarisation decreased in a dose dependent manner, indicating the requirement for both cytoplasmic Ca^{2+} and active calmodulin in this process. It was hypothesised that localised calmodulin activity was part of the signal transduction pathway between light stimulus and cytoplasmic polarisation. To test this hypothesis, artificially increasing the calmodulin concentration in polarising zygotes to disrupt any endogenous calmodulin gradient was proposed. However, given the evolutionary divergence of the Phaeophyceae, further information regarding the sequence of brown algal calmodulin was required.

Large scale purification of calmodulin from *F. serratus* tissues proved impractical due to the presence of algal polysaccharides which rendered cell lysates extremely viscous. Attempts to clone the calmodulin cDNA and gene were also hindered by polysaccharides which inhibited the activity of DNA modifying enzymes. As an alternative, the calmodulin cDNA was cloned from *Macrocystis pyrifera*, a commercial brown algal species and close relative of *F. serratus*. The cloned coding sequence was highly homologous to that of *Arabidopsis thaliana* and *Chlamydomonas reinhardtii*, the only algal calmodulin in the EMBL database. Amino acid homology to higher plant calmodulins was over 90%, but only 79% identical to that of *C. reinhardtii*.

Recombinant *M. pyrifera* calmodulin was expressed in bacteria, and purified using W7 affinity chromatography. Microinjection of this recombinant calmodulin into *F. serratus* eggs and polarising zygotes altered polarity. Results are discussed relative to current models of photopolarisation, and a refined model is proposed.

Chapter 1

Introduction

Multicellular organisms generally start life as a single, totipotent cell which gradually develops into a more or less complex array of differentiated cells. Differentiation is caused by variations in the biochemical environments between cells which, in turn, modifies gene expression between sister cells (Ilmansee and Mahowald, 1974). Asymmetric cell divisions, from which daughter cells inherit differing cellular environments, can therefore be viewed as the key to both cell differentiation and multicellular development.

Cell differentiation is controlled at several levels by the life history of the cell, by its immediate cellular environment, and by its integration within the organism as a whole (Slack, 1991). During embryogenesis, differentiation is more spectacular: Visible cytoplasmic asymmetries are partitioned during cytokinesis to form cells in which differing intracellular environments direct differential gene expression. However, the regionalised cytoplasm of zygotes is generally inherited from the maternal environment, and etched during oogenesis. Although the consequences of cytoplasmic heterogeneity in zygotes are apparent, the factors which initiate the cytoplasmic asymmetries controlling differentiation are not usually amenable to direct scrutiny.

Eggs of the Fucoid algae (Phaeophyceae, Fucales) display no inherent order, but are released from the parent plant as spherically symmetrical cells. This symmetry is retained following fertilisation (Jaffe, 1968 ; Evans *et al.*, 1982), but is broken before first cytokinesis by the formation of a

localised protuberance, the rhizoid, at the surface of the zygote (Thuret, 1854 ; Farmer and Williams, 1896). Asymmetric cell division follows, perpendicular to the direction of rhizoid initiation, and results in a two celled embryo consisting of highly differentiated cells. Given this particularity, Fucoid zygotes have been widely used as a model system for studying the initiation of cell polarity and cytoplasmic asymmetry (Goodner and Quatrano, 1993).

1. 1 *Fucus serratus* and *Macrocystis pyrifera*

1. 1. 1 Taxonomy

Algae are defined as plants which lack roots, stems and leaves, have chlorophyll *a* as their primary photosynthetic pigment, and lack a sterile covering of cells around the reproductive cells (Lee, 1980). This definition spans a range of plant forms with widely varying biochemistries, intracellular structures and cellular organisations. Life histories present complex alternations between haploid and diploid, motile and immobile, sessile and free-living, planktonic and macroscopic organisms. Currently six algal divisions have been recognised which differ from each other mainly in the organisation of the storage products and the structure of the chloroplast. Each division contains only one class, with the exception of the Chromophyta which is composed of ten classes including the brown algae. The Phaeophyceae (Chromophyta), or brown algae, first appear in the fossil record from 25 million years ago. These algae are almost exclusively marine with a parenchymatous organisation of tissues. The thallus is formed of three parts: A photosynthetic frond, or blade, constitutes the bulk of the organism. At the base, a holdfast secures the plant to a steady substratum. A stipe connects holdfast and frond. The Phaeophyceae include 7 orders, the Ectocarpales, the Desmarestiales, the Cutleriales, the

Laminariales, the Sphacelariales, the Dictyotales and the Fucales. Biochemistry and cellular organisation within the Phaeophyceae varies little (Parker, 1971), differences between families being mainly reproductive, morphological and ecological (Lee, 1980).

1. 1. 2 Macrocystis pyrifera

Macrocystis sp. (Lessoniaceae) are large brown algae of the sub-tidal zone (Figure 1-1-1) and close relatives of the *Laminaria sp.* common on northern european atlantic coasts. They inhabit the temperate waters of the Pacific Ocean, but are also found along the whole Pacific coast of America (Neushul, 1971 ; North, 1971). The life cycle of *Macrocystis* is typical of the Laminariales. A macroscopic sporophyte produces motile zoospores which swim for approximately 48 h before settling on the substratum to produce microscopic gametophytes of either sex. Male gametophytes bear several, branched antheridia, each of which produce a single antherozoid. Female gametophytes are practically reduced to a single oogonium, and beget a single egg. Following fertilisation and embryonic development, the young sporophyte develops meristematically. The meristem splits to form secondary stipes and blades (Parker, 1971 ; Lee, 1980). *M. pyrifera* live for about 8 years, and may reach over 150 m in length. The algae sustain a complex littoral ecosystem with over 300 species directly dependent on it for support (North, 1971). In the past, the laminariales have been used for food, "Kelp ash" for pottery glazing and glassmaking, and as a source of iodine (in 1846 there were 20 iodine manufacturers in Glasgow extracting about 15 kg of iodine per ton of algae). Currently, 300 tons of *Macrocystis* is harvested per day to produce the alginates required for the food, cosmetics and plastics industries. Productivity is solely sustained by natural regeneration.

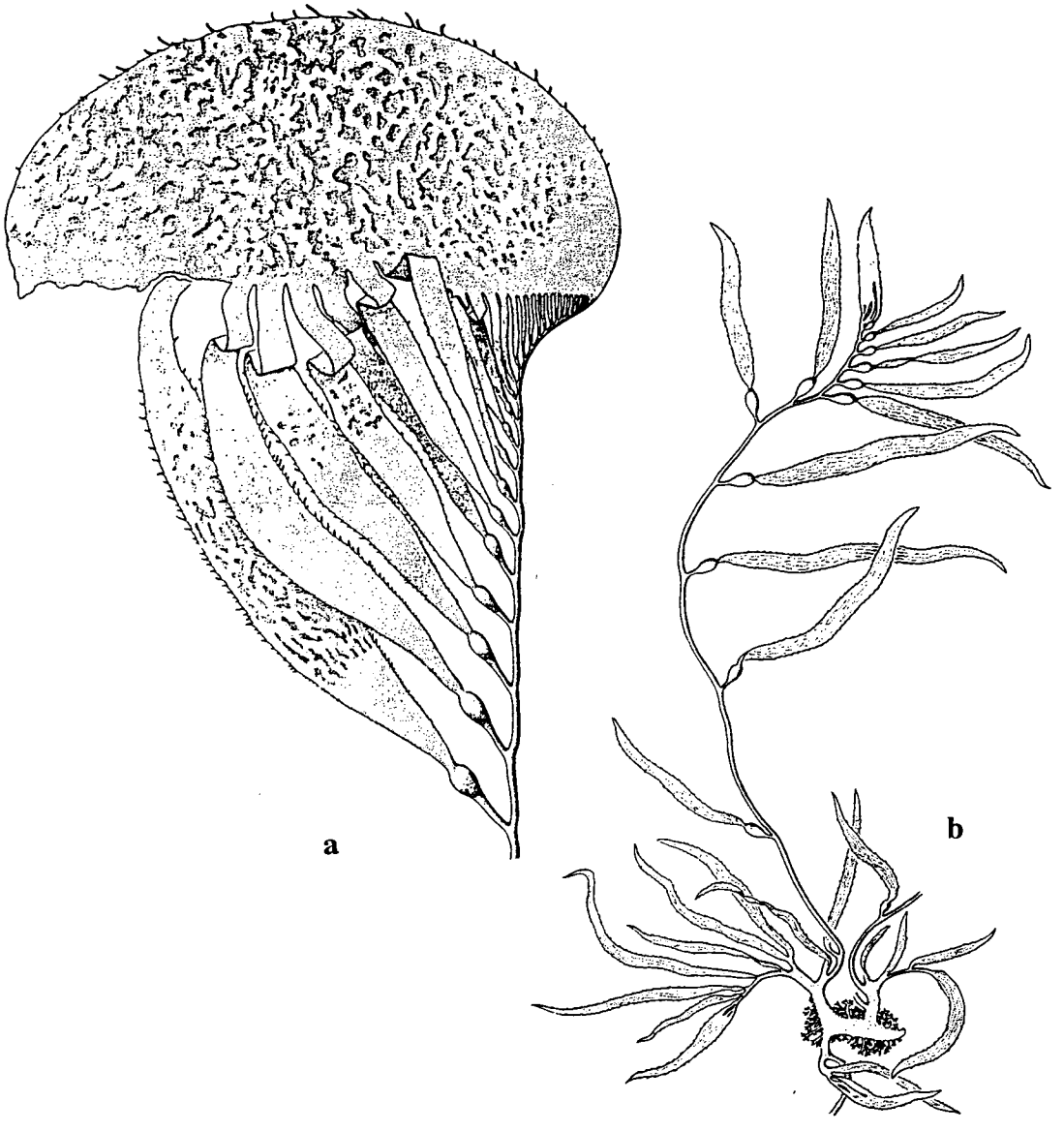

Figure 1-1-1. *Macrocystis pyrifera.*

a: Apex of *M. pyrifera* showing the splitting of the meristematic region to form secondary fronds.

b: Diagram of the thallus of *M. pyrifera.*

After Smith (1989).

1. 1. 3 Morphology of Fucus serratus

In the Fucales, growth originates from an apical cell which rarely divides, but stimulates division among the surrounding cells, effectively producing an apical meristem called the promeristem. The apical cell imposes apical dominance on the tissues below. The outer row of cells derived from the promeristem, the meristoderm, divides periclinally producing new cells on the inside of the thallus. Cellulose, alginic acid and fucoidin are the major components of the cell wall. Relative quantities of these components vary between and within species depending on ecological conditions and developmental stage. Chloroplasts possess three thylakoids per band, and are surrounded by a double endoplasmic reticulum membrane, as well as the chloroplast membrane. Chlorophylls *a*, *c1* and *c2* are present but there is no chlorophyll *b*. The major carotenoid is fucoxanthin. The Fucales are further divided into four families, Cystoseiraceae, Sargassaceae, Himanthaliaceae, and Fucaceae. Differences between the four families rest on variations in the morphology of the apical cell (Moss, 1967) and the presence or absence of branching of the frond. Both the Cystoseiraceae and the Sargassaceae possess a three-sided apical cell, but the former shows no branching of the thallus which is present in the latter. The thallus of the Himanthaliaceae is differentiated into a conical, sterile portion at the base, which supports a fertile strap-like segment. In the Fucaceae, the thallus is branched, with a four-sided apical cell in mature plants. The Fucaceae consist of three genera, *Pelvetia*, *Ascophyllum* and *Fucus* (Figure 1-1-2). There is no alternation of generations: Plants are diploid and reproduce oogamously.

F. serratus is prevalent in the northern hemisphere where it occupies rocky, marine habitats of the middle to lower intertidal zone. Individuals

Figure 1-1-2. Fucoid algae at low tide.

Algae were photographed in October, at Barnsness, East Lothian. The flattened frond and bright orange receptacles of a mature, male specimen of *F. serratus* are visible at the right of the photograph.

vary in size, mainly due to the ecological constraints of exposure to wave action, but may reach more than a metre in length. The frond is composed of flattened segments approximately 4 cm in width. Each segment possesses an elevated midrib flanked by two wings, the edges of which are serrated and give the species its name (Figure 1-1-3). The apical cell occasionally divides, resulting in branching which, due to the mutual effects of the daughter apical cells on each other, is unequal and dichotomous (Moss, 1967).

F. serratus is dioecious. Reproductive structures, termed conceptacles, are embedded under the epidermis in the receptacles, an accumulation of sterile tissues and mucilage at the distal portions of the frond. Conceptacles are hollow spheres approximately 0.5 mm in diameter, and opened to the outside via a pore, or ostiole, through which ripe gametes are secreted. Mature plants are recognised and sexed by the characteristic colour of ripe conceptacles. Antheridia are bright orange, whereas oogonia are dull green (Figure 1-1-4). *F. serratus* is sexually mature all year round, with a lull during the spring phase of vegetative growth, and the hottest months of summer. Under laboratory conditions, gametes are readily secreted (Jaffe, 1954 ; Kropf and Quatrano, 1987), hence an abundant supply of experimental material may be relied upon (Figure 1-1-5). Furthermore, as the species is dioecious, fertilisation may be experimentally controlled and synchronous zygote cultures established (Kropf, 1992).

1. 1. 4 Gametogenesis of Fucus serratus

Conceptacles are lined by a single layer of cells which functions as a germinal epithelium to produce the gametangia. Numerous papillae project from these epithelial cells into the conceptacle lumen, and form either the gamete mother cells (oocytes or spermatocytes) or sterile, elongated cells

Figure 1-1-3. *Fucus serratus*

A ripe, female specimen of *F. serratus* is shown. The length of the plant was approximately 30 cm. Branching is dichotomous, and the characteristic serrated edge of the frond is clearly visible. Receptacles are present at the distal portions of several branches, and appear as a rough, localised thickening of the frond.

Figure 1-1-4. Mature conceptacles of male and female *Fucus serratus*.

Receptacles were bisected to expose the conceptacles within. Conceptacles from male plants are bright orange due to the carotenoid-rich eyespot of mature sperm, whereas conceptacles from female plants are dull green.

Figure 1-1-5. Sperm secretions of a male *Fucus serratus*.

Under laboratory conditions (Section *2. 1. 2*), gametes are readily secreted from *F. serratus*. Secretions cover the receptacle and are easily purified (Section *2. 1. 3*).

called paraphyses (Figure 1-1-6). Gametangia differentiate at the conceptacle base, away from the ostiole and are carried towards the conceptacle lumen on an elongated cellular projection (Mc Cully, 1968).

Antheridial mother cells are meristematic and contain a large nucleus, surrounded by dense cytoplasm (Mc Cully, 1968). A succession of one meiotic and four mitotic divisions without cytokinesis produces a syncitium of 64 haploid nuclei (Mc Cully, 1968 ; Berkaloff and Rousseau, 1979). During this phase, organelle multiplication occurs. Each haploid nucleus then associates with a single chloroplast and, immediately prior to cell cleavage, two centrioles congregate close to each chloroplast, lying parallel to each other and perpendicular to the plasma membrane. Simultaneously, vesicles invade the chloroplast stroma to form the eyespot which becomes bright orange in colour due to the accumulation of caretinoids within it (Callow *et al.*, 1985). The nucleoplasm acquires a dense, homogeneous appearance due to chromatin condensation. With cytokinesis all but complete, flagellae extend from each centriole (Berkaloff and Rousseau, 1979). The anterior flagellum measures 45 µm and is conspicuously shorter than the other (Manton and Clarke, 1956). It is carried erect and bears helical rows of small, membrane extensions, called mastigonemes, which are believed to be involved in egg recognition (Jones *et al.*, 1988). The second flagellum is used for propulsion. As sperm mature, they become guttiform and the relative positions of each organelle is established (Figure 1-1-7). Mature sperm are 5 µm in length.

Like the production of sperm, the first stages of oogenesis are syncitial (Mc Cully, 1968). A meiotic division yields four haploid nuclei which remain clustered at the centre of the oogonium. A subsequent mitotic division results in eight nuclei which condense and disperse throughout the

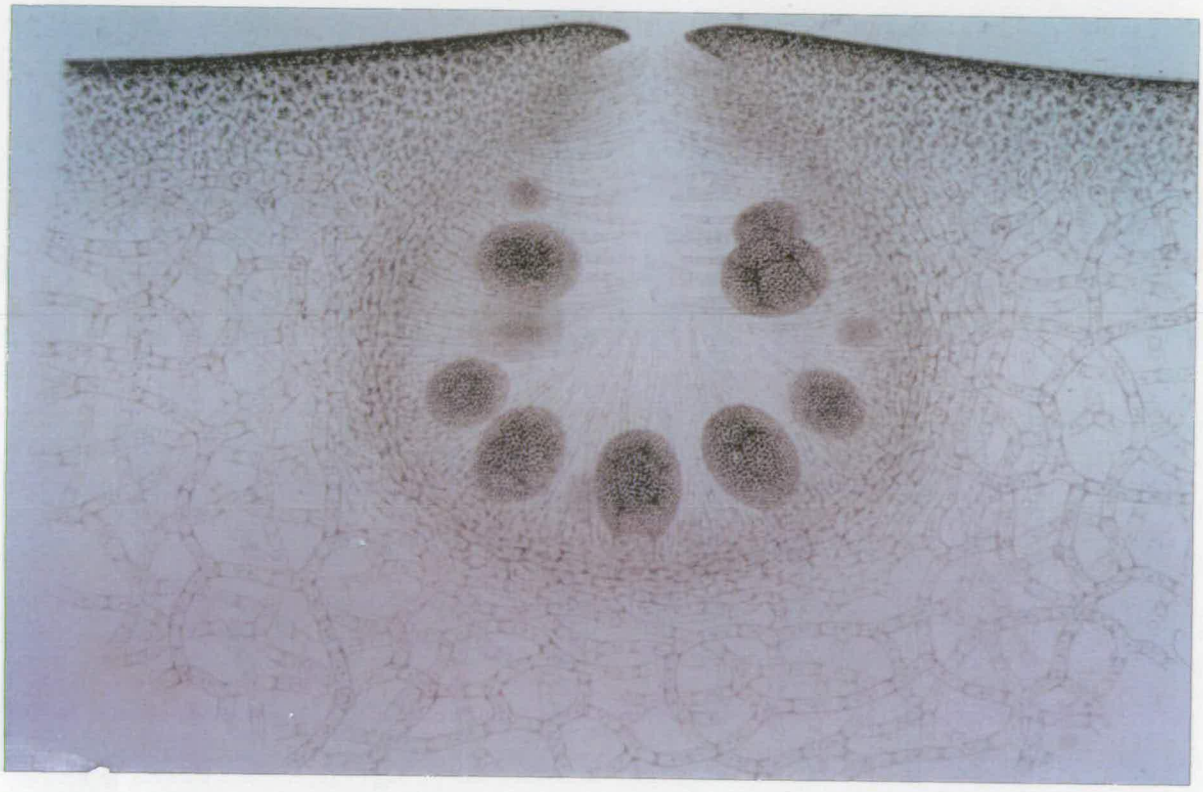

Figure 1-1-6. Female conceptacle of *Fucus vesiculosus.*

The conceptacle is in transverse section. Several oogonia at various stages of development are shown growing from the germinal epithelium, a single cell layer lining the interior of the conceptacle. Eight eggs are formed per oogonium. Sterile oogonia, the paraphyses, appear as thin cellular extensions growing into the lumen, mainly near the ostiole.

From Thuret, 1854.

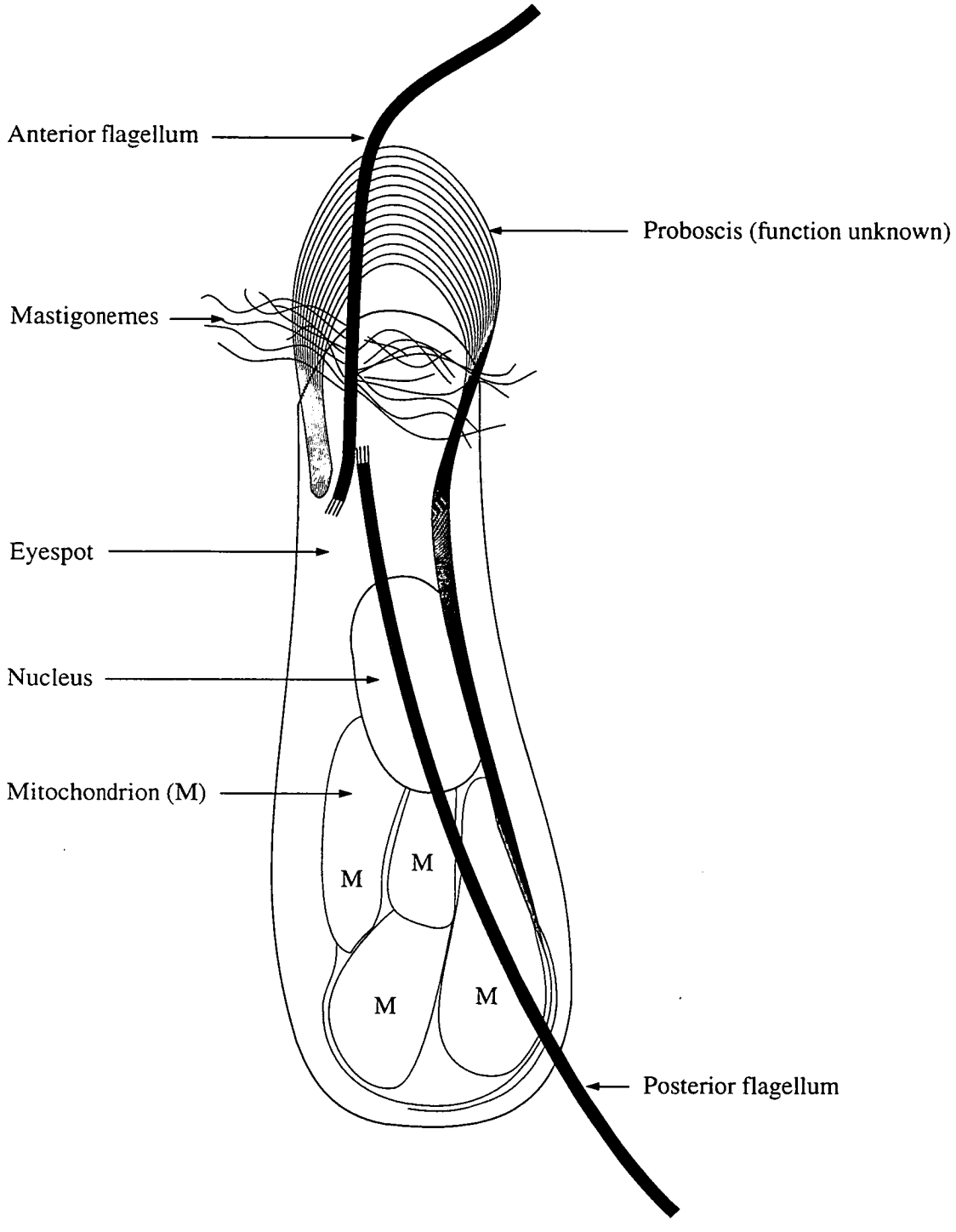

Figure 1-1-7. Diagram of the sperm of *Fucus serratus.*

After Berkaloff and Rousseau (1978).

oogonium. After a brief pause, cytokinesis occurs, to yield eight eggs, or oospheres, per oogonium (Thuret, 1854) (Figure 1-1-8). Maturation of the oogonium is accompanied by the appearance and concentration of polyphenolic rich and of polysaccharide rich vesicles (Mc Cully, 1968). When released from the oogonium, eggs rapidly become spherical (Thuret, 1854 ; Whitaker, 1931), measuring between 60 µm and 80 µm in diameter (Figure 1-1-9). The nucleus is central, with mitochondria and vesicles located nearer the cortical cytoplasm (Brawley *et al.*, 1976). Eggs are bound only by a plasma membrane, though a mucilage layer may coat freshly released eggs giving the impression of a cell wall (Levering, 1952). Protruding, polysaccharide filled, cortical vesicles confer a rough surface to the egg (Brawley *et al.*, 1976 ; Callow *et al.*, 1978). Fucoid eggs are apolar (Jaffe, 1958) and, although recent work suggests that the egg plasma membrane may be organised into domains (Stafford *et al.*, 1992), such an organisation does not imply functional asymmetry.

1. 1. 5 Fertilisation

Fertilisation occurs in the surrounding medium (Figure 1-1-10). *F. serratus* sperm are unspecifically attracted to eggs by fucoserratene, a pheromone-like substance belonging to a class of eight carbon chemicals which basic structure is 1,3-trans, 5-cis octatriene (Müller and Gassmann, 1978). Fucoserratene is active at concentrations of 10^{-6} M. *F. serratus*, *F. vesiculosus* and *F. spiralis* eggs secrete fucoserratene, but *A. nodosum* eggs radiate an affiliated compound, finavarrene, which contains the basic fucoserratene skeleton (Müller and Gassmann, 1984 ; Müller, 1989).

Although sperm attraction is unspecific (Thuret, 1854; Whitaker, 1931; Müller and Gassmann, 1978), cross fertilisation does not occur (Whitaker, 1931 ; Bolwell *et al.* 1977). Eggs therefore recognise sperm

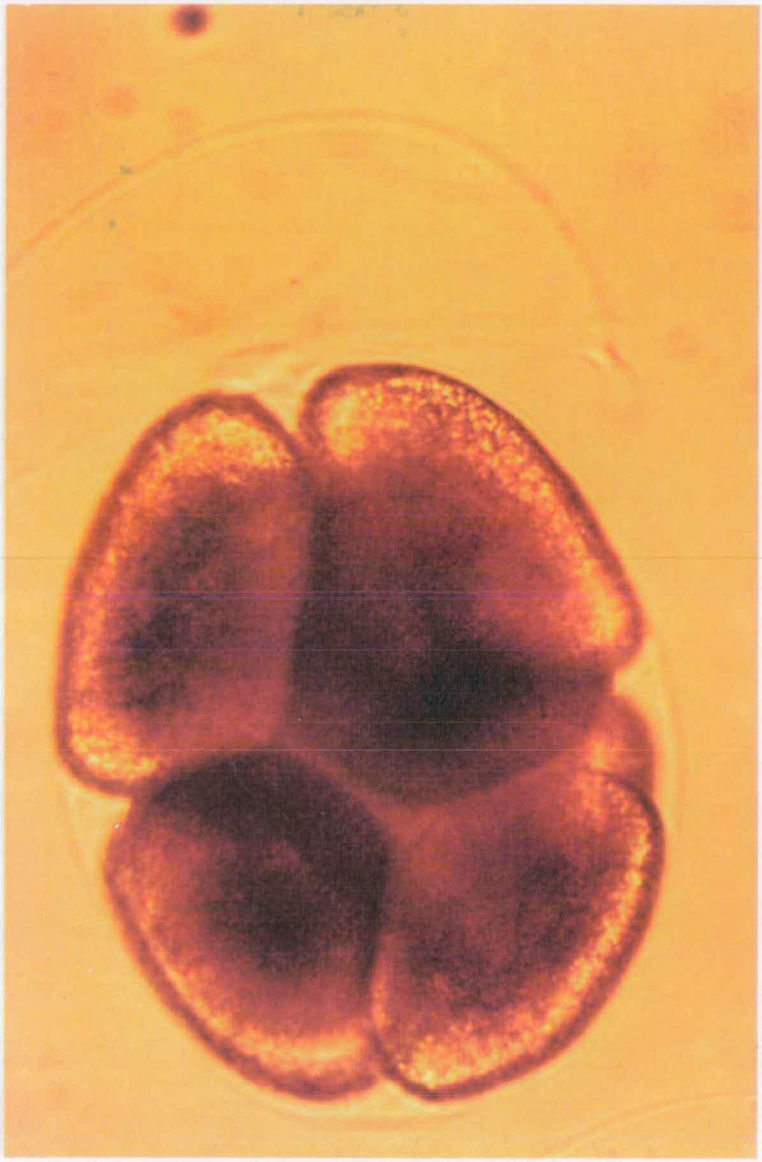

Figure 1-1-8. Mature oogonium of *Fucus serratus*.

Eight eggs are present in each oogonium (See text for details). The polysaccharide wall which surrounds the oogonium is visible.

Figure 1-1-9. Eggs of *Fucus serratus*.

Eight eggs are produced from a single oogonium. Eggs are spherical, approximately 70 μm in diameter, and disperse rapidly following secretion.

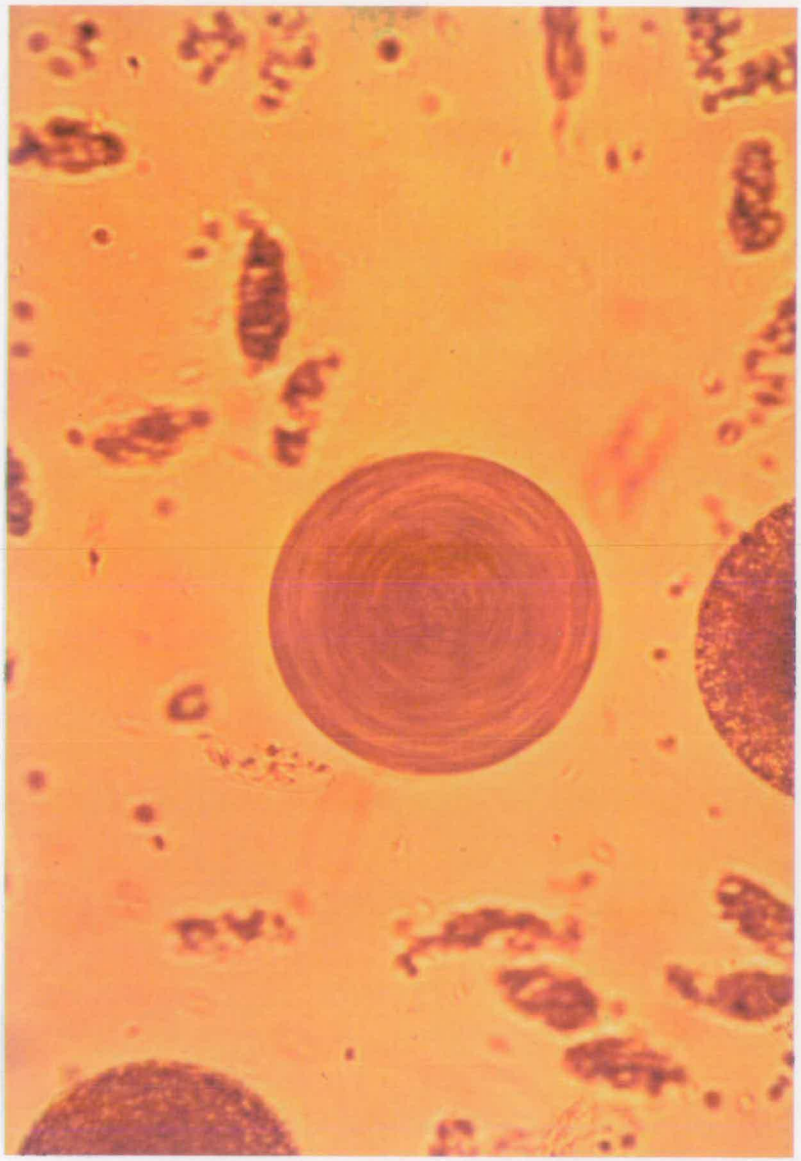

Figure 1-1-10. Fertilisation of a *Fucus serratus* egg.

During fertilisation, sperm swarm around the egg, attracted by fucoserratene. In the photograph, the egg is rotating due to the beating of sperms' flagellae. Sperm are barely visible on the egg surface.

prior to fusion, either by specific cell surface recognition and binding between gametes (Bolwell *et al.*, 1979) and/or by specific surface membrane fusion mechanisms (Bolwell *et al.*, 1977, 1979 and 1980 ; Callow, 1985 ; Callow *et al.*, 1978 and 1985 ; Evans *et al.*, 1982 ; Jones *et al.*, 1988). At concentrations of 50-100 sperm per egg, 50% fertilisation is achieved (Bolwell *et al.*, 1979). Despite quantifying fertilisation and not actual sperm binding, this result indicates that eggs bind a set number of sperm, and supports the notion that sperm bind to discrete complementary sites of the egg surface. Moreover, although sperm swarm round unfertilised eggs, scanning electron micrographs of fertilising oospheres show few attached sperm (Callow *et al.*, 1978). Whereas fixing procedures might have detached previously bound sperm, it does appear that the amount of sperm which bind to an egg is a fraction of the amount which swarm around it (Callow, 1985 ; Callow *et al.*, 1985). Therefore, either there are few sperm binding sites on the egg, or sperm which are already bound to the oosphere inhibit further binding by others. On average, eggs possess $2.5 \cdot 10^9$ sperm-specific receptors per cell, and sperm possess $1.8 \cdot 10^6$ egg receptors (Bolwell *et al.*, 1980). These numbers lend weight to the idea that, in some way, bound sperm inhibit the binding of others. There also appears to be a threshold ratio below which sperm do not fertilise the egg. This may be explained in two ways; either that in an average suspension the amount of sperm which are able to fertilise the egg is low, or the egg "permits" fertilisation only when enough sperm receptor sites are occupied. The kinetics of binding between gametes in *Fucus* indicate a requirement for a local confluence of several different sperm receptors in the egg membrane which is a possible control mechanism for specificity (Bolwell *et al.*, 1980). This possibility is supported by antibody labelling which recognised two different types of sperm receptor on the egg plasma

membrane: A first class of abundant, non-specific sperm receptors, and a second group of few, possibly localised, highly specific sperm receptors (Catt *et al.*, 1983 ; Stafford *et al.*, 1992). Before binding to the egg, sperm are observed to probe its plasma membrane with their anterior flagellum (Jones *et al.*, 1988), as though searching for a receptor site. 12 monoclonal antibodies were raised to sperm surface antigens of which 4 bound exclusively to the mastigonemes and recognised 40-250 kDa proteins (Jones *et al.*, 1988 and 1990). These proteins which may be the egg receptors of the sperm, are currently being characterised (Callow, *pers. comm.*, 1993).

Approximately 10 min after mixing gametes, one sperm penetrates the periphery of the egg cytoplasm (Farmer and Williams, 1896 ; Brawley *et al.*, 1977) causing a cascade of events resulting in egg activation, inhibition of polyspermy, cell wall secretion, and syngamy.

Within a second of gamete fusion, a transient depolarisation of the plasma membrane, the fertilisation potential, is observed. From a resting potential of -75 mV *Fucus* eggs depolarise to an average -33 mV for 7 min and *Pelvetia* to -28 mV for 11 min (Robinson *et al.*, 1981). In animal oocytes, the fertilisation potential induces a sharp rise in the concentration of cytosolic free Ca^{2+} ($[Ca^{2+}]_{cyt}$) (Jaffe, 1980 and 1983 ; Kline and Kline, 1992) which is thought to trigger egg activation and embryonic development. In *F. serratus*, however, no such cytosolic Ca^{2+} explosion has been observed. Instead, imaging with the high molecular weight dextran linked Ca^{2+} sensitive dye, Fura-2, has shown there to be a small, transient rise in $[Ca^{2+}]_{cyt}$, localised at the cortex, and due to increased Ca^{2+} permeability of the plasma membrane (Roberts *et al.*, 1994). When this small rise in cortical $[Ca^{2+}]$ is inhibited by the Ca^{2+} chelating drug Br_2BAPTA (bromo-1,2 bis (2 Aminophenoxy) ethane-N,N,N',N' tetraacetic

acid), the fertilisation potential is prolonged, and later events associated with egg activation, such as cell wall secretion do not occur. Although it has been argued that this data indicates a role for Ca^{2+} in egg activation, it may also be that this transient rise in $[Ca^{2+}]_{cyt}$ is more involved with linking fertilisation potential and cell wall secretion, rather than, as is the case in animals, with egg activation itself. Other experiments dealing with egg activation are also flawed; prolonged exposure to Ca^{2+} ionophores and sea water with a low sodium content resulted in an unsustained parthenogenic egg activation, as measured by cell wall secretion (Brawley and Bell, 1987). Given the importance of Ca^{2+} on exocytosis, the role of Ca^{2+} in Fucoid egg activation will only be resolved by the use of another marker for activation than wall secretion.

Polyspermy, the penetration of the egg by several sperm, is lethal. Eggs avoid polyspermy by a three-way block comprising a fast, an intermediate (hypothetical) and a slow component. Patch clamp inhibition of the fertilisation potential in *F. distichus*, *F. vesiculosus* and *Pelvetia fastigiata* result in polyspermic eggs, indicating that the fertilisation potential also acts as the first, fast polyspermy block (Brawley, 1987) . This idea is corroborated by identical ionic dependency between the fast block and the fertilisation potential (Brawley, 1987, 1990 and 1991). Soon after plasmogamy, sperm are actively repelled from the egg, leading to speculation on the existence of an intermediate polyspermy block, enzymatic in nature, which may destroy sperm surface antigens, thus rendering them useless for fertilisation (Brawley, 1991). Finally, cell wall secretion is generally held to act as a third, slow block to polyspermy (Pollock, 1970), even though wall synthesis is effectively too late to prevent multiple fertilisations.

On insemination, vesicles of the egg cortex fuse with the plasma membrane discharging their contents which form an incipient cell wall to the developing zygote (Brawley *et al.*, 1976*a* and 1976*b* ; Callow *et al.*, 1978) (Figure 1-1-11). Although secretion of wall material originates from the point of sperm entry (Brawley and Bell, 1987 ; Evans *et al.*, 1982), it does not proceed over the zygotic surface in a wave-like fashion, but is secreted in patches due to the fertilisation induced Ca^{2+} influx across the plasma membrane (Roberts *et al.*, 1994).

Pronuclear fusion occurs approximately 10 min after sperm penetration. Prior to fusion, egg mitochondria become asymmetrically distributed around the female pronucleus, and concentrate towards the migrating male pronucleus. This asymmetry is lost following syngamy, and there is no evidence to support the suggestion that the site of sperm entry affects polarisation in *Fucus* zygotes (Knapp, 1931).

1. 2 Embryogenesis: Polar axis formation in Fucoid zygotes

"The same day or, at the latest, the day after <fertilisation>, a first partition appears, which divides the spore in two; simultaneously, a small thickening of the membrane is distinguished at a point of the circumference, and the spore, which forms a protuberance on this side, becomes ovoid or pyriform. This elongation of the spore is nearly always perpendicular to the afore mentioned first partition... The portion of the spore which formed a protuberance, continues to elongate more and more, and finishes by converting to a hyaline filament, a sort of radicle, which is almost totally devoid of chlorophyll, and contains only a few yellowish granules at the apex. Soon several of these radicles are borne at the base of the spore, and are essential to the attachment of the young frond."

Thuret, 1854, on the embryogenesis of F. vesiculosus.

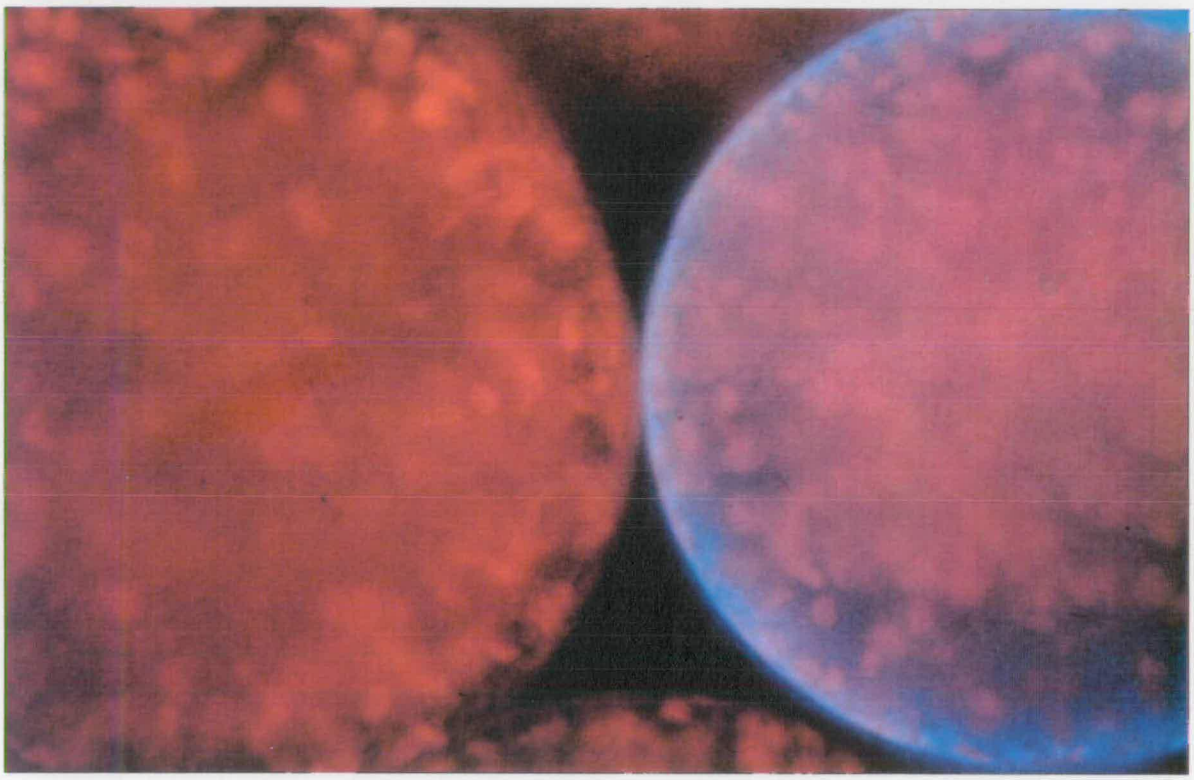

Figure 1-1-11. Fluorescence-micrograph of fertilisation-induced cell wall formation in *Fucus serratus*.

The fertilisation potential causes cell wall secretion. The egg on the right of the photograph has been fertilised and secreted a cell wall which was stained by 0.1% calcofluor white, and visualised under blue light. The egg on the left does not possess a cell wall. The red, granular appearance of the cells is due to the fluorescence of chlorophyll within the chloroplasts.

1. 2. 1 Polarisation

Following fertilisation, Fucoid zygotes gradually experience a process of cytoplasmic re-organisation during which the spherical symmetry of the early zygote is replaced by a highly polarised morphology (Figures 1-2-1, 1-2-2, 1-2-3 and 1-2-4). Polarisation is visualised by the emergence of a bulge, the rhizoid, from the surface of the zygote. By convention, the direction of rhizoid germination is the direction of the new-formed polar axis. First cytokinesis is invariably perpendicular to the polar axis, resulting in an asymmetric, two celled embryo. The larger cell, the thallus cell, is rich in chloroplasts, and gives rise to the blade, whereas the elongated rhizoid cell engenders the mature holdfast. Polarisation is developmentally programmed into Fucacean zygotes but the position of rhizoid germination, that is the orientation of the polar axis, can be determined by various environmental cues (Section *1. 2. 4*). Zygotes perceive these stimuli and organise cytoplasmic asymmetries accordingly. Sensitivity to polarising cues precedes morphological expression of the polar axis (Kniepp, 1907 ; Whitaker and Lowrance, 1936). For example, unilateral illumination between 11 and 13 h after fertilisation (AF) caused zygotes of *F. vesiculosus* and *F. spiralis* to initiate rhizoids on the shaded side of the cells approximately 4 h after the stimulus ended (Kniepp, 1907). For a while, the polar axis is labile, and will re-orient in response to a change in the direction of polarising cues. However, shortly before rhizoid germination, axis re-orientation is no longer possible. Consequently, polarisation has often been divided into three consecutive periods. Axis formation, during which environmental information is perceived and integrated into a labile polar axis. Axis fixation, refers to the period when the axis can no longer be re-oriented by environmental stimuli and zygotes are still spherical. Finally rhizoid germination, when the axis is morphologically expressed (Whitaker

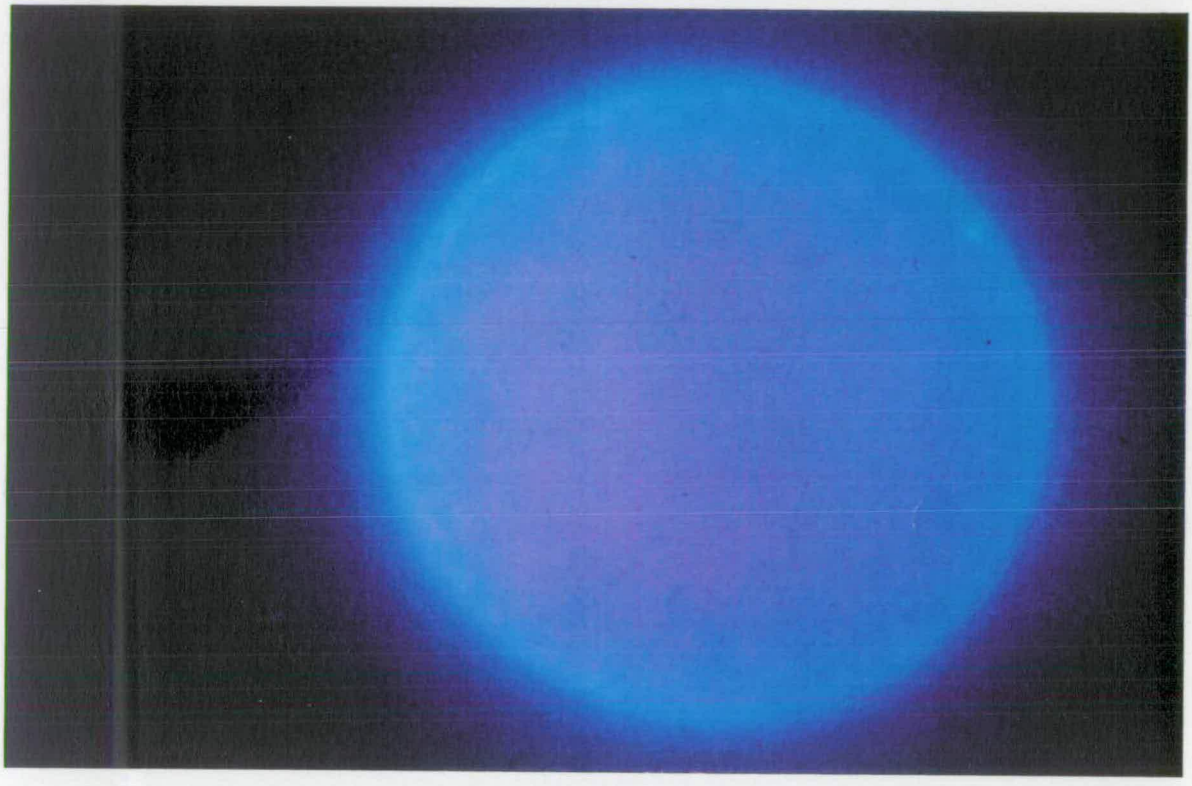

Figure 1-2-1. *Fucus serratus* zygote just after fertilisation.

The cell wall was visualised with calcofluor white (see Figure 1-1-11). Zygotes in the early stages of development are spherically symmetrical.

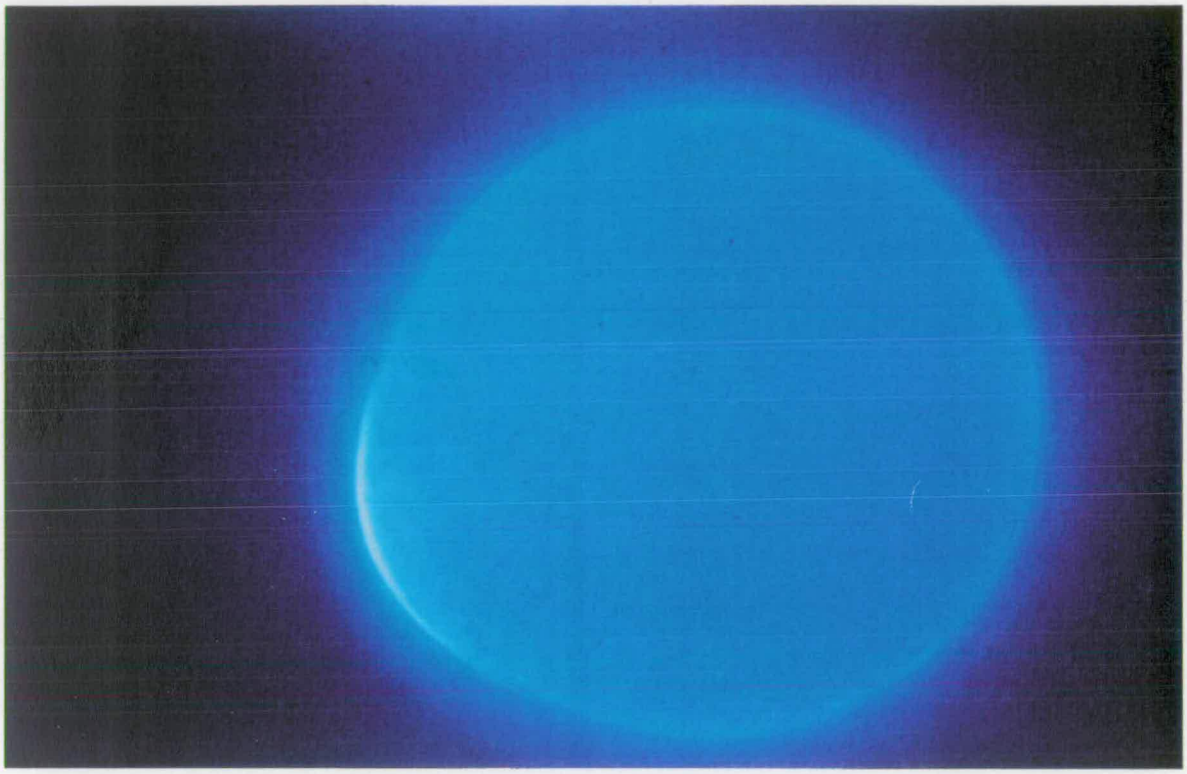

Figure 1-2-2. *Fucus serratus* zygote at 20 h AF.

The cell wall was visualised with calcofluor white. At this stage the spherical symmetry of the early zygote is morphologically broken by the appearence of a polar bulge, the rhizoid. In the photograph the rhizoid is the thickening of the cell wall, visible as a white line at 8 o'clock on the circumference of the zygote.

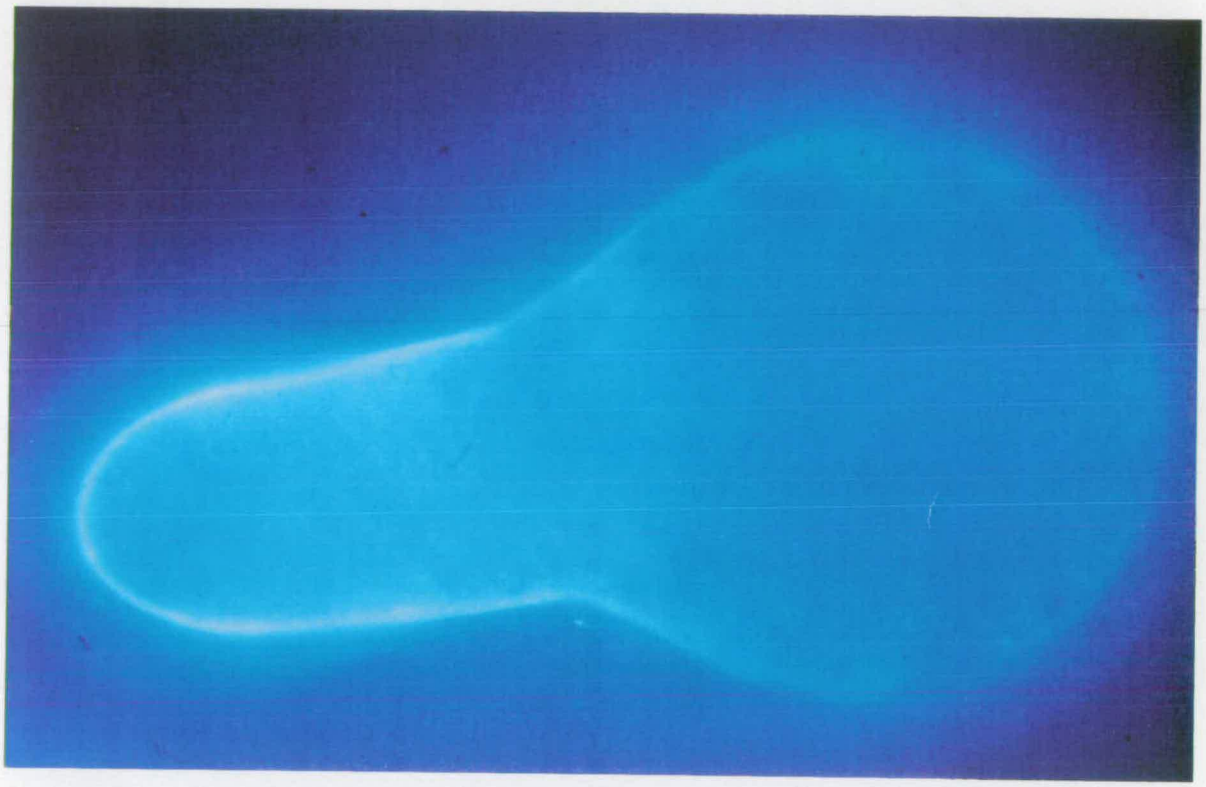

Figure 1-2-3. *Fucus serratus* zygote at 48 h AF.

The cell wall was visualised with calcofluor white. The embryo is at the two-cell stage. The elongated portion of the embryo is the rhizoid cell which gives rise to the stipe and holdfast of the mature plant. The thallus cell is spherical and produces the mature frond. The direction of rhizoid germination defines the polar axis of the zygote, and the longitudinal axis of the mature organism. Polar formation is therefore an essential feature of morphogenesis in Fucoid algae.

Figure 1-2-4. *Fucus serratus* zygote at 48 h AF.

The embryo is at the two-cell stage. The division between the elongated rhizoid cell and the thallus cell is visible, perpendicular to the polar axis. Note also that the thallus cell is richer in chloroplasts than is the rhizoid, and that cortical clearing occurs at the rhizoid tip.

and Lowrance, 1936 ; Quatrano, 1972 and 1973).

1. 2. 2 The polar axis is epigenic

For a century, the origin of the polar axis in fucacean eggs and zygotes in the early stages of development was conjecture: Were eggs and zygotes truly apolar and the axis formed *de novo*, or were the cells intrinsically polarised in an invisible, labile, manner (Whitaker, 1938)? Early evidence supported the first alternative, but was largely circumstantial: Unlike other embryos, no cytoplasmic asymmetries were observed in developing zygotes prior to rhizoid germination. Moreover, zygotes in which the cytoplasm was stratified by centrifugation responded normally to polarising cues (Whitaker, 1937) indicating that despite abnormal cytoplasmic asymmetry imposed from within, zygotes formed a normal polar axis by asymmetries imposed from without. An internal "deep" axis based on a cytoplasmic gradient was thought to be incompatible with this observation as it should be disrupted by centrifugation (Whitaker, 1938). Convincing evidence regarding the origin of the polar axis stemmed from studies of the effect of plane polarised light on zygotic development (Jaffe, 1956). Plane polarised light resulted in 45% of cultured zygotes to form two rhizoids at 180 ° of each other, germinating in opposite directions. This form of development is inexplicable by the rotation of an intrinsic polar axis, and can only be accounted for by the formation of two independent polar axes (Jaffe, 1958 and 1968). Fucoid zygotes are therefore apolar and the embryonic axis is epigenic.

1. 2. 3 Timing of polarisation

In *F. vesiculosus, F. serratus* or *F. furcatus*, rhizoid germination occurs between 18 and 21 h AF whereas a zygote of *P. fastigiata* reaches the same morphological stage between 8 and 12 h AF (Lowrance, 1937 ; Feucht and Bentrup, 1972 ; Kropf and Quatrano, 1987). However, when expressed

relative to the duration of the first cell cycle (1 developmental unit, or 1 DU), the timing of rhizoid formation is identical between species, approximately between 0.52 and 0.7 DU (Kropf and Quatrano, 1987). Moreover, the chronological timing of other polarisation events such as photosensitivity (Section *1. 2. 4* and Figure 1-2-8) or axis fixation are species dependent, but occur at the same moment with relation to the cell cycle, *i.e.* when expressed in DU. For example, *F. distichus, F. vesiculosus* and *P. fastigiata* fix the polar axis at different real times (~16 h AF, ~17 h AF and ~8 h AF respectively) but between 0.4 and 0.55 DU regardless of species. Similarly, at 0.5 DU, polar axes are fixed but not yet expressed (Kropf and Quatrano, 1987). The timing of developmental stages in Fucoid algae seems therefore to follow the cell cycle, with specific differences a consequence of variations in the duration of the cell cycle, without modification in the proportion of time allotted to a particular developmental stage.

1. 2. 4 Environmental cues and the effect of unilateral light

During the phase of polar axis induction the direction of polarity can be oriented by numerous environmental stimuli including mechanical signals (Knapp, 1931 ; Bentrup and Jaffe, 1968), electrical potentials (Lund, 1923 ; Novák and Bentrup, 1973), temperature gradients (Lowrance, 1937), chemical gradients, for instance of dinitrophenol (Whitaker and Berg, 1944), of auxin (du Buy and Olson, 1937*a* and 1937*b*), of K^+ (Bentrup *et al.*, 1966), of pH (Whitaker, 1938 ; Bentrup *et al.*, 1966 ; Gibbon and Kropf, 1991), and of Ca^{2+} (Robinson and Jaffe, 1976 ; Robinson and Cone, 1979), the proximity of neighbouring zygotes (Hurd, 1920 ; Whitaker, 1931, 1937 and 1938 ; du Buy and Olson, 1937*b* ; Jaffe, 1955 ; Bentrup and Jaffe, 1968 ; Jaffe and Neuscheler, 1969), and the direction of illumination (Thuret,

1854 ; Hurd, 1920 ; Whitaker and Lowrance, 1936 ; Jaffe, 1958 ; Bentrup, 1963 ; Feucht and Bentrup, 1972). In *F. serratus* the phase of axis induction, or axis lability, lasts from fertilisation to approximately 17 h AF during which time zygotes are apolar (Jaffe, 1958 and 1968) or weakly polar (Evans *et al.*, 1982). Zygotes experience sequential periods of sensitivity to polarising cues (Figure 1-2-5) and are polarised by the latest perceived stimulus, or by a compromise of several stimuli (Jaffe, 1968).

Light is arguably the most important natural polarising stimulus and the easiest experimental cue to apply in the laboratory. Zygotes polarise away from light (Figure 1-2-6), parallel to the vector of illumination (Thuret, 1854). Conventionally, zygotes are described as polarising on the shaded side of the cell (Whitaker, 1936 ; Bentrup, 1963 ; Jaffe, 1958) but recent evidence suggests that zygotes may, in fact, focus light onto the "shaded" hemisphere, paradoxically causing more intense illumination in that region (Berger and Brownlee, 1994). This suggestion, however, is tentative and requires further experimentation. Photopolarisation is caused by irradiation only with blue light, from $\lambda = 400\text{-}580$ nm (Hurd, 1920). Light is apparently perceived by a light-inactivated pigment (Bentrup, 1964 ; Jaffe, 1968). A plasma membrane redox chain then appears to be involved in transducing the blue light signal to the cell, possibly creating a labile map of the plasma membrane (Berger and Brownlee, 1994). This concept of light receptor to redox chain corroborates data showing acidification at the site of presumptive rhizoid formation which is dependent not on proton leak, nor on H^+-ATPases or Na^+/H^+ antiports, but on metabolic activity (Gibbon and Kropf, 1991).

Reciprocity holds true in photopolarising Fucoid zygotes (Figure 1-2-7). For example, 1 s irradiation with $4.48 \cdot 10^{15}$ quanta$\cdot$cm$^{-2}\cdot$s^{-1}

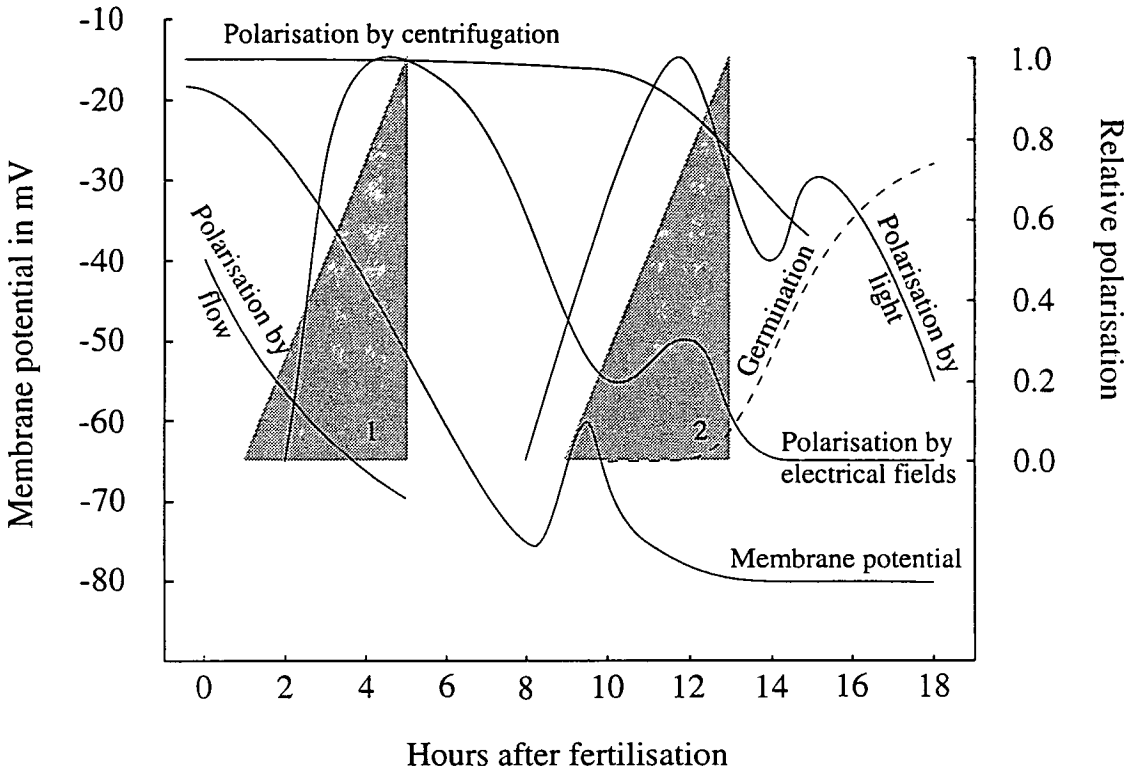

Figure 1-2-5. Developmental phases of *Fucus* zygotes and sensitivity to polarising cues.

Fluctuations in membrane potential and the periods of photopolarisation (40 W for 1 h), electric polarisability (30 mV per egg diameter for 2 h) and rhizoid germination are shown for *F. serratus*. Periods when polarisation is inducible by centrifugation (150,000 g for 5 min) or by flow (1 $m \cdot s^{-1}$, for 1 h) are presented for *F. furcatus*. Periods of RNA (1) and protein synthesis (2) essential for rhizoid formation, are in grey. These periods are for *F. vesiculosus*. The three species represented exhibit similar time courses of polarisation.

After Whitaker (1936), Jaffe (1968), Quatrano (1968), and Feucht and Bentrup (1972).

Figure 1-2-6. Polar orientation of *Fucus serratus* zygotes.

The polar axes of *F. serratus* zygotes was oriented by a pulse of unilateral white light, administered from 10-13 h AF. Light was incident from the top of the photograph. Zygotes polarise away from incident light.

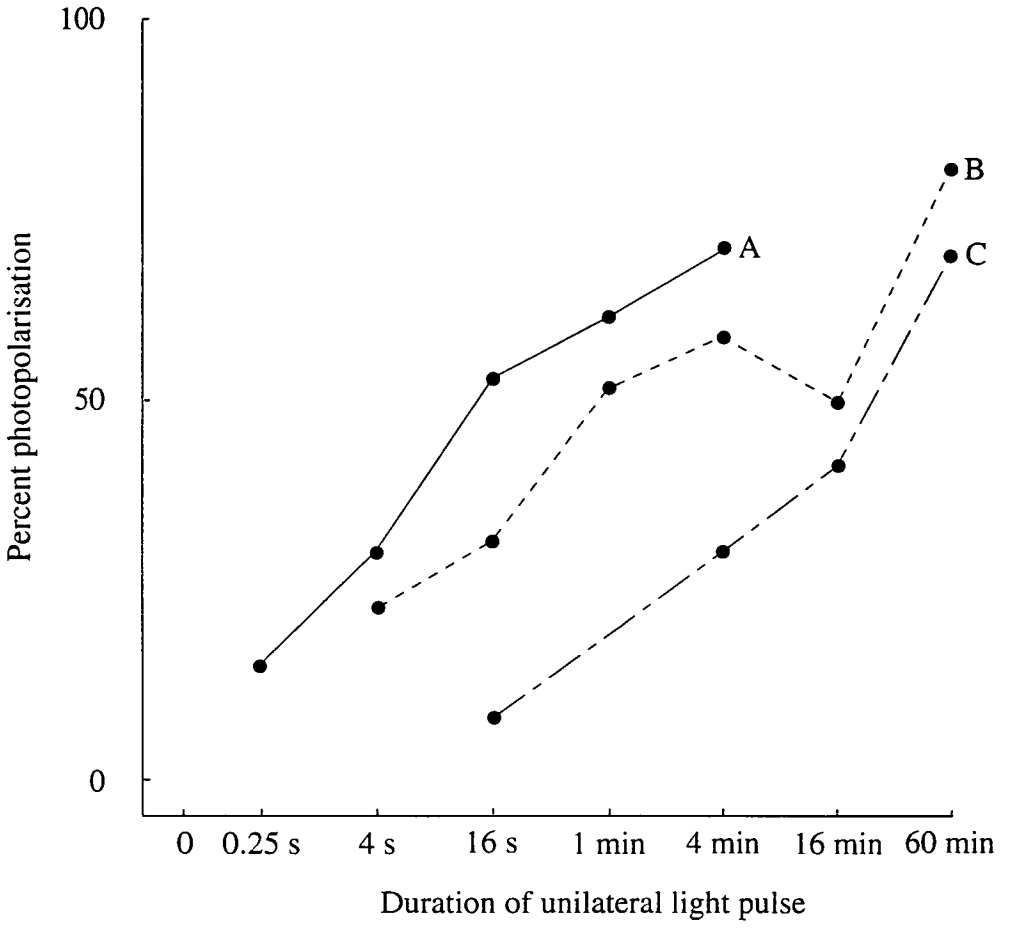

Figure 1-2-7. Reciprocity in photopolarising *Fucus serratus* zygotes.

The effect of different illumination regimes (light intensities and duration) on the photopolarisation of *F. serratus* zygotes are shown. Light was administered during the photosensitive period, for the duration shown on the abscissa. $\lambda = 254$ nm.
Light intensity (I) was based on $I = 2.5 \cdot 10^{13}$ quanta$\cdot$cm$^{-2}\cdot$s^{-1}. Curve A represents the effect on polarisation of a light intensity of 10 I, curve B the effect of 5 I and curve C the effect of 1 I.

From Bentrup (1963).

of light at $\lambda = 439$ nm yielded approximately 38% photopolarisation, and 4 s of irradiation with $1.12 \cdot 10^{15}$ q·cm^{-2}·s^{-1} were required to yield approximately 36% photopolarisation (Bentrup, *pers. comm.*, 1993 ; Bentrup, 1963). Less than 1 s of illumination is necessary to orient polarity in *F. serratus* zygotes (Bentrup, 1963).

As previously explained (Section *1. 2. 3*), real developmental timing varies between species in the Fucales. Consequently, the photosensitive period of a population of Fucoid zygotes (PSP_{pop}) is also dependent on species (Figure 1-2-8). Zygotes of *F. spiralis*, *F. vesiculosus* and *F. serratus* are maximally sensitive to polarising light from 10-13 h AF (Whitaker and Lowrance, 1936 ; Bentrup, 1963). However, in a single *F. serratus* zygote, the photosensitive period (PSP_{cell}) lasts approximately 1 h (Feucht and Bentrup, 1972). The duration of PSP_{pop} relative to PSP_{cell} reflects the distribution of asynchrony in populations of developing zygotes. Furthermore, illumination has a direct effect on the rate of progression through polarisation: The development of zygotes incubated in the dark is 28% slower than that of zygotes incubated in uniform light (Whitaker, 1936).

1. 2. 5 Ionic currents during polarisation

With the onset of rhizoid germination, approximately 200 zygotes of *F. furcatus* placed in file within a glass capillary drove an electrical current through themselves (Jaffe, 1966). Current intensity was approximately 60 pA per zygote, and consisted of a flow of positive ions entering at the presumptive rhizoid pole and exiting from the thallus pole (Jaffe, 1966). When polarity was induced and re-oriented by a unilateral light pulse, the electrical current flowed accordingly through the cytoplasm, and persisted after the polarising cue was removed (Jaffe, 1968). Measurement of

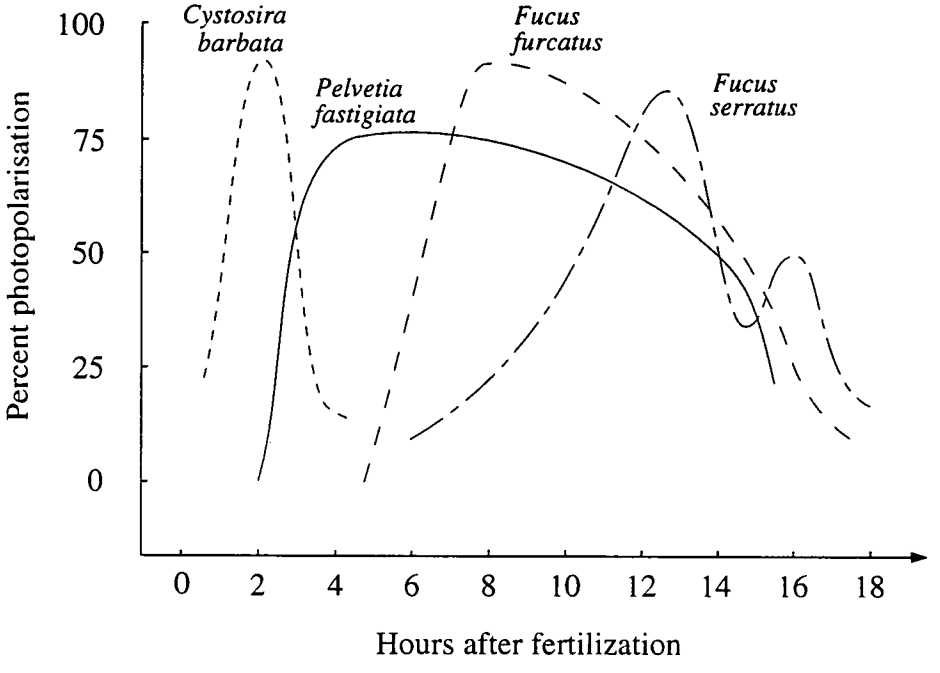

Figure 1-2-8. Timing of photopolarisation between Fucoid species.

A one hour unilateral white light pulse was administered to polarising zygotes and the orientation of polarity scored. PSP_{pop} is species dependent.

From Bentrup, *pers. comm.* 1993.

transcellular ion fluxes revealed an increase in inward flux of K^+, while Cl^- flux remained constant and the flux of Na^+ decreased by 60% (Robinson and Jaffe, 1973). When the ionic conductances were multiplied by the intensity of electrical fields which orient polarity (Novák and Bentrup, 1973), a value comparable to that of the self-generated ion current was found, indicating that the endogenous current might also feedback to polarise zygotes (Robinson and Jaffe, 1973 ; Jaffe *et al.*, 1974). A finer experimental protocol demonstrated that the transcellular current is initiated during axis formation (Nuccitelli and Jaffe, 1974) and oriented by polarising cues such as unilateral light (Robinson and Jaffe, 1975). In *P. fastigiata*, this current was 2 pA per zygote and carried by Ca^{2+} during axis formation. By axis fixation, however, Ca^{2+} carried only a fraction of the total potential; 0.4 pA per zygote (Robinson and Jaffe, 1975). Using the vibrating probe which determines the electrical potential round a single cell rather than in a population (Nuccitelli and Jaffe, 1975), it was found that the intensity of this current was, theoretically, sufficient to segregate differently charged membrane proteins (large, negative molecules at the rhizoid pole), and to produce substantial ion gradients through the embryo (Nuccitelli, 1978 ; Jaffe, 1977), thus creating asymmetries in the plasma membrane of the zygote.

1. 2. 6 Intracellular localisations

In addition to the polarised ionic currents, a small degree of structural polarisation occurs during axis formation. Polarised plasmolysis (cortical clearing) occurs at the presumptive rhizoid pole (Reed and Whitaker, 1941). Adhesive polysaccharides, notably fucoidin, are secreted at the presumptive rhizoid, at 4 h AF (~0.4 DU) in *P. fastigiata*, at 9 h AF (~0.4 DU) in *F. vesiculosus*, and at 10 h AF (~0.5 DU) in *F. spiralis*. Contrary to previous

opinion (Novotny and Foreman, 1974), polarised secretion of cell wall components starts several hours before axis fixation, is oriented by polarising cues, and is labile (Schröter, 1978).

From the electrical data previously presented, a Ca^{2+} gradient was predicted to accompany polar induction (Jaffe *et al.*, 1974 ; Kropf and Quatrano, 1987). A gradient of membrane bound Ca^{2+}, visualised with the fluorescent probe chlorotetracycline (CTC), has been observed in 20% of *Fucus* zygotes coinciding with axis formation. However, when polarity was oriented by unilateral illumination, all zygotes showed symmetric CTC fluorescence. The authors concluded that there was no reason to believe that an asymmetric distribution of membrane bound Ca^{2+} was involved in polar formation (Kropf and Quatrano, 1987). Conversely, a gradient of cytoplasmic free Ca^{2+} has been detected in polarising *F. serratus* zygotes using the Ca^{2+} indicator dye calcium green, linked to high molecular weight dextran (Berger and Brownlee, 1993). The gradient was oriented by unilateral light. However, this result must be treated with caution as microinjection into zygotes disrupts the timing of polarisation in an unpredictable manner: Zygotes might therefore have reached a later stage than assumed. In summary, although predicted, no convincing intracellular Ca^{2+} gradient has yet been detected during polar induction in Fucoid zygotes.

Finally, a labile, localised acidification has been detected around polarising *P. fastigiata* zygotes (Gibbon and Kropf, 1991). The future rhizoid is more basic due to an extrusion of H^+ into the extracellular medium (Gibbon and Kropf, 1993). This acidification of the medium adjacent to the zygote is labile and oriented by polarising cues. It has been proposed that an intracellular pH gradient is involved in maintaining and,

possibly, in generating regional differentiation (Gibbon and Kropf, 1991 and 1994). However, localised pH changes might also be viewed as reflections of the metabolic changes which occur during cue perception (Berger and Brownlee, 1994) and axis formation, rather than as a real polarising mechanism.

The irreversible commitment to form a rhizoid at a particular site is prerequisite to the morphological expression of the induced polar axis (Quatrano, 1978). Indeed, a fixed axis is required to direct polar transport of intracellular components (Quatrano, 1990). While a degree of structural polarisation is observed during an extended period of axis formation, it is minor compared with that which occurs rapidly, at axis fixation (Quatrano, 1972). At axis fixation, zygotes of *F. vesiculosus* and *F. gardneri* oriented by unilateral light display localised accumulation of mitochondria, ribosomes and vesicles at the site of future rhizoid germination. Such organelle accumulations are never observed in the light hemisphere of photopolarised zygotes (Quatrano ,1972).

Visualisation of actin distribution with the fluorescent probe rhodamine phalloidin revealed a uniform distribution of actin during axis formation, followed by a gradual localisation at the rhizoid pole at axis fixation (Kropf *et al.*, 1989). Such actin localisations have also been observed during bud site selection in yeasts (Welch *et al.*, 1994). Zygotes exposed to the inhibitor of actin polymerisation, cytochalasin D, and illuminated by unilateral light, did not fix a polar axis, but retained a labile axis until inhibition ceased (Quatrano, 1973). Furthermore treatment of developing *F. vesiculosus*, *F. distichus* and *P. fastigiata* zygotes with cytochalasins B and D inhibited events normally associated with polarisation, notably the trans-cytoplasmic electrical current (Brawley and

Robinson, 1985). Neither the microtubule network, nor cytoplasmic Ca^{2+} mobilisation appear to affect axis fixation (Kropf and Quatrano, 1987), although each are required for cytokinesis (Kropf *et al.*, 1990 ; Allen and Kropf 1992) and for rhizoid germination respectively (Brownlee and Wood, 1986 ; Brownlee and Pulsford, 1988 ; Brownlee, 1989).

1. 2. 7 Importance of the cell wall in polarity

At fertilisation, the cell wall is 60% alginic acid and 40% cellulose. Fucose containing polymers (fucoidin), existing only as traces at this stage, are deposited 1 h AF (Brawley *et al.*, 1976*a*). At 6 h AF, the relative amount of alginic acid is unchanged (60%), but the cellulose content of the wall is is 20% of the total polysaccharide content, with the remaining 20% being recently synthesised fucoidin (Ley and Quatrano, 1973). Novel synthesis of wall material, as opposed to the fertilisation-induced cell wall secretion, occurs from 6 h AF (Novotny and Foreman, 1975) and is accompanied by a localisation of fucoidin to the presumptive rhizoid pole (Novotny and Foreman, 1974 and 1975 ; Quatrano *et al.*, 1991). Enzymatic removal of the cell wall in polarised zygotes re-established a labile axis (Kropf *et al.*, 1988). The cell wall is therefore fundamental to axis fixation, yet unnecessary for axis formation (Kropf *et al.*, 1988 ; Quatrano, 1990 ; Quatrano *et al.*, 1991) and maintains the memory of polarity.

The establishment of a fixed, polar axis involves interaction between asymmetrically distributed elements of the zygote's cytoplasm, the cytoskeletal, microfilament network, elements of the plasma membrane, and the cell wall (Quatrano, 1990 ; Quatrano *et al.*, 1991 ; Kropf, 1992 ; Goodner and Quatrano, 1993*a*). Molecules involved in animal foetal contacts, vinculin, integrin and vitronectin, and in yeast bud formation, BUD1 and CDC 42 have been immunologically identified in *Fucus* zygotes

(Quatrano *et al.*, 1991 ; Goodner and Quatrano, 1993*b*). Vitronectin was localised at the rhizoid site (Wagner *et al.*, 1992) where it is thought to play a role in cell adhesion to the substratum.

Unilaterally illuminated zygotes in which turgor was reduced yielded multicellular, apolar embryos (Torrey and Galun, 1970). When turgor was returned to normal, zygotes developed multiple rhizoids, each originating from a single cell. Although unlike normal polarisation, this case suggests the rhizoid differentiation stimulus is different from polarisation transduction processes, and was inherited by several cells which probably originate from what would have been the initial rhizoid. Hence the cells of the early embryo have restricted developmental fates. This line of thought has recently been supported by further experimental evidence: Following ablation of the rhizoid cell, no replacement was produced from the thallus portion of the embryo which continued along its own developmental path (Kropf *et al.*, 1993). Rhizoid protoplasts prepared by enzymatic digestion lost their polar identity, though regenerated into globular embryos. Loss of the wall resulted in loss of microtubule organisation within the rhizoid. Hence the wall seems to maintain polarity by interaction with the cytoplasmic cytoskeleton (Kropf *et al.*, 1993). Rhizoid protoplasts isolated by laser microsurgery acted as zygotes, *i.e.* resorted to an apolar, undifferentiated state with polar induction following the same progression as for normal zygotes (Berger *et al.*, 1994). Moreover, thallus or rhizoid cells differentiate into the opposing cell type if put in contact with the alternative cell wall type. A positional information signal of unknown nature which determines the state of differentiation therefore seems to exist within the cell wall itself (Berger *et al.*, 1994). However, isolated rhizoid hairs regenerate into normal plants (Mc Lachlan and Chen, 1972) indicating that this positional information might only act in the early embryo.

1. 3 Models of polar axis formation

3. 1. 1 An invisible axis oriented by metabolic gradients

In the absence of other polarising cues, it was proposed that the point of sperm/egg fusion polarised zygotes (Knapp, 1931). Hence, if polarity were effectively established at fertilisation, from that time onwards a labile polar axis existed within the cell. By analogy with typical, polarised embryos, this axis was conceived to be a labile structure within the cell. Subsequent polarising cues would rotate the existing axis, guided by metabolic gradients within the cell (Child, 1929). A substantial body of experimental evidence supported the concept of a polar axis oriented by a pH gradient (Hurd, 1920 ; Whitaker, 1937, 1938 and 1940), despite the nature of the axis itself, and whether it was established or superseded by a gradient was unclear (Whitaker, 1938).

1. 3. 2 Cortical epigenesis and an electrical polar axis

As previously explained (Section *1. 2. 2*), zygotes illuminated by plane polarised light formed two rhizoids at diametrically opposite points of the cell circumference, demonstrating that "*polarity <is> not established through the rotation of some pre-formed asymmetric inclusion... it must arise in a more epigenic manner*", with the origin of the polar axis in the cortical cytoplasm (Jaffe, 1958 and 1968).

The trans-cytoplasmic, ionic currents which flow during polarisation (Section *1. 2. 5*) were proposed as a means for self-reinforcing asymmetry in Fucoid zygotes (Jaffe *et al.*, 1974 ; Nuccitelli and Jaffe, 1974 ; Robinson and Jaffe, 1975 ; Nuccitelli, 1978): Asymmetric, environmental cues would cause a localised alteration of the cytoplasm, leading to an asymmetric localisation of cations, notably Ca^{2+} (Robinson and Jaffe, 1975). The

resulting increase in localised cortical charge (1 mV across the cell) was calculated to be sufficient to polarise membrane-bound proteins, by lateral electrophoresis, in approximately 3 h (required theoretical differential 0.8-4 mV across the zygote) (Jaffe, 1977). As a result, Ca^{2+} channels would segregate within the plasma membrane to the presumptive rhizoid pole causing a passive inward Ca^{2+} leak, and Ca^{2+} pumps would redistribute to the thallus pole where ions are actively exported (Robinson and Jaffe, 1975). The trans-cytoplasmic potential thus initiated would feed back to cause further membrane protein segregation, both reinforcing itself and the membrane asymmetries it generates (Jaffe *et al.*, 1974). The current would guide F-actin assembly which would eventually stabilise and fix the generated axis (Brawley and Robinson, 1985). In this model, the trans-cytoplasmic current is, effectively, the polar axis (Figure 1-3-1). It explained both the observed data, and fitted the philosophical climate of the time.

Electrical fields exist in many developing and growing systems (Fulton, 1980). Furthermore, change in the direction and intensity of ionic currents reinforced polar structures in molluscan embryos (Zivkovic and Dohmen, 1991 ; Créton *et al.*, 1993) and oriented growth in chick embryos (Hotary and Robinson, 1992). However, transcellular currents and the cellular processes which they apparently guide are too closely linked to determine causal relationships. Current models of polarisation therefore lessen the role of the trans-cytoplasmic current and refrain from identifying it as the polar axis.

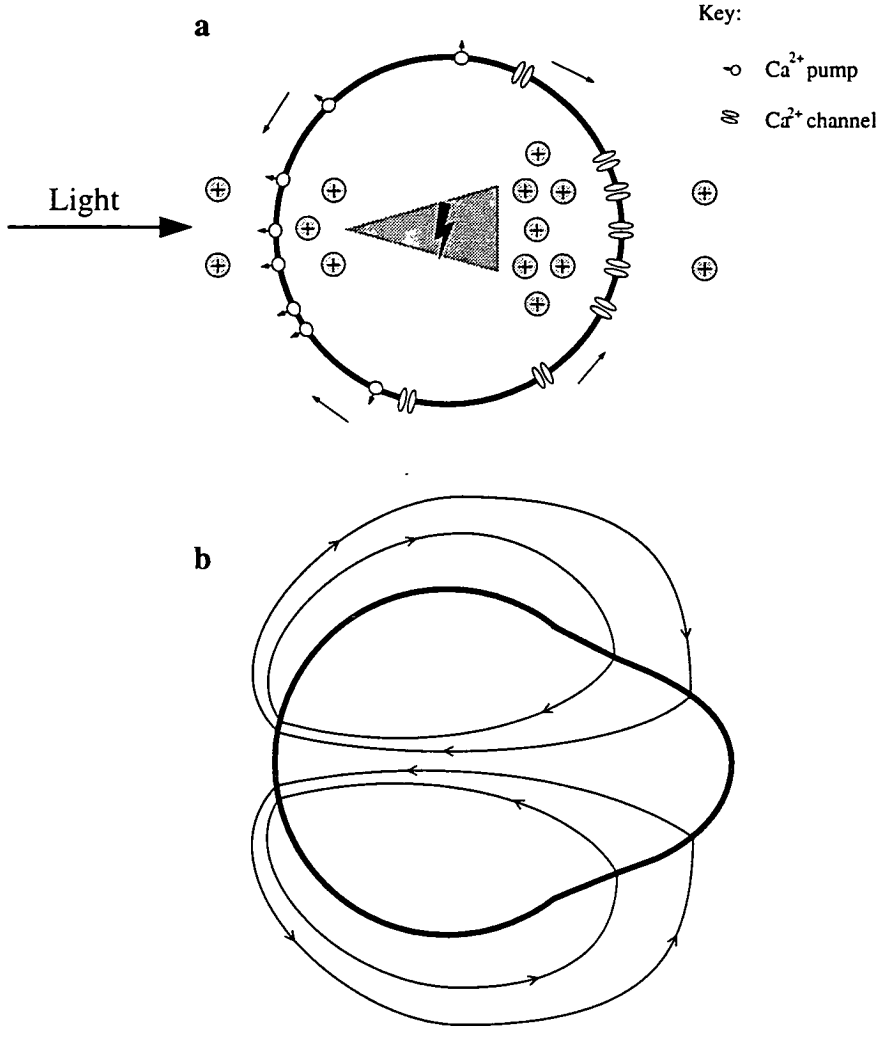

Figure 1-3-1. Lateral electrophoresis model of polarisation.

a: Polar trans-cellular electrical currents caused by ion flux through the cytoplasm cause lateral electrophoresis of membrane proteins, resulting in an epigenic, cortical asymmetry. The electrical current, represented by the grey triangle, is self re-enforcing and effectively is the polarising force (see text for details). The direction of polarising light is indicated.

b: Polar ionic currents round a developing *Fucus* zygote as measured with the vibrating probe (Nuccitelli, 1978).

1. 3. 3 Cortical epigenesis and Ca^{2+}

The most recent models of polarisation in Fucacean zygotes (Kropf and Quatrano, 1987 ; Quatrano, 1978 ; Brawley and Robinson, 1985 ; Kropf, 1989 and 1992 ; Goodner and Quatrano, 1993a) are greatly inspired by the aforementioned electrical axis model. It is now known that elevations in [Ca2+]cyt act as a second messenger between numerous environmental stimuli and cellular response in plant cells (Section 1. 4).

Early signal transduction events are thought to cause a localised rise in the concentration of $[Ca^{2+}]_{cyt}$ in polarising Fucoid zygotes. This initial Ca^{2+} asymmetry in the cell cortex generates a disequilibrium in plasma membrane permeability to Ca^{2+} resulting in lateral electrophoresis (Jaffe, 1977) of Ca^{2+} channels to the rhizoid hemisphere and Ca^{2+} pumps to the thallus hemisphere (Robinson and Jaffe, 1976). The asymmetric concentration of Ca^{2+} channels and pumps establishes a self-reinforcing cytosolic Ca^{2+} gradient through the cell, ionic currents being consequential of polarisation rather than causal (Figure 1-3-2). The transcellular Ca^{2+} gradient would mediate and guide the assembly of cytoskeletal components (Brawley and Robinson, 1985 ; Kropf, 1989 ; Quatrano, 1990), and polarisation of organelles (Section *1. 2. 5*). Cytoskeletal elements which interact with the cell wall would fix the polar axis (Brawley and Quatrano, 1979 ; Kropf *et al.* 1988 ; Quatrano, 1990 ; Wagner *et al.*, 1992).

The model has been refined (Kropf, 1992 ; Goodner and Quatrano, 1993) to encompass polarised pH gradients (Gibbon and Kropf, 1991, 1993 and 1994), metabolic processes (Schröter, 1978 ; Berger and Brownlee, 1994) and cell wall-plasma membrane bridges (Kropf *et al.*, 1988 ; Quatrano *et al.*, 1991 ; Kropf *et al.*, 1993). Consequently, the axis cannot be identified with a structure or with a force, but is perceived as a dynamic

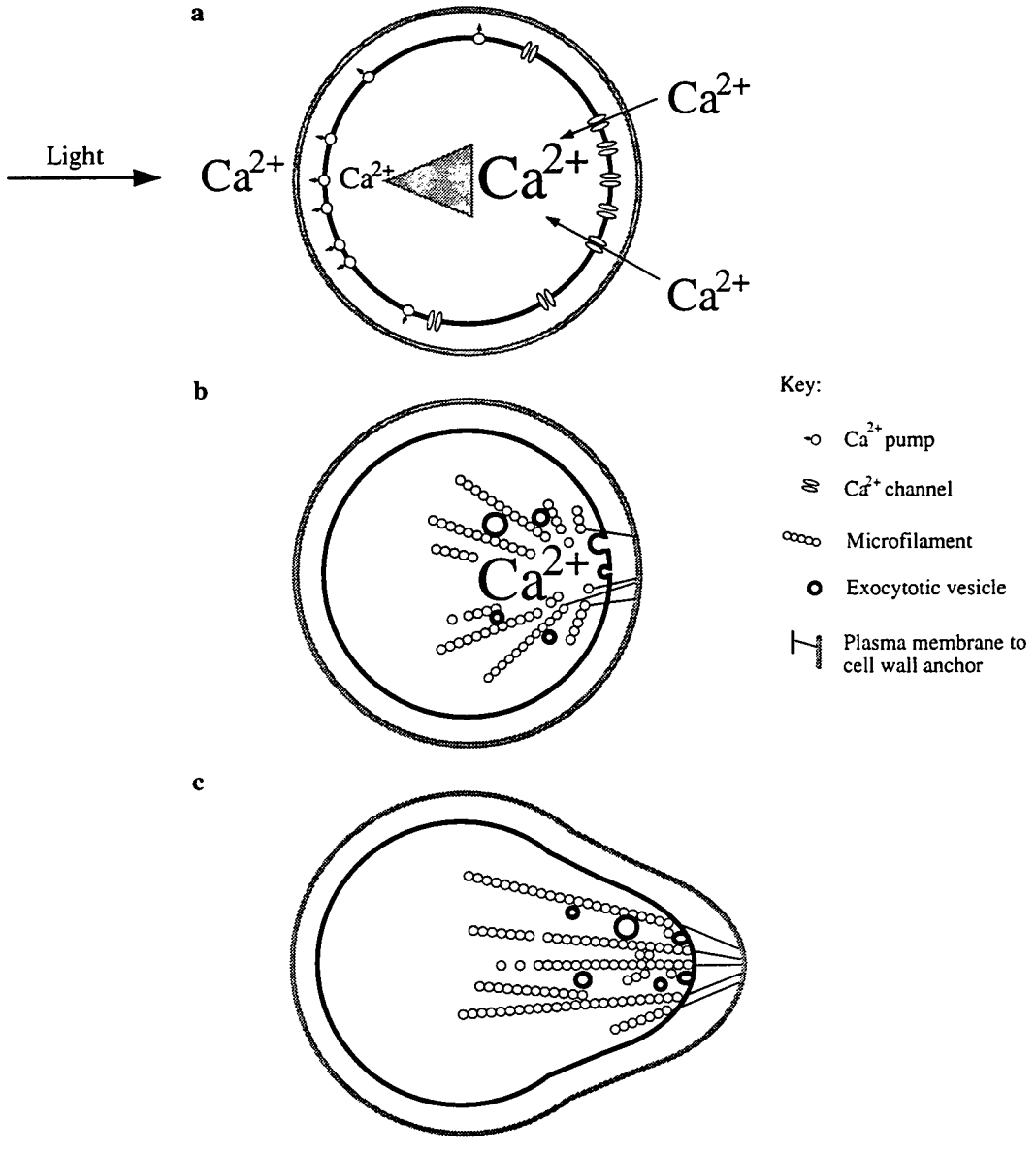

Figure 1-3-2. Polarisation by a dynamic transcellular Ca^{2+} gradient.

a: The polarising stimulus generates an asymmetric, passive influx of Ca^{2+} which, in turn, polarises Ca^{2+} channels to the presumptive rhizoid pole and Ca^{2+} pumps to the future thallus pole. The asymmetric distribution of membrane proteins re-enforces the cytoplasmic asymmetry, and enhances the trans-cytoplasmic Ca^{2+} gradient. The cell wall is represented by the grey ring.

b: A cytoplasmic Ca^{2+} gradient guides microfilament assembly and polarised secretion of wall material. The axis remains labile.

c: Cytoskeletal-plasma membrane-cell wall bridges then fix polarity.

interaction of signal transduction pathways, mainly involving changes in cytosolic [Ca^{2+}] at the presumptive rhizoid.

The central role of Ca^{2+} in this model has been challenged. The Ca^{2+} gradient itself appears unnecessary for axis fixation (Kropf and Quatrano, 1987 ; Kropf, 1989), casting doubt over its involvement in guiding microfilaments to the presumptive rhizoid. Moreover, visualisation of membrane-bound Ca^{2+} in polarising zygotes show a uniform Ca^{2+} distribution (Kropf and Quatrano, 1987). A convincing gradient of cytosolic Ca^{2+} has not been observed during axis formation (Section *1. 2. 5*), as opposed to the Ca^{2+} gradients readily observed at rhizoid initiation and during rhizoid elongation (Brownlee and Wood, 1986 ; Brownlee, 1989). This, however, may only be due to limits inherent in the *Fucus* system, such as opacity of zygotes, or in the Ca^{2+} visualisation technologies currently available, or in the Ca^{2+} dyes themselves disrupting what might be a minute, though functional, Ca^{2+} gradient. Furthermore, *P. fastigiata* zygotes formed a polar axis with respect to unilateral illumination in the absence of external Ca^{2+}, and indeed in the absence of all external ions bar K^+ (Hurst and Kropf, 1991). The authors concluded that whereas no specific ion (K^+, Na^+, Ca^{2+}, Mg^{2+}, Cl^- and SO_4^{2-}) was essential for photopolarisation, an ionic component was required in the medium and that the polar ionic current must therefore have a function. Although Ca^{2+} circulation through the polarising zygote, as proposed by the model, appeared not to be required for polarisation, these experiments take no account of Ca^{2+} release from intracellular Ca^{2+} stores. Microinjections of the Ca^{2+} buffer, BAPTA, inhibited polarisation and the intracellular events normally associated with the expression of polarity, notably the inward Ca^{2+} current at the presumptive rhizoid, and rhizoid germination (Speksnijder *et al.*, 1989). BAPTA is thought to significantly increase Ca^{2+} mobility in the cytoplasm,

thereby destroying any cytoplasmic free Ca^{2+} gradient. Current evidence therefore suggests that polarisation of Fucoid zygotes involves a cytoplasmic Ca^{2+} gradient sustained by Ca^{2+} from intracellular Ca^{2+} stores, rather than from Ca^{2+} import.

The concept of an epigenic and dynamic axis in polarising Fucoid zygotes is widely accepted, based on an interaction of signal transduction pathways, mainly involving changes in cytosolic $[Ca^{2+}]$ at the presumptive rhizoid. Localised perturbations in $[Ca^{2+}]_{cyt}$ are recognised by the cell and eventually fixed into a morphological reality. However, despite active research, the precise role of Ca^{2+} in polarisation remains unclear.

1. 4 Ca^{2+} as a second messenger in plant cells

Variations in the concentration of cytosolic free Ca^{2+} control many aspects of cell function (Burgoyne and Cheek, 1991 ; Bush, 1993). Due to the cytotoxic effects of Ca^{2+}, eukaryotic cells maintain concentrations of cytoplasmic Ca^{2+} between 10^{-6}-10^{-5} M (Gilroy *et al.*, 1987*a*). Homeostasis is achieved by several mechanisms (Lytton and Nigam, 1992 ; Gilroy *et al.*, 1993) including active export of Ca^{2+} from the cell, Ca^{2+} sequestration by intracellular stores (Burgoyne and Cheek, 1991) such as the endoplasmic reticulum (Koch, 1990) or the vacuole (Poovaiah and Reddy, 1987 ; Bush, 1993), and Ca^{2+} binding to regulatory proteins (Gilroy *et al.*, 1987*b* ; Heizmann and Hunziker, 1991). Ca^{2+} is exported from the cytosol by membrane bound Ca^{2+}-ATPases, or Ca^{2+} pumps (Gilroy *et al.*, 1987*a* ; Trewavas and Gilroy, 1991). Channels in the plasma membrane or in the membranes of intracellular Ca^{2+} stores allow controlled Ca^{2+} influx into the cytosol (Trewavas and Gilroy, 1991 ; Schroeder and Thuleau, 1991). Little is known about the mode of action of plant Ca^{2+} channels. As yet, only inositol 1,4,5-triphosphate (IP_3) is known to cause Ca^{2+} release from

intracellular Ca^{2+} stores in plant cells (Alexandre *et al.*, 1990 ; Schroeder and Thuleau, 1991), though Ca^{2+} induced Ca^{2+} release (CICR) channels (Schroeder and Thuleau, 1991) and G-protein activated Ca^{2+} channels (Delisle, 1991) are also thought to exist in plants. Free Ca^{2+} is quasi immobile in the cytoplasm (Allan and Trewavas, 1987 ; Allbritton *et al.*, 1992) and therefore accumulates in the cytoplasm where it was secreted. This low cytoplasmic mobility, and low background concentration coupled with tight control of Ca^{2+} fluxes within cells are essential to the second messenger role of Ca^{2+} in signal transduction and cellular control. Ca^{2+} may modulate cell activity through a sustained, localised rise in $[Ca^{2+}]_{cyt}$, for instance in pollen tube elongation (Jaffe *et al.*, 1975), or by single or multiple transient elevations in $[Ca^{2+}]_{cyt}$ (Hepler, 1990 ; Jaffe, 1991), propagated through cells in "Ca^{2+} waves" of CICR and re-sequestration (Berridge and Moreton, 1991 ; Kasai *et al.*, 1993). The Ca^{2+} wave starts by a localised increase in $[Ca^{2+}]_{cyt}$. This in turn causes CICR from nearby Ca^{2+} stores. In this way, CICR progresses through the cell, driven by increased $[Ca^{2+}]_{cyt}$. Behind the wave front, further Ca^{2+} release is blocked by the effect of high $[Ca^{2+}]_{cyt}$. Ca^{2+} is then actively exported from the cytoplasm into Ca^{2+} stores, ending the cycle and re-charging the system (Jaffe, 1991).

Although work on signal transduction and Ca^{2+} fluctuations in plant cells lags behind its animal counterpart, a substantial body of circumstantial evidence (Allan and Trewavas, 1987 ; Gilroy *et al.*, 1987*a*), and an increasing amount of direct evidence (Saunders and Hepler, 1983 ; Mc Ainsh *et al.*, 1990) suggests that Ca^{2+} acts as a second messenger in plant cells, coupling environmental signal and cellular response (Hepler and Wayne, 1985 ; Trewavas and Gilroy, 1991). To ascertain whether Ca^{2+} acts as a second messenger, three criteria must apply (Jaffe, 1980): First,

agonist-induced stimulation should be accompanied by a change in $[Ca^{2+}]_{cyt}$. Second, inhibition of changes in $[Ca^{2+}]_{cyt}$ should inhibit the presumed effect. Third, an artificial increase in $[Ca^{2+}]_{cyt}$ should stimulate the event in the absence of a normal agonist. Evidence suggests that Ca^{2+} mediates cell responses to both endogenous and exogenous stimuli. For example, in the moss *Funaria*, a rise in $[Ca^{2+}]_{cyt}$ was implicated in the cytokinin-induced formation of buds from the early protonema (Saunders and Hepler, 1983 ; Hahm and Saunders, 1991). Similarly, increased $[Ca^{2+}]_{cyt}$ following treatment of *Commelina communis* guard cells by abscisic acid has been shown to precede stomatal closure (Mc Ainsh *et al.*, 1990). Many studies have indirectly shown that changes in $[Ca^{2+}]_{cyt}$ mediate responses to environmental stimuli such as gravity or light (Allan and Trewavas, 1987). Currently, imaging using Ca^{2+} sensitive dyes or bioluminescent proteins is providing more direct evidence for the role of Ca^{2+} in signal transduction (Trewavas and Gilroy, 1991 ; Shacklock *et al.*, 1992 ; Knight *et al.*, 1991 ; Read *et al.*, 1992). For example, the use of the Ca^{2+} indicator dye, Fluo-3, revealed a rise in $[Ca^{2+}]_{cyt}$ which preceded red light induced swelling and rapid protein phosphorylation in etiolated *Triticum aestivum* leaf protoplasts, (Shacklock *et al.*, 1992 ; Fallon *et al.*, 1993). Furthermore artificial rises in $[Ca^{2+}]_{cyt}$ by intracellular release of microinjected, caged Ca^{2+} mimicked the effect of red light (Shacklock *et al.*, 1992) demonstrating a direct causal link between increased $[Ca^{2+}]_{cyt}$ and protoplast swelling. Transgenic expression of the Ca^{2+} sensitive bioluminescent protein aequorin in *Nicotiana plumbaginifolia* has shown that various environmental stimuli such as mechanical perturbation, temperature variations or chemical compounds cause transient, intracellular Ca^{2+} movement (Knight *et al.*, 1991, 1992 and 1993).

Cytosolic free Ca^{2+} interacts with numerous proteins, directly modulating their activity and subsequently the activity of the cell (Heizmann and Hunziker, 1991 ; Roberts and Harmon, 1992 ; Bush, 1993). Increased $[Ca^{2+}]_{cyt}$ promotes microtubule depolymerisation, (Weisenberg, 1972) and is therefore involved in regulating cytoskeletal and spindle assembly (Hepler *et al.*, 1990). High $[Ca^{2+}]_{cyt}$ has been detected, localised at the spindle poles (Keith *et al.*, 1985 ; Ratan and Shelanski, 1986) and is thought to be involved in mitotic control and aspects of cell cycle regulation (Iida *et al.*, 1990). Cytosolic Ca^{2+} also activates several regulatory proteins, notably calmodulin, which interacts with, and modulates the activity of yet other proteins or cell processes (Roberts and Harmon, 1992). These Ca^{2+} activated regulatory proteins can be viewed as a second link in the Ca^{2+} transduction chain, a sort of "tertiary messenger", which further control the specificity of the Ca^{2+} signal.

1. 5 Calmodulin

1. 5. 1 Calmodulin structure and activation

Calmodulin was first identified as a cyclic 3',5'-nucleotide phosphodiesterase activator (Cheung, 1970) and is the main regulatory protein linking Ca^{2+} signals and the activities of numerous proteins and enzymes in plant cells (Allan and Hepler, 1989 ; Klee *et al.*, 1980). Calmodulin is a small, acidic protein of approximately 148 amino acids and a molecular weight of 16-19 kDa (Figure 1-5-1). The primary structure comprises 4 Ca^{2+} binding loops, also called EF hands, of 12 amino acids in length (Martin, 1987 ; Babu *et al.*, 1988). The crystal structure of calmodulin reveals two globular domains, each containing two EF hands with a double-stranded, antiparallel β-sheet between each adjacent loop (Babu *et al.*, 1988). A large hydrophobic cleft, believed to be the binding

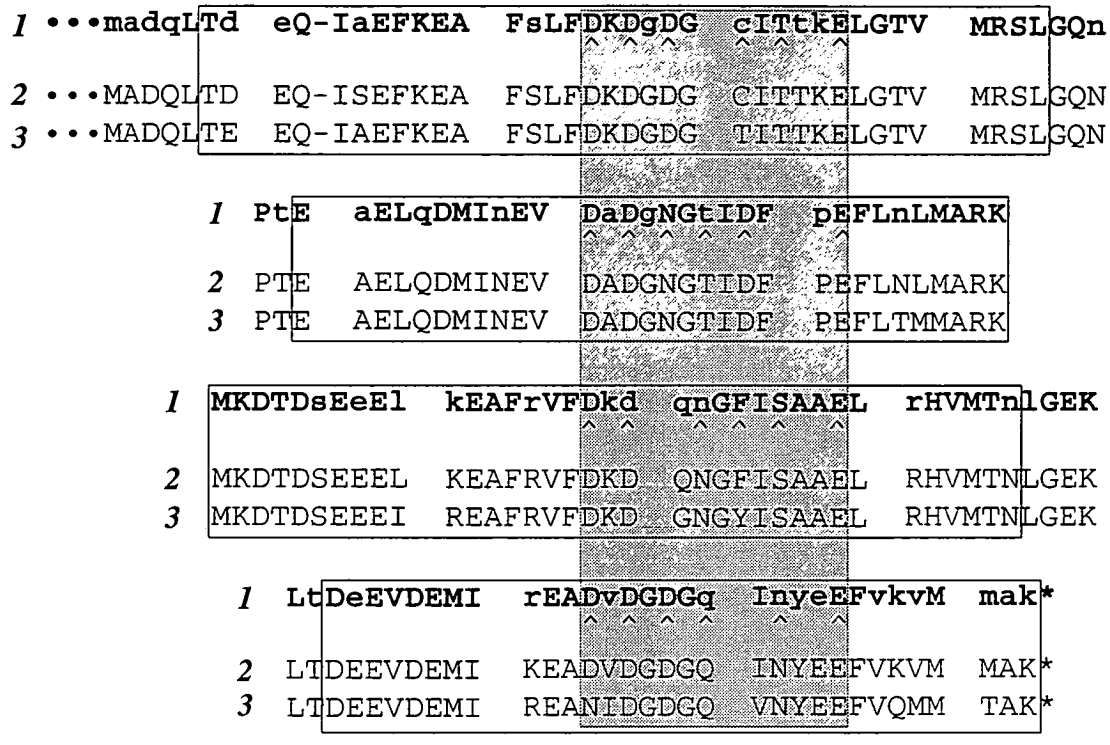

Figure 1-5-1. Amino acid sequence of calmodulin.

Three calmodulin sequences are presented using the single letter amino acid code. Sequences are aligned by the four Ca^{2+} binding loops which are shaded in grey (Babu *et al.*, 1988). Ca^{2+} binding residues are indicated by (^). The globular domains are boxed.

1: The consensus sequence of 18 plant and fungal calmodulins (Figure 2-11-1). Amino acids for which there are no or only one heterology throughout the species screened are indicated in capitals. Amino acids which show at least two heterologies are in lower case.

2: *A. thaliana* calmodulin (EMBL identifier; em_pl:atcam2).

3: *Rattus norvegicus* calmodulin (EMBL identifier; em_ro:rncam).

site for target proteins, runs along each globular domain (Babu et al., 1988 ; O'Neil and DeGrado, 1990 ; Williams, 1992 ; Ikura *et al.*, 1992) which are linked by a 7-turn α-helix (Babu *et al.*, 1990) (Figures 1-5-2 and 5-1-3).

EF hand and Ca^{2+} binding occurs in a 1 : 1 ratio. The dissociation constant (Kd) for Ca^{2+}/calmodulin ranges from 10^{-6}-10^{-5} M, with at least one Ca^{2+} binding site having a Kd of 10^{-6} M (Manalan and Klee, 1984). The sequence of the EF hand alone does not account for the Kd of Ca^{2+} to calmodulin as estimates of Kd values between Ca^{2+} and a single EF hand approximate 10^{-4} M (Williams, 1992). The central feature of calmodulin is the pairing of EF hands, which confers the low Kd observed between Ca^{2+} and the molecule as a whole (Williams, 1992). Ca^{2+} binding in each of the globular domains is negatively cooperative.

Under physiological conditions, notably with respect to Mg^{2+} concentration, calmodulin binds 3 Ca^{2+} ions (Cox, 1986). Calmodulin activation occurs in two steps. First Ca^{2+} binds to the molecule causing a conformational change which results in a 5-10% increase in α-helix content (Klee *et al.*, 1980) and exposes the hydrophobic region of each domain (Manalan and Klee, 1984). The conformational change is independent of Ca^{2+} occupying any particular EF hand (Cox, 1986). The Ca^{2+}-calmodulin complex (active calmodulin or Ca^{2+}-CaM) then binds to its target proteins, modulating their properties (Klee *et al.*, 1980). Ca^{2+}-CaM binding to polypeptides and activation of the Ca^{2+}-calmodulin-polypeptide complex may be controlled by the degree of Ca^{2+} occupancy of the EF hands. For instance, following binding of two Ca^{2+} ions, calmodulin attaches to calcineurin. Activation, however, only occurs when at least a third Ca^{2+} ion binds to the Ca^{2+}-CaM-calcineurin complex (Allan and Hepler, 1989).

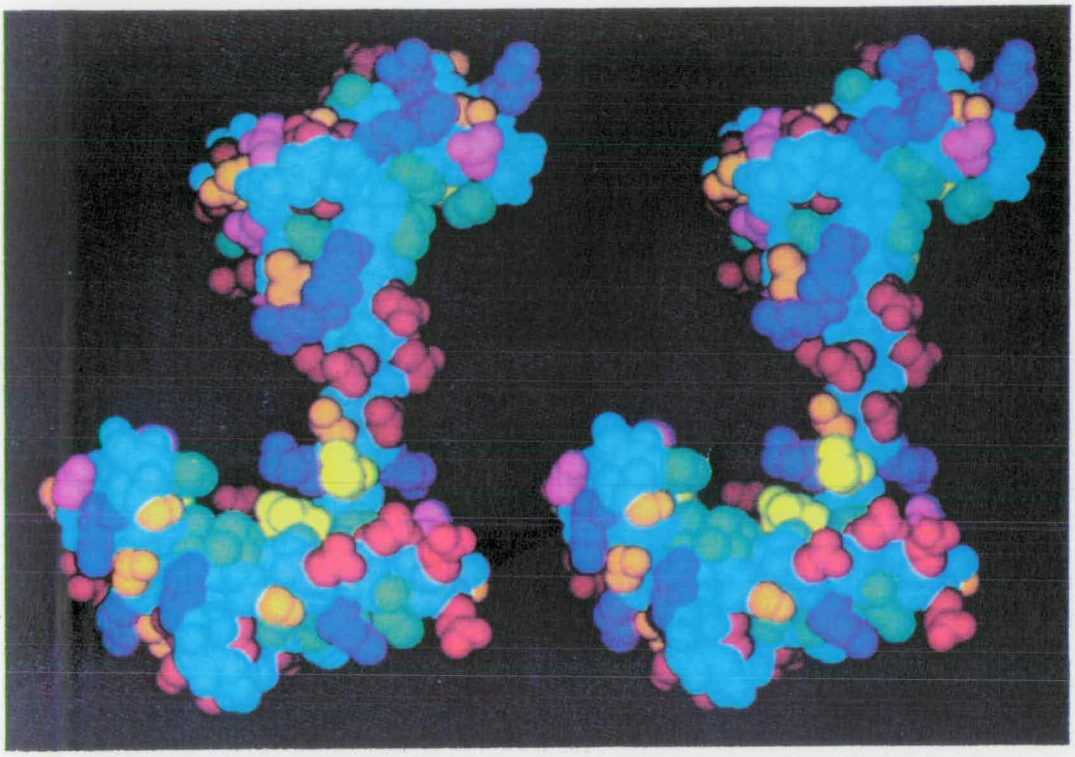

Figure 1-5-2. Secondary structure of calmodulin.

Stereo space-filling model of the crystal structure of *Rattus norvegicus* calmodulin. Note the two globular domains connected by a central helix. The N-terminal domain is at the top. Lys75 is positioned at the top of the central helix pointing to the right.

The amino acid residues are colour coded as follows.
Blue: Arginine, lysine, histidine (positively charged residues).
Red: Aspartic acid, glutamic acid (negatively charged residues).
Green: Alanine, valine, leucine, isoleucine, phenylalanine (hydrophobic, non-polar residues).
Purple: Asparagine, glutamine (polar but uncharged residues).
Orange: Serine, threonine, tyrosine (polar but uncharged residues).
Cyan: Proline (hydrophobic residue), glycine (polar, uncharged residue).
Yellow: Methionine.

From Babu *et al.* (1988).

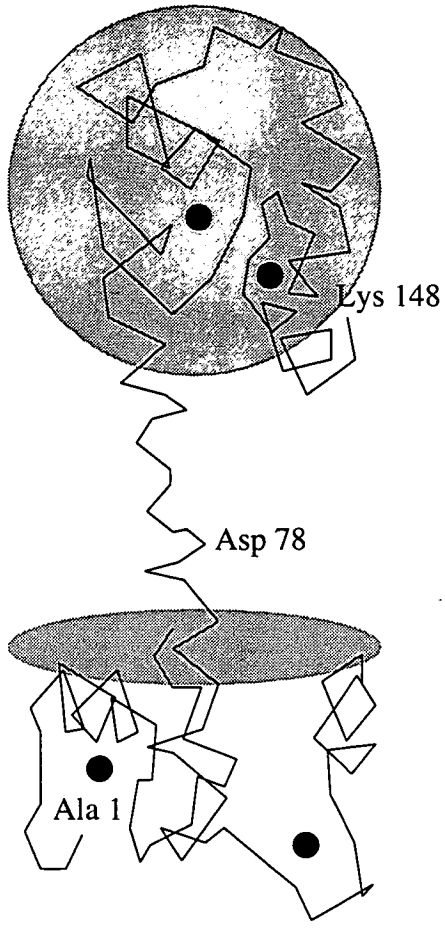

Figure 1-5-3. Secondary structure of calmodulin.

Stick model of the crystal structure of calmodulin. Note the two globular domains connected by a central helix. The positions of Ca^{2+} binding are indicated by a black dot within each of the 4 EF hands. The positions of the hydrophobic cleft of each domain are indicated in grey.

From O'Neil and DeGrado (1990).

Although there is the potential for two protein binding sites per calmodulin molecule, one on each globular domain, the binding of Ca^{2+}-CaM to target proteins occurs in a 1 : 1 stochiometry. Moreover, many of the spectral and binding properties of Ca^{2+}-CaM can be interpreted as the sum of the properties of the two globular domains. It therefore appears that both domains come closer together, and act in concert with the target protein (Kretsinger, 1992). Because this model of calmodulin activation requires a flexible link between both domains, it is known as the "flexible tether" model (Figure 1-5-4). Calmodulin interacts with many polypeptides by recognising and binding to a specific region of 20 amino acids, rich in positively charged amphiphillic helices, contained within the target peptides. The method by which Ca^{2+}-CaM binds to so many different peptides is still poorly understood, but may lie, among others, in the presence of high methionine concentrations (methionine puddles) in the hydrophobic clefts which could accommodate the fine details of variable target sequences while maintaining a rigid backbone to the binding site (O'Neil and DeGrado, 1990). Currently, molecular techniques such as mutation analysis (Davis, 1992*a* ; Ohya and Botstein, 1994) are being used to identify amino acid residues essential to various calmodulin functions.

Ca^{2+}-CaM regulates the activity of many different proteins such as cyclic nucleotide phosphodiesterase (Cheung, 1970), adenylate cyclase, inositol 1,4,5- triphosphatase, NAD kinase (Means *et al.*, 1991 ; Poovaiah and Reddy, 1987), histones (Wolff *et al.*, 1981), Ca^{2+} pumps of the endoplasmic reticulum and plasma membrane (Katz and Remtulla, 1978 ; Larsen and Vincenzi, 1979 ; Preston *et al.*, 1991), myosin light chain kinase (Hartwig *et al.*, 1992 ; Ikura *et al.*, 1992) and tubulin (Cyr, 1991). The concentration of calmodulin required for half maximal activation ($Ka_{0.5}$) of target proteins varies from 10^{-9}-10^{-6} M (Manalan and Klee, 1984). In

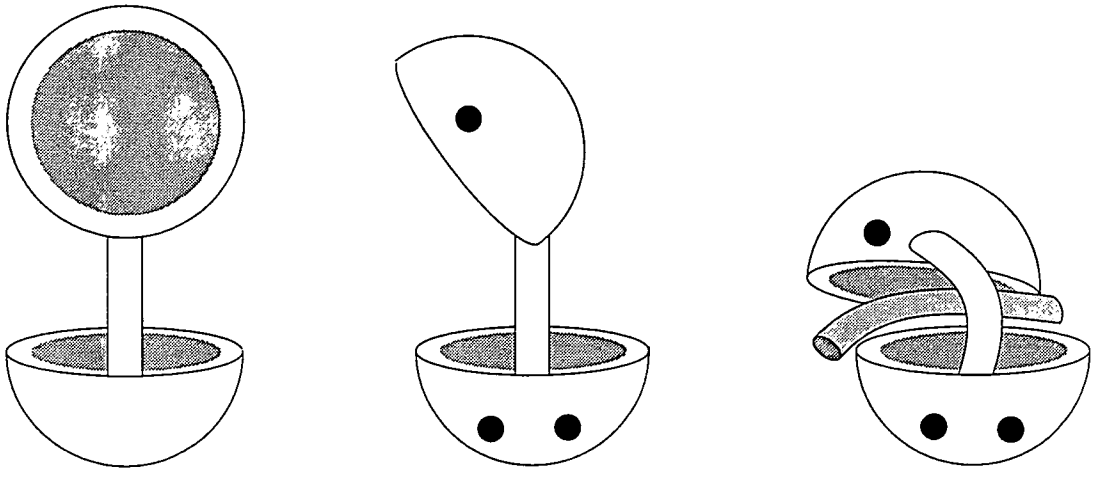

Figure 1-5-4. "Flexible tether" model of Ca^{2+}-CaM interaction with target peptides.

The diagram represents the relationship between the two Ca^{2+} binding domains of calmodulin, the central α-helix and a target peptide.

1: Inactive calmodulin. The globular domains are represented by hemispheres, with hydrophobic patches shown in grey.. The a-helix links both domains. (Figure 1-5-3).

2: Calmodulin is activated by binding 3 Ca^{2+} ions, represented by black dots.

3: The linker region of the central α-helix bends permitting the hydrophobic patches of both domains to enfold the helical portion of a target protein.

From Kretsinger (1992).

plants, calmodulin content varies between organs, although an average figure for calmodulin content in plant tissue is 15 $\mu g \cdot g^{-1}$, with approximately 10^{-7}-10^{-6} M calmodulin concentration per plant cell (Marmé and Dieter, 1983). Calmodulin availability is not therefore a limiting factor for the processes in which it is involved (Poovaiah and Reddy, 1987).

1. 5. 2 Evolutionary conservation of calmodulin

Calmodulin is viewed as a highly conserved protein throughout evolution (Watterson *et al.*, 1980 ; Manalan and Klee, 1984 ; Moncrief *et al.*, 1990 ; Roberts and Harmon, 1992 ; Stanovasnik *et al.*, 1993). The phosphodiesterase activities of plant and animal calmodulins are more or less equal (Watterson *et al.*, 1980 ; Schleicher *et al.*, 1983 ; Poovaiah and Reddy, 1987) and comparison between calmodulin amino acid sequences from protists, animals, fungi and plants show at least 60% homology between sequences. It has been argued that heterology between calmodulin sequences is not mirrored by functional divergence and that calmodulins are interchangeable across the phylogenetic barrier. For example, the calmodulin amino acid sequence of *Xenopus laevis* differs from that of *S. cerevisiae* by 60 amino acids out of 148 (40.5% heterology), yet transformation with the *X. laevis* calmodulin gene under control of the Gal 4 promoter restores normal growth to lethal *S. cerevisiae* mutants in which the calmodulin gene (CMD1) is lacking (Davis *et al.*, 1986 ; Davis and Thorner, 1989). However, saving lethal mutants is a gross effect and is not comparable with the more subtle functions of calmodulin. Effectively, mutation of selected amino acids within a specific calmodulin by genetic engineering has identified amino acids which are essential for certain cell functions (Davis, 1992*b* ; Lu *et al.*, 1993 ; Ohya and Botstein, 1994 ; Zielinski, *pers. comm.*, 1994). Mutation of phenylalanine residues 64 and

68 to alanine is sufficient to disrupt nuclear division in *Aspergillus nidulans* (Ohya and Botstein, 1994). With subtle changes in calmodulin sequences (*e.g.* one or two amino acid mutations) being increasingly attributed to a given function, the concept that all calmodulins across the phylogenetic range are functionally identical is simplistic and should be considered with caution.

1. 5. 3 Calmodulin involvement in the cell cycle

Regulation of the cell cycle is intimately connected with calmodulin dynamics (Rasmussen and Means, 1989*a* ; Rasmussen *et al.*, 1992) (Figure 1-5-5). At the G1-S phase boundary, the intracellular concentration of calmodulin doubles (Chafouleas *et al.* 1982 ; Rasmussen and Means, 1989*b*). Calmodulin was shown to be essential for progression through G1 and mitosis (Rasmussen and Means, 1989*b*). Increased concentrations of calmodulin shortened G1, thereby hastening entry into S phase, and accelerated progression through G2 and mitosis (Rasmussen and Means, 1989). Calmodulin depletion caused cell cycle arrest (Sasaki and Hidaka, 1982 ; Eilam and Chernichovsky, 1988). In the yeasts *S. cerevisiae* and *Schizosaccharomyces pombe*, disruption of calmodulin gene expression is lethal with the cell cycle block occurring at the transition between G2 and mitosis (Davis *et al.*, 1986 ; Takeda and Yamamoto, 1987 ; Ohya and Anraku, 1992). Homologous recombination in *A. nidulans* with a calmodulin fragment under the control of the alc A inducible promoter from *A. nidulans*, was used to replace the wild type calmodulin promoter. In presence of glucose or acetate, calmodulin expression was repressed and blocked cell cycle progression at the G2-M transition and at the G1-S transition (Rasmussen *et al.*, 1992). In cultured murine cells, this block occurs at the metaphase/anaphase boundary (Rasmussen and Means,

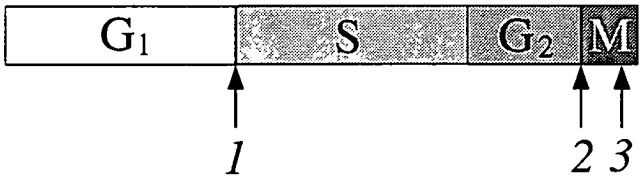

Figure 1-5-5. Calmodulin control of the cell cycle.

The points at which calmodulin controls the cell cycle are shown (see text for details):

1: Between G_1 and S phase.
2: Between G2 and Mitosis (M).
3: Between metaphase and anaphase.

1989*b*). Amphibian oocytes, arrested in late G2 of the meiotic cycle, resumed normal development when injected with 3-4 pmol of active calmodulin (Ca^{2+}-CaM) (Wasserman and Smith, 1981).

1. 5. 4 Calmodulin in polarity

Calmodulin has been visualised at the growing tip of polarised plant cells such as root hairs and pollen tubes (Haußer *et al.*, 1984). A calmodulin gradient is also present in the periphery of developing *Micrasterias*, a freshwater desmid (Kiermayer, 1981). Significantly, cytoplasmic Ca^{2+} gradients have also been identified in the same systems and are essential for normal development (Meindl, 1982). In *S. cerevisiae* the distribution of calmodulin varies during the cell cycle, with calmodulin polarised to the site of presumptive budding (Sun *et al.*, 1992 ; Brockerhoff and Davis, 1992). The yeast cdc 24 mutant, which displays defective budding at low temperatures, does not localise calmodulin at the bud site (Sun *et al.*, 1992). Mutations at phenylalanine residues 16 and 19 to alanine resulted in the loss of calmodulin localisation during budding (Ohya and Botstein, 1994). Polar distribution of actin has also been observed at the germination site (Welch *et al.*, 1994). In yeast, a single calmodulin mutation (F92A) resulted in a loss of actin localisation (Ohya and Botstein, 1994) demonstrating that calmodulin was involved in controlling the asymmetric distribution of F-actin towards yeast bud sites. F-actin is essential to polarity in *Fucus* (Brawley and Robinson, 1985) and is localised at the presumptive rhizoid pole during axis fixation of *F. distichus* zygotes (Kropf *et al.*, 1989), although no F-actin localisation was observed during axis formation. Given this parallel, a localisation of calmodulin activity during axis formation which precedes and guides the polar accumulation of F-actin at axis fixation is possible in Fucoid zygotes. Thus an asymmetric distribution of active

calmodulin may be a step between polarising stimulus, Ca^{2+} mobilisation, and F-actin redistribution.

1. 5. 5 Calmodulin during Fucus embryogenesis

Little is known about calmodulin in the Fucales. A putative calmodulin, 17 kDa-Ca^{2+} binding protein (17 kDa-CBP) was extracted from *P. fastigiata* sperm, egg and zygote lysates and identified among 10 other Ca^{2+} binding proteins by $^{45}Ca^{2+}$ overlay (Brawley and Roberts, 1989). Like calmodulin, 17 kDa-CBP migrated with an apparent molecular weight of 16-18 kDa in SDS PAGE, and displayed increased electrophoretic mobility in the presence of Ca^{2+} than when Ca^{2+} was chelated with EGTA. 17 kDa-CBP co-migrated with bovine brain calmodulin in the presence of Ca^{2+}, but faster than the vertebrate calmodulin in the presence of EGTA. Similar observations have been made with *Spinacia oleracea* and with *Hordeum vulgare* calmodulins (Watterson *et al.*, 1980 ; Schleicher *et al.*, 1983). Furthermore, 17 kDa-CBP was immunologically recognised by sheep polyclonal antibodies raised against bovine testis calmodulin.

The only algal calmodulin sequence present in the EMBL database was that of *C. reinhardtii* (Chlorophyceae). The amino acid sequence of *C. reinhardtii* calmodulin (Figure 1-5-6) differs significantly from higher plant calmodulins by an extra three amino acids at the N terminus of the protein, and ten amino acids more at the carboxyl terminus (Zimmer *et al.*, 1988). This characteristic "tail" enhances *in vitro* NAD reductase activity of *C. reinhardtii* calmodulin (Poovaiah and Reddy, 1987). It is unknown whether this trait is found in other algae, or whether it is unique to *Chlamydomonas*.

```
1  •••••••LT•  •QI•EFKEAF  •LFDKDGDG•  ITTKELGTVM  RSLGQNPTEA
2  •••madqLTd  dQIsEFKEAF  sLFDKDGDGc  ITTKELGTVM  RSLGQNPTEA
3  maanteqLTe  eQIaEFKEAF  aLFDKDGDGt  ITTKELGTVM  RSLGQNPTEA

1  ELQDMI•E•D  •D••GTIDFP  EFL•LM•RKM  •••D•E•E••  EAF•VFD•D•
2  ELQDMInEvD  aDgnGTDIFP  EFLnLMaRKM  kdtDsEeElk  EAFrVFDkDq
3  ELQDMIsEvD  aDgnGTIDFP  EFLmLMaRKM  ketDhEdElr  EAFkVFDkDg

1  NG•ISAA••R  HVMTNLGEKL  •••EVDEMI•  EAD•DGDG••  NYEEFV••M•
2  NGfISAAelR  HVMTNLGEKL  tdeEVDEMIk  EADvDGDGql  NYEEFVkvMm
3  NGfISAAelR  HVMTNLGEKL  seeEVDEMIr  EADvDGDGqv  NYEEFVrmMt

1  ••*•••••••  ••••
2  sk*
3  sgatddkdkk  ghk*
```

Figure 1-5-6. Amino acid sequence of plant calmodulins.

Amino acids are represented by the single letter code. Note the extra amino acids at the start and end of the *C. reinhardtii* sequence (shaded in grey).

1: Consensus sequence of 18 plant and fungal calmodulins (Figure 2-11-1).

2: Sequence of *A. thaliana* calmodulin (EMBL identifier; em_pl:atcam2).

3: Sequence of *C. reinhardtii* calmodulin (EMBL identifier; em_pl:crcam).

1. 6 Hypothesis and project plan

1. 6. 1 Background summary

A substantial amount of evidence supports the involvement of Ca^{2+} in polar formation during the early stages of Fucoid embryogenesis (Robinson and Jaffe, 1974 ; Brawley and Robinson, 1985 ; Speksnijder *et al.*, 1989). Briefly, the current model of fucoid polarisation proposes that environmental stimuli induce a secondary messenger-like release of cytoplasmic Ca^{2+}. This in turn locally alters the membrane potential, causing lateral electrophoresis, within the lipid bilayer, of Ca^{2+} channels to the presumptive rhizoid pole and of Ca^{2+}-ATPase export pumps to the future thallus pole. Consequently the intracellular Ca^{2+} distribution is altered, causing further protein segregation, resulting in a self sustaining polarisation mechanism (Kropf, 1992 ; Goodner and Quatrano, 1993). Implicit in this model is a cytoplasmic Ca^{2+} gradient. However, despite major advances in intracellular Ca^{2+} imaging techniques (Read *et al.*, 1992) and identification of Ca^{2+} gradients in elongating *Fucus* rhizoids (Brownlee and Wood, 1986), the evidence for Ca^{2+} gradients during axis induction remains circumstantial. Furthermore, the essential involvement of Ca^{2+} during axis induction has recently been questioned (Kropf and Quatrano, 1987 ; Hurst and Kropf, 1991).

Studies of budding in *S. cerevisiae* concluded that calmodulin, the main regulatory protein of calcium in cells, and the only Ca^{2+} regulator protein identified in plants to date, is required for polar development (Davis *et al.*, 1986 ; Sun *et al.*, 1992 ; Brockerhoff and Davis, 1992). Calmodulin localises to the future bud site where it guides the polarisation of F-actin (Ohya and Botstein, 1994 ; Welch *et al.*, 1994). Calmodulin has been identified in sperm, eggs and zygotes of *P. fastigiata* and *F. distichus*

(Brawley and Roberts, 1989), but further information is lacking. Moreover, F-actin localisations are essential to polar axis fixation in Fucoid zygotes (Quatrano, 1973 ; Kropf *et al.*, 1989), and might also be required during axis formation (Brawley and Robinson, 1985 ; Quatrano, 1973).

1. 6. 2 Hypothesis

By comparison with budding in *S. cerevisiae*, it was proposed that, in *F. serratus* zygotes, a localised concentration of active calmodulin is involved in polar induction. This working hypothesis suggested that polarisation cues cause a small, localised rise in $[Ca^{2+}]_{cyt}$, resulting in a polarised increase in calmodulin activity. Active calmodulin (Ca^{2+}-CaM) was conceived to link the initial, asymmetric variation in $[Ca^{2+}]_{cyt}$ during axis formation with the localised distribution of F-actin at axis fixation.

1. 6. 3 Project plan

To investigate the above hypothesis, *F. serratus* zygotes were studied during photopolarisation. First, the roles of Ca^{2+} and calmodulin during photopolarisation were assessed using transient application of various inhibitors of Ca^{2+} and active calmodulin to photopolarising *F. serratus* zygotes (Figure 1-6-1_1).

To elucidate further the role of calmodulin during polarisation, it was proposed to analyse the effects of artificially elevating the concentration of this protein during polarisation. However, although calmodulin is present in Fucoid tissues (Brawley and Roberts, 1989), the sequence, structure and activity, of Phaeophycean calmodulin is unknown. Evidence shows calmodulin to be structurally (Roberts and Harmon, 1992) and functionally conserved (Davis and Thorner, 1989), but subtle variations in calmodulin amino acid sequence are sufficient to cause the breakdown of specific, even essential, functions (Schaefer *et al.*, 1987 ; Davis, 1992 ; Lu *et al.*, 1993 ;

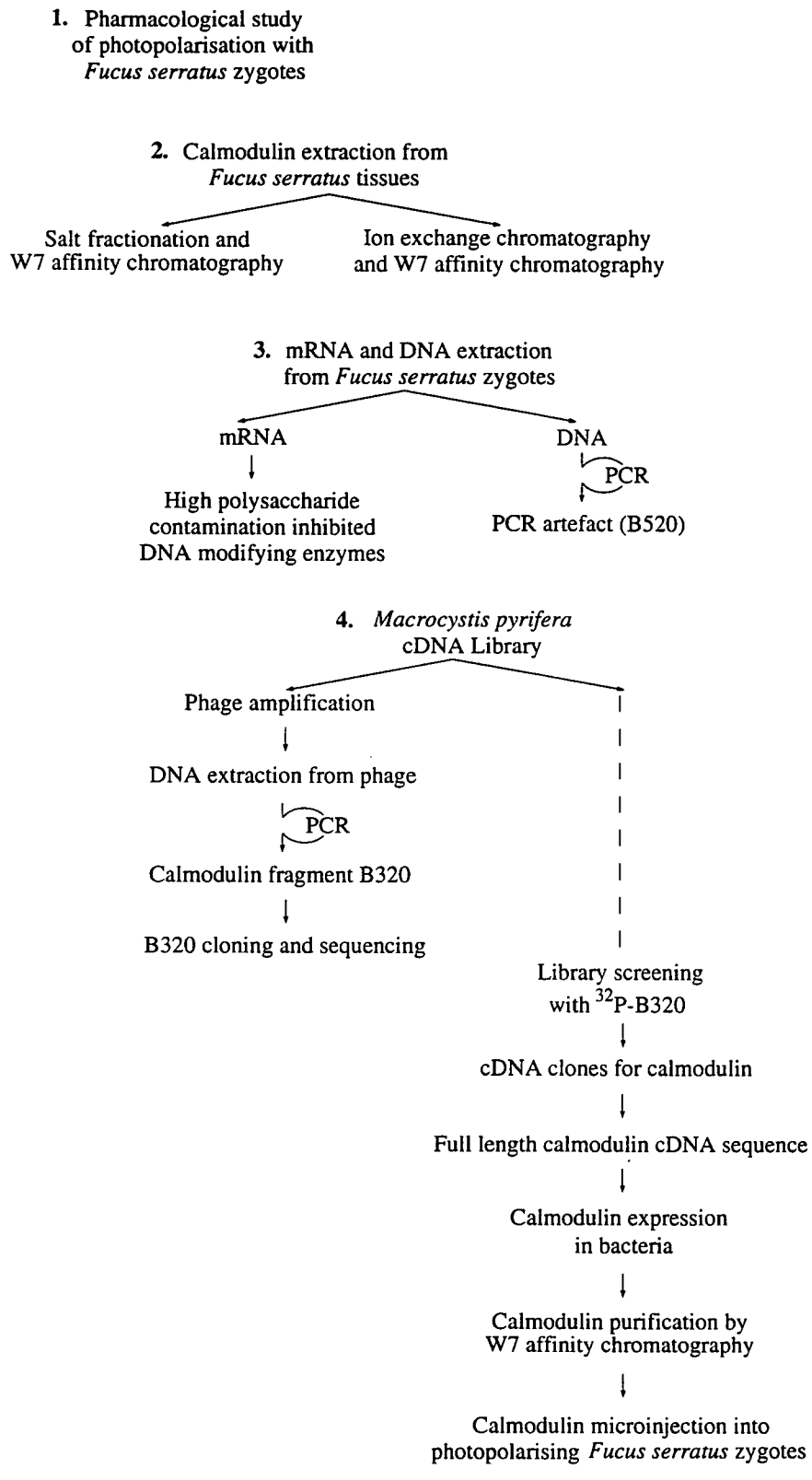

Figure 1-6-1. Flow diagram of the practical work performed during the study of the role of calmodulin in *Fucus serratus* photopolarisation.

Ohya and Botstein, 1994). To date, the only algal calmodulin sequenced, that of *C. reinhardtii*, is heterologous to higher plant calmodulins by possessing an extra 11 amino acids at the carboxyl terminus of the protein (Zimmer *et al.*, 1988) which affect certain *in vitro* activities (Poovaiah and Reddy, 1987). Furthermore, the evolutionary relationships between the Phaeophyceae, *C. reinhardtii* and the higher plants are uncertain, and gave no hint as to the possible structure of brown algal calmodulin. Consequently, further information regarding the structure of *F. serratus* calmodulin, was required.

Calmodulin was extracted from *F. serratus* eggs and sperm initially using gross purification by ammonium sulphate precipitation (Watterson *et al.*, 1980) or ion-exchange chromatography (Brawley and Roberts, 1989). Finer purification was performed by W7 affinity chromatography (Means *et al.*, 1991). Each method was assessed in terms of protein yield, purity and consistency (Figure 1-6-1_2).

Molecular biological techniques were employed to clone and sequence the calmodulin cDNA or gene from *F. serratus*, but were hampered by persistent molecular artefacts (Figure 1-6-1_3). Instead, the calmodulin cDNA was cloned from *M. pyrifera*, engineered into bacteria, and recombinant protein expression induced (Figure 1-6-1_4). Following purification, recombinant *M. pyrifera* calmodulin was microinjected into *F. serratus* eggs and photopolarising zygotes to disrupt any polarised calmodulin gradients (Figure 1-6-1_4). The basic assumption of this altered approach is that both algae are sufficiently related for high homology between their respective calmodulin sequences.

The respective roles of Ca^{2+} and calmodulin in photopolarisation are discussed with particular attention drawn to the responses of a zygote

population *vis á vis* those of a single cell. Calmodulin extraction and cloning from *F. serratus* are then discussed. The features of *M. pyrifera* calmodulin are examined at the nucleotide and amino acid levels and compared with those of other plant calmodulins. Finally, the effects of microinjecting recombinant *M. pyrifera* calmodulin into *F. serratus* zygotes are considered and a refined model for photopolarisation in *F. serratus* zygotes is proposed.

Chapter 2

Materials and methods

2. 1 Laboratory culture of *Fucus serratus* zygotes

2. 1. 1 General culture media

Artificial sea water (ASW): 450 mM NaCl, 30 mM $MgCl_2$, 16 mM $MgSO_4$, 10 mM KCl, 9 mM $CaCl_2$, 2 mM $NaHCO_3$, pH 8.0.

Ca2+ depleted artificial sea water (DASW): 450 mM NaCl, 30 mM $MgCl_2$, 16 mM $MgSO_4$, 10 mM KCl, 27 mM sucrose, 2 mM $NaHCO_3$, pH 8.0.

2. 1. 2 Gamete purification

Mature fronds of *F. serratus* were harvested at Barnsness, East Lothian, Scotland. Plants were segregated according to sex, and ripe receptacles cut from fronds. Receptacles were washed three times in distilled water at room temperature, blotted dry, and stored between paper towels, in the dark, at 4 °C. This treatment caused abundant gamete secretion from the conceptacles within 24 h.

To collect eggs, female receptacles were washed in ASW and floated in ASW, under fluorescent white light, for 4 h at 14 °C. Spent receptacles were removed and the eggs were separated from immature oogonia and algal debris by gentle filtration through a 100 µm nylon mesh. Eggs were allowed to decant and were rinsed three times in ASW.

Sperm were activated immediately prior to fertilisation by washing the orange secretions off two or three male receptacles with approximately 5 ml ASW, at 14 °C. Sperm activity was monitored under the microscope at

magnification x100. Numerous, fast swimming sperm were sought and if immature antheridia were present, or sperm were mostly inactive, a new suspension was prepared.

2. 1. 3 Fertilisation and zygote culture

Sperm were added to eggs and gametes mixed by gentle shaking. Gametes were sampled and their interaction observed at x100 magnification. Fertilisation was carried out under fluorescent white light at 14 °C and considered complete 20 min after gamete unification (Brawley, Wetherbee & Quatrano, 1976). Zygotes were sown in sparse lawns upon glass coverslips to which they adhered firmly within five hours of fertilisation. Cultures were grown in ASW, in darkness and at 14 °C. Zygote populations developed synchronously (Quatrano, 1978).

2. 2 Inhibition of photopolarisation

2. 2. 1 Inhibitors

Inhibitors used were ethylene glycol-bis (β-aminoethyl ether) N,N,N',N'-tetraacetic acid (EGTA), $LaCl_3$, (8-N,N-diethylamino) octyl-3,4,5-trimethoxybenzoate (TMB-8), nifedipine, verapamil, bepridil, N-(6-aminohexyl)-5-chloro-1-naphthalenesulfonamide (W7), trifluoperazine (TFP), calmidazolium, colchicine, cytochalasin-B, neomycin, and acridine orange, all purchased from Sigma Chemical Company, U.K.

5 M EGTA was dissolved in distilled water and the pH of the solution adjusted to 8.0. $LaCl_3$ and colchicine were dissolved in distilled water to 1 M stock solutions. The other inhibitors were dissolved in dimethylsulfoxide (DMSO), also to 1 M stocks. Stock solutions were diluted to working concentrations in DASW thereby enhancing physiological effects of the inhibitors, and cooled to 14 °C. The maximum

concentration of DMSO in working solutions (0.01%) was added to DASW controls, and had no adverse effects on zygotes. TMB-8 and nifedipine were also dissolved in ASW.

2. 2. 2 Experimental protocol

Zygote cultures were established as described previously. 9 h 30 min AF, under red light which had no effect on zygotes (Hurd, 1920), ASW was replaced by approximately 40 ml of inhibitor solutions. Zygotes were unilaterally illuminated with 325 $\mu mol \cdot m^{-2} \cdot s^{-1}$ white fluorescent light (Osran liteguard warm white, 15 W) between 10 and 13 h AF, the phase during which the polar axis is most sensitive to orientation by light (Whitaker and Lowrance, 1936 ; Feucht and Bentrup, 1972). At 13 h AF, illumination was again switched to red (Hurd, 1920). Inhibitor solutions were discarded and zygotes rinsed three times in ASW. Zygotes were cultured further, in ASW, in darkness, for approximately 36 h (Figure 2-2-1). As a control for the photosensitive period of the zygote population (Feucht and Bentrup, 1972), zygotes were also cultured in ASW, under permanent illumination, for approximately 36 h.

Cultures were examined under the dissecting microscope, at x30 magnification. The position of the base of the embryonic rhizoid from the centre of the thallus cell indicated the orientation of the polar axis in the zygote (Figure 2-2-1). Photopolarisation was determined by the cosine of the angle θ between the direction of rhizoid germination and the direction of the unilateral light pulse. All embryos in randomly selected fields of view were observed. To minimise group effects (Whitaker, 1931 ; Jaffe and Neuscheler, 1969), only zygotes more than 4 egg diameters from their neighbours were scored (Bentrup and Jaffe, 1968). Over 200 embryos per treatment were counted and each experiment was replicated 5 times. The

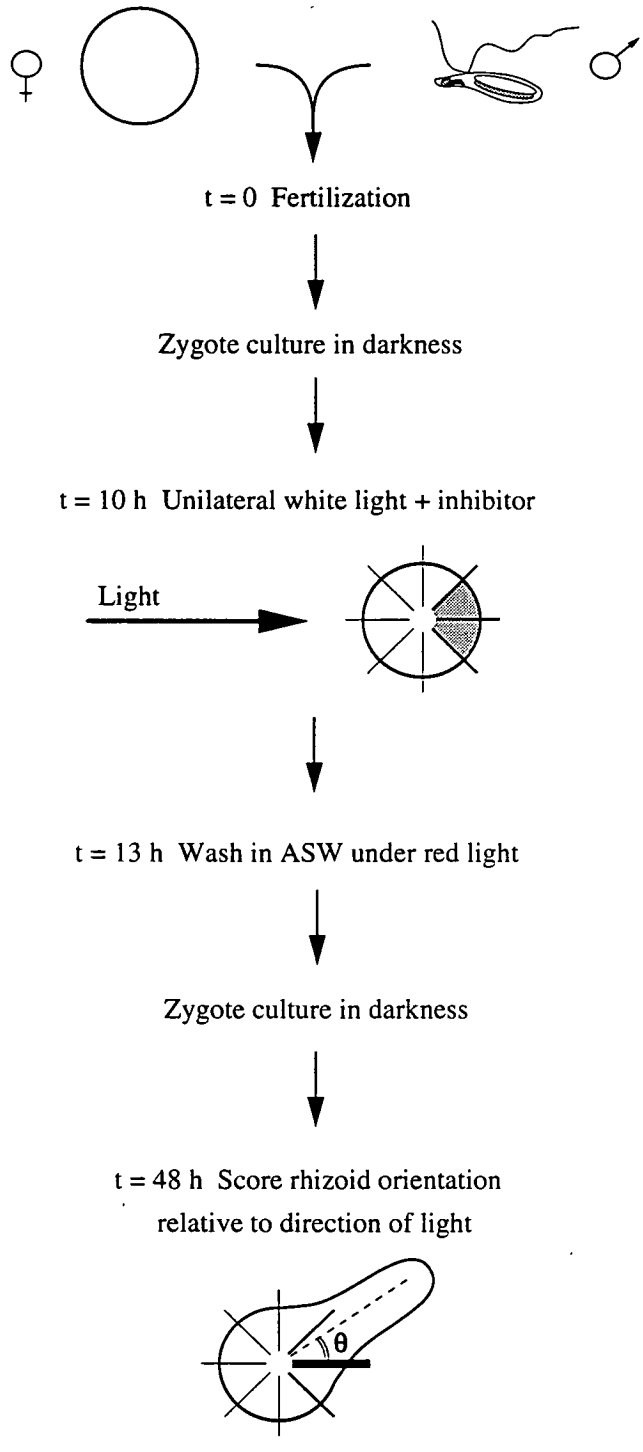

Figure 2-2-1. Inhibitor protocol.

The protocol used to test the action of various pharmacological inhibitors on photopolarisation of *F. serratus* zygotes is diagrammed. The shaded area of the zygote indicates the region of rhizoid germination corresponding to photopolarisation. The angle between incident light and rhizoid germination (θ) represents the orientation of the polar axis established in the zygote.

percentage of photopolarised zygotes was calculated by the equation;

$$P = \frac{\Sigma \cos\theta}{n} \times 100$$

Where "P" is the percentage of photopolarised zygotes (percent photopolarisation), "θ" is the angle between the vector of incident light and the direction of rhizoid germination, and "n" is the total number of zygotes scored. The calculated value reflects the degree by which the light vector and the average polarity within a zygote population are aligned: 100% photopolarisation indicates that all zygotes' axes are aligned with the light vector. 0% photopolarisation represents random axis orientation; on average, zygotes polarised by chance in the direction of applied light are balanced by those which polarise in the opposite direction. A decrease in the percentage of photopolarisation represents increased randomisation of zygotes' axes relative to the direction of polarising light.

2. 2 Calmodulin purification from *Fucus serratus* tissues

For all protein extractions, glassware, centrifuge tubes, pestles, mortars and spatulas were autoclaved for 20 min, at 121 °C, at 1 bar. Manipulations were carried out on ice and centrifugations were at 4 °C. Solutions were autoclaved prior to adding β-mercaptoethanol. Reagents were purchased from Fisons, U.K. or from Sigma Chemical Company, U.K.

2. 2. 1 Tissue preparation

Algae were collected and prepared as explained in Section **2. 1.** Eggs were purified (Section *2. 1. 2*), and centrifuged in a MSE Microcentaur, at 3,000 r.p.m., for 1 min, at 14 °C. The supernatant was discarded. Pelleted eggs were snap frozen in liquid nitrogen and stored at -80 °C. A concentrated suspension of sperm and antheridia was prepared by repeatedly

washing approximately 3 kg ripe, male fronds in 50 ml ice cold ASW. 250 ml of sperm were collected and filtered through 2 layers of muslin. The suspension was very dense due to polysaccharide secreted by receptacles. Sperm were concentrated by centrifugation in a Mistral 4L centrifuge using a swing out rotor, at 3,500 r.p.m., for 30 min, at 4 °C. Sperm were resuspended in 50 ml ice cold ASW, and dripped into liquid nitrogen. Frozen sperm "pearls" were collected and stored at -80 °C.

2. 2. 2 Calmodulin extraction by salt fractionation

10 g frozen sperm or 2 ml packed eggs were ground in liquid nitrogen and gradually added to 3 volumes ice cold Buffer E (50 mM Tris-HCl pH 7.5, 10 mM EGTA, 4 mM 3-[(3-cholamidopropyl)-dimethyl ammonio]-1-propane sulfonate (CHAPS), 1 mM β-mercaptoethanol ; 1% w/v polyvinylpyrrolidone (PVP-40)). After each addition, the lysate was vortexed briefly. The lysate was then homogenised in an ice cold glass-teflon homogeniser, and the volume of the homogenate determined. An equal volume of Buffer E was added to the homogenate, and stirred for 10 min at 4 °C.

0.351 g pulverised $(NH_4)_2 SO_4$ was added per ml homogenate over a 2 h period at 4 °C, gradually increasing $[(NH_4)_2 SO_4]$ of the homogenate to 55% w/v. The pH of the suspension was adjusted to 7.0, and stirring continued for 1 h. 55% $(NH_4)_2 SO_4$ at neutral pH caused isoelectric precipitation of a substantial amount of protein, but calmodulin remained in solution. The suspension was cleared by centrifugation in a Sorvall® RC-5B centrifuge, using a Sorvall® SS34 rotor, at 10,500 r.p.m., for 1 h, at 4 °C. The supernatant was acidified to pH 4.1 with 2.5 N $H_2 SO_4$ saturated to 55% $(NH_4)_2 SO_4$, and stirred at 4 °C for 2 h causing calmodulin precipitation. Following centrifugation in a Sorvall® RC-5B centrifuge,

using a Sorvall® SS34 rotor, at 10,500 r.p.m., for 1 h, at 4 °C, the calmodulin containing pellet was resuspended in 5 ml Buffer F (200 mM NaCl, 10 mM Tris-HCl pH 8.0, 1 mM $MgCl_2$, 1 mM $CaCl_2$, 1 mM β-mercaptoethanol). $(NH_4)_2 SO_4$ was removed by overnight dialysis against 2 l Buffer F at 4 °C to re-dissolve calmodulin (Englard and Seifter, 1990).

The dialysate was clarified by centrifugation in a MSE Microcentaur, at 13,500 r.p.m., for 30 min, at 4 °C. The supernatant was heated to 100 °C for 2 min and chilled on ice. Calmodulin is stable for 3 min at 100 °C, but other proteins were denatured and precipitated. The resulting suspension was clarified as before and the supernatant retained.

2. 2. 3 Calmodulin extraction by ion-exchange chromatography

5 g frozen, concentrated sperm were ground under liquid nitrogen and the powder gradually added to 5 ml ice cold lysis buffer (50 mM sodium 3-[N-morpholino] propane sulphonic acid (MOPS) pH 7.4, 2 mM ethylene diaminetetraacetic acid (EDTA), 50 mM sodium ascorbate, 1 mM dithiothreitol (DTT), 4 mM CHAPS, 1% w/v polyvinylpolypyrrolidone (PVPP) (Brawley and Roberts, 1989). The lysate was vortexed for 3 min and centrifuged in a Sorvall® RC-5B centrifuge, using a Sorvall® SS34 rotor at 10,000 r.p.m., for 10 min, at 4 °C. The supernatant was retrieved and diluted in 3 volumes exchange buffer A (25 mM MOPS, pH 7.4, 1 mM β–mercaptoethanol, 1 mM EDTA).

A sterile chromatographic column (Pharmacia) was packed with 20 ml DE52 diethylaminoethyl cellulose (Whatman®) suspended in exchange buffer A (Gopalakrishna and Anderson, 1982 ; Brawley and Roberts, 1989 ; Wilson and Goulding, 1988). The column was equilibrated overnight with buffer A, at 4 °C. Chromatography was carried out at 4 °C. The sperm extract was loaded onto the ion-exchange column and unbound, positive and

neutral proteins were eluted in 1 ml fractions until the spectrophotometric absorbance at 280 nm (Abs_{280}) was under 0.05 (Philips PU 8625 UV/VIS spectrophotometer). Two negative protein fractions, NP1 and NP2, were then eluted from the column. NP1 was eluted with 10 ml exchange buffer B (200 mM NaCl, 25 mM MOPS pH 7.4, 1 mM β–mercaptoethanol, 1 mM EDTA). NP2 was then eluted with 10 ml exchange buffer C (300 mM NaCl, 25 mM MOPS pH 7.4, 1 mM β-mercaptoethanol, 1 mM EDTA).

2. 2. 4 Calmodulin purification by W7 affinity chromatography

1 ml W7-agarose (Sigma) was aliquoted into a sterile chromatography column (5 mm internal diameter) at 4 °C (Wilson and Goulding, 1988 ; Englard and Seifter, 1990). The column was washed with 100 column volumes Buffer F, allowed to drain until the meniscus was just above the affinity matrix, and clamped. Samples (final supernatant from salt fractionation (Section *2. 2. 2*), NP1 or NP2 (Section *2. 2. 3*)) were applied to the column, and incubated for 10 min. The Ca^{2+}-calmodulin complex bound tightly to the W7-agarose matrix. Unbound protein was flushed from the column in 20-drop fractions until $Abs_{280} < 0.005$. The column was clamped, 2 column volumes Buffer G (200 mM NaCl, 10 mM Tris-HCl pH 8.0, 10 mM EGTA, 1 mM β–mercaptoethanol) added, and the column allowed to equilibrate for 10 min. EGTA chelated all Ca^{2+} causing dissociation between calmodulin and the W7-agarose matrix. Calmodulin was eluted in 15-drop fractions (~150 µl) with Buffer G until $Abs_{280} < 0.005$. Fractions with high absorbance levels were pooled. Calmodulin was stabilised by adding $CaCl_2$ to 15 mM final concentration. Protein samples were assayed by sodium dodecylsulfate (SDS) polyacrylamide gel electrophoresis (PAGE) (Section **2. 3**).

2. 3 Gel electrophoresis of proteins

2. 3. 1 Gels, buffers and stains

Resolving gel: 12% v/v acrylamide, 0.32% v/v N,N-methylene bisacrylamide, 750 mM Tris-HCl pH 8.9, 0.1% w/v SDS, 0.1% w/v ammonium persulfate (AMPS), 0.04% v/v N,N,N',N'-tetramethylethylene-diamine (TEMED).

Stacking gel: 5% v/v acrylamide, 0.13% v/v N,N-methylenebisacrylamide, 125 mM Tris-HCl pH 6.9 ; 0.1% w/vSDS, 0.1% w/v AMPS, 0.1% v/v TEMED.

5x Running buffer: 250 mM Tris-HCl pH 8.3, 1 M glycine, 0.5% w/v SDS. Autoclaved and stored at room temperature.

2x Sample buffer: 125 mM Tris-HCl pH 6.8, 4% w/v SDS, 20% w/v glycerol, 10% v/v β-mercaptoethanol, 0.02% w/v bromophenol blue. Stored at -20 °C.

Coomassie blue stain: 0.025% w/v brilliant blue R, 40% v/v methanol, 7% v/v ethanoic acid.

Destain: 7% v/v ethanoic acid, 4% v/v methanol, 1% v/v glycerol.

Glycerol fixative: 7% v/v ethanoic acid, 4% v/v methanol, 1% v/v glycerol.

2. 3. 2 Sample preparation and electrophoresis

Samples were diluted with an equal volume 2x sample buffer and incubated at 100 °C for 3 min to denature proteins. Samples were chilled on ice, centrifuged in a MSE Microcentaur at 13,000 r.p.m. for 2 min and then loaded onto the polyacrylamide gel. Proteins were separated by electrophoresis under 1x running buffer, at 50 mA, until the dye front had

run the full length of the gel. Gels were stained with coomassie blue for 30 min, then de-stained twice for 30 min. Gels were photographed using a CCD camera (Cohu) linked to a video copy processor (Mitsubishi). Gels were then incubated, overnight, in glycerol fixative before being mounted on a paper base and dried, under vacuum, at 60 °C for 1 h (Model 583 gel dryer, Bio-Rad).

2. 4 Electrophoresis of nucleic acids and DNA purification from agarose gels

2. 4. 1 Buffers and solutions

50x TAE: 40 mM Trizma® base pH 8.0, 5.7% ethanoic acid, 50 mM EDTA. The solution was filtered, autoclaved, and stored at room temperature.

10x TBE: 0.89 M boric acid, 0.89 M Trizma® base, 25 mM EDTA. The solution was filtered, autoclaved, and stored at room temperature.

50x MOPS buffer: 1.0 M MOPS pH 7.0, 0.25 M sodium citrate (CH_3COONa), 0.05 M EDTA. The solution was sterilised by ultrafiltration through 0.8 µm/0.2 µm filters (Acrodisc® PF, Gelmann Sciences) and stored at 5 °C.

6x DNA loading buffer: 0.25% w/v bromophenol blue, 0.25% w/v xylene cyanol FF, 15% v/v Ficoll™ 400 (Pharmacia). The solution was stored at room temperature.

1x RNA loading buffer: 1x MOPS buffer, 50% v/v formamide, 6.6% v/v formaldehyde, 3% v/v Ficoll™ 400, 0.02% w/v bromophenol blue, 50 $\mu g \cdot ml^{-1}$ ethidium bromide (EtBr). The solution was stored at -20 °C.

High salt buffer: 1.5 M NaCl, 10 mM Tris-HCl pH 8.0, 1 mM EDTA. The solution was sterilised by ultrafiltration through 0.8 µm/0.2 µm Acrodisc® PF filters and stored at room temperature.

2. 4. 2 Agarose gel electrophoresis of DNA

Small DNA fragments (under 500 bp) were resolved using 3 % w/v agarose gels (Sambrook *et al.*, 1989). Larger fragments were resolved on 1 % w/v gels. The required percentage of agarose was dissolved in 1x TAE or 0.5x TBE. When solutions were hand-hot, 0.2 µg EtBr was added per ml gel and gels cast.

Samples were diluted in 6x DNA loading buffer and loaded onto the gel. 1 µg of 1 kb DNA ladder (GIBCO, BRL) were also loaded as standards. Gels were electrophoresed under 1x TAE, at 50 mA for 30-90 min. Nucleic acid, stained with EtBr, was visualised under U.V. light (λ = 312 nm). Gels were photographed either using a Polaroid instant camera and Polaroid Type 667 film, or with a CCD camera (Cohu) linked to a video copy processor (Mitsubishi).

2. 4. 3 Agarose gel electrophoresis of RNA

1.3% w/v agarose was dissolved in 0.8 final gel volume 1x MOPS buffer and left to cool. 6.6% final volume formaldehyde was added to the gel, and the final volume made up with DEPC-H_2O (Section *2. 5. 1)* prior to casting.

RNA samples were desiccated under vacuum and re-dissolved in 15 µl RNA loading buffer. Samples were incubated at 65 °C for 10 min to denature RNA, ice-chilled, and applied to gel. Gels were run under 1x MOPS buffer, at 50 mA for approximately 1 h. Nucleic acid was viewed as previously explained. Photographs were taken using a Polaroid instant camera and Polaroid Type 667 film.

2. 4. 4 DNA purification from TAE-agarose gels

DNA was electrophoresed in agarose-TAE gels and bands to be

excised were identified. Gels were cut above and below bands of interest and strips of NA 45 DEAE membrane (Schleicher and Schuell) inserted into the incisions. Gels were electrophoresed until bands had completely run into membranes. Membranes towards the positive pole of the electrophoresis system bound the fragments of interest. These membranes were collected, rinsed in 1x TAE, cut into small pieces, and incubated in 200 µl high salt buffer for 10 min, at 37 °C. Under these conditions DNA entered into solution. The solution was retrieved, fresh buffer added to the membranes and incubated as before. Both samples were pooled. DNA was precipitated by addition of an equal volume isopropanol and collected by centrifugation in a MSE Microcentaur at 13,000 r.p.m., for 15 min, at 4 °C. Following a wash in ice cold 70% ethanol, DNA was desiccated under vacuum, dissolved in 20 µl H_2O and stored at -20 °C. The total amount of DNA retrieved was estimated assuming total recovery.

2. 5 General purification techniques of molecular biology.

For all molecular biology solutions, plastic-ware, and utensils were autoclaved at 121 °C, for 20 min, at 1 bar, unless delivered sterile from the manufacturer. For RNA extractions, glassware, spatulas, pestles and mortars were autoclaved and baked for at least 8 h at 120 °C. General chemicals were from Sigma Chemical Company, U.K. Enzymes and special reagents for molecular biology were produced by a range of companies, which are named where relevant. Unless otherwise indicated, all manipulations were carried out on ice.

2. 5. 1 Solutions and buffers

Diethyl pyrocarbonate (DEPC) treated H_2O (DEPC-H_2O): 0.1% v/v DEPC was added to double distilled water. The emulsion was incubated overnight at room temperature and autoclaved.

TE: 10 mM Tris-HCl pH 8.0, 20 mM EDTA.

Chloroform: 24 : 1 v/v chloroform : isoamyl alcohol.

Tris buffered phenol: 0.1% hydroxyquinoline was dissolved in 1:1 v/v phenol : 0.5 M Tris-HCl pH 8.0. The organic phase was retrieved, mixed with an equal volume of 0.1 M Tris-HCl pH 8.0, and stirred for 1 h at 4 °C. This step was repeated until the pH of the phenol was over 7.8. The buffered phenol was retrieved and mixed with 0.1 volumes of 0.1 M Tris-HCl pH 8.0 containing 0.2% v/v β-mercaptoethanol. Solutions were stored at -80 °C.

Phenol: Equal volumes of Tris buffered phenol and of chloroform were mixed and the emulsion allowed to settle. The subnatant, organic phase was used during extractions. Phenol was stored at 5 °C.

2. 5. 2 Phenol extraction and chloroform extraction

Organic solvents enable separation of nucleic acids from contaminating proteins. An equal volume of phenol or chloroform was added to the nucleic acid sample and mixed (vortexed) using a Whirlmixer (Fisons). The phases of the emulsion were separated by centrifugation: Samples less than 1 ml in volume were centrifuged in a MSE Microcentaur (Fisons), at 13,000 r.p.m., for 2 min, at room temperature. Samples over 1 ml were either centrifuged in a Mistral 4L centrifuge using a swing out rotor, at 3,500 r.p.m., for 20 min, at 4 °C, or in a Sorvall® RC-5B centrifuge using a Sorvall® HB4 (swing out) rotor, at 13,000 r.p.m. for 5 min, at 4 °C. The aqueous phase which contained the nucleic acid, was retrieved.

Chloroform extractions are performed following phenol extractions to decontaminate the sample of any phenol (Sambrook *et al.*, 1989).

2. 5. 3 Ethanol precipitation

Under high salt conditions, nucleic acids precipitate from solution upon addition of ethanol. 0.1 volumes of 3M sodium acetate pH 5.0 (Na-Ac) and 2.5 volumes of ice cold 100% ethanol were added to a nucleic acid solution, and incubated at -80 °C for 30 min. The precipitate was collected by centrifugation, for ml volumes in a MSE Microcentaur at 13,000 r.p.m., for 30 min, at 4 °C, and for larger volumes in a Sorvall® RC-5B centrifuge using a Sorvall® SS34 rotor, at 13,000 r.p.m., for 30 min, at 4 °C. The supernatant was discarded and the pellet of precipitated nucleic acid retrieved. To wash away contaminating salts, 1-2 ml ice cold 70% ethanol was gently added to the pellet and incubated, on ice, for 5 min. The supernatant was discarded and the pellet desiccated under a vacuum of -1 bar (Gyro Vap, Howe).

2. 5. 4 Plasmid DNA purification from bacteria

For small scale purification of bacterial plasmid DNA ("miniprep"), 1.5 ml cell suspension from a 5 ml (overnight) culture (Section **2. 6**) was centrifuged at 13,000 r.p.m. for 5 min. The supernatant was discarded and cells suspended in 0.25 ml STET buffer (8% w/v sucrose, 5% v/v Triton X-100, 50 mM EDTA, 50 mM Tris-HCl pH 8.0). 20 µl of 10 mg·ml^{-1} lysozyme was added to the suspension, and vortexed briefly. The lysate was incubated at 100 °C for 40 s to denature proteins. RNA and chromosomal DNA was precipitated by addition of 0.27 ml 5 M LiCl and incubated on ice for 15 min. The suspension was cleared by centrifugation in a MSE Microcentaur at 13,000 r.p.m. for 15 min at 4 °C. Pellets were removed with sterile toothpicks. Plasmid DNA was ethanol precipitated and dissolved in 50 µl H_2O.

For DNA sequencing, high plasmid purity was required to minimise the generation of artefacts (Stephen *et al.*, 1990). Bacteria were harvested as before from 3 ml liquid culture. The supernatant was discarded. Cells were resuspended in 100 µl 25 mM Tris-HCl pH 8.0, 50 mM glucose, 10 mM EDTA and left at room temperature for 5 min. Cells were lysed by adding 200 µl freshly prepared alkaline-detergent solution (0.2 M NaOH, 1% w/v SDS). The lysate was mixed by inversion, and stored on ice for 5-10 min. 150 µl ice cold 5 M potassium acetate (K-Ac) pH 4.8 was added to the lysate, mixed by inversion and incubated on ice for 15-30 min. Following centrifugation at in a MSE Microcentaur at 13,000 r.p.m., for 5 min, at 4 °C, the supernatant was retained and extracted once with phenol and then with chloroform. Plasmid DNA was ethanol precipitated and dissolved in 50 µl H_2O. 1 µl 10 mg·ml^{-1} heat treated RNase A was added to the solution and incubated at 37 °C for 60 min. Following a further phenol and chloroform extraction, plasmid DNA was ethanol precipitated and dissolved in 50 µl H_2O.

Plasmid DNA was also purified using Wizard™ minipreps (Promega). Extractions were carried out on 3 ml bacterial cultures, following manufacturer's instructions. DNA produced by this method was uncontaminated. The volume of retrieved DNA solution was 50 µl with concentrations of 0.5-1 µg·µl^{-1}.

2. 5. 5 DNA insertion into a plasmid vector

DNA fragments were inserted into the appropriate restriction sites in the multiple cloning site (MCS) of the plasmid vector pBluescript SK- (Figure 2-5-1). Blunt ended fragments (Section *2. 11. 4*) were inserted at the *Sma* I site. Fragments with exposed terminal restriction sites were ligated at the corresponding position in the MCS. pBluescript SK- contains an

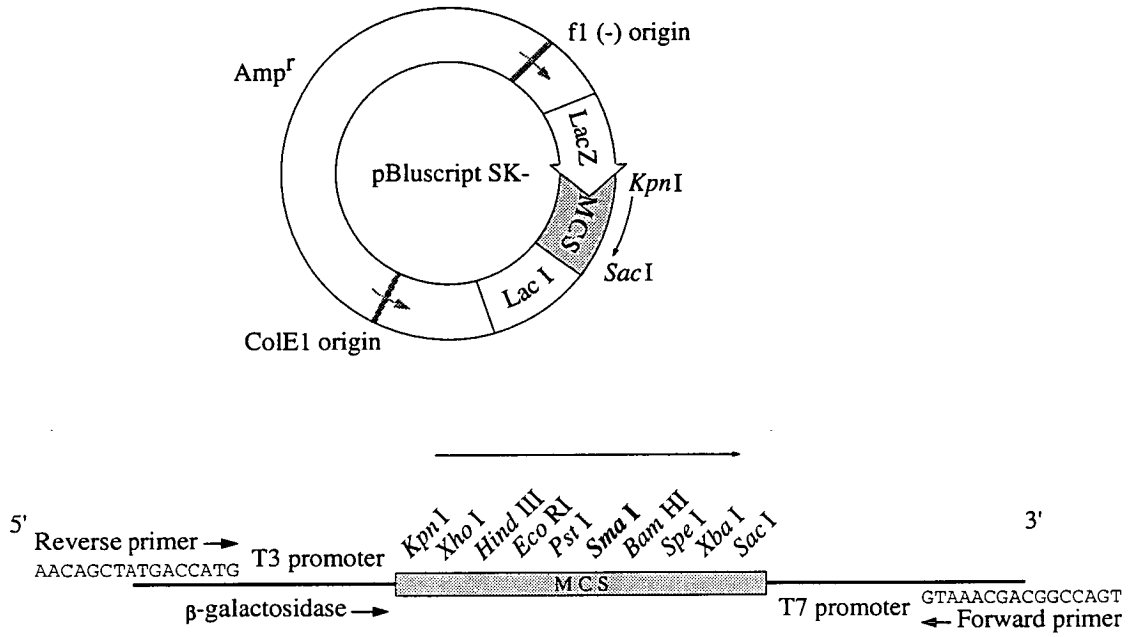

Figure 2-5-1. Diagram of the plasmid vector pBluescript SK-.

The plasmid measures 2958 bp. It possesses a f1 phage origin, a col E1 origin and T3 and T7 promoters flanking the MCS (shaded). The plasmid also contains a *lacZ* promoter for blue/white colour selection or fusion protein induction by IPTG.

The SK- designation indicates that the polylinker is oriented such that β-galactosidase transcription proceeds through the *Sac* I site first and the *Kpn* I site last. The polylinker is given in more detail under the plasmid map.

Reverse and forward primers used for sequencing cloned DNA fragments are shown and their nucleotide sequences given (nucleotide bases represented by their initials). Most commonly used restriction sites of the MCS are indicated. The *Sma* I site, which generates blunt ended cuts, and was used for cloning PCR fragments is in **bold type**.

ampicillin resistance gene, allowing resistance based selection of bacterial transformants.

20 µg pBluescript SK- was digested with the appropriate restriction endonuclease(s) to linearise the plasmid and expose restriction sites (Sambrook *et al.*, 1989). Endonucleases were removed by phenol extraction and DNA ethanol precipitated. Dissolution in 10 µl H_2O yielded a linear plasmid vector concentration of 2 $\mu g \cdot \mu l^{-1}$. DNA was stored at -20 °C. Insert and linearised plasmid vector were ligated using T4-DNA-ligase (Boehringer Mannheim Biochemica). Ligation was optimum at a 3 : 1 insert : vector molar ratio (Sambrook *et al.*, 1989). 200 ng linearised vector (15 nmol) was used per ligation reaction. Ligations (reaction L_1) were carried out in 10 µl volumes containing 1x ligation buffer (66 mM Tris-HCl pH 7.5, 5 mM $MgCl_2$, 1 mM dithioerythritol (DTE), 10 mM adenosine triphosphate (ATP)), 45 nmol DNA insert, 15 nmol linearised pBluescript SK- and 4 U T4-DNA-ligase (Boehringer Mannheim Biochemica). Control reactions were prepared either containing no insert (reaction L_2) or containing no insert nor T4-DNA-ligase (reaction L_3). Reactions were incubated for at least 12 h at 16 °C.

2. 5. 6 Plasmid digestion with restriction endonucleases

Plasmids were digested with restriction endonucleases which cut the DNA strand at unique restriction sites within the MCS. Plasmids can therefore be analysed for cloned inserts by selecting sites which flank the the insertion site(s) (Sambrook *et al.*, 1989). Reactions were prepared in 20 µl volumes containing 1x appropriate restriction buffer (BRL), 0.5-1 µg plasmid DNA, and 5-12 U appropriate restriction endonuclease. Following incubation at 37 °C for 1-2 h, the reaction products were analysed by TAE-agarose gel electrophoresis (Section *4. 2. 8*).

2. 6 Bacterial cell culture

2. 6. 1 Culture media

All media were autoclaved at 121 °C, for 20 min, at 1 bar.

Luria-Bertani (LB) agar: 1.5% w/v bacto agar, 1% w/v bacto tryptone, 0.5% w/v bacto yeast extract, 1% w/v NaCl, pH 7.0.

LB broth: 1% w/v bacto tryptone, 0.5% w/v bacto yeast extract, 1% w/v NaCl, pH 7.0.

Colour selection medium: LB-Agar, 238 $mg \cdot ml^{-1}$ isopropyl β-D-thiogalactoside (IPTG), 20 $mg \cdot ml^{-1}$ 5-bromo-4-chloro-3-indolyl-β-D-galactopyranoside (X-Gal), 10 $\mu g \cdot ml^{-1}$ tetracycline, 100 $\mu g \cdot ml^{-1}$ ampicillin. The medium is for *Escherichia coli*, strain XL-1 Blue transformed with pUC or pBluescript SK- and derivatives.

2. 6. 2 Bacterial culture on solid medium

Molten LB agar was poured into sterile petri dishes and allowed to set. Agar was enriched with the appropriate selection antibiotic (*e.g.* 100 $\mu g \cdot ml^{-1}$ ampicillin or 5 $\mu g \cdot ml^{-1}$ tetracycline). Using sterile microbiological practise, *E. coli* were plated onto the culture medium. Plates were incubated, overnight, at 37 °C. Bacterial colonies are the progeny of a single bacterium, and therefore represent a single genetic clone (Sambrook *et al.*, 1989).

2. 6. 3 Bacterial culture in liquid medium

A single bacterial colony was picked from solid culture and inoculated into LB broth containing the appropriate antibiotic. Cultures were incubated, with shaking, overnight, at 37 °C.

2. 7 Transformation of bacterial cells with plasmid DNA

2. 7. 1 Solutions and buffers

TSS medium: 1% w/v tryptone, 0.5% w/v yeast extract, 1% w/v NaCl, 20 mM MgSO4, 20 mM piperazine-N-N'-bis [2-ethanesulfonic acid] (PIPES) pH 6.6, 10% w/v polyethylene glycol (PEG 3350), 5% v/v DMSO (BDH SpectrosoL® grade flushed with N_2 and stored at -80 °C). DMSO was initially omitted and TSS autoclaved, then stored at 4 °C until required. DMSO was added to the medium immediately prior to use.

SOC medium: 2% Bacto tryptone, 0.5% Bacto yeast extract, 20 mM glucose, 10 mM NaCl, 10 mM $MgCl_2$, 10 mM $MgSO_4$, 2.5 mM KCl.

2. 7. 2 Transformation by DMSO

200 µl XL-1 Blue liquid culture was diluted 20 ml LB broth (1 : 100 dilution). Bacteria were incubated, with shaking, at 37 °C, until $0.3 < Abs_{600} < 0.4$ (Philips PU 8625 UV/VIS spectrophotometer). At this point, bacteria were in exponential growth phase. The culture was chilled in ice for 10 min and centrifuged in a Mistral 4L centrifuge using a swing out rotor, at 3,500 r.p.m., for 10 min, at 4 °C. The supernatant was discarded, tubes allowed to drain, and cells gently re-suspended in 2 ml (0.1 original volume) TSS. Re-suspended bacteria were kept on ice (Chung *et al.*, 1989).

For transformation, 0.1 ml TSS-cell suspension was aliquoted to 5 pre-chilled eppendorfs and kept on ice. 5 µl of each ligation reaction (approximately 100 ng vector DNA) was added to each aliquot:

Tube 1: Minus DNA control.

Tube 2: 20 ng plasmid vector (Positive transformation control)

Tube 3: 5 µl ligation reaction L_1 (Ligation)

Tube 4: 5 µl ligation reaction L_2 (Re-circularisation control)

Tube 5: 5 µl ligation reaction L_3 (Enzyme control)

Tubes were inverted 3 times and incubated on ice for 30 min. 0.9 ml LB broth enriched to 10 mM glucose was added to each transformation, mixed by inversion, and incubated at 37 °C for 90 min to allow expression of plasmid-borne genes. 0.1 ml transformed bacteria were then plated on appropriate solid culture media and incubated overnight at 37 °C (Sambrook *et al.*, 1989).

2. 7. 3 Transformation by electroporation

Bacterial transformation by electroporation was 10-100 fold more efficient that the DMSO method (Chung *et al.*, 1989) presented previously. A single *E. coli* colony was cultured in 5 ml LB broth with the appropriate antibiotic. 500 µl of this culture was diluted in 50 ml LB broth (100 fold dilution) and incubated on a shaker, at 37 °C, until $0.5 < Abs_{600} < 0.7$ (Philips PU 8625 UV/VIS spectrophotometer). Cells were chilled on ice and centrifuged in a Mistral 4L centrifuge, using a swing out rotor, at 3,500 r.p.m., for 20 min, at 4 °C. The supernatant was discarded and pelleted cells drained. To eliminate salts from the culture medium which would decrease the electrical resistance of the bacterial suspension and impede electroporation, cells were re-suspended in 50 ml ice cold H_2O, centrifuged as before, and the pellets drained. Bacteria were sequentially pelleted and re-suspended, again, in 50 ml H_2O, then, in 25 ml H_2O, in 5 ml 10% glycerol, and, finally, in 0.1 ml 10% glycerol. All solutions were ice

cold. Cells were aliquoted in 40 µl volumes and either stored on ice for immediate use, or frozen in liquid nitrogen and stored at -80°C. Frozen aliquots were thawed on ice immediately prior to use.

2 µl of each ligation reaction (Section *2. 5. 5* and Section *2. 7. 2*) or approximately 1 ng purified plasmid DNA was added to a 40 µl aliquot of bacterial cells prepared for electroporation. Cells and DNA were transferred to an ice chilled electroporation cuvette (Bio-Rad gene pulser®/*E. coli* pulser™ cuvette). The cuvette was placed between the electrodes of a Bio-Rad pulse controller, linked to a Bio-Rad gene pulser™. The apparatus was optimised for *E. coli* electroporation following manufacturer's instructions with resistance set at 200 Ω and capacitance at 25 µF. A single, square electric pulse of 2.5 kV was administered to bacteria for 3-5 ms. 1 ml SOC medium was immediately added to electroporated cells. Bacteria were then incubated at 37 °C for 2 h to allow expression of plasmid borne genes. 0.1 ml cell suspension was spread onto the appropriate solid culture medium (Section *2. 6. 2*) and incubated, overnight, at 37 °C. Bacterial growth was analysed as explained in Section *2. 7. 3*.

2. 7. 4 Colour selection of transformant bacteria

Bacteria which absorbed the plasmid acquired ampicillin resistance. pBluescript allowed for blue/white transformant selection when plated on IPTG-XGal rich medium (Section *2. 6. 1*). Bacteria in which the plasmid contains an insert in the MCS produce white colonies whereas those in which the plasmid does not contain a cloned insert generally produce blue colonies (Sambrook *et al.*, 1989). Transformation efficiency and the degree of plasmid re-circularisation was assessed by analysing bacterial growth on each plate, notably the controls (from Tubes 1, 2, 4 and 5). White transformant colonies (from Tube 3) were selected and cultured, overnight,

in 5 ml liquid cultures with 10 $\mu g \cdot ml^{-1}$ tetracycline and 100 $\mu g \cdot ml^{-1}$ ampicillin.

2. 8 Double stranded DNA sequencing

DNA fragments cloned into the MCS of pBluescript SK- were sequenced using the T7 Sequencing™ Kit (Pharmacia). Each DNA template was sequenced in both sense and antisense directions using the Forward and Reverse priming sites of pBluescript SK- (Figure 2-5-1). The method yields ^{35}S-labelled, dideoxy base terminated DNA fragments which are separated by electrophoresis in a 5% polyacrylamide-TBE denaturing gel containing 7 M urea. Radioactive isotopes were manipulated and disposed of according to the directives of the Radiation Protection Committee of the University of Edinburgh.

2. 8. 1 Sequencing reaction 1: Primer annealing

DNA was purified for sequencing as explained in Section *2. 5. 4.* For each sequencing reaction, 2 µg template DNA was dehydrated under vacuum, and dissolved in 9 µl H_2O. To denature DNA and also hydrolyse any RNA present in the solution, 1 µl 2 M NaOH was added to the DNA and incubated for 15 min at 37 °C. 1 µl 10 µM stock Forward or Reverse primer was added to each reaction. Solutions were vortexed and the pH neutralised with 3 µl 5 M K-Ac, causing primers to anneal to their sites in pBluescript SK-. DNA was ethanol precipitated. The pellet was invisible, so great care was taken while it was washed with ice cold 70% ethanol and dried under vacuum. Annealed template and primer were then dissolved in 12 µl H_2O, and 2 µl annealing buffer (Pharmacia) added. Solutions were kept on ice.

2. 8. 2 Sequencing reaction 2: Labelling and extension reactions

Sequencing reactions were performed following manufacturer's instructions in the T7 Sequencing™ Kit. The method is based on two-stage extension of the primers by T7 DNA polymerase. First, a single labelling reaction in presence of all four deoxynucleotide bases, one of them radiolabelled (^{35}S-dATP) was carried out. Second, four separate extension and termination reactions, each with one quarter of the labelling reaction and including a single dideoxynucleotide, were carried out. The addition of a dideoxynucleotide to the end of DNA polymer caused extension to terminate. Incorporation into the DNA strand was random for each dideoxynucleotide, hence all fragments between approximately 50-500 bp were represented.

2. 8. 3 Denaturing polyacrylamide gel electrophoresis

Chain-terminated reaction products were separated by electrophoresis in 5% polyacrylamide denaturing gels (5% acrylamide, 0.3% N,N-methylenebisacrylamide, 7 M urea, 1x TBE, 0.04% w/v AMPS, 0.2% v/v TEMED). The sequencing gel apparatus (Sequi-Gen® nucleic acid sequencing cell, Bio-Rad) was mounted and sequencing gels poured according to manufacturer's instructions. Gels were 0.4 mm thick. Gels were run in 1x TBE (Section *2. 4. 1*) and heated to 50 °C prior to sample loading. Samples were incubated at 80 °C for 3 min to denature DNA and loaded onto sequencing gels in the order G-A-T-C (nucleotide bases represented by their initials). Samples were electrophoresed at an appropriate current and tension to maintain gels at a temperature of 50 °C. Generally 48 well gels were run at 80-90 W and 24 well gels at 45-60 W. Electrophoresis was halted when the xylene cyanol dye front (light blue) had migrated 40 cm from the wells.

Gels were fixed in 2.5 l 10% v/v ethanoic acid, 10% v/v methanol for 30-45 min. Gels were drained for 2 min, blotted dry and transferred to Whatman® 3MM paper. Mounted gels were dried under vacuum (Model 583 Gel Dryer, Bio-Rad) at 80 °C for 1 h and allowed to cool. Gels were then autoradiographed using Cronex blue base X-ray film (Dupont).

2. 9 DNA transfer to membranes

2. 9. 1 Buffers and solutions

20x SSC: 3 M NaCl, 0.3 M sodium citrate.

Denaturing buffer: 1.5 M NaCl, 0.5 M NaOH.

Neutralisation buffer: 1.5 M NaCl, 0.5 M Tris-HCl pH 7.2, 1 mM EDTA.

Wash buffer: 0.2 M Tris-HCl pH 7.5, 2x SSC.

Denhardt's solution: 2% w/v bovine serum albumin (BSA), 2% w/v Ficoll™ 400, 2% w/v PVP-40.

Dextran sulfate: 50% w/v Dextran sulfate stock solution.

Hybridisation buffer: 4x SSC, 1% w/v SDS, 2x Denhardt's solution, 10% w/v Dextran sulphate, 20 mM Tris-HCl pH 7.6.

2. 9. 2 Southern blotting

DNA was transferred from an agarose gel to Hybond-N nylon membrane (Amersham) by Southern blotting (Southern, 1975). Transfer was at room temperature. The gel was bathed for 10 min in 250 ml 0.25 M HCl to nick DNA strands by brief depurination, thereby enhancing DNA transfer to the membrane. Following 3 rinses in H_2O, the gel was immersed in 250 ml denaturation buffer for 30 min with shaking. The gel was rinsed again in H_2O and incubated in neutralisation buffer for 15 min with shaking. This step was repeated twice.

The Hybond-N membrane was cut to the dimensions of the gel (110 mm x 140 mm) and orienting marks made. The membrane was then saturated with 20x SSC. Approximately 20 sheets of Whatman® 3MM paper were cut to the dimensions of the gel, carefully layered, and saturated with 20x SSC. The gel was laid, face down, on top of the paper, and the membrane placed over the gel accordingly. A further 20 sheets of Whatman® 3MM Paper, cut to the dimensions of the gel and saturated with 20x SSC, were layered over the membrane. Care was taken to ensure that no air bubbles, which would interfere with DNA transfer, were allowed between layers. 20 sheets of dry blotting paper cut to the dimensions of the gel, then 40-50 dry paper towels (Pullman, Scott), folded to the dimensions of the gel were placed on the Whatman® 3MM Paper. Finally, a glass plate and a 750 g-1 kg weight crowned the set-up. Towels were changed after 1 h. The blot was left overnight. Capillary action drew liquid from wet to dry paper, across both gel and membrane. DNA was carried from the gel to the membrane to which it bound. The membrane was washed in 2x SSC for 10 min and left to dry on blotting paper. DNA was fixed to the membrane matrix by irradiation with 0.4 $J \cdot cm^{-2}$ U.V. light (λ=312 nm).

2. 9. 3 Plaque blotting (cDNA library analysis)

cDNA library phage cultures were incubated at 4 °C for at least 2 h to ensure maximum adhesion between top and bottom agars (Section *2. 12. 6*). Plaques were blotted onto Hybond-N transfer membranes (Amersham). Filters were cut to the appropriate size, labelled in pencil, carefully laid on the top agar surface and left in place for 2 min. Three orientation marks were made through the filters, into the agar, using a syringe needle dipped in indian ink. Filters were then carefully removed and dipped, sequentially, in 500 ml denaturing buffer for 2 min, 500 ml neutralising buffer for 5 min,

500 ml wash buffer for 30 s, then allowed to dry on blotting paper. DNA was crosslinked to filters by irradiation with 0.4 $J \cdot cm^{-2}$ U.V. light (λ=312 nm). Duplicate filters were blotted for each library plate.

2. 9. 4 Radioactive probe synthesis

Radioactive isotopes were manipulated and disposed of following the advice of the Radiation Protection Committee of the University of Edinburgh.

DNA probes were radiolabelled with ^{32}P following the method by Feinberg and Vogelstein (1982 and 1983). DNA was denatured for 3 min at 100 °C and kept at 37 °C until added to the reaction. The labelling reaction was performed in a 50 µl volume by the addition of the following reagents in the stated order: H_2O, 10 µl oligo-labelling buffer (50 mM Tris-HCl pH 7.5, 10 mM $MgCl_2$, 1 mM DTT), 2 µl of 10 $mg \cdot ml^{-1}$ BSA, 50 ng DNA, 50 µCi ^{32}P-dCTP, 2 U DNA polymerase I (Klenow fragment). The reaction was incubated overnight at room temperature. Radiolabelled DNA was purified from unincorporated radio-nucleotides by gel filtration through a 1 ml Sephadex G25 (Pharmacia) spin column (Sambrook *et al.*, 1988).

2. 9. 5 Probe hybridisation

The probe hybridisation protocol is essentially identical for Southern and plaque blots. Blotted membranes were placed between 220 mm x 220 mm nylon mesh (100 µm pore size), wetted with 5 ml hybridisation buffer, rolled and placed in a Hybaid HB-OV-BL hybridisation cylinder. Cylinders were placed in a rotating hybridisation oven (Hybaid). To avoid non-specific binding of the probe to the blots, membranes were pre-hybridised against 25 ml hybridisation buffer for at least 30 min at 65 °C. The radiolabelled DNA probe was denatured for 5 min at 100 °C, ice-chilled, and added to 10 ml hybridisation buffer. The

buffer from the pre-hybridisation was drained, and replaced with the probe-buffer mix. The probe was hybridised to the blots overnight at 65 °C.

Following hybridisation, the spent probe was collected and stored. Filters were washed by incubating, twice, with 50 ml 2x SSC at 65 °C for 15 min, then with 50 ml 2x SSC, 0.1% w/v SDS at 65 °C for 30 min, and finally with 0.1x SSC at 65 °C for 10 min (high stringency wash). Membranes were sealed, wet, between plastic sheets (Saran, Dow), and autoradiographed (Cronex® blue base X-ray film) at -80 °C.

2. 10 Nucleic acid extraction from *Fucus serratus* tissues

Eggs or 24 h zygotes were purified as explained previously (Section *2. 1. 2*). Following each extraction, the spectrophotometric absorbance of the nucleic acid sample was analysed from 220-320 nm using a Beckman DU-64 spectrophotometer. Control scans within the same wavelengths were also performed on algal polysaccharides.

2. 10. 1 RNA extraction by isopycnic separation

3 ml packed eggs were finely ground in liquid nitrogen and the powder gradually added to 10 ml ice cold lysis buffer (4 M guanidine thiocyanate, 25 mM sodium citrate pH 7.0, 0.5% w/v SDS, 0.1 M β–mercaptoethanol). After each addition, the mixture was vortexed to avoid freezing the buffer. Once all the material had been added, the lysate was vortexed for 2 min (Okayama *et al.*, 1987). 7 ml Tris buffered phenol and 2 ml chloroform were added and vortexed for 30 s. The phases of the resulting emulsion were separated by centrifugation in a Mistral 4L centrifuge using a swing-out rotor, at 4,000 r.p.m., for 20 min, at 4 °C. The aqueous solution was collected and phenol extracted.

CsCl was dissolved in the aqueous phase to a concentration of

0.5 g·ml^{-1}. The solution was carefully overlaid onto 4 ml 5.7 M sucrose, avoiding mixing between the two solutions and centrifuged in a Sorvall® OTD50B ultracentrifuge, under vacuum, with a Sorvall® AH629 rotor, at 27,000 r.p.m., for 96 h, at 20 °C. Proteins, polysaccharides, DNA and other cell contaminants accumulated at the interface between the CsCl solution and the high-density sucrose cushion. The RNA pelleted to the bottom of the tube. The CsCl solution, the interface, and a third of the sucrose cushion were removed by aspiration, and the remaining solution discarded. Tubes were then cut approximately 1 cm from the bottom. The pellet was dissolved in 100 µl DEPC-H_2O and collected for analysis. Following ethanol precipitation, RNA was dissolved in 10 µl DEPC-H_2O, frozen in liquid nitrogen, and conserved at -80 °C.

2. 10. 2 RNA extraction by repeated phenol extractions

1 ml packed eggs or 24 h zygotes were ground in liquid nitrogen, gradually homogenised in 2 ml extraction buffer (150 mM LiCl, 100 mM Tris-HCl pH 9.0, 5 mM EDTA, 1% w/v SDS, 1000 U RNasin (RNase inhibitor (Promega)) and vortexed for 2 min (Masters *et al.*, 1992). The homogenate was phenol extracted and the aqueous phase collected and stored at -20 °C. The organic phase was then back extracted with an equal volume of extraction buffer, the phases of the emulsion separated as for phenol extraction, and the second aqueous layer retrieved and pooled with the first.

The pooled sample was subsequently phenol extracted four times, until no solid interface was present between organic and aqueous phases. 2 volumes 3 M LiCl were added to the final aqueous phase and RNA precipitated by overnight incubation at -20 °C. RNA was collected by centrifugation in a Sorvall® RC-5B centrifuge, using a Sorvall® HB4 rotor,

at 13,000 r.p.m., for 30 min, at 4 °C. The supernatant was discarded and the white, translucent pellet dissolved in 200 µl extraction buffer. The solution was incubated at 65 °C for 5 min with vortexing at 1 min intervals and ice-chilled. Undissolved material was removed by centrifugation in a Sorvall® RC-5B centrifuge, using a Sorvall® HB4 rotor, at 6,000 r.p.m., for 4 min, at 4 °C. RNA was ethanol precipitated from the supernatant, dissolved in 20 µl DEPC-H_2O, frozen in liquid nitrogen and stored at -80 °C.

2. 10. 3 Guanidinium extraction of RNA and NaCl-ethanol wash

1 ml packed eggs or 24 hour zygotes were ground in liquid nitrogen and gradually added to 3 ml extraction buffer containing 4 M guanidine thiocyanate, 150 mM LiCl, 100 mM Tris-HCl pH 9.0, 5 mM EDTA, 1% v/v Triton X-100. The lysate was vortexed after each addition, and finally for 2 min (Chomczynski and Sacchi, 1987).

The lysate was phenol extracted twice and RNA ethanol precipitated from the resulting supernatant. The pellet, large and with a gelatinous aspect, was dissolved in 5 ml TE. [NaCl] of the solution was taken to 2 M, and 2 volumes of 100% ethanol were added to precipitate nucleic acid, whilst leaving most contaminating polysaccharide in solution (Fang *et al.*, 1992). Precipitated RNA was pelleted as following ethanol precipitation and dissolved in 1 ml DEPC-H_2O. RNA was precipitated from the solution by adding 2 volumes 3 M LiCl and incubating the mixture overnight at 4 °C. The precipitate was pelleted by centrifugation in a Sorvall® RC-5B centrifuge, using a Sorvall® HB4 rotor, at 13,000 r.p.m., for 30 min, at 4 °C. The pellet, a thin, almost transparent layer was dissolved in 200 µl DEPC-H_2O. Following a further ethanol precipitation, RNA was dissolved in 20 or 100 µl DEPC-H_2O, frozen in liquid nitrogen and stored at -80 °C.

2. 10. 4 RNA extraction with acid phenol

1 ml packed zygotes were ground in liquid nitrogen and gradually homogenised in 2 ml extraction buffer (4 M guanidine thiocyanate, 25 mM sodium citrate pH 7.0, 10 mM EDTA, 0.5% w/v SDS). The lysate was vortexed for 2 min, acidified by adding 400 µl 2 M Na-Ac, pH 4 (Logemann, *et al.,* 1987), vortexed briefly, and then phenol extracted. The acid pH drove DNA and proteins into the organic phase and the solid interface. RNA was ethanol precipitated from the resulting aqueous phase, dried briefly under vacuum, and dissolved in 5 ml TE. The solution was adjusted to 2 M NaCl, and 2 volumes 100% ethanol added in order to precipitate nucleic acid, while leaving most contaminating polysaccharide in solution (Fang *et al.,* 1992). RNA was pelleted as before, dried briefly, and dissolved in 1 ml DEPC-H_2O. RNA was precipitated from the solution by addition of 2 volumes 3 M LiCl and incubated overnight, at 4 °C. Following centrifugation in a Sorvall® RC-5B centrifuge, using a Sorvall® HB4 rotor, at 13,000 r.p.m., for 30 min, at 4 °C, the RNA pellet was dissolved in 200 µl DEPC-H_2O. Finally, the RNA was ethanol precipitated, dissolved in 20 µl DEPC-H_2O, frozen in liquid nitrogen and stored at -80 °C.

2. 10. 5 RNA extraction, polyphenol, quinone and polysaccharide cleansing

2 ml packed eggs and 2 g fresh frond apices were ground in liquid nitrogen. Each powder was homogenised for 2 min in 6 ml ice cold extraction buffer (150 mM Tris-borate pH 7.5, 50 mM EDTA, 2% SDS, 1% β-mercaptoethanol). The lysate was vortexed with 0.25 buffer volume 100% ethanol for 1 min, and then with 0.11 buffer volume 5 M K-Ac for 1 min (Su and Gibor, 1988). The homogenate was extracted with chloroform, then with phenol and again with chloroform.

β–mercaptoethanol was added to the resulting aqueous phase to 1% final concentration. 0.33 final volume 3 M LiCl was then added to the sample, vortexed, and incubated at -20 °C overnight to precipitate RNA. Precipitated material was pelleted by centrifugation in a Sorvall® RC-5B centrifuge, using a Sorvall® HB4 rotor, at 10,000 r.p.m., for 90 min, at 4 °C. The supernatant was discarded and the pellet re-suspended in 0.02 original volume 0.5x extraction buffer. 0.25 buffer volume ice cold 100% ethanol was added to the solution and vortexed for 1 min. 0.11 buffer volume 5 M K-Ac was added and the solution vortexed for 1 min. The solution was extracted with chloroform, then three times with phenol, and finally, once again with chloroform.

Mixing gently, 1% w/v solid $NaBH_4$ was added to the resulting aqueous phase, reducing oxidised compounds such as quinones. Once bubbles (H_2) had dissipated, 2 volumes DEPC-H_2O, 1 volume 12 M LiCl and 1% v/v β-mercaptoethanol were added to the solution and incubated overnight, at -20 °C to precipitate RNA. RNA was pelleted by centrifugation in a Sorvall® RC-5B centrifuge, using a Sorvall® HB4 rotor, at 10,000 r.p.m., for 90 min, at 4 °C. The pellet was dissolved in the same volume of DEPC-H_2O as for the last LiCl precipitation. An equal volume 1 M $CaCl_2$ was added to the solution, vortexed, and incubated on ice for 30 min. This caused RNA precipitation while leaving neutral compounds (*e.g.* polyphenols) in solution. Precipitated RNA was collected as before and dissolved in 1 ml TE. 250 µl 5 M NaCl was added to the RNA solution, which was then extracted, twice, with phenol. Finally, RNA was ethanol precipitated from the recovered aqueous solution, dissolved in 20 µl DEPC-H_2O, frozen in liquid nitrogen and stored at -80 °C.

2. 10. 6 CTAB extraction of RNA

1 ml packed cells was ground in liquid nitrogen to a fine powder and gradually added to 10 ml lysis buffer containing 1.5 M NaCl, 2% w/v hexadecyltrimethylammonium bromide (CTAB), 10 mM EDTA, 10 mM DTT, 1 mM Tris-HCl pH 7.5. The lysate was vortexed for 10 min at room temperature, during which time the colour changed from brown to olive green. The homogenate was chloroform extracted and vortexed for 2 min. The resulting emulsion was centrifuged in a Sorvall® RC-5B centrifuge, using a Sorvall® HB4 rotor, at 10,000 r.p.m., for 20 min, at room temperature. A very solid, light green interface separated the organic and aqueous phases (Apt, *pers. comm.* 1993).

0.25 volumes 100% ethanol were slowly added to the recovered aqueous phase with gentle, constant swirling. This step caused some degree of polysaccharide precipitation, resulting in a translucent suspension. Ethanol was removed from the aqueous solution by chloroform extraction. A pure white pad of polysaccharide was present at the interface between the organic and aqueous phases. RNA was precipitated from the aqueous solution by addition of 0.25 volume 12 M LiCl and overnight incubation at -20 °C. RNA was pelleted by centrifugation in a Sorvall® RC-5B centrifuge, using a Sorvall® HB4 rotor at 10,000 r.p.m., for 45 min, at 4 °C. The pellet was dissolved in 1 ml TE and the solution extracted with phenol, then with chloroform. RNA was ethanol precipitated from the resulting supernatant and dissolved in 100 µl DEPC-H_2O. RNA was frozen in liquid nitrogen and stored at -80 °C.

2. 10. 7 RNA extraction from sperm

20 g concentrated sperm suspension (Section *2. 2. 1*) were ground under liquid nitrogen and homogenised in 40 ml 4 M guanidine thiocyanate, 25 mM sodium citrate pH 7, 10 mM EDTA, 0.5% w/v SDS using a glass-teflon homogeniser (Chomczynski and Sacchi, 1987). The homogenate was then divided equally between 6, 30 ml baked corex tubes and acidified with 0.2 volumes 2 M Na-Ac pH 4.0 (Logemann *et al.*, 1987). Each acidified lysate was phenol extracted and the aqueous layers pooled. Nucleic acid was ethanol precipitated from the pooled sample and dissolved in 2 ml DEPC-H_2O. The solution was adjusted to 3 M LiCl and incubated overnight at -20 °C to precipitate RNA. Following centrifugation in a Sorvall® RC-5B centrifuge, using a Sorvall® HB4 rotor, at 10,000 r.p.m., for 30 min, at 4 °C, the pellet was dried briefly and dissolved in 100 µl DEPC-H_2O. RNA was again ethanol precipitated, dissolved in 40 µl DEPC-H_2O, frozen in liquid nitrogen and stored at -80 °C.

2. 10. 8 DNA extraction from sperm

10 g concentrated sperm suspension were ground in liquid nitrogen and gently lysed in 20 ml ice-cold extraction buffer (2 M Tris-HCl pH 8.0, 0.5 M EDTA, 1.5% v/v β-mercaptoethanol, 1% w/v SDS). The lysate was treated with care to avoid shearing genomic DNA. Solid CsCl was dissolved in the lysate to a final density of 1.58. EtBr was added to the solution to a final concentration of 0.2 $mg \cdot ml^{-1}$. The solution was centrifuged under vacuum, in a Sorvall® OTD50B ultracentrifuge, using a Sorvall® AH629 rotor, at 27,000 r.p.m., for 60 h, at 20 °C. Genomic DNA, visualised under long wave U.V. irradiation (λ= 366 nm), formed a single band in the density gradient set up by the CsCl. DNA was removed from the CsCl gradient using 19G 1½ Microlance sterile hypodermic needles.

Extracted bands were pooled and diluted in a CsCl solution at a density of 1.58 with 0.2 mg·ml^{-1} EtBr. Samples were centrifuged under vacuum, in a Sorvall® OTD50B ultracentrifuge, using a Sorvall® AH629 rotor, at 45,000 r.p.m., for 48 h, at 20 °C. DNA bands were visualised and collected as before.

EtBr was removed from the solution by addition of an equal volume isopropanol, saturated with H_2O and with NaCl. Both phases were gently mixed causing EtBr transfer to the isopropanol, colouring it pink. The emulsion was stood on ice to allow organic and aqueous phases to separate. The supernatant, pink isopropanol was removed and this cleansing procedure repeated until the supernatant isopropanol was colourless. The DNA solution was purified from contaminating traces of isopropanol by phenol extraction. Organic and aqueous phases were gently mixed, not vortexed. The mixture was centrifuged in a Sorvall® RC-5B centrifuge, using a Sorvall® HB4 rotor, at 10,000 r.p.m., for 10 min, at 4 °C, the aqueous phase retained and chloroform extracted in a similar manner. DNA was ethanol precipitated from the recovered aqueous phase and re-hydrated, overnight, in 2 ml H_2O, at 4 °C.

2. 10. 9 cDNA synthesis

The reaction was performed in a 50 µl volume containing 1x first strand buffer (50 mM Tris-HCl pH 8.3, 75 mM KCl, 5 mM $MgCl_2$), 1 mM dNTP (1 mM each of dGTP, dATP, dTTP and dCTP, pH 7.0), 10 mM DTT, 0.1 mg·ml^{-1} BSA, 1 U·µl^{-1} RNasin (Promega), 100 µg·ml^{-1} oligo dT (12-18 thymine oligonucleotide) or 100 µg·ml^{-1} random base hexamer, *F. serratus* RNA, and 200 U M-MLV reverse transcriptase (GIBCO, BRL). The reaction mix was prepared without RNA or reverse transcriptase and kept on ice.

RNA was denatured at 70 °C for 5 min, ice chilled for 2 min, and added to the reaction mix. Reverse transcriptase was then added, and the reaction incubated at 37 °C for 1 h. The oligo dT or the random base hexamer annealed to the RNA, either on the poly A tail in the former case, or randomly in the latter. Reverse transcriptase recognises the double stranded region to which it binds. The enzyme then uses the RNA sequence as a template to synthesise the complimentary DNA strand. The reaction was stopped by incubation at 100 °C for 3 min, and then chilled on ice for 10 min. Denatured proteins were pelleted by centrifugation in a MSE Microcentaur, at 13,000 r.p.m., for 5 min, at 4 °C. The cDNA solution was retrieved and stored at -20 °C.

2. 11 *In vitro* amplification of calmodulin nucleotide sequences

2. 11. 1 Oligonucleotide primers

Degenerate oligonucleotides were designed representing highly conserved regions of an amino acid consensus sequence of 12 plant and 6 fungal calmodulins (Figure 2-11-1) (McPherson *et al.*, 1991). Three "forward primers" (236 V, A 657, 113 Y) annealing to the antisense strand of the gene, and one "reverse primer" (Q 34) annealing to the coding strand of the gene were devised.

236 V: 5' ATG GCX GAY CAR YTX ACX G 3'

A 657: 5' TTY GAY AAR GAY GGX GAY GG 3'

113 Y: 5' GAY ATG ATX AAY GAR GTX GAY GCX GAY GG 3'

Q 34: 5' ATC ATY TCR TCX ACY TCY TC 3'

"G" represents guanine, "A" represents adenine, "T" represents thymine, "C" represents cytosine, "R" represents A or G, "Y" represents C or T and "X" represents G, A, T or C.

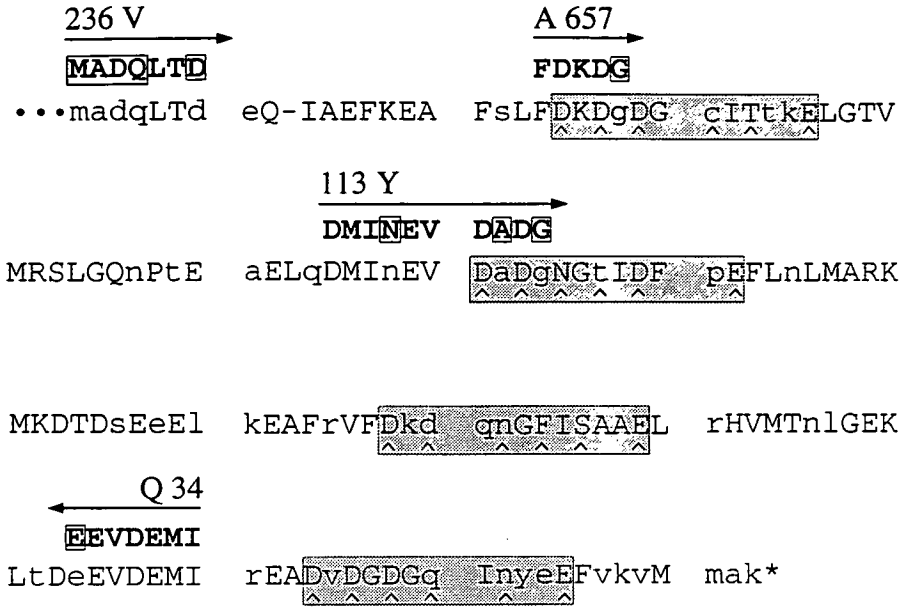

Figure 2-11-1. Amino acid consensus sequence of calmodulin.

12 plant (*Arabidopsis thaliana, Chlamydomonas reinhardtii, Cucumis melo, Daucus carota, Hordeum vulgare, Lycopersicon esculentum, Medicado sativa, Oryza sativa, Petunia hybrida, Solenum tuberosum, Spinacia oleracea, Triticum aestivum*) and 6 fungal (*Achyla klebsiana, Aspergillus nidulans, Candida albicans, Phyophthora infestans, Saccharomyces cerevisiae, Schizosaccharomyces pombe*) calmodulin amino acid sequences were aligned and analysed for homology.
Amino acids are represented by the single letter code. Capitals indicate that the residue is identical for that amino acid position in at least 17 of the 18 species screened, less conservation being indicated by lower case letters. In this case the residue shown is the most represented among the screened sequences. The EF-hands are shaded. (^) points out the Ca^{2+} binding residues.
Oligonucleotide primers 236 V, A 657, 113 Y and Q34, representing conserved regions of the calmodulin consensus sequence, are shown **in bold** and their priming directions indicated by an arrow. Heterologies are boxed. Nucleotide sequences for each primer are given in the text.

2. 11. 2 In vitro amplification of Fucus serratus calmodulin DNA fragment

In vitro amplification of specific DNA fragments by the polymerase chain reaction (PCR) was performed in 50 µl volumes. Reaction mixes contained 1x reaction buffer (10 mM Tris-HCl pH 8.8 at 25 °C, 50 mM KCl, 1.5 mM $MgCl_2$, 0.01% v/v Triton X-100), 200 µM dNTP, 2.5% formamide (Sarkar *et al.,* 1990), 2 µM reverse primer (Q 34), 4 µM forward primer (236 V, A 657 or 113 Y), target DNA (all *F. serratus* cDNA from a cDNA synthesis reaction or 1 µg *F. serratus* genomic DNA), and 2.5 U thermalase (thermostable DNA polymerase, Kodak).

Reaction mixes were kept on ice and overlaid with 40 µl mineral oil. Thermal cycling was carried out using a Hybaid omnigene automatic thermal cycler. Thermal cycling programs were optimised for each set of primers to maximise target fragment amplification, while minimising artefacts. Single primer and minus DNA control reactions were performed. 12 µl samples from each reaction were analysed by gel electrophoresis.

2. 11. 3 In vitro amplification of Macrocystis pyrifera calmodulin DNA fragment

Amplification reactions were prepared as previously explained. Forward priming was with A 657 or 113 Y. Target DNA was 1 µg DNA extracted from a *M. pyrifera* cDNA library (Section *2. 12. 5*). In addition to the controls carried out before, a positive control containing 1 pg of a plasmid containing the calmodulin cDNA clone from *C. reinhardtii*, p6-8.11, (Zimmer *et al.,* 1988) was amplified. Amplification of the A 657-Q 34 PCR product (Bjourson and Cooper, 1992) using primers 113 Y and Q 34 was also carried out as a further control (nested PCR).

2. 11. 4 Blunt ending PCR fragments

Thermostable DNA polymerases add an extra nucleotide base, usually an adenine, to the 3' end of amplified DNA fragments (Holland, 1993). Prior to cloning, fragments were blunt ended using the proofreading properties of T4 DNA polymerase.

Reactions were performed in 50 µl volumes containing 1x incubation buffer (50 mM Tris-HCl pH 8.8, 15 mM $(NH_4)_2SO_4$, 7 mM $MgCl_2$, 0.1 mM EDTA, 10 mM β-mercaptoethanol, 0.2 mg·ml^{-1} BSA), 20 µM dNTP, ~0.5 µg amplified DNA fragment and 4 U T4 DNA polymerase (Boehringer Mannheim Biochemica). Reactions were incubated for 30 min at 12 °C. DNA was ethanol precipitated, dissolved in H_2O to give an approximate fragment concentration of 0.05 µg·µl^{-1}, and stored at -20 °C.

2. 12 Cloning *Macrocystis pyrifera* calmodulin from a cDNA library

2. 12. 1 Media and solutions

BBL bottom agar: 1% w/v Difco agar, 1% w/v BBL trypticase, 0.5% w/v NaCl.

BBL top agar: 0.65% w/v Difco agar, 1% w/v BBL trypticase, 0.5% w/v NaCl.

Host cell buffer: 10 mM Tris-HCl pH 7.5, 10 mM $MgSO_4$.

Phage buffer: 1 M Tris-HCl, pH 7.5, 0.58% w/v NaCl, 0.2% w/v $MgSO_4 \cdot 7H_2O$, 5 ml 2% w/v gelatin.

2. 12. 2 Macrocystis pyrifera cDNA library

The cDNA library was a kind gift from Kirk Apt, Carnegie Institution of Washington, Stanford, California. cDNA from *M. pyrifera* female gametophytes was cloned into λ-Zap II XR (Stratagene) at the *Xho* I and

Eco RI sites (Figure 2-12-1). The library titer was $71 \cdot 10^5$ phage per ml prior to mailing.

2. 12. 3 cDNA library titer

A single colony of *E. coli,* strain XL1 Blue, was inoculated into 20 ml LB broth enriched to 0.2% maltose and 10 mM $MgSO_4$ (enriched LB broth), and cultured overnight, at 37 °C. The presence of maltose and $MgSO_4$ activated the λ bacteriophage receptor of *E. coli*, thereby inducing phage infection. Cells were pelleted by centrifugation in a Mistral 4L centrifuge using a swing-out rotor, at 3,500 r.p.m., for 10 min, at 4 °C and the supernatant discarded. Pellets were re-suspended in 20 ml host cell buffer. The suspension was diluted to $Abs_{600} = 0.5$ (Philips PU 8625 UV/VIS spectrophotometer). Cells prepared in this way, hereafter referred to as λ-host cells, were stored on ice.

The cDNA library was diluted in phage buffer to 10^{-2}, 10^{-3}, 10^{-4} and 10^{-5} aliquots. 20 µl each dilution was added to 200 µl λ-host cells and incubated at 37 °C for 20 min to permit infection of the bacteria by the library phage. For each dilution, two replicate infections were prepared. Each infection was added to 3 ml molten BBL top agar enriched to 10 mM $MgSO_4$, at 45 °C. Cells and agar were mixed, spread over 50 ml BBL bottom agar plates, and allowed to set. Infection plates were incubated overnight, at 37 °C. Following incubation, phage plaques, which show up as clear discs on an opaque bacterial lawn, were counted. The phage titer was determined in phage, or "plaque forming units (pfu)", per ml library stock ($pfu \cdot ml^{-1}$). In this case library titer was $3.1 \cdot 10^5$ $pfu \cdot ml^{-1}$.

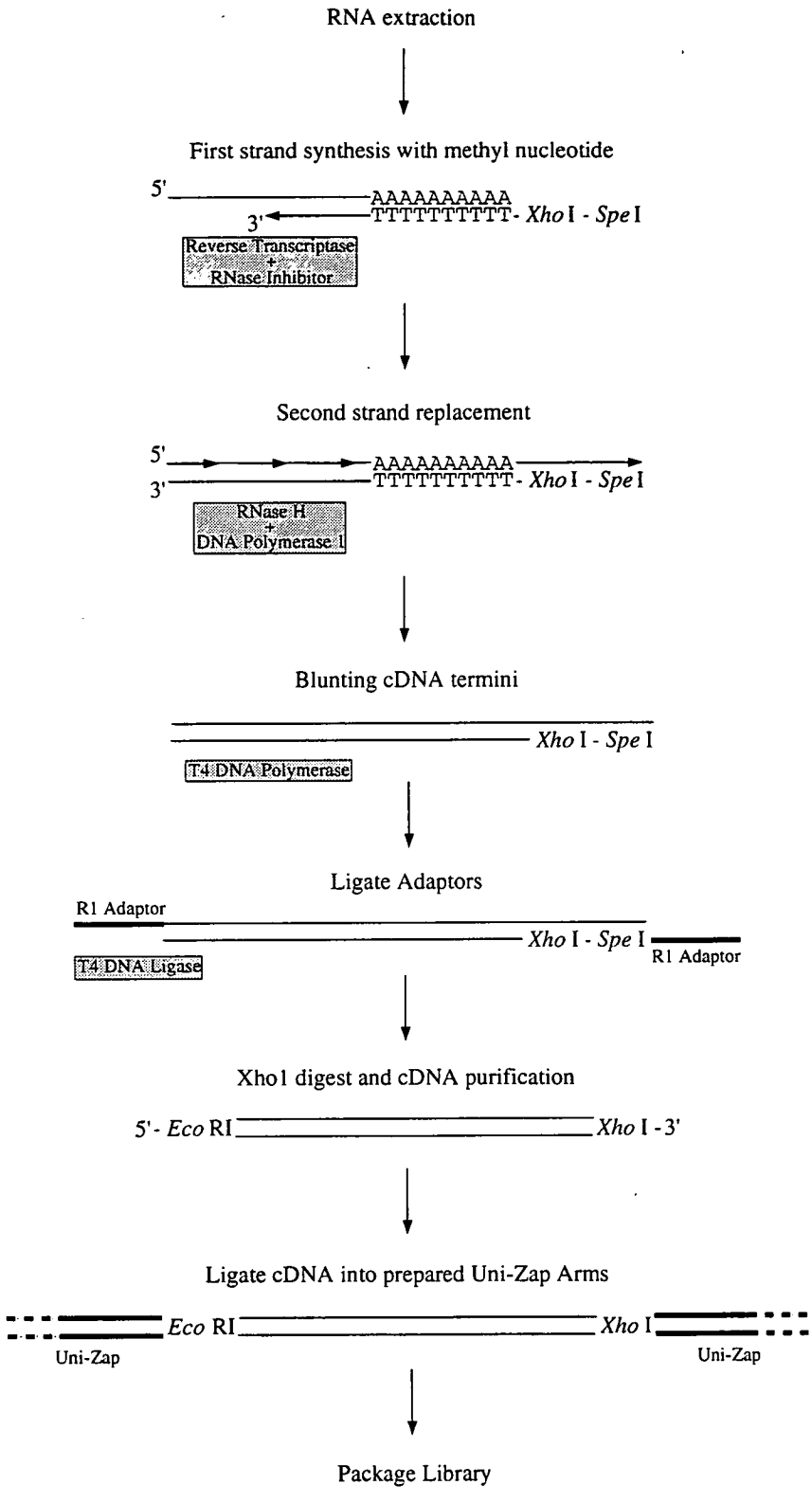

Figure 2-12-1. Diagram of λ-Zap II XR cDNA library construction.

The main phases of cDNA library construction are indicated. Special importance is given to the linkers and cloned restriction sites (*Eco* RI and *Xho* I) which orient the cDNA insertion into the phage. Enzymes used at

2. 12. 4 Library amplification

The library was amplified following the same general protocol as for the titer: Library stock was diluted to 10^{-1} and 10^{-2} aliquots. Each dilution and a zero dilution control were used to infect 200 µl λ host cells. The cells were incubated at 37 °C for 20 min, mixed with 3 ml enriched BBL top agar and 2 ml LB broth, and spread over set BBL bottom agar. Four replicate dilutions and two replicate zero controls were prepared.

Following overnight incubation at 37 °C, 10^{-2} dilutions yielded confluent plaques (the only visible bacterial culture was a lattice of thin lines marking the junction between adjacent plaques). 5 ml phage buffer was added to each 10^{-2} infection plate and incubated overnight at 4 °C. Replicated λ phage were secreted from infected bacteria and collected in the supernatant buffer. The phage-buffer suspension was harvested from each plate and kept in a sterile plastic tube at 4 °C. 1 ml fresh phage buffer was added to the plates which were then stored, for 15 min, at 4 °C, in a tilted position to allow draining to one area. The buffer was collected and pooled with the previously collected phage suspension samples. 0.1 ml pure chloroform was added to phage samples which were then centrifuged in a Mistral 4L centrifuge, using a swing-out rotor, at 3,500 r.p.m., for 10 min, at 4 °C, to pellet any residual agar. The supernatant phage suspension was recovered.

2. 12. 5 DNA extraction from cDNA library phage

DNA was isolated from 5 ml amplified phage suspension. 10 µl DNase I and 10 µl RNase I (5 $mg \cdot ml^{-1}$ of each in 50% glycerol) were added to the phage stock, vortexed and incubated for 30 min at 37 °C to remove contaminating bacterial DNA and RNA while leaving the phage intact. 250 µl 0.5 M EDTA were added causing phage disruption. The mix was

briefly vortexed and placed on ice. To ascertain disruption of all phage, 5 µl Proteinase K were quickly added to the lysate and vortexed. 500 µl 3 M Na-Ac were added and the solution extracted with phenol. An equal volume of isopropanol was added to the recovered aqueous phase and incubated at 20 °C for 5 min to allow DNA precipitation. DNA was pelleted in a Sorvall® RC-5B centrifuge using a Sorvall® HB4 rotor, at 13,000 r.p.m. for 15 min at 20 °C. Pelleted DNA was washed in ice cold 70% ethanol, dried under vacuum and dissolved in 200 µl TE. 0.1 $mg \cdot ml^{-1}$ BSA were added to the DNA sample to complex bacterial polysaccharides.

2. 12. 6 cDNA library screening for calmodulin clones

Two 243 x 243 x 18 mm sterile bio-assay dishes (Nunc, Inter Med) were cast with 500 ml BBL bottom agar enriched to 10 mM $MgSO_4$. The desired phage concentration for the first screen was 150,000 pfu per plate. 2 ml λ-host cells were incubated for 20 min, at 37 °C with, 150,000 pfu library bacteriophage from the original stock. Two replicates were prepared. Infected cells were mixed with 30 ml enriched BBL top agar, overlaid onto the prepared bio-assay plates and incubated at 37 °C, overnight. Bio-assay plates were incubated at 4 °C for at least 2 h to ensure maximum adhesion between top and bottom agars. Plaques were blotted onto Hybond-N membranes as explained in Section *2. 9. 3.* Blots were probed with a ^{32}P-labelled calmodulin PCR fragment amplified from the library (Section *2. 11. 3*), called ^{32}P-B320. Positive plaques were identified by comparing autoradiographs of replicate filters. Plates were placed over the autoradiographs and aligned with the ink marks on the gel. Positives were picked off using the wide end of sterile pasteur pipettes and cores suspended in 1 ml phage buffer, vortexed, and incubated at 20 °C for 2 h. Agar was pelleted by centrifugation in a MSE Microcentaur, at 13,000 r.p.m., for

2 min, at 20 °C. For each core, the supernatant phage suspension was titered as described in Section *5. 2. 3.*

Phage from the first screening were then screened individually. 200 pfu per clone were plated on 120 x 120 mm plates, resulting in discrete plaques. After blotting and probing with ^{32}P-B320, positive, secondary clones were identified and numbered. Individual positive plaques were cored and suspended in 1 ml phage buffer.

2. 12. 7 In vivo excision of cDNA containing plasmids from λ Zap

The l-Zap II XR (Uni-ZAP™) vector was designed to allow *in vivo* excision and recircularisation of any cloned insert contained within the λ phage vector to form a phagemid (Stratagene). *In vivo* excision required engineering of the λ phage genome to include the f1 bacteriophage origin of replication, which sites of initiation and of termination flank the sequence to be excised, upstream (5') and downstream (3') respectively. In the case of the l-Zap II XR vector, this included all sequences of the phagemid, pBluescript SK-, and cloned insert. Moreover, all sequences of normal λ phage vectors were positioned outside of the f1 initiator and terminator signals and were therefore not contained within the circularised DNA (Figure 2-12-2). The λ phage was made accessible to the f1 derived proteins by simultaneously infecting *E. coli* with both λ phage (target phage) and f1 bacteriophage (helper phage). Proteins from f1 bacteriophage (helper proteins) recognised the initiator site within the λ phage genome and nicked one of the two DNA strands, initiating single strand DNA synthesis, and duplicating sequences downstream of the initiator. When the f1 terminator was reached, DNA synthesis stopped. The single DNA strand was then circularized by a gene II product of the f1 bacteriophage. DNA circularisation automatically recreated a functional f1 origin (initiator and

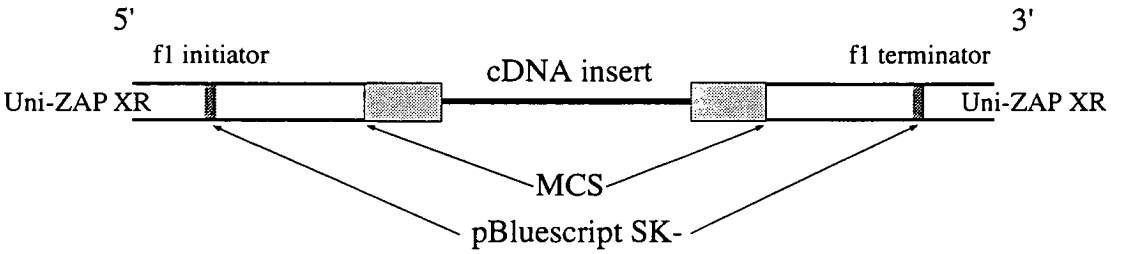

Figure 2-12-2. Diagram of the pBluescript SK- phagemid within λ-Zap.

The relative positions of the cDNA insert, the MCS and core of pBluescript SK-, and the f1 initiator and terminator signals are shown within the Uni-ZAP XR genome.
cDNA-pBluescript SK- phagemids can be cloned directly and *in vivo* from the phage (see text for details).

terminator) as in the f1 bacteriophage or phagemids. Packaging signals, contained within the f1 terminator of the newly circularized phagemid, caused the DNA to be packaged and secreted from the host bacterium (rescued phagemid). Following phagemid secretion, bacteria were killed by heating, and the packaged, single stranded, pBluescript SK- phagemid transformed into competent *E. coli* (λ-host cells) within which synthesis of the phagemid's complementary DNA strand took place. Transformant bacterial colonies were selected by ampicillin resistance.

Phage clones from the second screen were titered as explained previously (Section *5. 2. 2*) and diluted to working suspensions of $25 \cdot 10^4$ pfu·μl^{-1}. 200 μl suspension of each phage clone was added to 200 μl λ-host cells and 1 μl R408 helper phage (> 10^6 pfu·ml^{-1}). Cells were incubated at 37 °C for 15 min. As a negative control, host cells and helper phage alone were combined, with no recombinant λ phage. Following addition of 5 ml phage buffer, the inoculum was incubated at 37 °C, for 3 h. During this period, saved phagemids were secreted into the medium. Bacteria were killed by heating the suspension to 70 °C for 20 min. Following centrifugation in a Mistral 4L centrifuge, using a swing-out rotor, at 3,500 r.p.m., for 5 min, at 20 °C, the supernatant phagemid suspension was retrieved.

Phagemids were diluted 100 fold, 20 μl added to 200 μl λ-host cells, and incubated for 15 min, at 37 °C, to allow phagemid absorption. Cells were then diluted 10^{-1}, 10^{-2} and 10^{-3} fold. For each clone, 2 replicate 50 μl aliquots were plated onto LB-agar containing 5 μg·ml^{-1} tetracycline and 100 μg·ml^{-1} ampicillin. Plates were incubated overnight, at 42 °C, to inhibit growth of any bacteria infected with helper phage, even though helper phage alone do not contain ampicillin resistance genes. Colonies which

appeared on plates contained the double stranded pBluescript SK- plasmid with cloned insert. For each clone, 3 recombinant colonies were selected, labelled "a", "b" or "c", and cultured in 5 ml LB-broth containing 100 $\mu g \cdot ml^{-1}$ ampicillin and 5 $\mu g \cdot ml^{-1}$ tetracycline.

2. 12. 8 Clone selection by sequencing and PCR

Plasmid cDNA clones were purified from *E. coli*, using Wizard™ minipreps from Promega (Section *2. 5. 4*). Each clone was tentatively sequenced using the Forward and Reverse priming sites of pBluescript SK- (Section **2. 8**). Clones which failed to produce a sequence, or did not possess either one of the restriction sites used during library construction (*Xho* I or *Eco* RI) were discarded.

1 ng of each retained plasmid cDNA clone was analysed for the calmodulin cDNA insert by *in vitro* amplification with the calmodulin PCR primers A 657 and Q 34 (Section *2. 11. 3*). Clones which yielded a PCR band of the expected size (320 bp) were selected and sequenced (Section **2. 8**).

2. 12. 9 Calmodulin cDNA clone sequencing

cDNA clones were first sequenced using the forward and reverse priming sites of pBluescript SK-. Regions approximately 100 bp from the 3' end of the sequenced portions were considered as novel sequence priming sites. Priming sites between 12 bp and 16 bp long, with over 60% G/C content were selected and checked for annealing both to pBluescript SK- and to the previously sequenced cDNA portion. The presence of guanine or cytosine at the primer termini, especially at the 3' end, were sought to enhance priming. The relative positions of each sequencing primer is diagrammed (Figure 2-12-3).

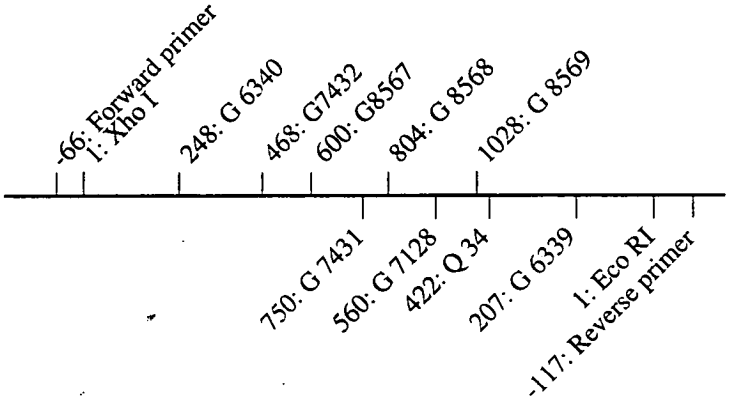

Figure 2-12-3. Positions of the primers used for sequencing clone 4.2a.

Oligonucleotide primers were synthesised to anneal to internal regions within the *M. pyrifera* calmodulin cDNA clone 4.2a. The position of each primer is indicated, in bp, relative to the *Xho* I and *Eco* RI cDNA linker sites.
Sequencing was carried out in portions on both DNA strands. Overlapping regions within these portions were identified and used to build the total nucleotide sequence of 4.2a. Both DNA strands were compared to confirm the deduced sequence (see text for details).

Forward primer: 5' GTA AAA CGA CGG CCA GT 3'

G 6340: 5' GGA AAG CCT CAC ATC 3'

G 7432: 5' CAG TAA CTA ACC AAG G 3'

G 8567: 5' GCT CTC CTA CAC CC 3'

G 8568: 5' CAG GAC ATG ATC AAC G 3'

G 8569: 5' GAC GAG ATG ATC CG 3'

Reverse primer: 5' AAC AGC TAT GAC CAT G 3'

G 6339: 5' CCT CAC GGC AGA ATA G 3'

Q 34: 5' ATC ATY TCR TCI ACY TCY TC 3'

G 7128: 5' CCG TGT CCT TCA 3'

G 7431: 5' GGC TGA AGG CTC CTT G 3'

2.13 *Macrocystis pyrifera* calmodulin expression in bacteria

2. 13. 1 Engineering a Nde I restriction site at the calmodulin start codon

Using the polymerase chain reaction, a *Nde* I restriction site (5' CAT$_{\wedge}$ATG) was engineered into the *M. pyrifera* calmodulin coding sequence (clone 4.2a) to overlap with the ATG (Start) codon. This *Nde* I site was used to insert the PCR (coding) fragment, in frame, with the T7 polymerase promoter of the expression vector pRSET A (Figure 2-12-4). The oligonucleotide G 9101 was designed to anneal to the antisense strand (forward primer) of the calmodulin cDNA clone, from base -11 to to +5, the "A" of the start codon being nucleotide +1 (Figure 2-12-5). The upstream portion of the primer was designed long to protect the restriction site (in bold) at the 5' end of the amplified product. Reverse priming was by the reverse primer of pBluescript SK- .

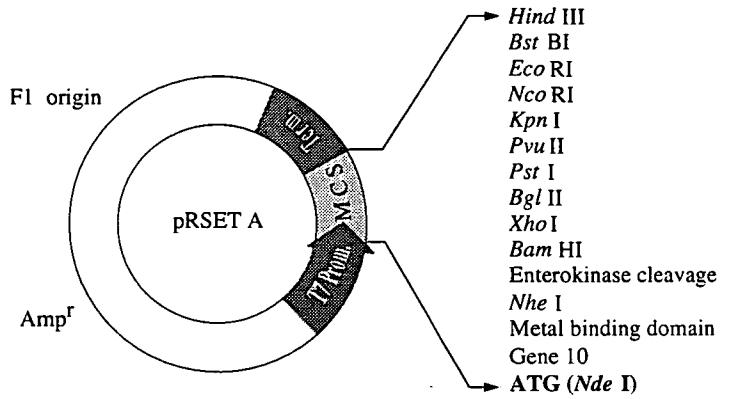

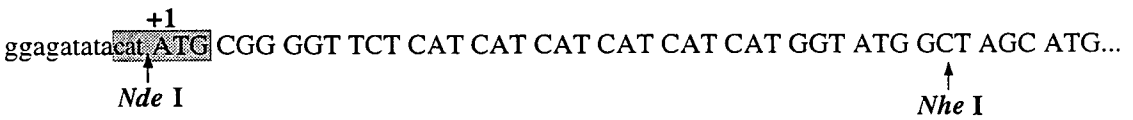

Figure 2-12-4. Diagram of the expression plasmid vector, pRSET A.

The MCS is shaded in light grey, and restriction sites shown. The plasmid enables in frame insertion of fragments under the control of the T7 promoter. Protein synthesis is induced by 4 M IPTG.
The last 12 bp of the T7 promoter, and the first 45 bp of the MCS are detailed. Fragments are inserted, in frame, at the *Nde* I restriction site.

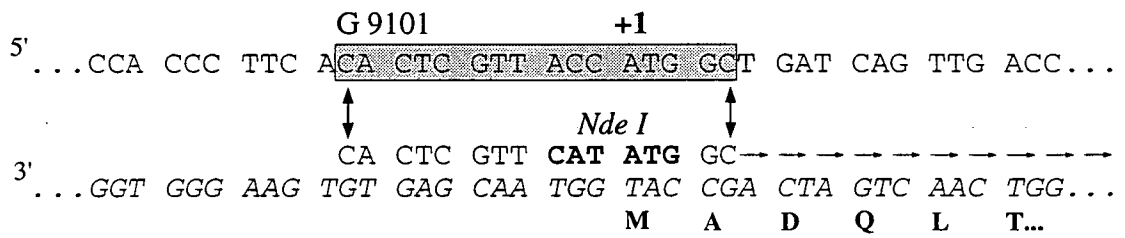

Figure 2-12-5. Diagram of G 9101 annealing to clone 4.2a.

The position of G 9101 on the coding strand of clone 4.2a is shown. Nucleotides are represented by their initials. Note that the primer possesses a *Nde* I restriction site ($^{5'}$CAT$_{\wedge}$ATG) which is absent from the clone (**bold type**). The primer anneals tightly to the antisense strand (italicised), the direction of PCR amplification being indicated by the row of arrows.
The amino acid translation is shown using the single letter code.

G 9101: $^{5'}$ CA CTC GTT CAT ATG GC $^{3'}$

In vitro amplification of the calmodulin sequence was performed as explained in Section **2. 11**. Reactions contained 1x reaction buffer, 200 μM dNTP, 2.5% formamide, 2 μM pBluescript SK- reverse primer, 2 μM G 9101, 5 ng clone 4.2a, 2.5 U Taq DNA polymerase (thermostable DNA polymerase, NBL). The PCR yielded an expected 920 bp DNA fragment which was cloned into the *Sma* I restriction site of pBluescript SK- (Section *2. 11. 4)* and transformed into *E. coli*, strain XL-1 Blue, by electroporation (Section *2. 7. 3*). Recombinant bacterial colonies were selected and plasmid DNA purified using Wizard® minipreps (Promega). DNA samples were analysed for the engineered calmodulin insert with restriction endonucleases Sst I, Nde I and Eco RI. A plasmid containing the insert was selected and labelled pB920.

2. 13. 2 pB920 insertion into the expression vector pRSET A

The engineered *Nde* I-calmodulin sequence was excised from pB920 with Nde I and Eco RI, yielding a 820 bp fragment labelled B820. The native *M. pyrifera* Stop and polyadenylation signals remained part of the engineered fragment, but downstream sequences were not included. The expression vector pRSET A was linearised, also with Nde I and Eco RI. B820 and linearised pRSET A were ligated and transformed into *E. coli*, strain XL-1 Blue, by electroporation. pRSET A does not enable colour selection of transformants. Instead, plasmid DNA was purified from 6 selected recombinant colonies using Wizard® minipreps (Promega), and analysed by restriction digestion with Nde I and Eco RI. All plasmids contained the appropriate insert (B820), one of which was selected and labelled pB820-E.

2. 13. 3 Calmodulin expression in bacteria and purification

E. coli, expression strain BL21-ΔDE3, was transformed with 1 ng pB820-E by electroporation. Recombinant colonies were selected and cultured in 5 ml LB broth with 200 $\mu g \cdot ml^{-1}$ ampicillin. BL21-ΔDE3 is not recombination inactive and loses plasmids over time. For this reason, antibiotic selection pressure was set at double the normal in order to maintain the plasmid longer. BL21-ΔDE3/pB820-E transformant colonies were cultured only once in liquid medium and used within 48 h. Recombinant bacteria were analysed for pB820-E by restriction digestion of purified plasmid DNA with Nde I and Eco RI (Section *2. 5. 6*).

2 ml BL21-ΔDE3/p820-E from a 5 ml overnight liquid culture was added to 38 ml LB broth containing 200 $\mu g \cdot ml^{-1}$ ampicillin. Two replicates were prepared; in one calmodulin synthesis was induced, whereas the replicate acted as a negative control. Cultures were incubated for approximately 2 h, at 37 °C, until $0.8 < Abs_{600} < 0.9$. Recombinant protein synthesis was induced by taking the IPTG concentration of cultures to 4 M. Cultures were incubated on a shaker for 1 h, at 37 °C. Rifampicin was added to 200 $\mu g \cdot ml^{-1}$ final concentration and incubated for 2 h at 37 °C. Rifampicin poisoned bacteria without affecting recombinant translation. Consequently, the production of bacterial proteins was minimised relative to that of the recombinant calmodulin (Das, 1990).

1 ml bacterial suspensions from induced and uninduced cultures were collected. Both aliquots and the remaining culture were frozen in liquid nitrogen and conserved at -80 °C. Aliquots were thawed on ice and sonicated at 20 μm, in an ice cold water bath, for 10 s. The lysate was centrifuged in a MSE Microcentaur, at 13,500 r.p.m., for 5 min, at 4°C. Supernatants (crude protein extract) were retrieved, and pellets conserved at

-80 °C in case calmodulin was secreted into bacterial inclusion bodies. 100 µl of the supernatant was added to 100 µl 2x SDS PAGE loading buffer and incubated at 100 °C for 3 min. 10 µl of this sample (corresponding to 5 µl supernatant) was analysed by SDS PAGE.

For large scale recombinant calmodulin purification, induced and uninduced 40 ml cultures were ice-chilled and centrifuged in a Mistral 4L centrifuge, using a swing out rotor, at 3,500 r.p.m., for 20 min, at 4 °C. The supernatant was discarded and cells re-suspended in 5 ml W7 affinity column loading buffer (Buffer F, Section *2. 2. 4*). Cell suspensions were frozen in liquid nitrogen, thawed on ice, and sonicated at 20 µm, in an ice-cold water bath, for 30 s. The lysate was centrifuged in a Sorvall® RC-5B centrifuge, using a Sorvall® HB4 rotor, at 15,000 r.p.m., for 15 min, at 4 °C. The supernatant was collected and a 100 µl sample retained for SDS PAGE analysis. Pellets were conserved at -80 °C.

Calmodulin was purified from the lysate by affinity chromatography through a 3 ml W7-agarose column (Section *2. 2. 4*). The column was washed with 3 column volumes (9 ml) Buffer F, and clamped. The supernatant from the induced bacterial lysate was loaded and unbound protein flushed from the column in 0.5 ml fractions. 200 wash fractions were collected.

Calmodulin was eluted with buffer G (10 mM EGTA) in 0.5 ml fractions until $Abs_{280} < 0.05$. 30 fractions were collected, of which 13 displayed high absorbance levels. 5 µl samples were collected from each fraction and analysed by SDS PAGE. Eluted calmodulin fractions were frozen in liquid nitrogen and stored at -80 °C.

2. 13. 4 Buffer replacement and calmodulin concentration

Calmodulin eluted from the W7 affinity column in buffer G (10 mM EGTA) could not be microinjected directly into developing *F. serratus* zygotes. For microinjection, buffer G was replaced with a solution containing the main ions present in the cytoplasm of 8 h zygotes of *P. fastigiata* (320 mM KCl, 40 mM NaCl, 25 mM $MgCl_2$, 4 mM $CaCl_2$) (Allen *et al.*, 1972).

Calmodulin fractions were pooled. Buffer transfer and protein concentration were performed simultaneously, by ultrafiltration in Centricon®-10 columns (Amicon®) according to the manufacturer's instructions. Calmodulin was concentrated to 5 $\mu g \cdot \mu l^{-1}$ and aliquoted into 10 µl volumes. Aliquots were frozen in liquid nitrogen and conserved at -80 °C.

2. 14 Calmodulin microinjections into developing *Fucus serratus* zygotes

2. 14. 1 Preparation of eggs and zygotes for microinjection.

F. serratus eggs were purified as described previously (Section *2. 1. 2*) and allowed to settle onto Chance Propper n° 1 coverslip glass, which had previously been rinsed with 0.01% poly-L-lysine for 30 s, and with distilled water for 2 min. Coverslips formed the base of a chamber filled with ASW. Orientation marks were inscribed on culture chambers. *F. serratus* zygotes were cultured on untreated glass to which they adhered naturally. Zygotes were cultured at 14 °C, in darkness, for 10 h, and illuminated by unilateral, white light (Section *2. 2. 2*) between 10 and 13 h AF.

2. 14. 2 Microinjection

Cells were microinjected with an artificial intracellular solution containing 5 $\mu g \cdot \mu l^{-1}$ recombinant *M. pyrifera* calmodulin (Section *2. 13. 4*) and 1 μM calcium green (Molecular Probes Inc., USA). Microinjection was performed over a 2 h period at 15-17 °C using a hydraulic pressure-probe (Figure 2-14-1) which permits controlled intracellular injection of complex solutions (Oparka *et al.*, 1991). Injection electrodes were pulled from 500 pcs filamented borosilicate glass capillaries (GC 100 F-10, Clark Electromedical Instruments, U.K.) using a Narishige PB-7 electrode puller. Electrodes were back-filled with 1 μl injection solution, completely filled with de-gassed silicone oil, and inserted into a Narishige stainless steel injection holder, H1-4A.

Cells were resolved using a Nikon-Diphot inverted microscope with either a x10 (Nikon Plan 10/0.25 DIC) or a x20 (Nikon PlanApo 20/0.75) objective. A 3 axis joystick hydraulic micromanipulator with extra fourth axis movement from Narishige (MMO-24,-24-D) was used to impale eggs or zygotes with an injection electrode. Electrodes were used once only. Impalement was performed under illumination by white light. Eggs adhered tenaciously to the poly-L-lysine treated glass (Section *2. 14. 1*), but zygotes were held in place by a holding pipette made from flexible fused silica capillary tubing (TSP/025/150) from Composite metal Services L^{TD}, U.K. The capillary was held by a quartz Inner-lok™ connector (Composite metal Services L^{TD}) attached to a vacuum system, and manipulated like the injection electrode. Microinjection was monitored by calcium green fluorescence. The excitation wavelength was determined by a 490 ± 10 nm interference filter (Ealing Electro-Optics, U.K.) mounted in a motor-driven excitation filter wheel (Newcastle Photometric Systems) in front of a super

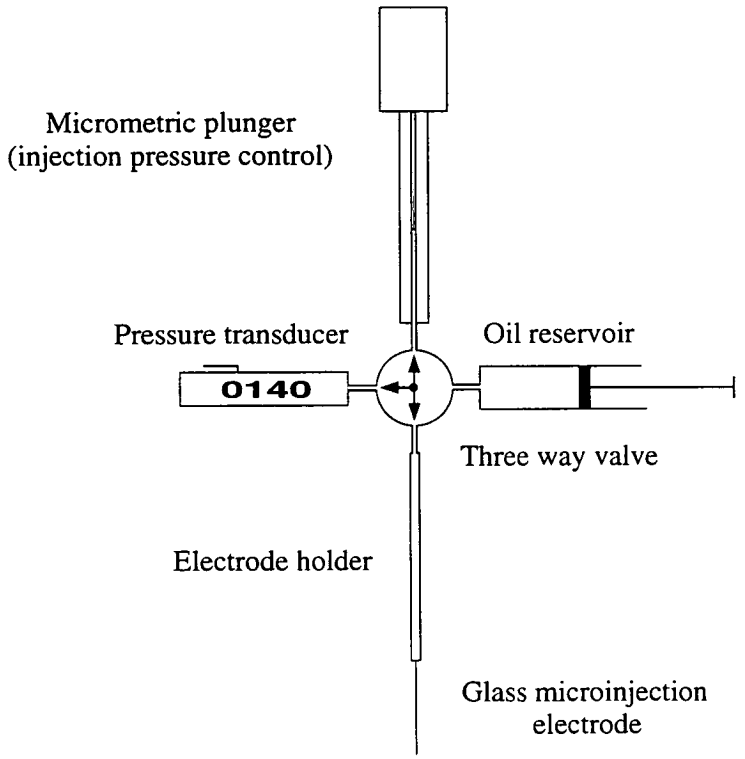

Figure 2-14-1. Diagram of the pressure probe used for microinjection. After Oparka *et al.* (1991).

high pressure mercury bulb (MBF 14343 100 wrth), powered by a Nikon HB10101 AF power pack. Fluorescence from the dye was monitored during injection with a 510 nm dichroic mirror coupled to a 520 nm long-pass filter.

Following microinjection, eggs were fertilised, cultured in darkness at 14 °C for 10 h, and exposed to unilateral white light from 10-13 h AF (Section *2. 2. 2*). Cells were then cultured in darkness, at 14 °C, for 48 h, and polar orientation scored relative to the direction of incident light. Microinjected zygotes were cultured in darkness at 14 °C, for 48 h and their direction of polarisation scored relative to the vector of applied light and to that of microinjection (Figure 2-14-2). For all microinjections, the direction of impalement and that of unilateral light were perpendicular. Polarisation was expressed as the mean of the cosine of the angle between the vector of applied stimulus (light or microinjection) and that of rhizoid germination.

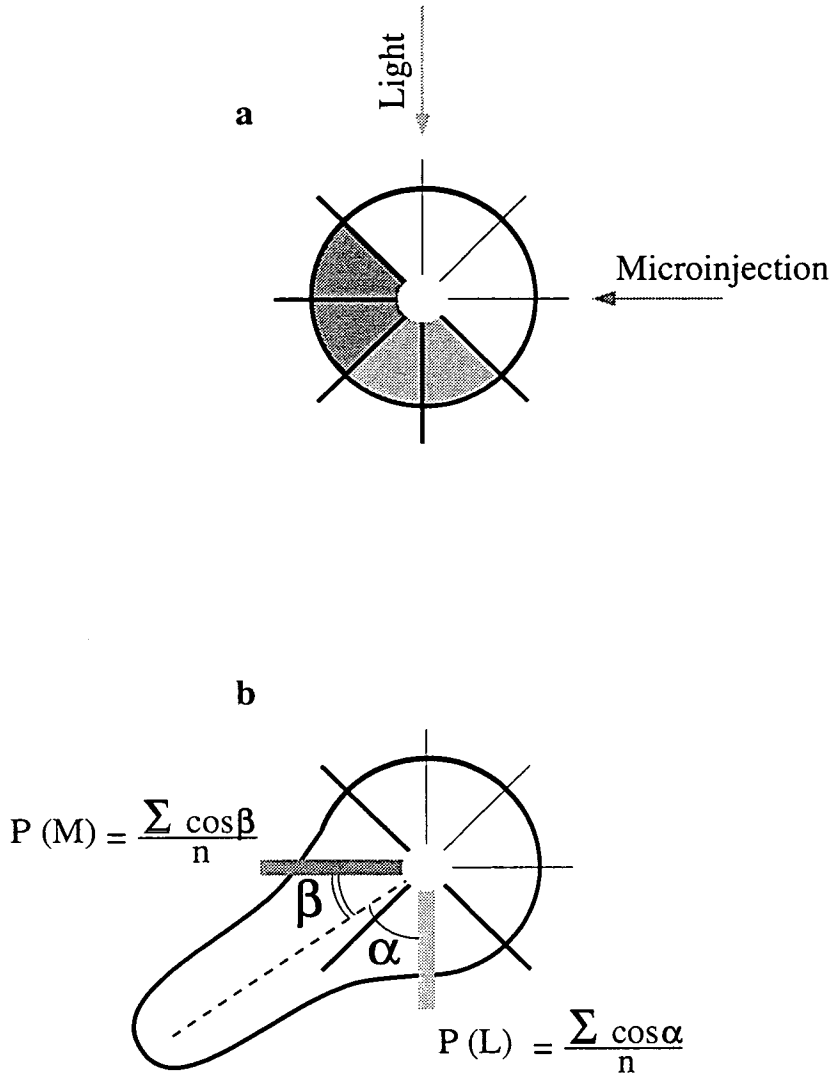

Figure 2-14-2. Orientation of *F. serratus* zygotes during microinjection.

a: *F. serratus* zygotes were recorded according to eight orientations. The direction of applied unilateral light (light grey) and that of microinjection (dark grey) were perpendicular. To maintain consistency with Section 2. 2. 2, polarisation was considered positive if zygotes germinated away from the polarising stimulus. In the case of unilateral light, polarisation is positive if zygotes germinate away from the light source (zone shaded in light grey), whereas for microinjection, polarisation is positive if zygotes germinate opposite the site of injection (zone shaded in dark grey).

b: Polarisation was determined by the cosine of the angle between applied stimulus and rhizoid germination. Photopolarisation is represented by P (L) and polarisation by microinjection is represented by P (M).

Chapter 3

Results

3. 1 Inhibition of photopolarisation

Inhibitors were applied to zygotes during the transient phase of photopolarisation and only zygotes which developed normally following inhibition were scored. Comparison between ASW and DASW controls excluded zygotes which did not perceive light, or in which the signal-response pathways were permanently uncoupled. Results therefore reflect as closely as possible the aspects involved in signal-response coupling between light perception and polar commitment.

A Mann-Whitney *U*-test was used to compare photopolarisation between zygotes incubated in ASW and zygotes incubated in DASW (null hypothesis: "The difference between means of the two groups is no greater than can be reasonably explained by chance"). For $n = 5$ (n being the number of replicates), significant $U = 2$ at the 5% probability level. If sample U for replicate experiments is strictly greater than significant U, the null hypothesis cannot be rejected, and the difference between the two groups is not significant. For each experiment, sample U is given in the corresponding figure legend.

3. 1. 1 Photopolarisation in ASW and under permanent illumination

Under normal conditions (incubation in ASW), the degree of photopolarisation reached a maximum 75-85%. Approximately one zygote in five therefore failed to either perceive or respond to the polarising stimulus given between 10 and 13 h AF. Under permanent illumination, 96.77% of zygotes formed a photopolarised axis indicating that that 12-22%

of zygotes which did not respond to light between 10 and 13 h AF had nevertheless the potential for phototropic response: "Blind" to the light pulse at 10-13 h AF, these zygotes could perceive light at other times and form axes accordingly. In these zygotes, the formation of a randomly oriented axis was not due to breakdown in perception-response coupling, but to a transient lack in perception. Conversely, the remaining 3% of zygotes which did not photopolarise at all either failed to do so because of a permanent breakdown in unilateral light perception, or because of a fault in the signal-response coupling. From the data collected, it is impossible to determine which possibility holds true.

3. 1. 2 Effect of Ca^{2+} inhibitors on photopolarisation

In all experiments barring those using $LaCl_3$ and cytochalasin-B, a Mann-Whitney *U*-test demonstrated no significant difference in polarisation between zygotes incubated in ASW during the period of unilateral illumination, and those bathed in DASW. Normal (9 mM) concentrations of free Ca^{2+} in the medium are not necessary for photopolarisation.

At a concentration of 10 mM, the Ca^{2+} chelating agent EGTA does not significantly reduce photopolarisation (Figure 3-1-1). Conversely, the inhibitor of plasma membrane Ca^{2+} channels, $LaCl_3$, reduced photopolarisation by a maximum 20% between 0.8 and 1 mM. Half (50%) inhibition was achieved at an approximate concentration of 0.5 mM $LaCl_3$ (Figure 3-1-2). While photopolarisation seems to proceed normally in the absence of extracellular free Ca^{2+}, it nevertheless requires an influx of external Ca^{2+}, albeit in a subpopulation of *F. serratus* zygotes. This ambiguous result is discussed in Section **4. 2.**

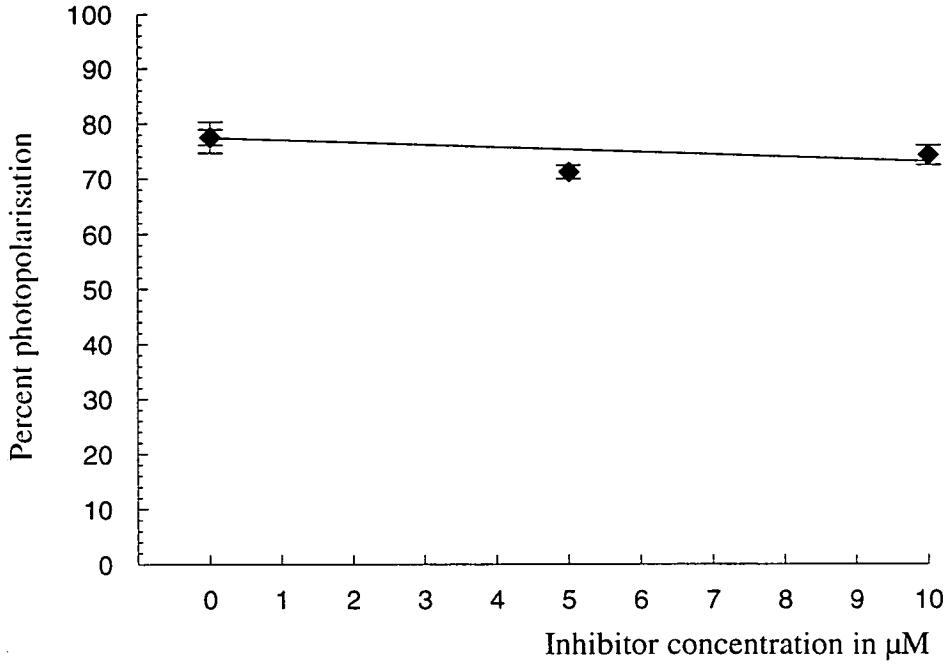

Figure 3-1-1. Effect of EGTA on photopolarisation at 10-13 h AF.

Each point represents the mean of 5 replicate experiments (see text for details). Standard error bars are shown.
There was no significant difference between zygotes incubated in ASW and those incubated in DASW as demonstrated by a Mann-Whitney *U*-test (sample $U = 12 >$ significant $U = 2$).

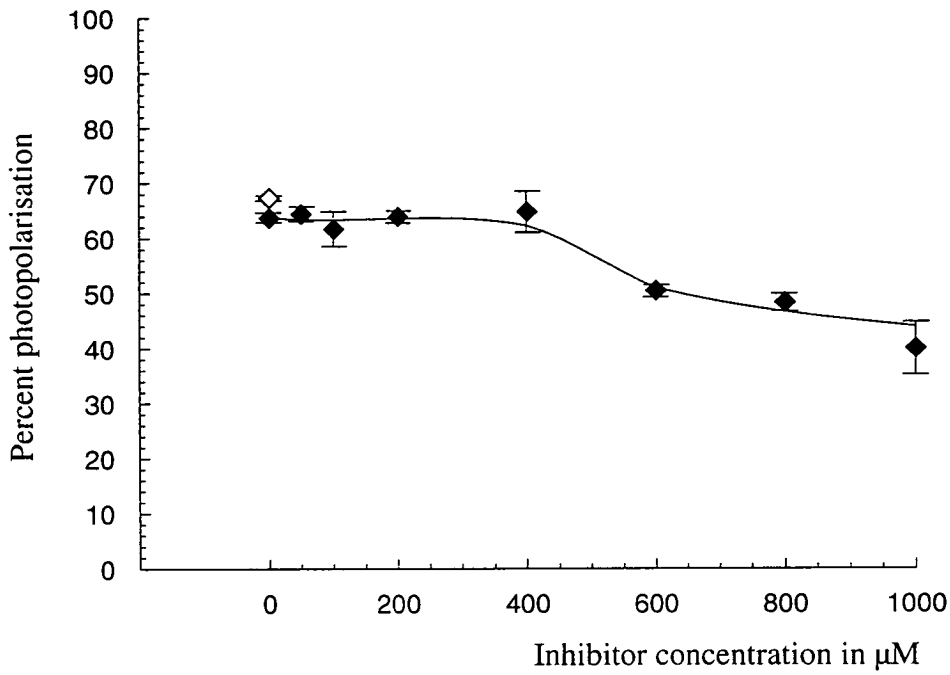

Figure 3-1-2. Effect of $LaCl_3$ on photopolarisation at 10-13 h AF.

Each point represents the mean of 5 replicate experiments. Standard error bars are shown. The difference in photopolarisation between zygotes incubated in ASW (open diamond) and those incubated in DASW (filled diamonds) is significant, as demonstrated by a Mann-Whitney *U*-test (sample $U = 1 <$ significant $U = 2$).

At $[LaCl_3] = 800$ μM, embryos loosened from coverslips. Loosening occurred at the rhizoid tip, cells remaining attached to the substrate only by the thallus. Consequently, certain cells were mobile around this single point of attachment and the orientation of the axis relative to incident light difficult to score accurately. At $[LaCl_3] = 1$ mM, approximately 10% of embryos were floating free of the substrate. This unforeseen effect on zygotes persisted 24-48 h after the inhibitor was washed from the culture medium.

Embryos normally adhere to the substratum by the rhizoid tip. $LaCl_3$ is therefore having a lasting effect on embryo development, though by which means remains unclear.

At 800 μM La^{3+}, the rhizoid tip of some embryos detached from coverslips. This effect was enhanced at 1 mM La^{3+}, causing certain polarised embryos to float free of the substratum. At these concentrations, the accurate determination of rhizoid direction relative to incident light became difficult; free floating embryos were easily discounted, but embryos with loosened rhizoid tips were less readily identified.

Exposure to the intracellular Ca^{2+} antagonist TMB-8 (Malagodi and Chiou, 1974 ; Lonergan, 1990 ; Saunders and Hepler, 1983) inhibited photopolarisation of *F. serratus* zygotes, in a dose dependant manner, from 75% in DASW to 30% at 80 μM TMB-8 (Figure 3-1-3). 50% inhibition occurred at approximately 20 μM. Increasing inhibitor concentrations from 60 μM had no increased effect on zygotes. The zygote population was therefore divided in the response to TMB-8 with approximately 40% of zygotes affected by the inhibitor. Consequently, for this group of zygotes, intracellular Ca^{2+} is required for photopolarisation. However, photopolarisation in 30% of the zygote population proceeded normally. These zygotes were either less sensitive to the effects of TMB-8, or did not require cytoplasmic free Ca^{2+} for photopolarisation. The effect of TMB-8 was reduced when dissolved in ASW. Previous research has shown that TMB-8 inhibition is reduced by the presence of Ca^{2+} in the incubation medium (Saunders and Hepler, 1983). In this case, 50% inhibition occurred at approximately 75 μM. The slope of inhibition in ASW was less abrupt than for DASW indicating a buffering of the drug's effect in Ca^{2+} containing media. This buffering suggests that TMB-8 is indeed inhibiting the action of Ca^{2+} with some degree of specificity.

The inhibitors Ca^{2+} channel antagonists, nifedipine, verapamil and bepridil reduced photopolarisation of *F. serratus* zygotes in a sensitive and

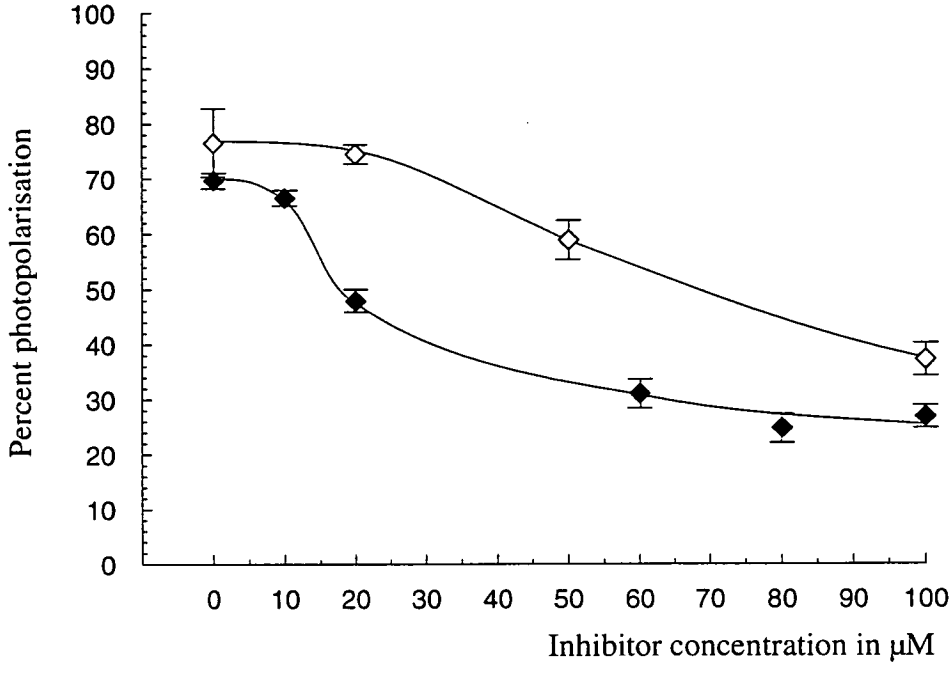

Figure 3-1-3. Effect of TMB-8 on photopolarisation from 10-13 h AF.

Each point represents the mean of 5 replicate experiments with standard error bars. Filled diamonds are for inhibitor dissolution in DASW and open diamonds represent inhibitor dissolution in ASW. There is no significant difference between zygotes incubated in ASW or in DASW, alone, as demonstrated by a Mann-Whitney *U*-test (sample $U = 12 >$ significant $U = 2$).

The presence of Ca^{2+} in the culture medium decreased the potency of TMB-8 at lower concentrations.

dose dependent manner.

In DASW, the intracellular Ca^{2+} channel antagonist nifedipine (Reiss and Herth, 1985 ; Schramm *et al.*, 1983 ; Heslop-Harrison and Heslop-Harrison, 1992) decreased photopolarisation by 40% to an average 30% at 50 μM (Figure 3-1-4). From 50 μM to 100 μM the inhibitor had no increased effect on photopolarisation. 50% inhibition was obtained from 10-20 μM. Dissolution in ASW attenuated the effect of nifedipine. Photopolarisation decreased by a maximum 10% at 20 μM, whereas in DASW 20 μM nifedipine reduced photopolarisation by 25%. Extracellular Ca^{2+} did not only slow inhibition by nifedipine, it also reduced the maximum inhibitory effect of the drug.

Verapamil, (Lee and Tsien, 1983 ; Saunders and Hepler, 1983 ; Lehtonen, 1984 ; Lonergan 1990) caused dose-dependent inhibition of photopolarisation (Figure 3-1-5). 50 μM verapamil gave half inhibition. From 10-30 μM inhibition was slight, but increased sharply at higher concentrations. The zygote population appears to be divided into zygotes sensitive to low concentrations of verapamil (below 30 μM) and zygotes responsive only to higher concentrations of the drug (over 30 μM). Concentrations exceeding 100 μM caused cell lysis.

Bepridil (Figure 3-1-6) gave the most potent effect of all intracellular Ca^{2+} channel inhibitors used and affected all zygotes. At 4 μM bepridil, zygote polarisation was random (10% and not significantly different from 0%). Half inhibition was reached at an approximate concentration of 2 μM. 5 μM bepridil was lethal to the vast majority of zygotes (>90%), although survivors showed random polarity (result not shown due to the low numbers of zygotes involved).

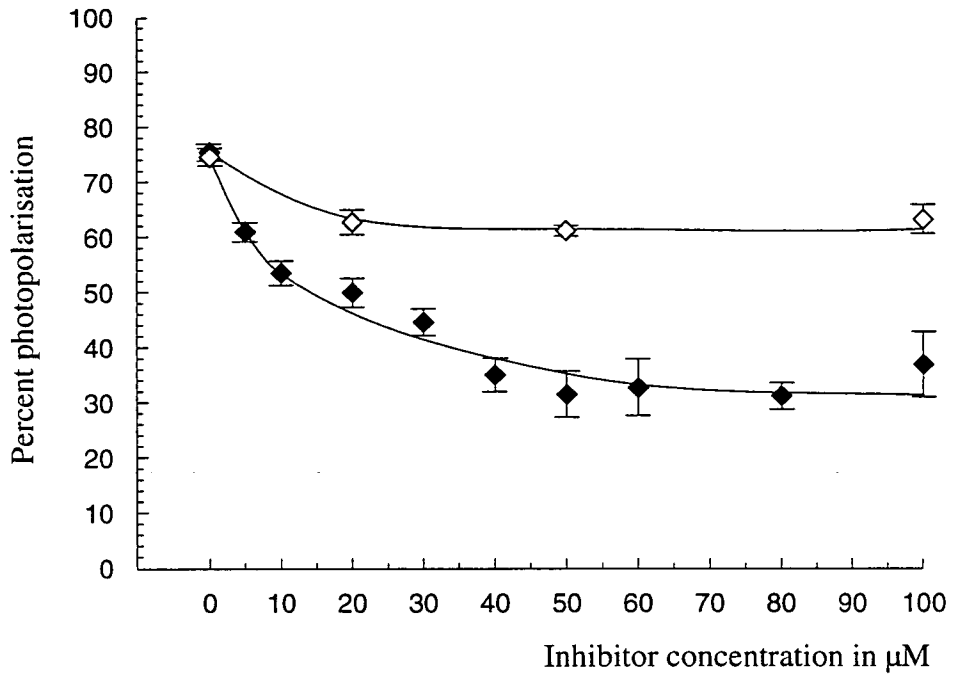

Figure 3-1-4. Effect of nifedipine on photopolarisation at 10-13 h AF.

Each point represents the mean value for 5 replicate experiments, with standard errors shown. Filled diamonds are for inhibitor dissolution in DASW, and open diamonds for dissolution in ASW. The presence of 9 mM Ca^{2+} in the medium reduced the effect of nifedipine to approximately half that when [Ca^{2+}] in the medium was reduced. Photopolarisation in DASW or ASW alone was not significantly different as demonstrated by a Mann-Whitney *U*-test (sample $U = 12 >$ significant $U = 2$).

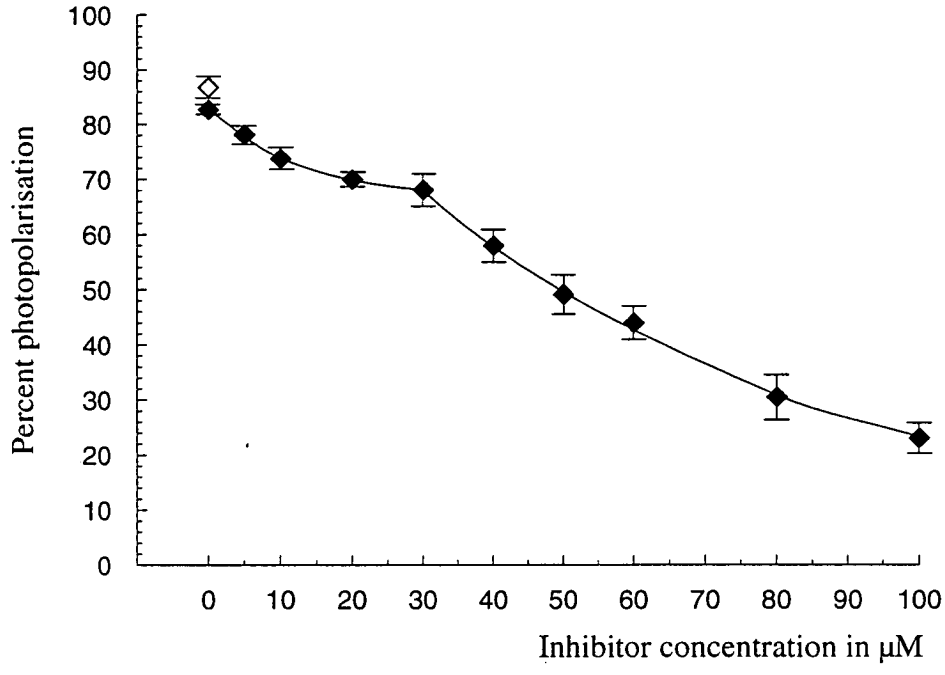

Figure 3-1-5. Effect of verapamil on photopolarisation at 10-13 h AF.

Each point represents the mean for 5 replicate experiments with standard errors. There was no significant difference between photopolarisation in ASW (open diamond) and in DASW (filled diamonds), as demonstrated by a Mann-Whitney *U*-test (sample $U = 4 >$ significant $U = 2$).
The graph displays a dichotomy in the action of verapamil on the zygote population. From 5 µM to 30 µM verapamil the inhibition is slight, but beyond 30 µM, inhibition increases sharply. The shape of the graph suggests that the zygote population is divided into two groups; a first group which is sensitive to verapamil, and a second which is only sensitive to the drug at higher concentrations. Different sensitivities may be due to zygotes primarily using one of alternative Ca^{2+} channel types which might differ in verapamil binding affinity.

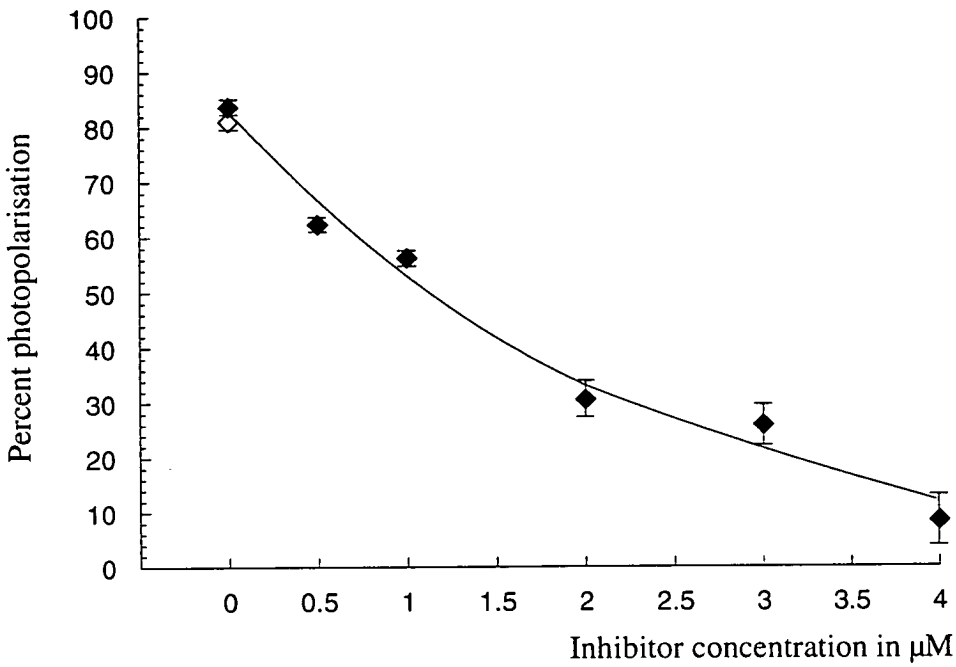

Figure 3-1-6. Effect of bepridil on photopolarisation at 10-13 h AF.

Points represent the mean value for 5 replicate experiments. Standard error bars are indicated. A Mann-Whitney *U*-test demonstrated no significant difference between percent photopolarisation in DASW (filled diamonds) and in ASW(open diamonds). For the test, sample $U = 6 >$ significant $U = 2$.

3. 1. 3 Effect of calmodulin inhibitors on photopolarisation

W7 binds to calmodulin, inhibiting the activities of calcium-calmodulin regulated enzymes (Hidaka *et al.* 1981 ; Poovaiah and Reddy, 1987). W7 caused dose dependent inhibition of photopolarisation in *F. serratus* zygotes (Figure 3-1-7). 50% inhibition occurred at approximately 30 μM. Below 20 μM, W7 had little effect but inhibition increased sharply between 20-50 μM. From 50-100 μM photopolarisation decreased further, and was random at approximately 80-100 μM.

TFP, a calmodulin antagonist chemically unrelated to W7 (Poovaiah and Reddy, 1987) inhibited photopolarisation in an almost linear manner (Figure 3-1-8). 4 μM TFP was fatal to over 90% of zygotes. Results at this concentration do not appear on the graph due to the small number of surviving embryos available for scoring. However, at 3 μM TFP enough zygotes survived the treatment for meaningful statistics ($n > 50$). At this concentration, photopolarisation was totally inhibited (0%). Approximately 2.5 μM gave 50% inhibition.

Calmidazolium (Figure 3-1-9) inhibited photopolarisation only in a sub-population of zygotes. From 0-3 μM, calmidazolium caused a 20% reduction in polarisation. Inhibition then increased sharply causing a further 20% reduction in photopolarisation, from 3-4 μM. Inhibitor concentrations exceeding 4 μM did not increase inhibition further. The percentage photopolarisation did not fall below a minimum 30%, indicating that approximately one third of the zygote population were insensitive to the drug. 50% inhibition was attained at 3 μM.

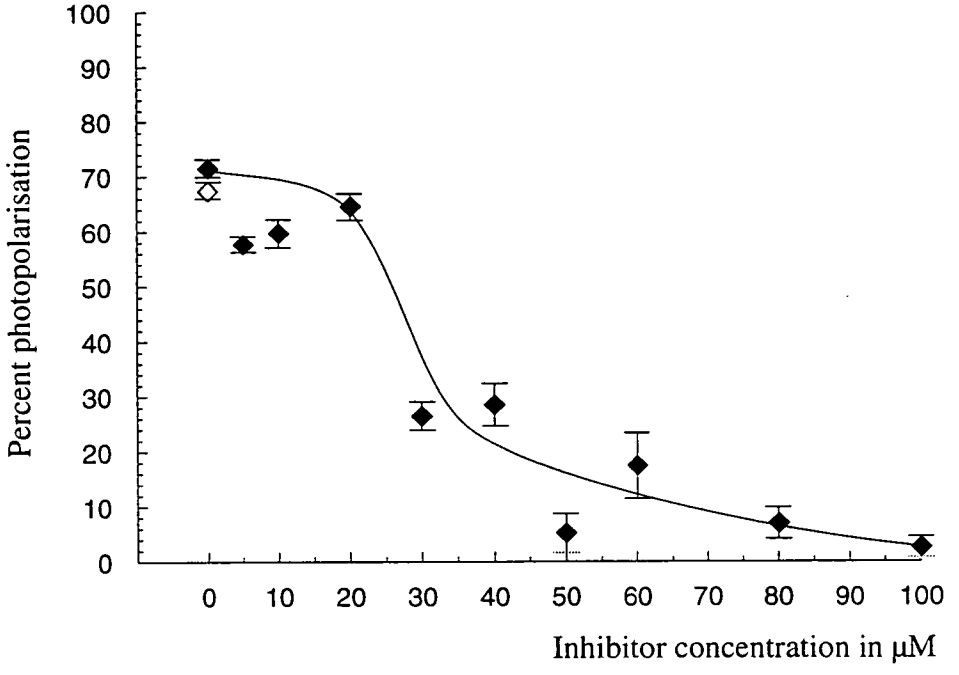

Figure 3-1-7. Effect of W7 on photopolarisation from 10-13 h AF.

Each point represents the mean of 5 replicate experiments with standard error bars shown. The difference in photopolarisation between zygotes incubated in ASW (open diamond) or in DASW (filled diamonds) is not significant (Mann-Whitney *U*-test: Sample $U = 5 >$ significant $U = 2$).

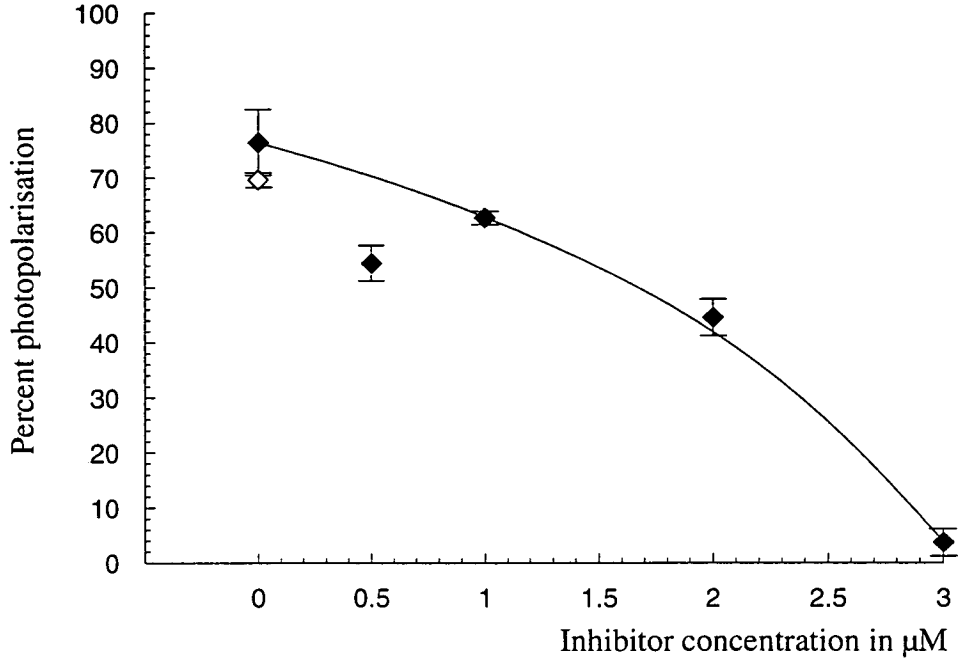

Figure 3-1-8. Effect of TFP on photopolarisation at 10-13 h AF.

Points represent the mean of 5 replicate experiments. Standard errors are indicated by bars. A Mann-Whitney *U*-test showed no significant difference (sample $U = 12 <$ significant $U = 2$) between photopolarisation in ASW (open diamond) or in DASW (filled diamonds).

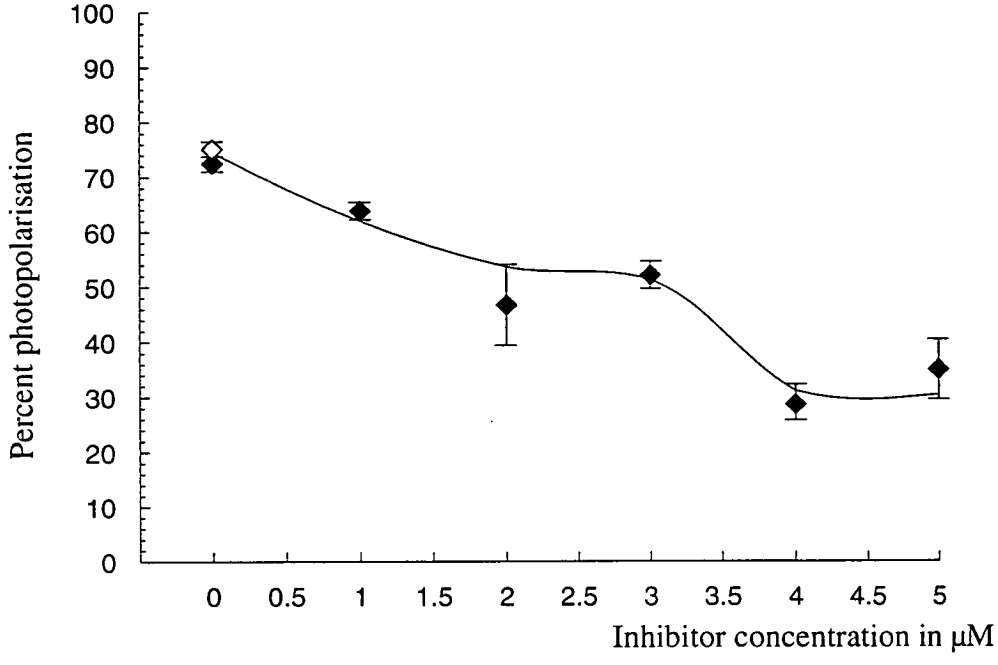

Figure 3-1-9. Effect of calmidazolium on photopolarisation.

Each point represents the mean value of photopolarisation for 5 replicate experiments. Standard error bars are given. There was no significant difference between photopolarisation of zygotes cultured in ASW (open diamond) and those cultured in DASW (filled diamond): Mann-Whitney *U*-test; sample $U = 6 >$ significant $U = 2$.

3. 1. 4 Effects of other inhibitors on photopolarisation

Colchicine, an inhibitor of microtubule polymerisation, cytochalasin B, a microfilament inhibitor, neomycin which suppresses the IP_3 mediated transduction pathway by inhibiting the release of IP_3 from plasma membrane bound PIP_2, and acridine orange, an inhibitor of protein kinase C all had no significant effect on photopolarisation of *F. serratus* zygotes, although inhibitors were administered to toxic levels (Figure 3-1-10).

3. 2 Calmodulin extraction from *Fucus serratus* tissues

To ascertain further the role of calmodulin during photopolarisation, further information regarding the calmodulin of *F. serratus* was required (Section *1. 6. 3*). The protein was extracted from egg and sperm lysates with a view to amino acid sequencing and eventual microinjection into developing zygotes. Extractions were therefore assessed in terms of calmodulin yield, purity, and consistency of the method.

3. 2. 1 Homogenates

Egg homogenates were extremely viscous due to algal polysaccharides. During ammonium sulphate fractionation, protein precipitation caused the viscosity of egg homogenates to increase until the added $(NH_4)_2 SO_4$ clumped in a cohesive mass which failed to dissolve homogenously. Consequently, it was impossible to gradually and uniformally increase $[(NH_4)_2 SO_4]$ in egg homogenates, and to accomplish protein fractionation. The viscosity of egg homogenates also impeded ion exchange chromatography by obstructing the free flow of buffer through the column. Sperm homogenates were also viscous, but amenable to both ammonium sulphate fractionation and ion exchange chromatography.

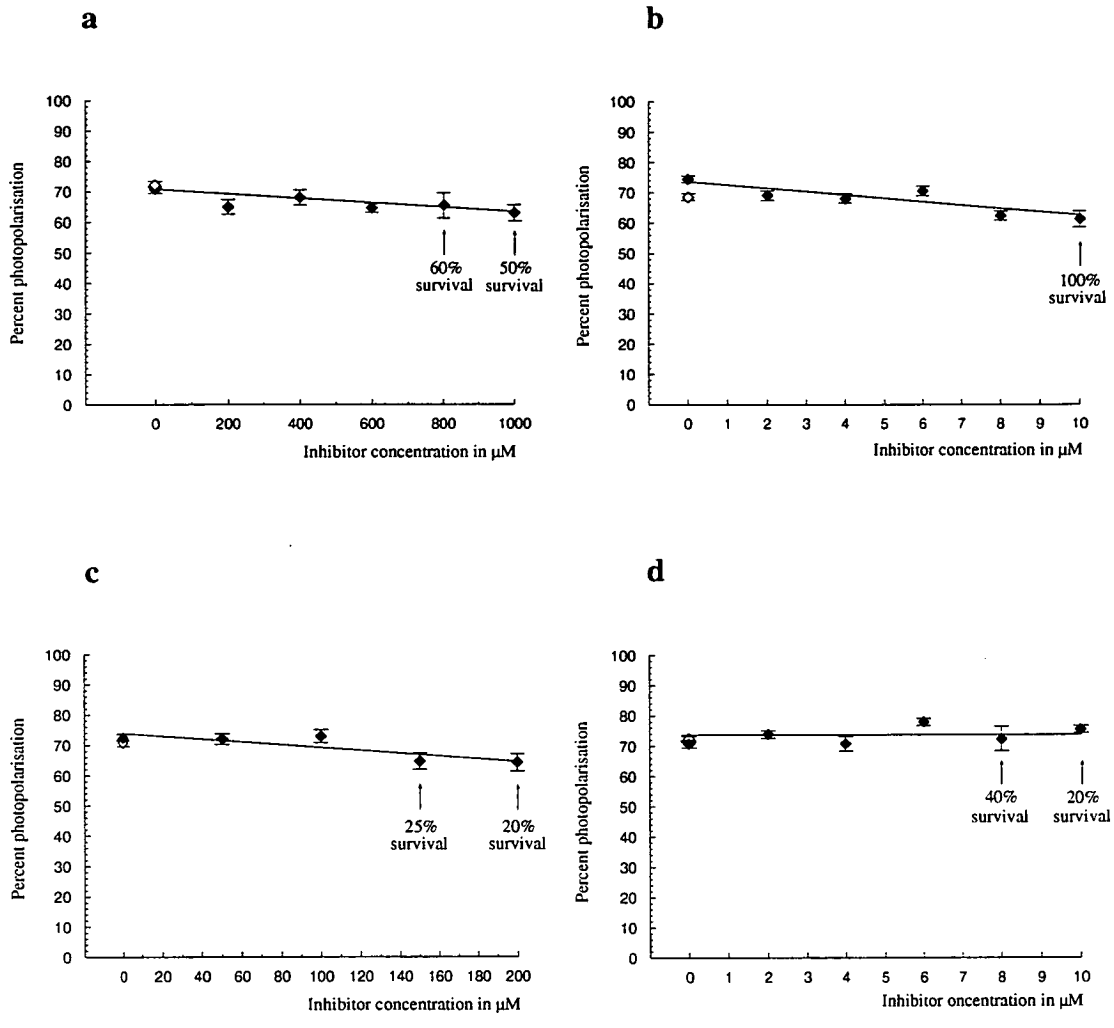

Figure 3-1-10. Effect of colchicine (**a**), cytochalasin B (**b**), neomycin (**c**) and acridine orange (**d**) on photopolarisation at 10-13 h AF.

Points represent the mean percent photopolarisation of 5 replicate experiments. Standard error bars are shown. For colchicine, neomycin and acridine orange there was no significant difference in photopolarisation between zygotes cultured in DASW (filled diamonds) or in ASW (open diamonds). In a Mann-Whitney *U*-test, sample $U = 6$, 7 and 7 respectively > significant $U = 2$). For cytochalasin B, the difference between photopolarisation in ASW and in DASW was significant (sample $U = 1$ < significant $U = 2$).
When cell survival was less than 100%, it is indicated on the figures.

3. 2. 2 Ammonium sulphate fractionation and W7 affinity chromatography

SDS PAGE analysis (Section **2. 3**) of protein fractions purified by ammonium sulphate fractionation and W7 affinity chromatography showed a single protein band with an electrophoretic mobility of approximately 16 kDa, corresponding to the molecular weight of calmodulin (Figure 3-2-1). The sample was one third of the total collected fraction. The amount of calmodulin loaded onto the gel was estimated to be 0.5 µg. Total calmodulin yield was therefore estimated at approximately 1.5 µg, that is 0.15 µg of calmodulin per gram of tissue, one hundredfold less than the average quantity of calmodulin extracted from plant tissues (Marmé and Dieter, 1983). One out of three replicate extractions yielded sufficient calmodulin to be detected by SDS PAGE.

3. 2. 3 Ion exchange chromatography and W7 affinity chromatography

Samples eluted from ion exchange chromatography and purified by W7 affinity chromatography showed no calmodulin protein band following SDS PAGE (Figure 3-2-2). A replicate extraction gave the same result.

3. 3 Cloning the calmodulin nucleotide sequence from *Fucus serratus*

Following the difficulties in extracting sufficient calmodulin from *F. serratus* tissues for sequencing and protein microinjection, it was proposed to clone the calmodulin cDNA or gene from *F. serratus*. This would lead to both knowledge of the calmodulin sequence and to production of *F. serratus* calmodulin in bacteria (Figure *1. 6. 3*).

3. 3. 1 RNA extraction

RNA was successfully extracted from eggs or 24 h zygotes of *F. serratus*, but not from sperm. For all RNA samples, polysaccharide contamination represented a major problem, and was assessed according to

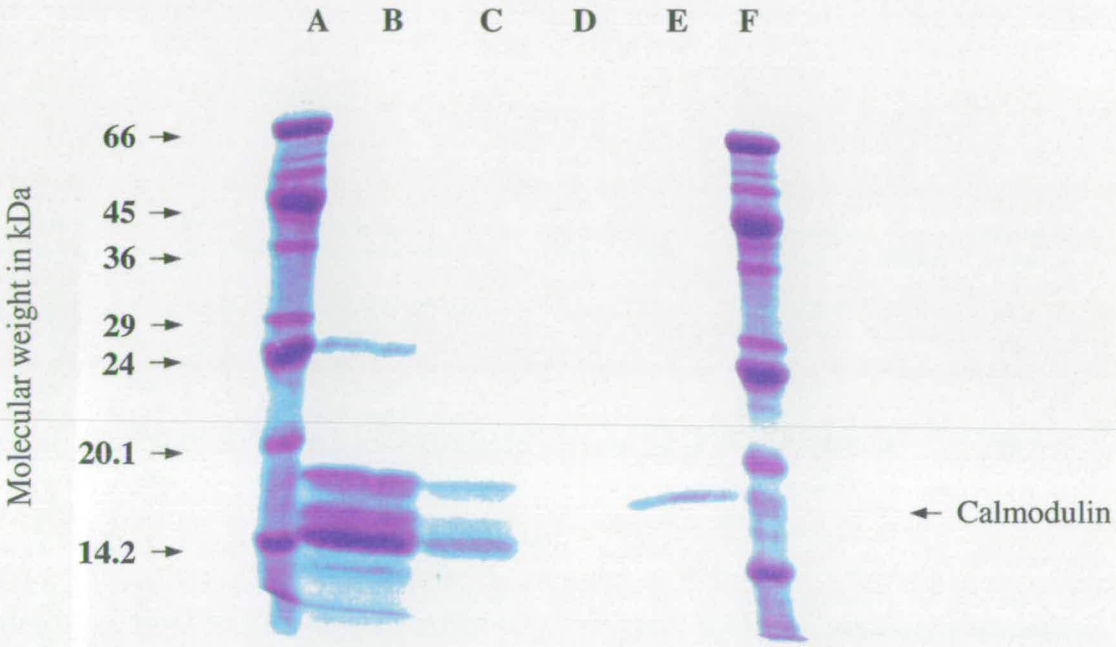

Figure 3-2-1. SDS PAGE of calmodulin purified by $(NH_4)_2 SO_4$ fractionation and W7 affinity chromatography.

Lanes A and F: Molecular weight markers (Sigma). 1 µg of each standard was loaded. Molecular weights are indicated.
Lane B: 50 µl W7 affinity column wash fraction 11.
Lane C: 50 µl W7 affinity column wash fraction 15.
Lane D: 50 µl W7 affinity column wash fraction 20.
Lane E: 50 µl calmodulin elution fraction 2. A single band migrating at approximately 16 kDa, the molecular weight of calmodulin, is evident. The estimated amount of protein present in the sample is 0.5 µg. Total fraction volume recovered was 150 µl.

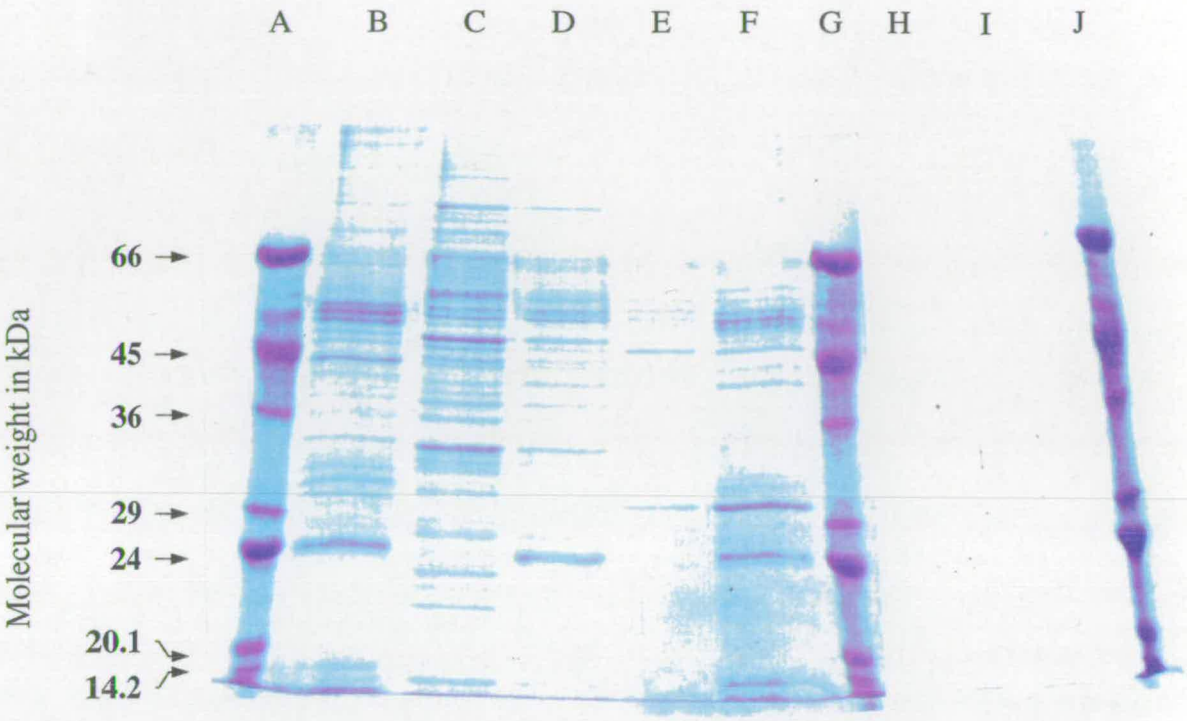

Figure 3-2-2. SDS PAGE of calmodulin purified by ion exchange chromatography and W7 affinity chromatography.

Lanes A, G and J: Molecular weight markers (Sigma). 1 µg of each standard was loaded. Molecular weights are indicated.
Lane B: 50 µl crude sperm extract.
Lane C: 50 µl NP1, fraction 6.
Lane D: 50 µl NP1, fraction 7.
Lane E: 50 µl NP2, fraction 6.
Lane F: 50 µl NP2, fraction 7.
Lane H: 50 µl calmodulin elution from W7 affinity column, fraction 2. A pooled sample of NP1, fractions 2-13, was loaded onto the W7 affinity column.
Lane I: 50 µl calmodulin elution from W7 affinity column, fraction 2. A pooled sample of NP2, fractions 6-9, was loaded onto the W7 affinity column.

several criteria including the aspect of RNA pellets at the different steps of extraction, the ease with which they dissolved, and the viscosity of the final RNA solution. Moreover, a spectrophotometric absorbance scan from λ = 320-220 nm was performed on RNA from each extraction method and compared against a scan of polysaccharides secreted by *F. serratus* fronds (Figure 3-3-1).

RNA purified by density separation over a sucrose cushion (Okayama *et al.*, 1987) exhibited a spectrophotometric absorbance curve similar to that of polysaccharides secreted by *F. serratus* (Figure 3-3-2). Following re-suspension of the polysaccharide-RNA pellet and RNA precipitation by LiCl, polysaccharide contamination was reduced, but RNA was lost.

Repeated phenol extractions (Masters *et al.*, 1988) yielded low amounts of RNA, with erratic results. Polysaccharide contamination was high in these samples (Figure 3-3-3). Enhancing RNA yield by increasing the amount of tissue used in the extraction was unsuccessful. Moreover, the cost of RNAsin required to inhibit RNA degradation during homogenisation rapidly became prohibitive for large amounts of tissue. RNasin was therefore replaced with 4 M guanidine thiocyanate, a potent denaturing agent and RNase inhibitor (Chirgwin *et al.*, 1979). Using this method, RNA was extracted from both eggs and 24 h zygotes (Figure 3-3-4). Yield, however, was low and erratic and polysaccharide contamination high. Back extraction of the first phenolic phase with extraction buffer enhanced polysaccharide contamination without increasing RNA yield. A mass of polysaccharide was ethanol precipitated from the lysate, along with RNA, prior to polysaccharide cleansing. The resulting gelatinous pellet was difficult to re-dissolve, and might partially account for the low RNA yield. It was hoped that the acidification of the phenolic phase, which drives DNA

a

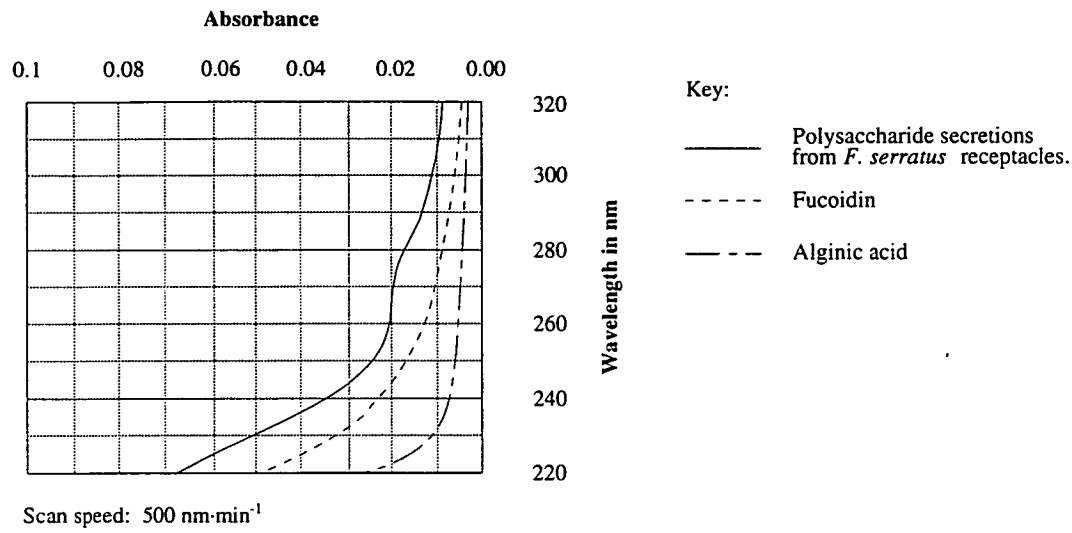

b

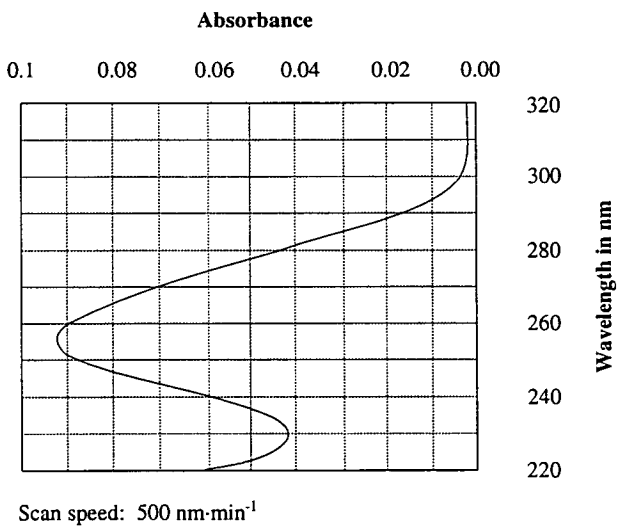

Figure 3-3-1. Spectrophotometric absorbance of *Fucus* polysaccharides and DNA.

a: Spectrophotometric absorbance of *Fucus* polysaccharides. Polysaccharides were secreted from *F. serratus* receptacles, bathed in ASW at 14 °C and the solution cleared by centrifugation in a MSE Microcentaur at 13,000 r.p.m. for 5 min. Fucoidin was extracted from *F. vesiculosus* fronds, and was a kind gift from L. Kennedy. Alginic acid was from Sigma Chemical company, U.K.

b: Spectrophotometric absorbance of *F. serratus* sperm DNA, extracted on a CsCl gradient (Section *2. 10. 8*).

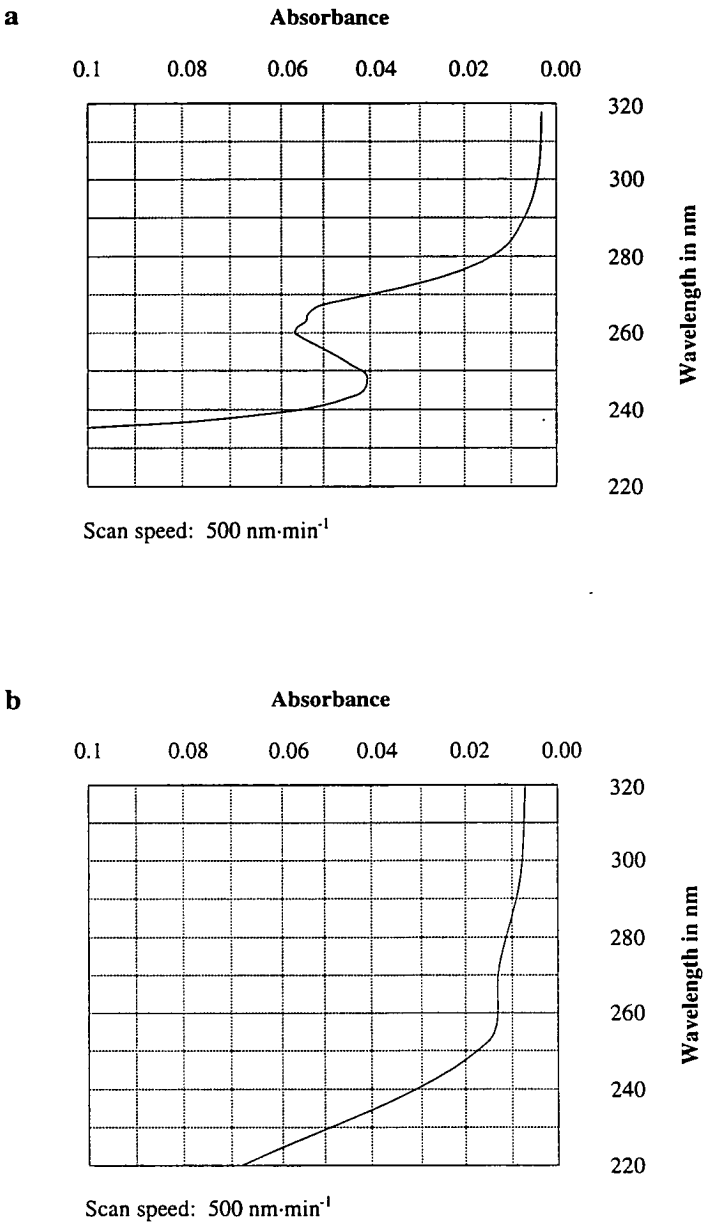

Figure 3-3-2. Spectrophotometric absorbance of RNA extracted from 1 g of *Fucus serratus* eggs, by density separation.

5 µl of each sample was diluted 100 fold in DEPC-H_2O.

a: Sample collected following isopycnic separation, prior to LiCl precipitation (5 µl sample from 100 µl). The curve shows both high RNA levels (280-260 nm) and considerable polysaccharide contamination of the sample (> 240 nm).

b: Final RNA sample (5 µl from 10 µl). RNA was lost (gel not shown) and polysaccharide contamination still considerable.

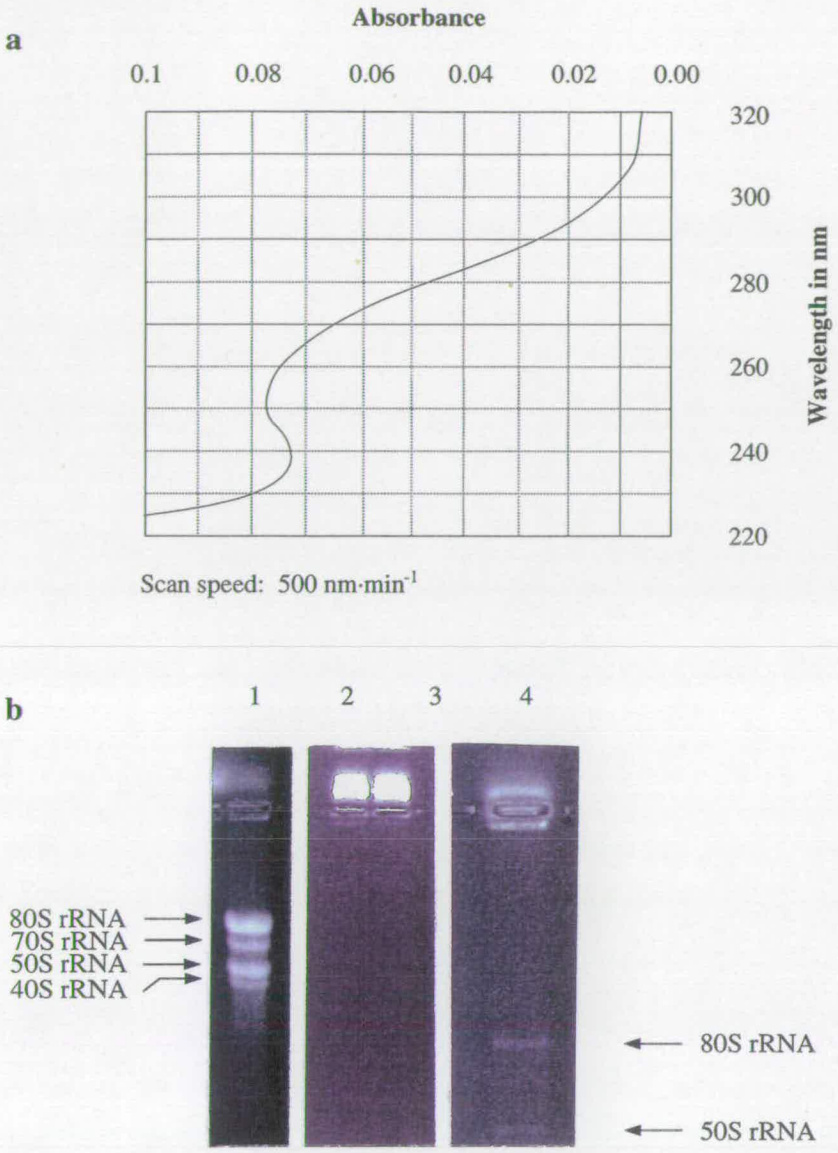

Figure 3-3-3. RNA, extracted from *Fucus serratus* eggs or zygotes by repeated phenol extractions.

a: Spectrophotometric scan of sample 1 ((**b**), track 1). 5 µl out of 20 µl sample was diluted to 500 µl in DEPC-H_2O.

b: Denaturing agarose gel electrophoresis of replicate RNA extractions. Samples in lanes **1** and **4** only gave visible RNA bands. Bands are rRNA, and their sizes are indicated.

Lane 1: 5 µl RNA from 20 µl sample, extracted from 1 ml packed eggs.
Lanes 2 and **4:** 10 µl RNA from 20 µl sample, extracted from 1ml eggs.
Lane 3: 10 µl RNA from 20 µl sample, extracted from 1 ml zygotes.

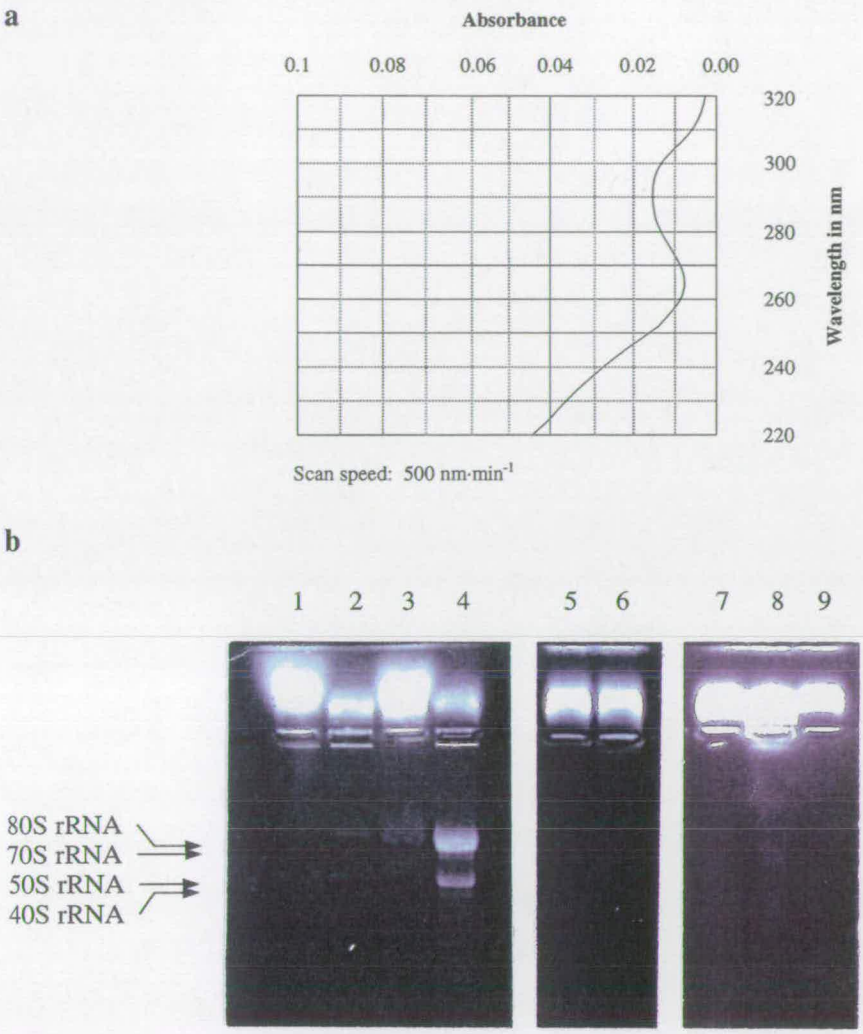

Figure 3-3-4. RNA extracted from *Fucus serratus* tissues by guanidine thiocyanate, followed by NaCl-ethanol wash.

a: Spectrophotometric absorbance of 5 µl out of 20 µl, diluted 100 fold.

b: Denaturing RNA gel of replicate extractions. rRNA sizes are shown.

Lanes 1 and **3:** 5 µl from 200 µl sample egg (**1**) or zygote (**3**) RNA, before LiCl precipitation (extracted from 1 ml tissue).
Lanes 2 and **4:** 5 µl from 20 µl sample egg (**2**) or zygote (**4**) RNA following LiCl precipitation. Note RNA in lane **4**.
Lanes 5 and **6**: 5 µl (**5**) and 20 µl (**6**) out of a 100 µl sample of RNA extracted from 1 ml packed zygotes. The final pellet was large, hence dissolution in 100 µl. The gel, coupled with a spectrophotometric scan showed the pellet to be precipitated polysaccharides.
Lane 7: 20 µl out of 100 µl sample RNA, extracted from 3 g zygotes.
Lane 8 and **9:** 20 µl out of two replicate, 100 µl RNA samples extracted from 3 g (fresh weight) of frond apices.

into organic solution (Logemann *et al.*, 1987), might also reduce polysaccharide contamination. Results, however, were negative (result not shown).

RNA extraction using a CTAB based lysis buffer (Apt, *pers. comm.* 1993) yielded high amounts of intact RNA from ml quantities of eggs and zygotes (Figure 3-3-5) with lower polysaccharide contamination. Replicate extractions, however, showed the method to be inconsistent.

The method of Su and Gibor (1988) was complex and produced no RNA, either from eggs or from fronds, in two replicate experiments (result not shown). Although successful for large amounts of algae, this method is not applicable to RNA extractions from small (~1 g) amounts of tissue.

3. 3. 2 DNA extraction and analysis

Spectrophotometric analysis of DNA extracted from 10 g concentrated *F. serratus* sperm suspension (Figure 3-3-6) showed a typical curve for pure DNA (Sambrook *et al.*, 1989). Methylation of DNA is known to impede PCR (McPherson *et al.*, 1991), hence DNA was digested with the restriction endonucleases Msp I and Hpa II (Promega) which recognise the $^{5'}$CC$^{\wedge}$GG nucleotide motif, cleaving between the two cytosines. Msp I is insensitive to internal cytosine methylation while Hpa II is sensitive to both internal and 5' cytosine methylation (Nelson and McClelland, 1991). Digestion with these two endonucleases gave a similar smear pattern on a 1% agarose-TAE gel, indicating no particular methylation of the DNA (Figure 3-3-6).

Southern blots were carried out on sperm DNA, treated with various restriction endonucleases (Figure 3-3-7). The calmodulin cDNA from *C. reinhardtii* (Zimmer *et al.*, 1988) hybridised to the Southern blot filter indicating that a homologous sequence is present in the genome of *F. serratus* (Figure 3-3-8). Without additional knowledge of the *F. serratus*

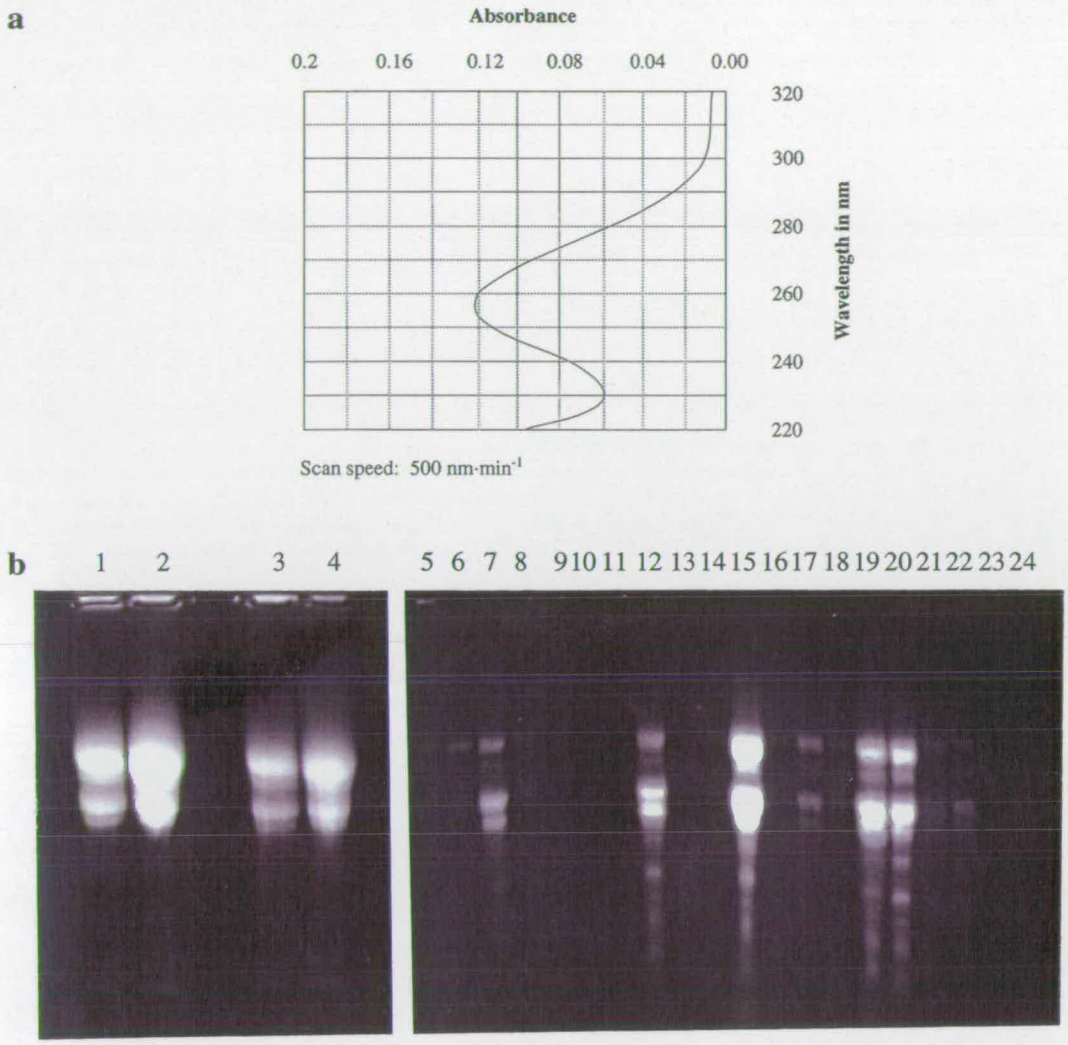

Figure 3-3-5. RNA extracted from eggs or zygotes using CTAB.

(a) Spectrophotometric scan of 5 µl RNA (from 100 µl sample), diluted 100 fold in DEPC-H_2O.

(b) Denaturing RNA gel of replicate RNA extractions. rRNA sizes are not indicated due to the differences between the gels, though rRNA bands are clearly visible. Note high RNA yield and variability of replicate extractions.

Lanes 1 and **2:** 2 µl (**1**) and 5 µl (**2**) from 100 µl RNA sample, extracted from 1 ml packed eggs.
Lanes 3 and **4:** 2 µl (**1**) and 5 µl (**2**) from 100 µl RNA sample, extracted from 1 ml zygotes.
Lane 4: Replicate RNA extraction from 1 g sperm suspension.
Lane 5: Replicate RNA extraction from 1 ml packed eggs.
Lanes 6-24: Replicate RNA extractions from 0.5-1 ml zygotes.

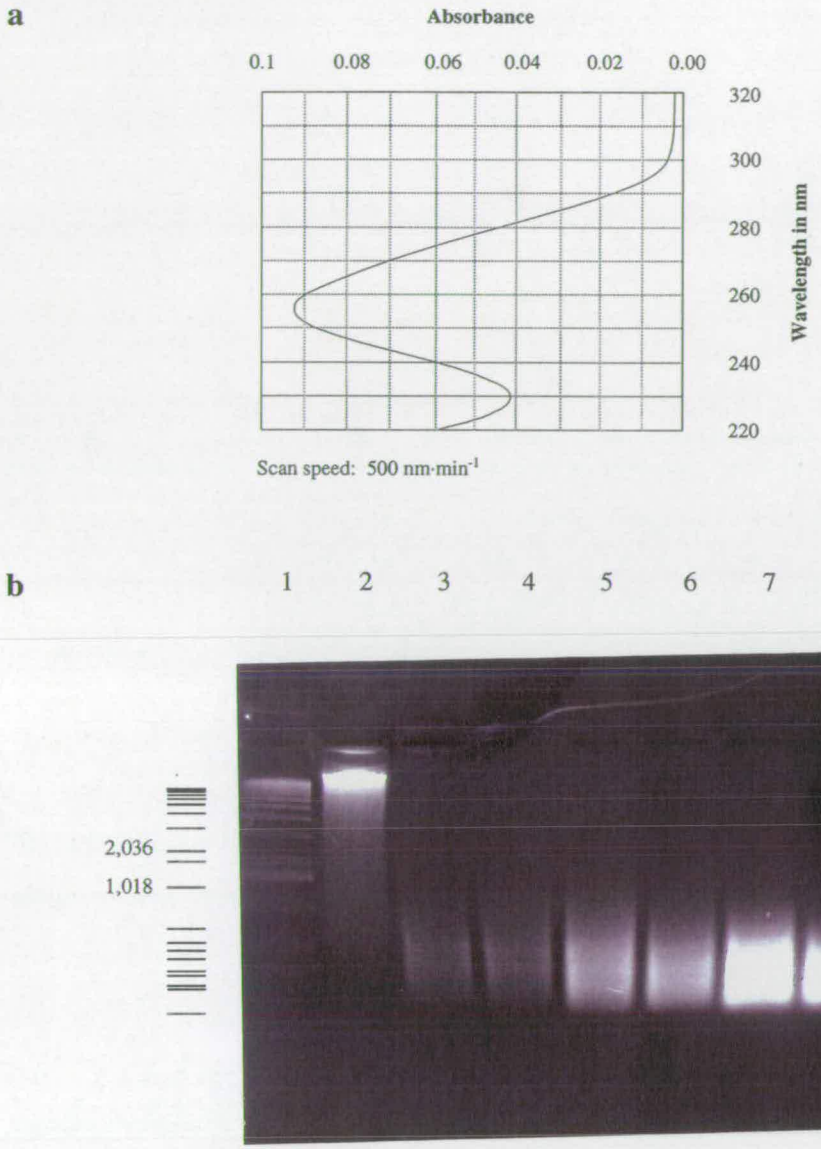

Figure 3-3-6. Analysis of *Fucus serratus* sperm DNA.

(a) Spectrophotometric absorbance of DNA. 10 µl DNA were diluted to 1 ml with H_2O.

(b) 1% agarose-TAE gel of sperm DNA digested with Msp I and Hpa II.

Lane 1: 1 µg 1 kb DNA Ladder (GIBCO).
Lane 2: 1 µg undigested sperm DNA.
Lanes 3, 5 and **7:** 0.5 µg, 1 µg and 2 µg of sperm DNA, digested with Msp I (methylation sensitive).
Lanes 4, 6 and **8:** 0.5 µg, 1 µg and 2 µg of sperm DNA, digested with Hpa III (methylation insensitive).

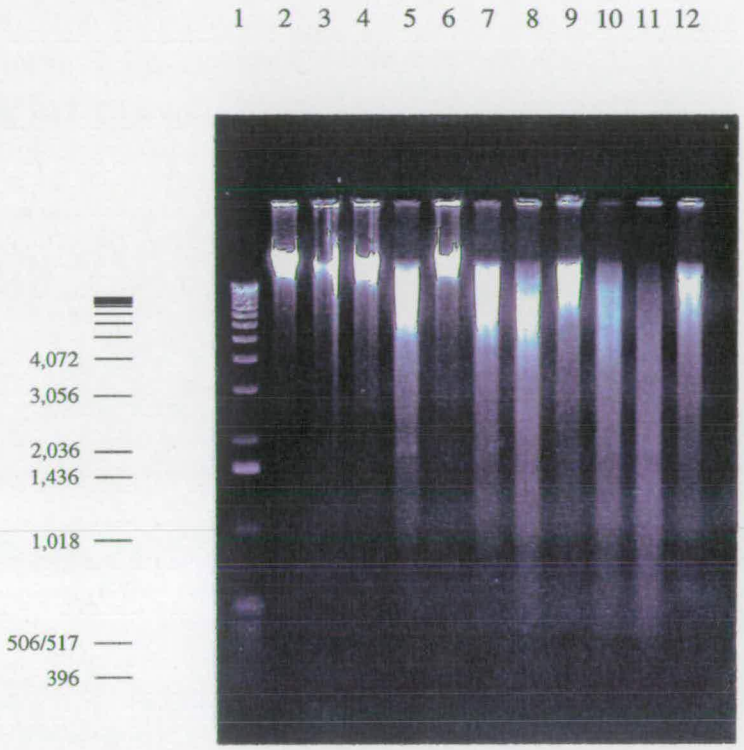

Figure 3-3-7. Restriction digests of *Fucus serratus* sperm DNA.

2 µg of sperm DNA was incubated in the appropriate buffer with 12 U of a restriction endonuclease, for 2 h, at 37 °C. A further 12 U of enzyme was added to the reaction which was incubated for another 3 h. Reactions were run on a 1% agarose-TAE gel, at 10 mA for 12 h. DNA was visualised by EtBr staining. DNA was then transferred to a nylon membrane by Southern blotting.

Lane 1: 1 µg 1 kb DNA ladder (GIBCO).
Lane 2: 2 µg undigested sperm DNA.
Lanes 3-12: 2 µg sperm DNA, respectively digested with 12 U Bam HI, Bcl I, Eco RI, Hind III, Nde I, Pst I, Sal I, Sac I, Sty I, and Xba I (GIBCO, BRL).

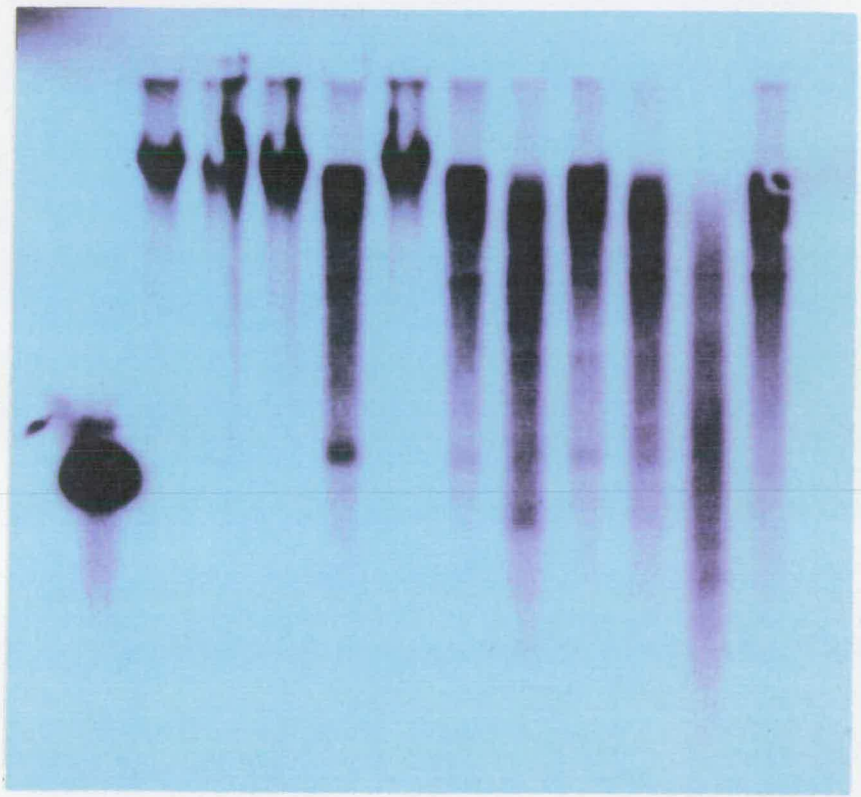

Figure 3-3-8. Autoradiograph of *Fucus serratus* sperm DNA Southern blot, probed with the *Chlamydomonas reinhardtii* calmodulin cDNA, labelled with ^{32}P.

DNA (Figure 3-3-7) was transferred to a Hybond membrane as described in Section *2. 9. 2.* The radioactive probe was hybridised to the blot overnight at 65 °C (Section *2. 9. 5*), and the blot autoradiographed for 8 h.

Several bands are visible in each track. Sequences exhibiting homology to the probe are therefore present in *F. serratus* genomic DNA.

calmodulin gene sequence, that is without a restriction map of the gene, further inferences regarding the characteristics of the calmodulin gene (*e.g.* the number of gene copies per genome) cannot be drawn.

3. 3. 3 In vitro amplification of Fucus serratus calmodulin nucleotide sequence

Using 236 V-Q 34 (Figure 3-3-9) or 113 Y-Q 34 (Figure 3-3-10) as primers, PCR of *F. serratus* cDNA produced no amplified product (thermal cycling programs indicated on the figures). cDNA was synthesised using RNA extracted using the method of Masters *et al.* (1992). Positive controls using p6-8.11 (Zimmer *et al.*, 1988) in the presence of 5 µg oligo dT or 5 µg random hexamer (Section *2. 11. 2*), demonstrated that the presence of these oligonucleotides did not impede the amplification process (Figure 3-3-10).

Using genomic DNA as template and 236 V-Q 34 as primers, *in vitro* amplification consistently synthesized a DNA fragment, migrating on a TAE-agarose gel with a molecular weight of approximately 517 bp, noted B517 (Figure 3-3-11). Due to possible introns, the expected size of the PCR fragment was impossible to determine. For example the *C. reinhardtii* calmodulin gene possesses 3 introns between 236 V and Q 34 (Zimmer *et al.*, 1988), giving a fragment size of 1017 bp. In *A. thaliana* (EMBL identifier; em_pl:s40050), the calmodulin gene yields a putative PCR fragment of 847 bp, between 236 V and Q 34. B517 amplification was dependent on both primer concentration and thermal cycling parameters. Following optimisation of the reaction, B517 was amplified in bulk, purified from the agarose gel, and cloned into the *Sma* I site of pBluescript SK-. 8 clones were identified as possessing the B517 insert and sequenced. Sequencing revealed that 7 cloned fragments were due to artefactual Q 34 annealing at both ends of the DNA product (Figure 3-3-12). The remaining clone displayed 236 V forward priming and Q 34 reverse priming, but the

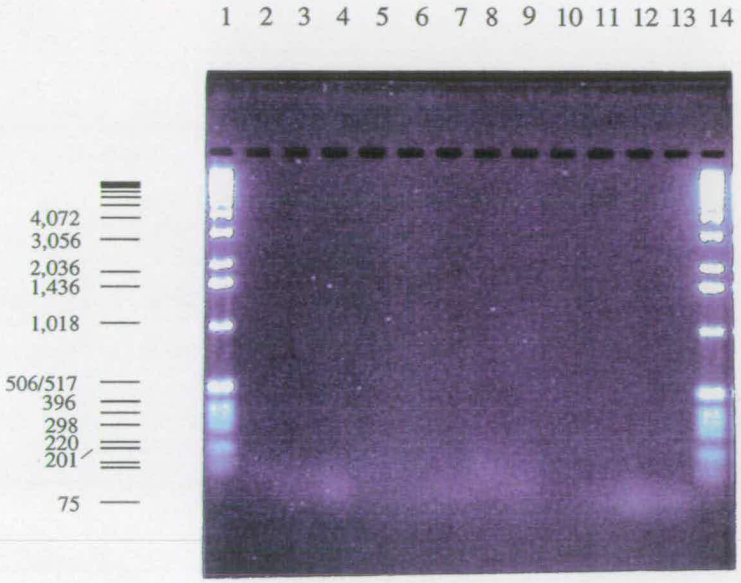

Figure 3-3-9. PCR of *Fucus serratus* cDNA (236 V-Q34).

The amplification reaction was performed as described in Section *2. 11. 2.* Priming was with 236 V and Q 34. The PCR program was 20 s denaturation at 94 °C, 1 min annealing at 40 °C and 1 min 30 s extension at 70 °C. PCR samples (12 µl) were analysed on a 3% agarose-TAE gel, after 30, 45 and 60 cycles. Results were similar over a range of annealing temperatures/times and extension times.

Lane 1: 1 µg 1 kb DNA Ladder (GIBCO, BRL).
Lanes 2-4: cDNA amplification after 30, 45 and 60 cycles, respectively.
Lanes 5-7: cDNA, 236 V single primer control (30, 45 and 60 cycles).
Lanes 8-10: cDNA, Q 34 single primer control (30, 45 and 60 cycles).
Lanes 11-13: Water control, no DNA present (30, 45 and 60 cycles).
Lane 14: 1 µg 1kb DNA Ladder (GIBCO, BRL).

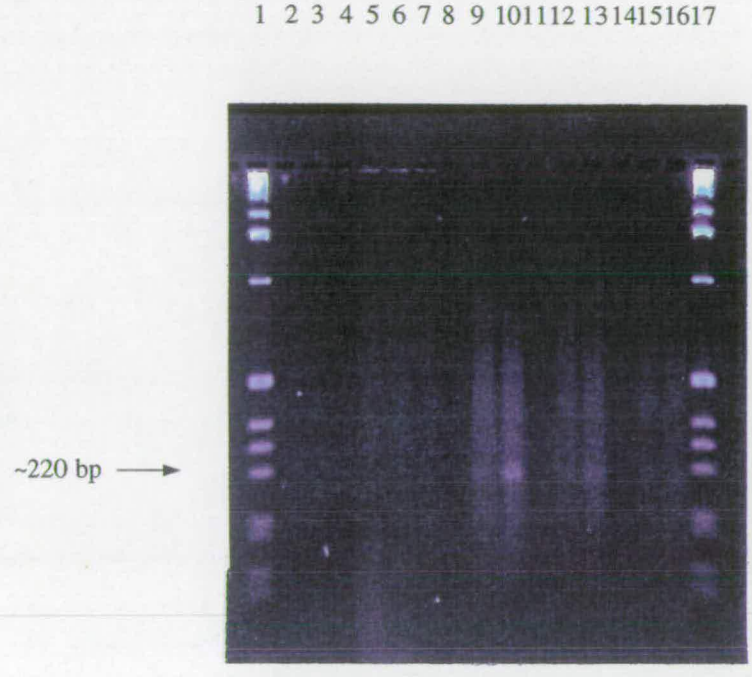

Figure 3-3-10. PCR of *Fucus serratus* cDNA (113 Y-Q34).

The amplification reaction was primed with 113 Y and Q 34, and performed as described in Section *2. 11. 2.* The target cDNA was synthesised with oligo-dT or with the random hexamer (noted T-cDNA and H-cDNA respectively). As a positive control, 1 pg *Chlamydomonas reinhardtii* calmodulin cDNA (p6-8.11) was amplified in the presence of 1 M oligo-dT or 1 M random hexamer. Thermal cycling was 30 s denaturation at 94 °C, 2 min annealing at 35 °C and 2 min extension at 70 °C. PCR samples (12 µl) were analysed on a 3% agarose-TAE gel, after 20, 40 and 60 cycles.

Lane 1: 1µg 1 kb DNA Ladder (GIBCO, BRL).
Lanes 2-4: T-cDNA amplification after 20, 40 and 60 PCR cycles.
Lanes 5-7: H-cDNA amplification (20, 40, 60 cycles).
Lanes 8-10: p6-8.11 / 1 M oligo-dT amplification (20, 40, 60 cycles).
Lanes 11-13: p6-8.11 / 1M random hexamer (20, 40, 60 cycles).
Lanes 14-16: Water control (20, 40, 60 cycles).
Lane 17: 1 µg 1 kb DNA Ladder (GIBCO, BRL).

Note a PCR fragment, migrating with the expected size of approximately 220 bp is present in the p6-8.11 controls (arrow). This demonstrates that the PCR was not impeded by the presence of either oligo-dT or the random hexamer.

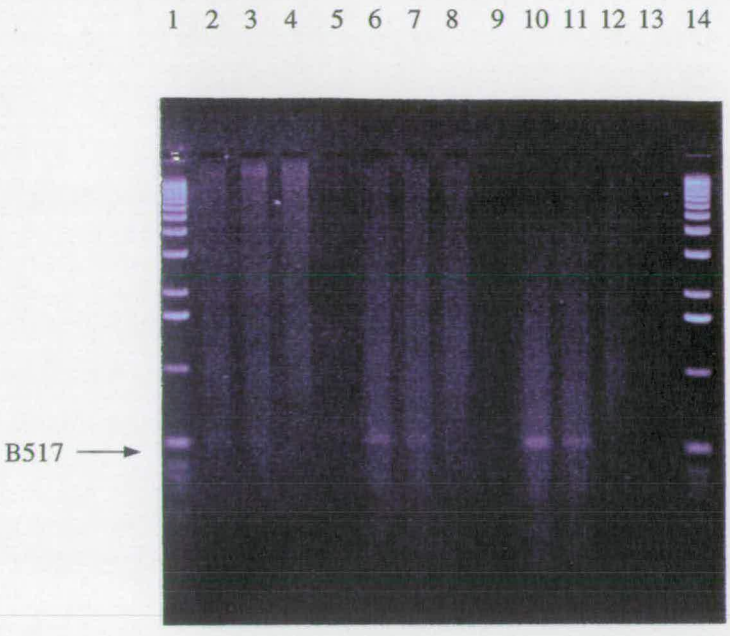

Figure 3-3-11. PCR of *Fucus serratus* genomic DNA (236 V-Q 34).

The amplification reaction was performed as explained in Section *2. 11. 2* and primed with 236 V and Q 34. Two replicates were performed. Thermal cycling was 30 s denaturation at 94 °C, 2 min annealing at 40 °C and 2 min extension at 70 °C. PCR samples (12 µl) were analysed on a 3% agarose-TAE gel, after 20, 30 and 40 cycles.

Lane 1: 1µg 1 kb DNA Ladder (GIBCO, BRL).
Lane 2: Genomic DNA amplification reaction 1, after 20 cycles.
Lane 3: Genomic DNA amplification reaction 2, after 20 cycles.
Lane 4: No primer control, after 20 cycles.
Lane 5: Water control (no DNA), after 20 cycles.
Lane 6: Genomic DNA amplification reaction 1, after 30 cycles.
Lane 7: Genomic DNA amplification reaction 2, after 30 cycles.
Lane 8: Control reaction without primers, after 30 cycles.
Lane 9: Water control (no DNA), after 30 cycles.
Lane 10: Genomic DNA amplification reaction 1, after 40 cycles.
Lane 11: Genomic DNA amplification reaction 2, after 40 cycles.
Lane 12: No primer control, after 40 cycles.
Lane 13: Water control (no DNA), after 40 cycles.
Lane 14: 1µg 1 kb DNA Ladder (GIBCO, BRL).

Note the consistent presence of a single PCR product, migrating at approximately 517 bp (labelled B517).

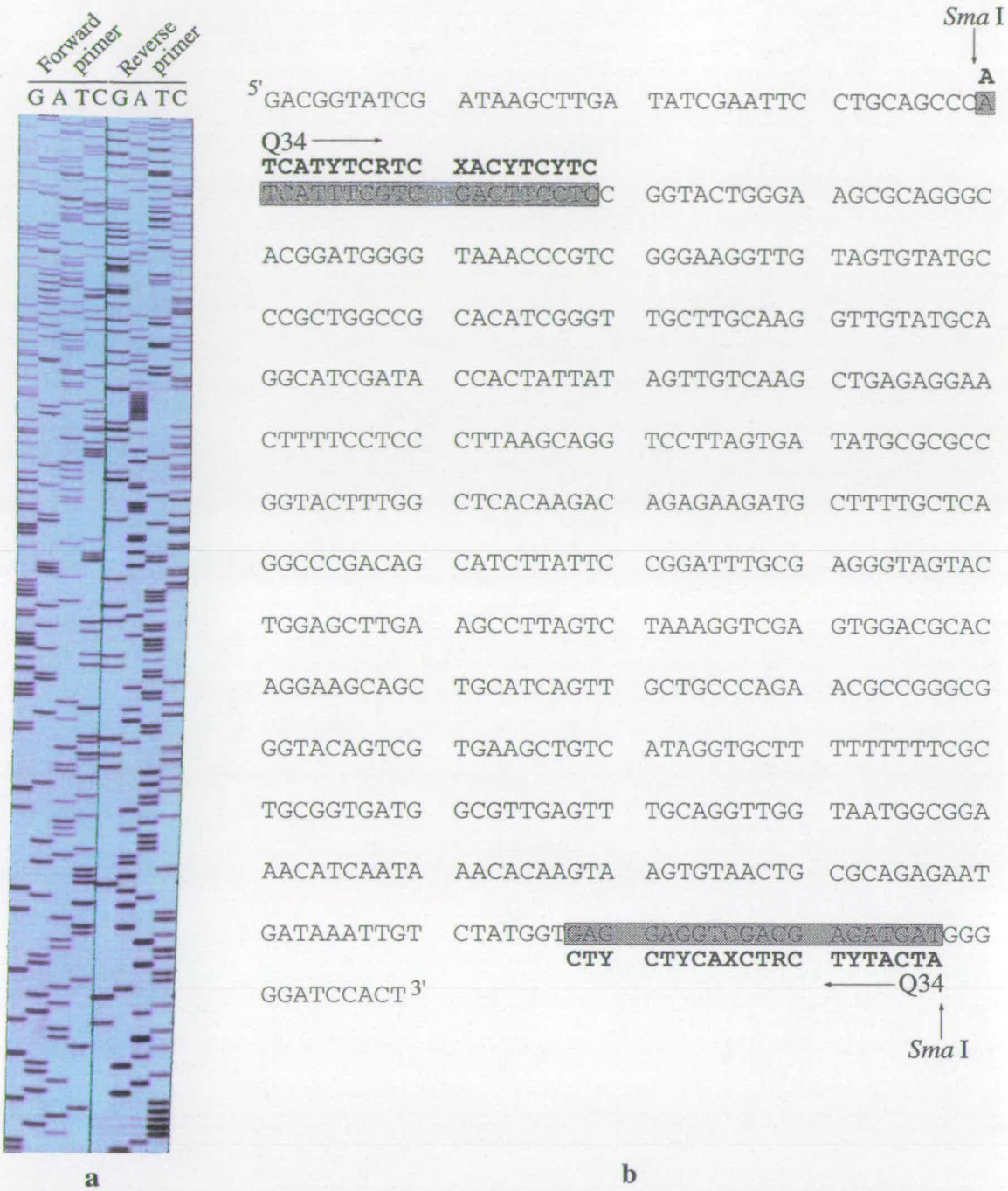

Figure 3-3-12. Sequence of B517 showing double Q34 annealing.

a: Autoradiograph of the B517 sequencing gel (Section **2. 8**).

b: Nucleotide sequence of B517. Nucleotides are represented by their initials. Primer Q 34 is shaded and its direction indicated. The sequence of Q 34 is given (**bold type**) to show its annealing to B517. The *Sma* I site of B517 insertion into pBluescript SK- is also indicated (Section *2. 11. 4*).

sequence bore no homology to calmodulin (result not shown).

Priming with 113 Y-Q 34 consistently produced an amplified fragment migrating between 201-220 bp on a 3% agarose-TAE gel, noted B220 (Figure 3-3-13). From the cDNA present in the EMBL database, the size of the 113 Y-Q 34 fragment in *A. thaliana* (EMBL identifier; em_pl:atcam2) was 206 bp. Cloning and sequencing B220 established that forward priming had been accomplished by a truncated version of 113Y (the 5' region of the primer, from base 1 to the inocine at base 9, did not anneal to the template DNA). The sequence of B220 bore no homology to calmodulin (Figure 3-3-14).

In vitro amplification on *F. serratus* genomic DNA, priming with A 657 and Q 34, produced no DNA fragment. Positive controls with *C. reinhardtii* genomic DNA, and with the *C. reinhardtii* calmodulin cDNA clone, p6-811, (Zimmer *et al.,* 1988) yielded DNA fragments of ~900 bp and ~360 bp, respectively (Figure 3-3-15). Failure to amplify a calmodulin fragment from *F. serratus* DNA was not, therefore, due to ineffectual PCR.

3. 4 Cloning the calmodulin cDNA from *Macrocystis pyrifera*

Due to the difficulties in cloning the calmodulin cDNA or gene from *F. serratus* it was proposed to clone the calmodulin cDNA from *M. pyrifera*, a close relative to *F. serratus* and the only brown alga for which a cDNA library was available (Section *1. 6. 3*).

3. 4. 1 Calmodulin amplification by PCR (B320)

Using A 657 and Q 34 as primers, *in vitro* amplification of λ phage DNA purified form the *M. pyrifera* cDNA library yielded three bands when analysed by TAE-agarose gel electrophoresis (Figure 3-4-1). Two of the resulting bands which migrated at approximately 240 bp and 400 bp were

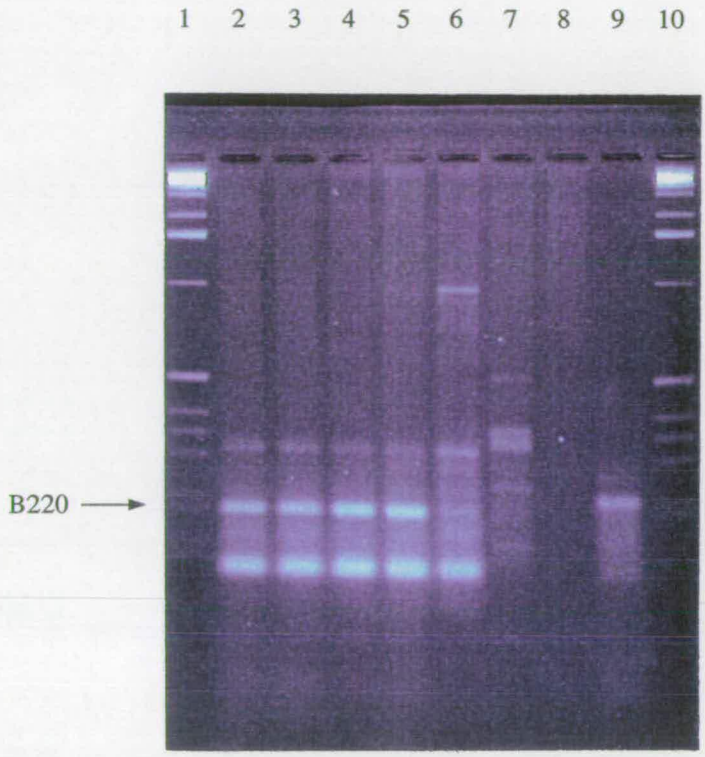

Figure 3-3-13. PCR of *Fucus serratus* genomic DNA (113 Y-Q 34).

The amplification reaction was performed as described in Section *2. 11. 2* and primed with 113 Y and Q 34. Thermal cycling was optimised at 30 s denaturation at 94 °C, 2 min annealing at 45 °C and 2 min extension at 70 °C for 40 cycles. PCR sample were analysed on a 3% agarose-TAE gel.

Lane 1: 1µg 1 kb DNA Ladder (GIBCO, BRL).
Lane 2: Genomic DNA amplification reaction 1 (20 µl).
Lane 3: Genomic DNA amplification reaction 1 (20 µl).
Lane 4: Genomic DNA amplification reaction 2 (20 µl).
Lane 5: Genomic DNA amplification reaction 2 (20 µl).
Lane 6: Genomic DNA, 113 Y single primer control (12 µl).
Lane 7: Genomic DNA, Q 34 single primer control (12 µl).
Lane 8: Genomic DNA, no primers present in reaction (12 µl).
Lane 9: Water control, no DNA present (12 µl).
Lane 10: 1 µg 1 kb DNA Ladder (GIBCO, BRL).

Note B220, an amplified fragment absent from single primer controls, and migrating between 201 and 220 bp. The expected fragment size was 206 bp.

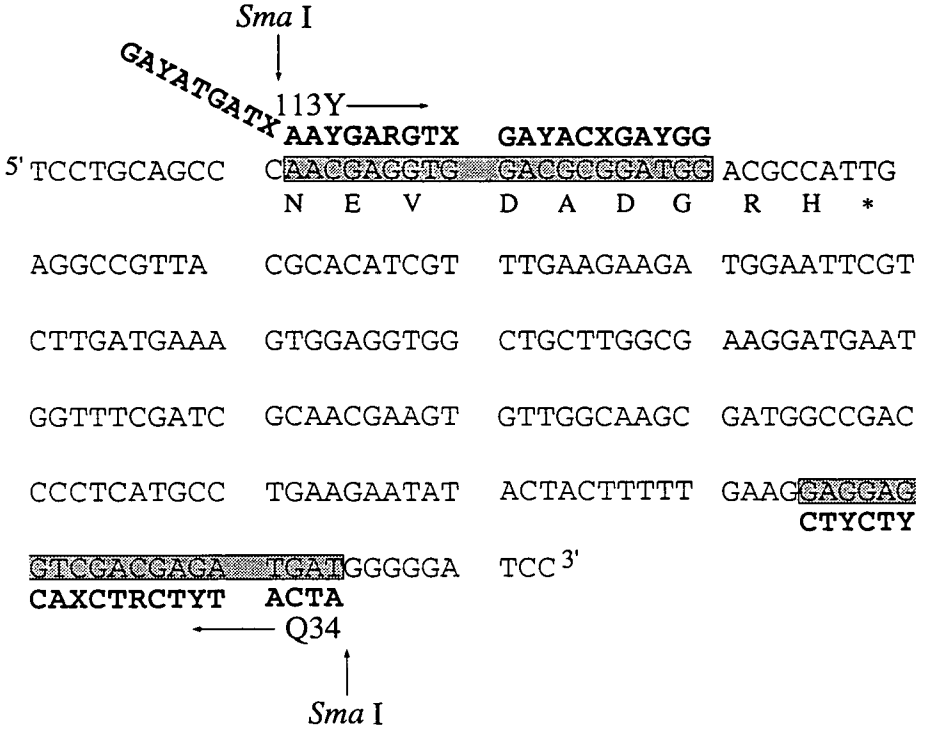

Figure 3-3-14. Sequence of B220 showing artefactual 113 Y annealing.

Nucleotide sequence of B220. Bases are represented by their initials. Primers 113 Y and Q 34 are shaded and their directions indicated. The sequence of the primers are given (**bold type**) to show annealing to B220. The *Sma* I site of B220 insertion into pBluescript SK- is also indicated (Section *2. 11. 4*).
The amino acid sequence of B220 is given using the single letter amino acid code. The translational Stop signal is represented by (*). B220 bore no homology to calmodulin.

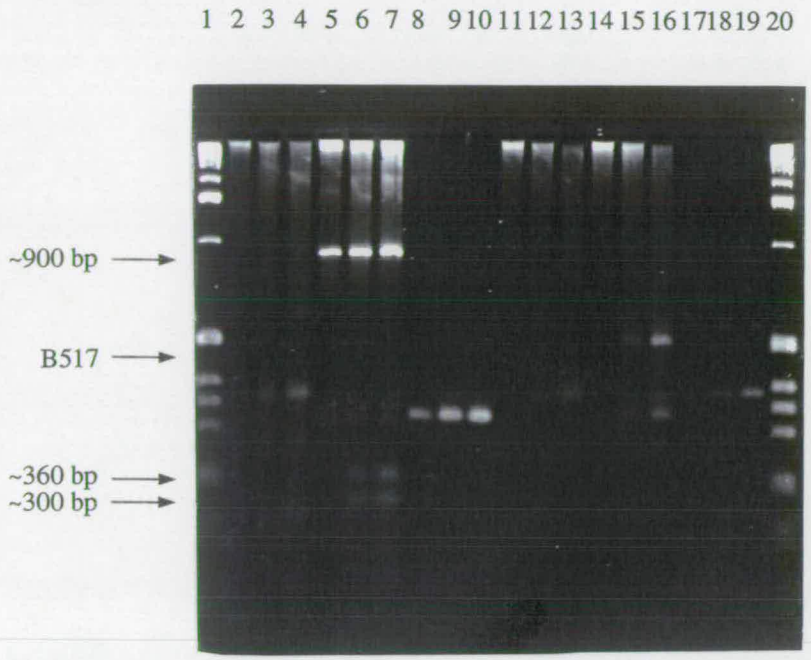

Figure 3-3-15. PCR of *Fucus serratus* genomic DNA (A 657-Q 34).

The amplification reaction was performed as explained in Section *2. 11. 2* and primed with A 657 and Q 34. Two positive controls were performed on 1 µg *C. reinhardtii* genomic DNA and on 1 pg p6-8.11 (*C. reinhardtii* calmodulin cDNA clone). Single primer controls were carried out using *F. serratus* genomic DNA as target. Thermal cycling was optimised as 94 °C for 30 s (denaturation), 55 °C for 2 min (annealing) and 70 °C for 2 min (extension) for 30, 45 and 60 cycles. PCR samples (12 µl) were analysed on a 3% agarose-TAE gel.

Lane 1: 1µg 1 kb DNA Ladder (GIBCO, BRL).
Lanes 2-4: *F. serratus* genomic DNA (1 µg), after 30, 45 and 60 cycles.
Lanes 5-7: *C. reinhardtii* genomic DNA (30, 45, 60 cycles).
Lanes 8-10: p6-8.11 (30, 45, 60 cycles).
Lanes 11-13: A 657 single primer control (30, 45, 60 cycles).
Lanes 14-16: Q 34 single primer control (30, 45, 60 cycles).
Lanes 17-19: Water control (30, 45, 60 cycles).
Lane 20: 1 µg 1 kb DNA Ladder (GIBCO, BRL).

Amplification of *F. serratus* DNA produced an artefactual fragment of approximately 360 bp due to A 657 alone. *C. reinhardtii* genomic DNA yielded a PCR product of 900 bp, and the calmodulin cDNA clone, a fragment of 300 bp. These fragment sizes were expected, showing that failure to obtain an amplified product using *F. serratus* genomic DNA was not a result of inefficient PCR.
Amplification with Q 34 alone produced the B517 artefact.

Figure 3-4-1. *In vitro* amplification of the calmodulin fragment B320.

The amplification was carried out as described in Section *2. 11. 3.* A 657 and Q 34 were used as primers. 40 PCR cycles were performed with 1 min at 94 °C (denaturation), 2 min at 40-60 °C in steps of 5 °C (primer annealing) and 2 min at 70 °C (product extension). Annealing temperatures for control reactions were 55 °C.
12 µl of each reaction were loaded onto a 3% agarose-TAE gel. A fragment of 320 bp was expected. The most efficient amplification reaction was achieved at an annealing temperature of 55 °C.

Lane 1: 1 µg 1 kb DNA ladder (GIBCO, BRL).
Lane 2: p6-8.11 (*C. reinhardtii* calmodulin cDNA).
Lane 3: Purified B320 (from PCR annealing at 55 °C).
Lane 4: *M. pyrifera* cDNA library DNA, annealing at 40 °C.
Lane 5: *M. pyrifera* cDNA library DNA, annealing at 45 °C.
Lane 6: *M. pyrifera* cDNA library DNA, annealing at 50 °C.
Lane 7: *M. pyrifera* cDNA library DNA, annealing at 55 °C.
Lane 8: *M. pyrifera* cDNA library DNA, annealing at 60 °C.
Lane 9: *M. pyrifera* cDNA library DNA, A 657 single primer control.
Lane 10: *M. pyrifera* cDNA library DNA, Q 34 single primer control.
Lane 11: *M. pyrifera* cDNA library DNA, water control (no DNA).
Lane 12: 1 µg 1 kb DNA ladder (GIBCO, BRL).

single primer artefacts produced from primer A 657. These artefacts flanked a single band, migrating at about 320 bp called B320. B320 was not present in single primer controls. A similar band was obtained with the positive control using p6-8.11 as template and A 657-Q 34 as primers. Finally, the length of B320 matches the expected size as determined from the plant and fungal calmodulin consensus sequence.

3. 4. 2 B320 cloning and sequencing

Following purification of B320 from TAE-agarose gels, blunt-ended ligation into the *Sma* I restriction site of pBluescript SK- and transformation into *E. coli*, strain XL1-Blue, 12 bacterial colonies were selected (Section 2.7). Of these, 6 possessed a cloned insert (Figure 3-4-2).

B320 was sequenced (Figure 3-4-3) and compared with the calmodulin nucleotide sequence of *A. thaliana* (EMBL database identifier; em_pl:atcam2). B320 and *A. thaliana* calmodulin overlap was 100%, with 75.42% identity between the two nucleotide sequences. A similar result was obtained with the *C. reinhardtii* calmodulin nucleotide sequence (EMBL database identifier; em_pl:crcam), homology being 69.30% in this case. At the amino acid level, homology between B320 and the plant and fungal consensus was 84.91%. B320 was therefore identified as a calmodulin fragment and used to probe the *M. pyrifera* cDNA library for homologous clones. The plasmid containing B320 was labelled pB320.

3. 4. 3 Library screens and in vivo excision

The first library screen with ^{32}P-B320 as probe, identified 8 positive plaques. A second screen of each plaque (Figure 3. 4. 4) yielded no positives for plaques 1, 2, 3 or 5, 3 positive plaques for plaque 4 (noted clones 4.1, 4.2 and 4.3), 5 positives for plaque 6 (6.1-6.5), 2 positives for

Figure 3-4-2. pBluescript SK-/B320 (pB320) restriction digests.

Recombinant bacterial colonies containing the pBluescript-B320 ligation (*Sma* I site) were identified by colour selection (Section *2. 7. 3*) and cultured in 5 ml LB broth. Plasmid DNA was purified and 1 µg digested with 12 U of Eco RI and Bam HI (BRL) for 1 h at 37 °C in 20 µl volumes.
Samples were analysed by electrophoresis on a 1% agarose-TAE gel. Plasmids exhibit B320 insertion, except for plasmid 12 which presents a band migrating at approximately 600 bp, and probably representing an end to end insertion of 2 B320 fragments.

Lane 1: 1 µg 1 kb DNA ladder (GIBCO, BRL).
Lane 2: pBluescript SK-, digested with Eco RI and Bam HI.
Lane 3: 1 µg pB320, number 1.
Lane 4: pB320, number 1, digested with Eco RI and Bam HI.
Lane 5: 1 µg pB320, number 2.
Lane 6: pB320, number 2, digested with Eco RI and Bam HI.
Lane 7: 1 µg pB320, number 4.
Lane 8: pB320, number 4, digested with Eco RI and Bam HI.
Lane 9: 1 µg pB320, number 6.
Lane 10: pB320, number 6, digested with Eco RI and Bam HI.
Lane 11: 1 µg pB320, number 11.
Lane 12: pB320, number 11, digested with Eco RI and Bam HI.
Lane 13: 1 µg pB320, number 12.
Lane 14: pB320, number 12, digested with Eco RI and Bam HI.

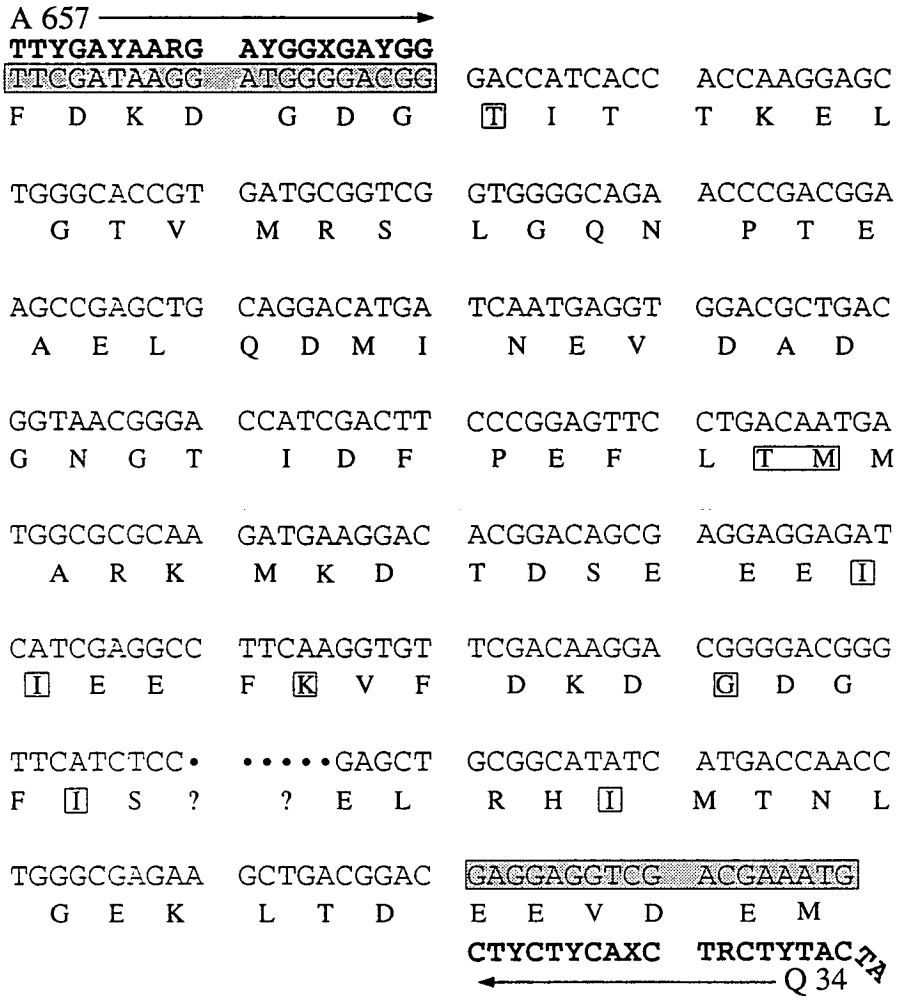

Figure 3-4-3. Nucleotide and deduced amino acid sequence of the *Macrocystis pyrifera* calmodulin PCR fragment, B320.

Nucleotide sequence of B320 as read from the dideoxynucleotide sequencing gel. Nucleotides are represented by their initials. PCR priming sites are shaded and primers given in **bold type**. The deduced amino acid sequence of B320 is shown using the single letter code. Amino acid heterologies with the plant and fungal consensus sequence are boxed. Homology is 84.91% at this level.

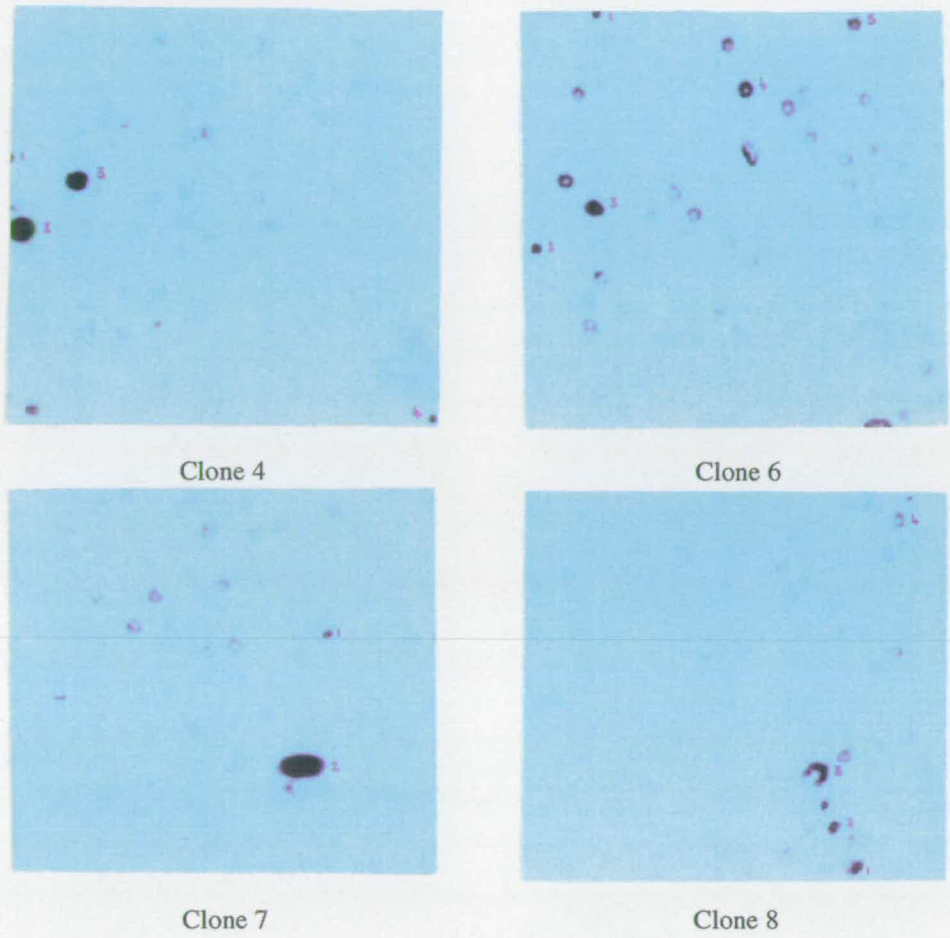

Figure 3-4-4. Second screen of *Macrocystis pyrifera* cDNA library, using ^{32}P-B320 as probe.

Clones 1-8 from the first screen were individually screened (200 pfu per plate) with ^{32}P-B320. Only those autoradiographs of plaque blots which yielded a positive signal are presented. Secondary, individual positive plaques were identified and attributed a second number. Clones 2 and 3 of screen 4 (clones 4.2 and 4.3) and clone 7.2 gave a strong signal.
All noted plaques were collected and phage retrieved. Following *in vivo* excision of cDNA containing plasmids, three bacterial colonies were selected per library clone and labelled a, b or c. Plasmids were then analysed by sequencing and PCR.

plaque 7 (7.1 and 7.2) and, finally, 4 positives for plaque 8 (8.1-8.4). Plaque 7.2 was lost during filter lifts.

Following *in vivo* excision, 3 recombinant bacterial colonies were selected per clone and labelled, for instance, 4.1a, 4.1b and 4.1c. Plasmid DNA was extracted from each clone.

3. 4. 4 cDNA clone selection

After preliminary sequencing, clones 6.1, 6.3, 6.4, 6.5, 8.1, 8.3, 8.4 were discarded, either because they yielded no sequence, or because they did not possess the library linker sites *Xho* I or *Eco* RI.

Using A 657-Q 34 as primers and each of the retained clones (4.1, 4.2, 4.3, 6.2, 7.1, 8.2) as targets, *in vitro* amplification produced a band migrating at 320 bp for clones 4.2a and 4.3a (Figure 3-4-5). Clone 4.2a produced no PCR artefacts.

3. 4. 5 Sequences of cDNA clones 4.2a and 4.3a

Sequencing cDNA clone 4.3a was hampered by a sequencing artefact which made the sequence illegible. Conversely, clone 4.2a gave a clean, clear sequence (Figure 3-4-6). Sequencing therefore concentrated on clone 4.2a and was carried out, in sections, along both the sense and antisense strand of the clone. For each section, a sequencing primer was designed (Figure 2-12-3). Sequencing gels were read sequentially and the total sequence of each DNA strand constructed from overlapping regions. The sequence of both DNA strands were then compared, giving the final nucleotide sequence of clone 4.2a (Figure 3-4-7). The sequence was analysed and found to contain an open reading frame, coding for a protein with high amino acid homology with the calmodulin consensus sequence.

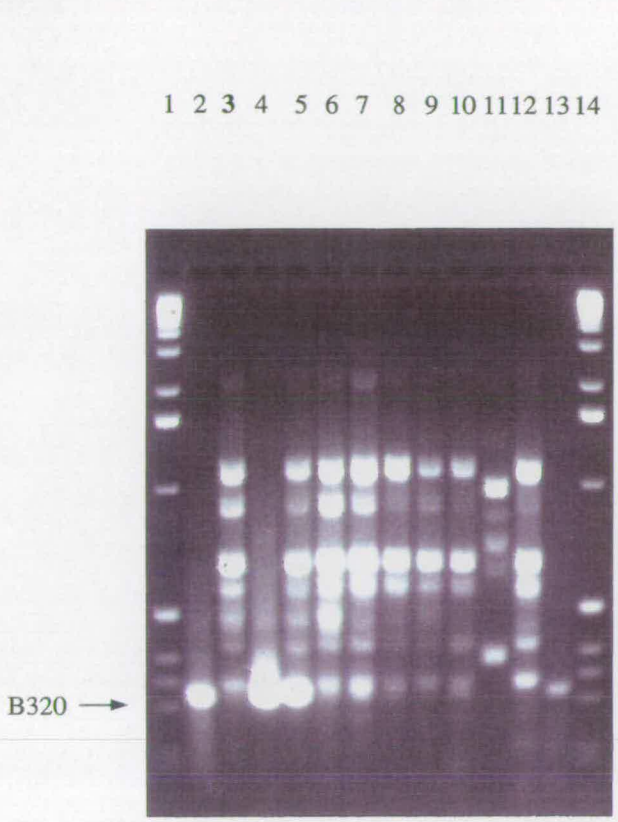

Figure 3-4-5. PCR analysis of cDNA clones.

A 657 and Q 34 were used as primers. PCR was for 40 cycles with 1 min at 94 °C (denaturation), 2 min at 55 °C (annealing) and 2 min at 70 °C (extension). The amplification reaction therefore expected to yield B320. Single primer controls were performed with DNA from clone 4.1c. 12 µl samples from each reaction were separated by electrophoresis in a 1% agarose-TAE gel.

Lane 1: 1µg 1 kb DNA ladder (GIBCO, BRL).
Lane 2: p6-8.11 amplification (positive control).
Lane 3: Clone 4.1c amplification.
Lane 4: Clone 4.2a amplification.
Lane 5: Clone 4.3a amplification.
Lane 6: Clone 6.2c amplification.
Lane 7: Clone 6.3c amplification.
Lane 8: Clone 7.1c amplification.
Lane 9: Clone 8.2a amplification.
Lane 10: Clone 8.2b amplification.
Lane 11: Q 34 single primer control.
Lane 12: A 657 single primer control.
Lane 13: p6-8.11 amplification (positive control).
Lane 14: 1 µg 1 kb DNA ladder (GIBCO, BRL).

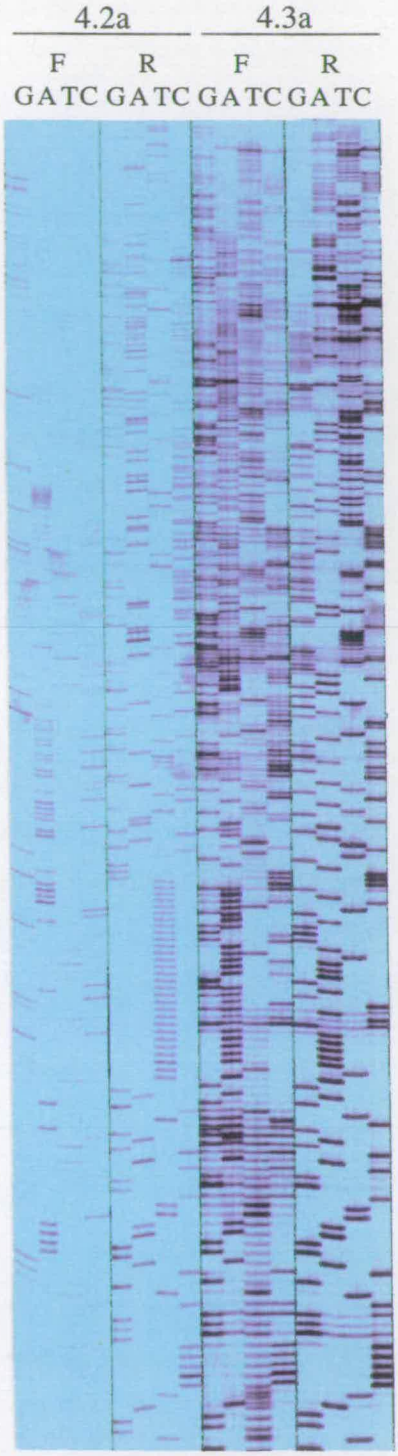

Figure 3-4-6. Autoradiographs of dideoxy-sequencing gels for the cDNA library clones 4.2a and 4.3a.

Nucleotide tracks are indicated by their initials. Sequencing was performed using the forward (F) and reverse (R) priming sites of pBluescript SK-. Although both 4.2a and 4.3a gave PCR band of 320 bp with A 657 and Q 34, only 4.2a yielded a legible sequence.

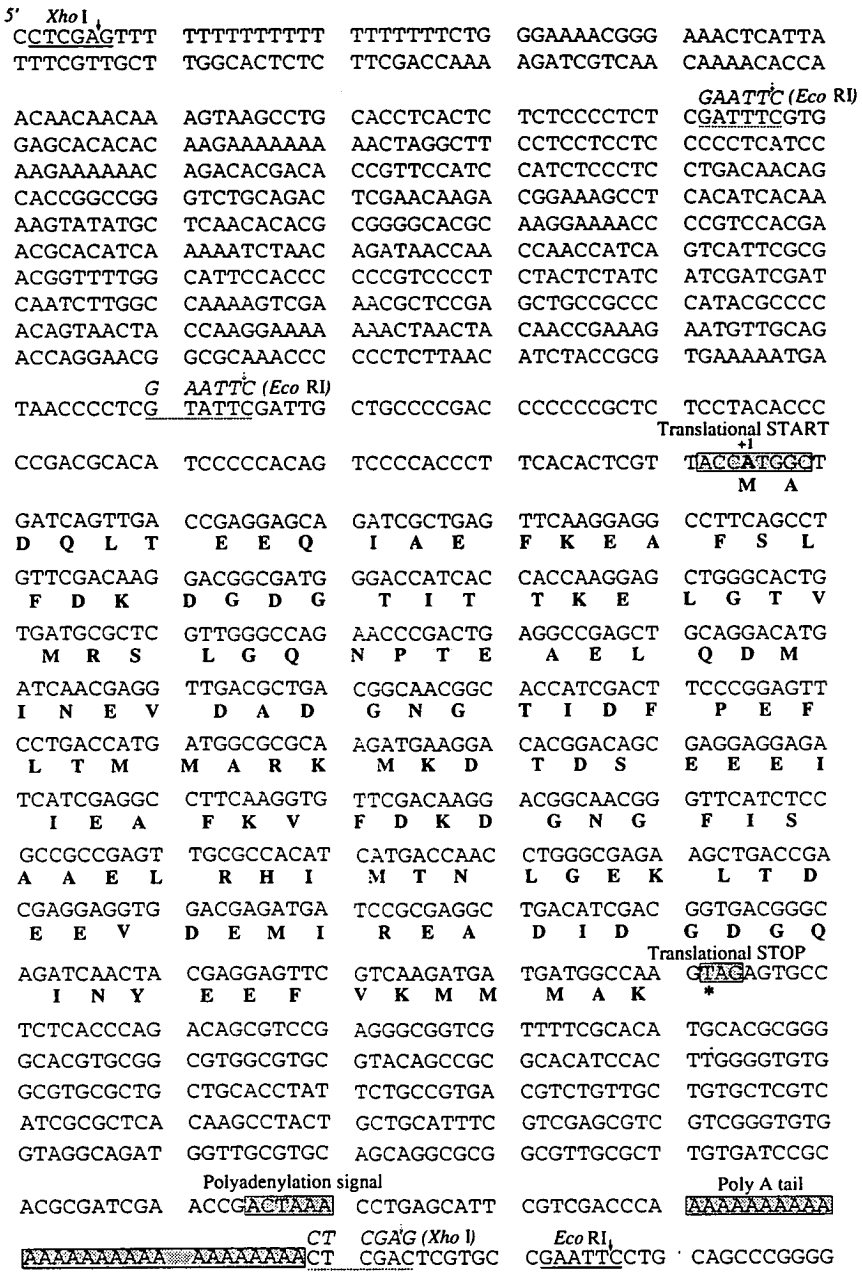

Figure 3-4-7. Complete nucleotide sequence of clone 4.2a.

Nucleotides are represented by their initials. *Eco* RI and *Xho* I restriction sites used during cDNA library construction are underlined. Possible, modified *Eco* RI and *Xho* I restriction sites are also underlined and the normal restriction sequence given. The translational Start and Stop sequences, polyadenylation signal, and poly A tail are shaded and labelled.

An open reading frame is present in the clone, and the amino acid translation given for each codon. Amino acids are indicated by the one letter code. The "A" of the translational Start codon (ATG) is noted "**+1**" and all nucleotides numbered accordingly.

3. 5 Bacterial expression and purification of *Macrocystis pyrifera* calmodulin

Following isolation of the calmodulin cDNA from *M. pyrifera*, the protein was expressed by bacterial genetic engineering.

3. 5. 1 Calmodulin expression plasmid pB820-E

A *Nde* I restriction site, 5' CAT$_{\wedge}$ATG, was engineered into the open reading frame of clone 4.2a by *in vitro* amplification using G 9101 and the reverse primer of pBluescript SK-. The amplification reaction yielded a 920 bp fragment (Figure 3-5-1) which was then cloned into the *Sma* I site of pBluescript SK-. The plasmid was labelled pB920. pB920 digestion with the restriction endonucleases Sst I, Eco RI, Nde I and Nde I - Eco RI identified plasmids with the B920 insertion and correct *Nde* I engineering (Figure 3-5-2). The calmodulin coding sequence was excised from pB920 by simultaneous restriction digestion with Nde I and Eco RI to yield a *Nde* I-calmodulin coding sequence called B820. Following B820 ligation into the bacterial expression vector pRSET A at the *Nde* I and *Eco* RI restriction sites of the MCS, the plasmid construct, labelled p820-E (Figure 3-5-1), was transformed into *E. coli*, strain XL-1 Blue. p820-E was analysed using restriction endonucleases and then transformed into *E. coli*, strain BL21-ΔDE3, for recombinant protein expression.

3. 5. 2 Calmodulin expression in Escherichia coli

Transformants were first cultured in 5 ml LB broth. A crude cell lysate of 6 different BL21-ΔDE3/pB820-E transformants (labelled MpCaM-E1 to MpCaM-E6) were analysed for calmodulin expression. SDS PAGE showed a strong protein band, migrating at approximately 15 kDa, and only present in bacterial cultures for which transgenic protein expression was induced by 4 M IPTG (Figure 3-5-3). Furthermore, when

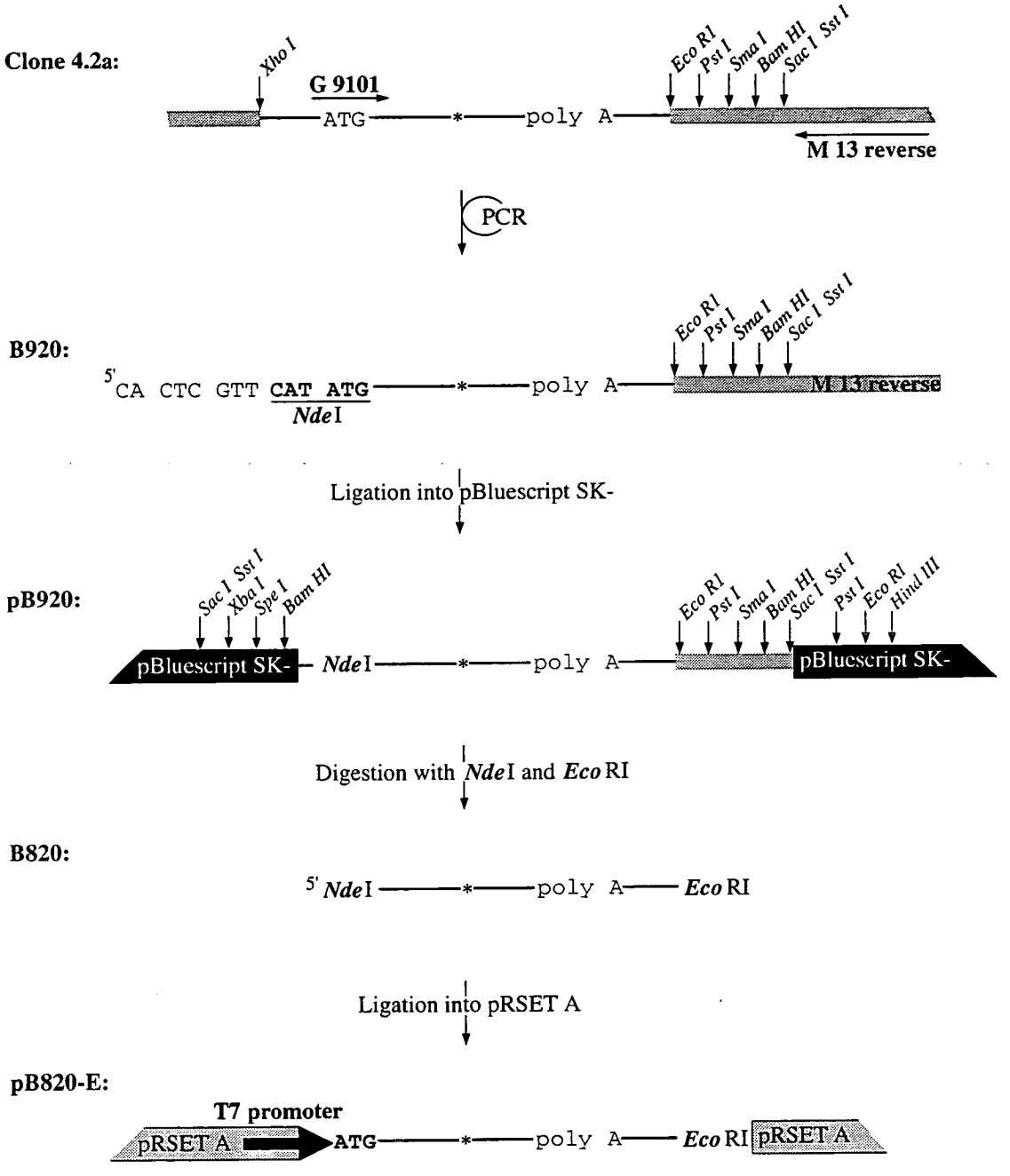

Figure 3-5-1. Construction of the *Macrocystis pyrifera* calmodulin expression plasmid, pB320-E, from the cDNA clone 4.2a.

The diagram represents the critical steps of pB320-E construction. Essential characteristics of the DNA constructs, such as restriction sites, are indicated for each step.

Figure 3-5-2. Restriction digest analysis of pB920.

pB920 was digested with Sst I, Nde I and Eco RI. If B920 were inserted in the direction indicated in Figure 3-5-1, the pattern of restriction, using these enzymes, was predicted: Sst I would cut in two places yielding bands corresponding to linear pBluescript SK- (~3,000 bp) and to B920 plus a portion of the pBluescript SK- MCS (~1,000 bp). Eco RI would cut at two sites yielding two bands, one corresponding to pBluescript SK- plus B820 (~3,800 bp), and one corresponding to the *Eco* RI-reverse primer portion of pBluescript amplified by PCR (~100 bp). Nde I would cut once, yielding a single band corresponding to linear pB920 (~4,000 bp). Cutting with both Eco RI and Nde I would yield 3 bands; linear pBluescript SK- (~3,000 bp), B820 and the previously described 100 bp band.

1 µg pB920 DNA was digested with 12 U of each enzyme for 1 h at 37 °C, in 20 µl volumes. Reactions were analysed by electrophoresis in 1% agarose-TAE gels. Bands displayed the predicted pattern, confirming both B920 insertion into pBluescript SK- and correct engineering of the *Nde* I restriction site.

Lane 1: 1 µg 1 kb DNA ladder (GIBCO, BRL).
Lane 2: Undigested pB920.
Lane 3: pB920, digested with Sst I.
Lane 4: pB920, digested with Eco RI.
Lane 5: pB920, digested with Nde I.
Lane 6: pB920, digested with Eco RI and Nde I (B820 excision).

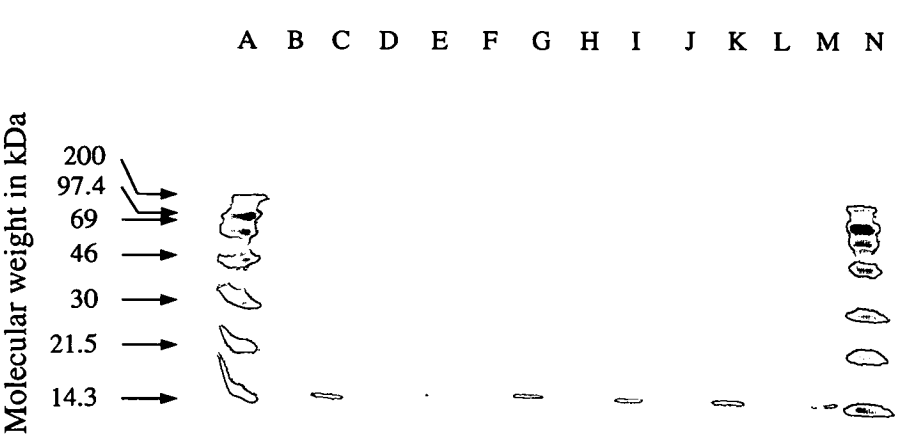

Figure 3-5-3. SDS PAGE of proteins extracted from bacterial colonies, strain BL21-ΔDE3 transformed with pB820-E (MpCaM-E).

Six transformant colonies (MpCaM-E1 to MpCaM-E6) were cultured in 40 ml LB broth and recombinant protein synthesis induced by 4 M IPTG. Controls without IPTG were performed simultaneously. Crude protein extracts were obtained from 1 ml cell suspensions by lysing bacteria. 5 µl of each extract was analysed by SDS PAGE.

Lanes A and N: 1 µl (~1.4 µg/band) High Range Rainbow Markers (Amersham). Molecular weights are indicated in kDa.
Lanes B, D, F, H, J, and L: Bacterial lysate (crude protein extract) from recombinant bacterial colonies MpCaM-E1 to MpCaM-E6, cultured in LB broth (recombinant protein expression non-induced).
Lane C, E, G, I, K, and M: Bacterial lysate from MpCaM-E1 to MpCaM-E6, cultured in LB broth enriched to 4 M IPTG (recombinant protein synthesis induced).

In cultures for which recombinant protein synthesis was induced by 4 M IPTG, a densely staining band was observed migrating with an apparent molecular weight of approximately 15 kDa, close to the molecular weight of calmodulin. This band was absent in control cultures without IPTG.

free Ca^{2+} was chelated by 10 mM EGTA, the induced protein band migrated slower, with an apparent molecular weight of approximately 18 kDa (Figure 3-5-4). This electrophoretic band shift due to the presence or absence of Ca^{2+} is characteristic of calmodulin, though is not as pronounced for plant calmodulins as it is for animal calmodulins (Watterson *et al.*, 1980). Comparing the band density of the bacterial extracts to that of the standards (~1.4 µg protein per band, Amersham), it was estimated that 1 ml of induced bacterial culture would yield 0.5 mg of crude calmodulin.

3. 5. 3 Calmodulin purification

Calmodulin was purified from crude bacterial lysates by W7 affinity chromatography. Following column wash with buffer F, calmodulin was eluted from the W7 matrix using 10 mM EGTA. This EGTA concentration impeded accurate spectrophotometric readings at Abs280 (Figure 3-5-5). Consequently, elution fractions were also analysed by SDS PAGE (Figure 3-5-6). Fractions 6 to 12 showed a densely staining calmodulin band and were pooled. Approximately 6 mg of pure calmodulin was recovered from the W7 affinity column, that is 30% of the crude calmodulin present in bacterial lysates. SDS PAGE analysis of wash fractions showed no calmodulin, indicating that the column was not saturated, and that the protein loss probably occurred by inefficient recovery from the column, rather than by a failure of matrix-calmodulin binding. Yield of purified calmodulin in these suboptimal conditions was therefore 0.15 mg of protein per ml of bacterial culture. The EGTA elution buffer was replaced by a physiological salt solution containing 25 mM $MgCl_2$ and 4 mM $CaCl_2$ (Section *2. 13. 4*). Calmodulin was concentrated to 5 µg·µl-1 (Figure 3-5-7).

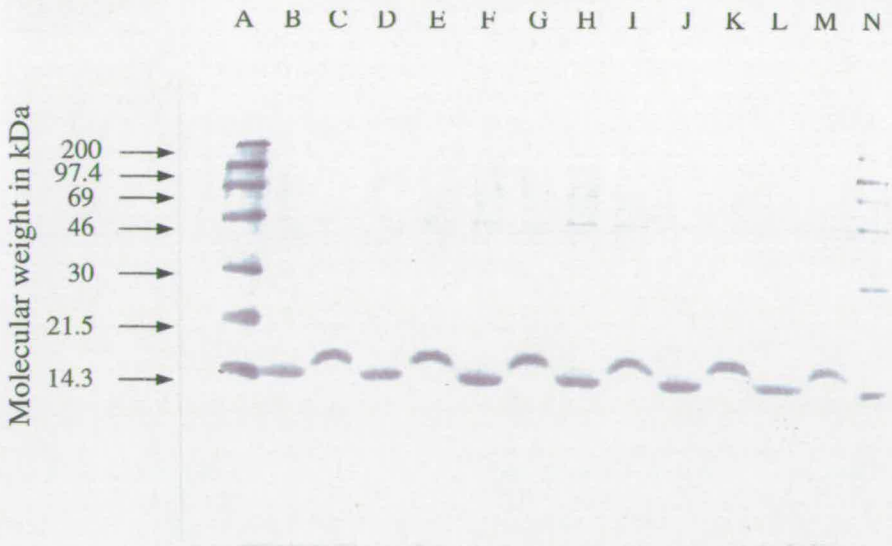

Figure 3-5-4. SDS PAGE of transformant bacterial lysates, MpCaM-E, showing Ca^{2+} dependent band shift of recombinant protein.

5 µl induced bacterial lysates (culture in LB broth enriched to 4 M IPTG) were loaded onto a SDS polyacrylamide gel. Molecular weights are indicated in kDa.

Lane A: 1 µl High Range Rainbow Markers (Amersham).
Lane B: MpCaM-E1 lysate.
Lane C: MpCaM-E1 lysate, buffered to 10 mM EGTA.
Lane D: MpCaM-E2 lysate.
Lane E: MpCaM-E2 lysate, buffered to 10 mM EGTA.
Lane F: MpCaM-E3 lysate.
Lane G: MpCaM-E3 lysate, buffered to 10 mM EGTA.
Lane H: MpCaM-E4 lysate.
Lane I: MpCaM-E4 lysate, buffered to 10 mM EGTA.
Lane J: MpCaM-E5 lysate.
Lane K: MpCaM-E5 lysate, buffered to 10 mM EGTA.
Lane L: MpCaM-E6 lysate.
Lane M: MpCaM-E6 lysate, buffered to 10 mM EGTA.
Lane N: 1 µl High Range Rainbow Markers (Amersham).

In the presence of free Ca^{2+}, the induced protein migrates faster that when Ca^{2+} is chelated with EGTA. This band shift is characteristic of calmodulin.

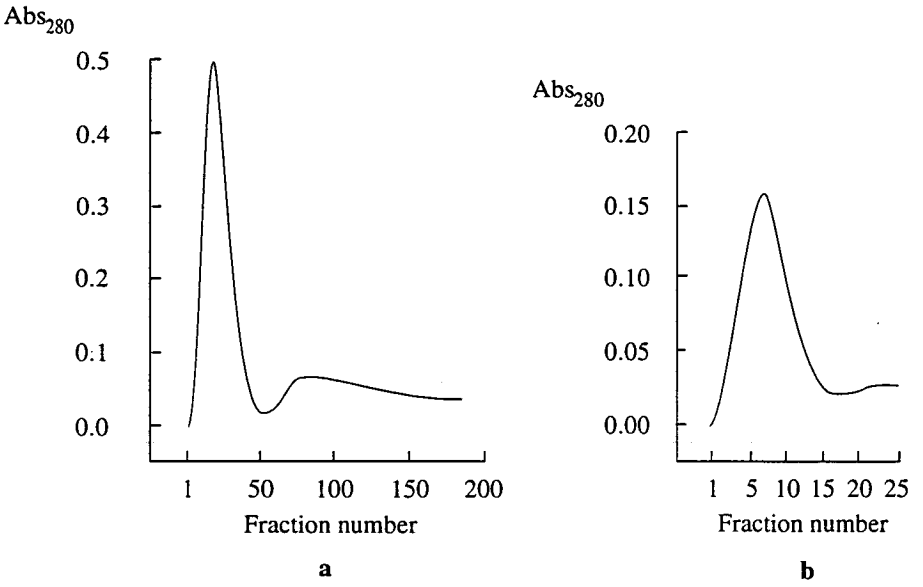

Figure 3-5-5. Elution profiles of recombinant calmodulin purification by W7 affinity chromatography.

a: Abs_{280} of W7 affinity column wash fractions (elution with Buffer F). Fractions 13, 14 and 10 were collected for analysis by SDS PAGE.

b: Abs_{280} of calmodulin elution fractions from W7 affinity column (elution with Buffer G containing 10 mM EGTA). The presence of EGTA caused inaccurate absorbance readings. Fractions 6, 7, 8, 9, 10, 11, 12 and 18 were analysed by SDS PAGE.
Note that the base of the absorbance peak is wide, spanning approximately 15 elution fractions. This is largely due to the length of the affinity column (30 mm) being too short relative to the column diameter (5 mm), resulting in sub-optimum separation (Wilson and Goulding, 1986 ; Ostrove, 1990).

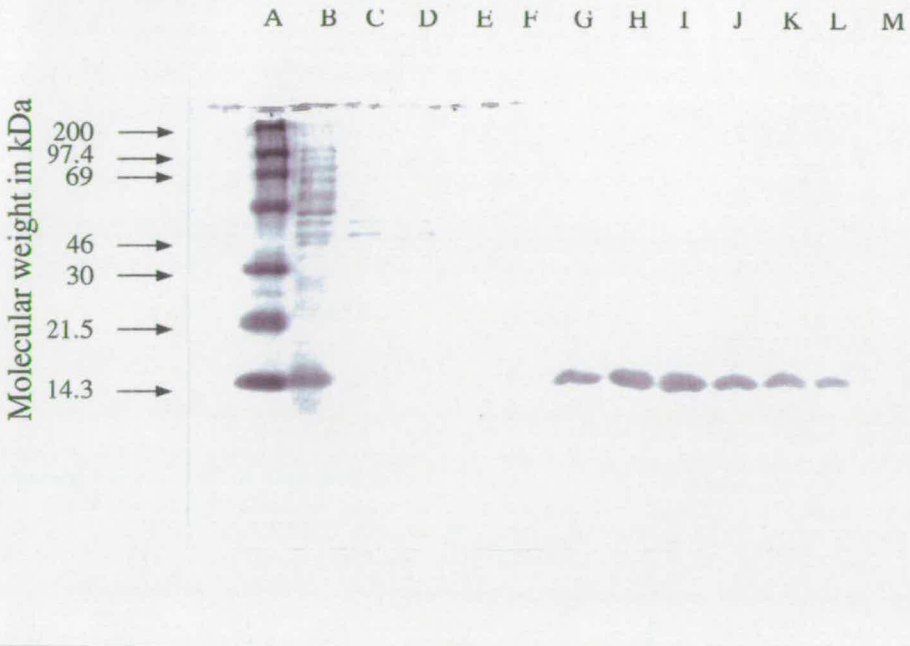

Figure 3-5-6. SDS PAGE of protein fractions from a lysate of induced MpCaM-E1 cultures, purified by W7 affinity chromatography.

Lane A: 1 µl High Range Rainbow Markers (Amersham). Molecular weights are given.
Lane B: 5 µl crude lysate from induced MpCaM-E1 (loaded onto W7 affinity column)
Lane C: 10 µl W7 affinity column wash fraction 13 (A_{280} = 0.43).
Lane D: 10 µl W7 affinity column wash fraction 14 (A_{280} = 0.46).
Lane E: 10 µl W7 affinity column wash fraction 23 (A_{280} = 0.31).
Lane F: 5 µl calmodulin elution (Buffer G) fraction 6 (A_{280} = 0.12).
Lane G: 5 µl calmodulin elution fraction 7 (A_{280} = 0.07).
Lane H: 5 µl calmodulin elution fraction 8 (A_{280} = 0.16).
Lane I: 5 µl calmodulin elution fraction 9 (A_{280} = 0.10).
Lane J: 5 µl calmodulin elution fraction 10 (A_{280} = 0.14).
Lane K: 5 µl calmodulin elution fraction 11 (A_{280} = 0.06).
Lane L: 5 µl calmodulin elution fraction 12 (A_{280} = 0.15).
Lane M: 5 µl calmodulin elution fraction 18 (A_{280} = 0.15).

The recombinant 15 kDa protein band (calmodulin) is present in the crude bacterial lysate (**Lane B**). The band is absent from W7 affinity column wash fractions (**Lanes C, D,** and **E**), indicating that the protein remained bound to the affinity matrix. The protein is eluted pure from the column (**Lanes F-M**) with Buffer G (10 mM EGTA). Note the discrepancy between A_{280} of samples, and the intensity with which bands stain on SDS polyacrylamide gels (*e.g.* **Lanes F** and **G**). This discrepancy is due to the high concentration of EGTA in Buffer G which impeded accurate spectrophotometric readings at A_{280}.

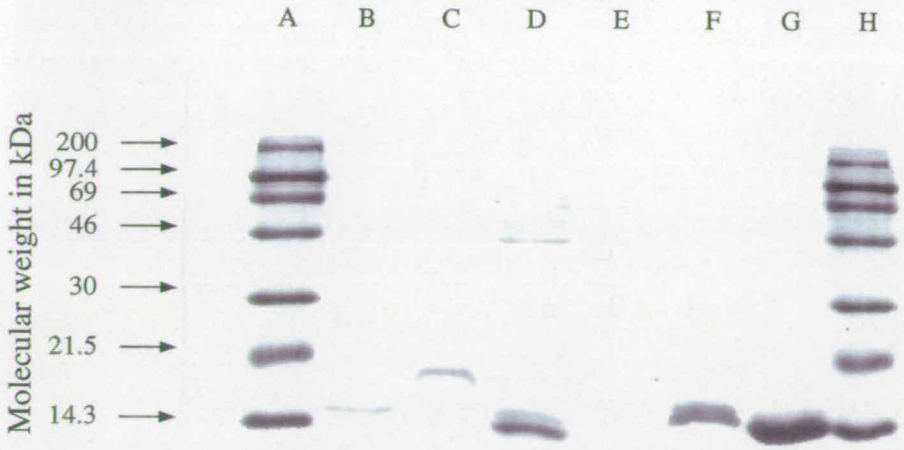

Figure 3-5-7. SDS PAGE analysis of recombinant *Macrocystis pyrifera* calmodulin production in bacteria and purification from bacterial lysates.

Lane A: 1 µl (~1.4 µg protein per band) High Range Rainbow Markers (Amersham). Molecular weights are given.
Lane B: 0.5 µg bovine brain calmodulin (Sigma) in 1 mM $CaCl_2$, migrating with an apparent molecular weight of 16 kDa.
Lane C: 0.5 µg bovine brain calmodulin (Sigma) in 10 mM EGTA, migrating with an apparent molecular weight of 20 kDa. This band shift in the presence or absence of free Ca^{2+} is characteristic of calmodulin.
Lane D: 5 µl bacterial lysate from MpCaM-E1 culture in which recombinant protein synthesis was induced by 4 M IPTG. The recombinant protein migrated with an apparent molecular weight of 15 kDa.
Lane E: 10 µl W7 affinity column wash fraction 14 (A_{280} = 0.46). Note the absence of the recombinant protein band.
Lane F: 5 µl W7 affinity column calmodulin elution fraction 7in 10 mM EGTA (A_{280} = 0.07), migrating with an apparent molecular weight of ~16 kDa.
Lane G: 2 µl purified, recombinant calmodulin, concentrated in a physiological salt solution containing 25 mM $MgCl_2$ and 4 mM $CaCl_2$. The band migrated with an apparent molecular weight of ~14.5 kDa, possibly due to the heavy sample load. The band shift between **Lanes F** and **G**, characteristic of calmodulin is nevertheless apparent, though not as pronounced as for the bovine calmodulin (**Lanes B** and **C**). The final calmodulin concentration was estimated at 5 $\mu g \cdot \mu l^{-1}$.
Lane H: 1 µl High Range Rainbow Markers (Amersham).

3. 6 Calmodulin microinjection into *Fucus serratus* eggs and zygotes

Given the high degree of homology between *M. pyrifera* and *A. thaliana* calmodulins, microinjecting the recombinant *M. pyrifera* calmodulin into *F. serratus* eggs and zygotes was justified (Section **4. 4**). Microinjections were proposed to disrupt any polarised calmodulin gradients (Section *1. 6. 2*), and affect polar formation in *F. serratus* zygotes.

3. 6. 1 Microinjection into eggs

Microinjection of 1 μM calcium green in the artificial intracellular solution (hereafter referred to as "calcium green") (Section *2. 14. 2*) into eggs and zygotes did not affect fertilisation and subsequent embryogenesis (Figures 3-6-1, 3-6-2, and 3-6-3). Microinjected eggs polarised normally relative to unilateral light applied from 10-13 h AF, with a mean photopolarisation score of 0.9 ± 0.063 ($n = 7$) (Figure 3-6-4). The fluorescent dye persisted during embryogenesis, and microinjected cells were therefore readily identified from those which were untreated (Figures 3-6-2 and 3-6-3).

Microinjections of the intracellular solution containing 1 μM calcium green and 5 μg·μl-1 recombinant *M. pyrifera* calmodulin caused the cytoplasm of injected eggs to congeal on the injection electrode, making electrode withdrawal difficult. A similar situation has previously been encountered following microinjection of active cytoskeletal proteins into plant cells, but not with calmodulin (Hepler, *pers. comm.*, 1994). Moreover, calmodulin injection into zygotes did not result in cytoplasmic stiffening. It therefore seems likely that microinjected calmodulin interacted with the egg cortical cytoskeleton or polysaccharide containing vesicles (Section *1. 1. 3*), causing this localised phenomenon. Eggs injected with calmodulin

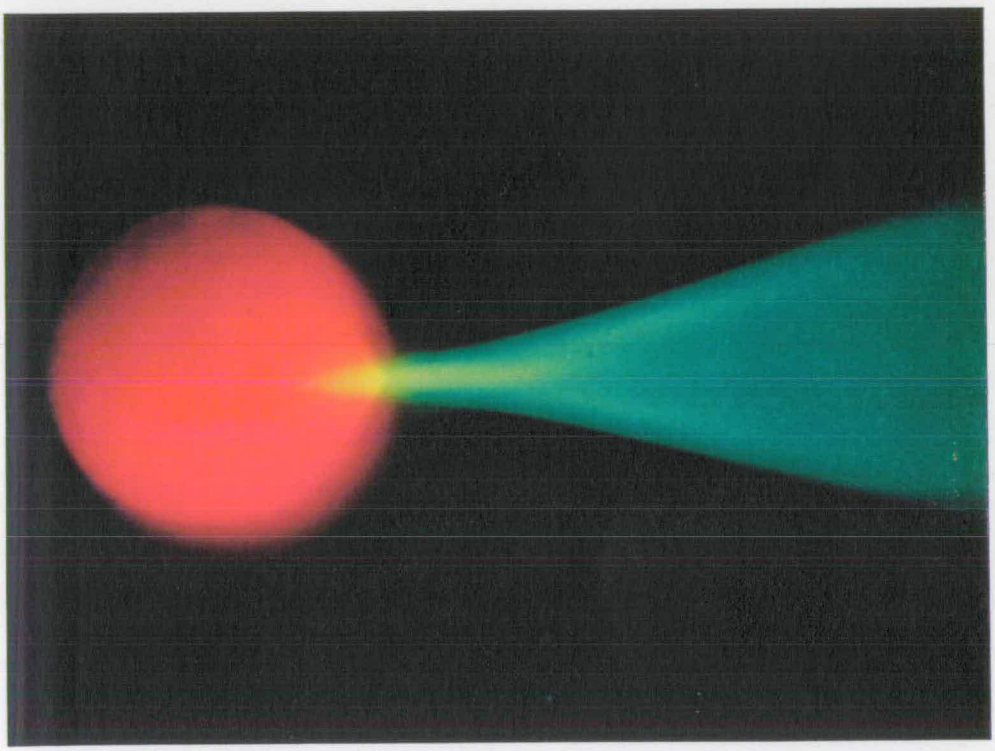

Figure 3-6-1. Calcium green microinjection into a *Fucus serratus* egg.

Calcium green fluorescence was visualised as described in Section *2. 14. 2.* The red colour of the egg is due to chlorophyll fluorescence. The dye is clearly visible in the electrode with which the egg is impaled.

a

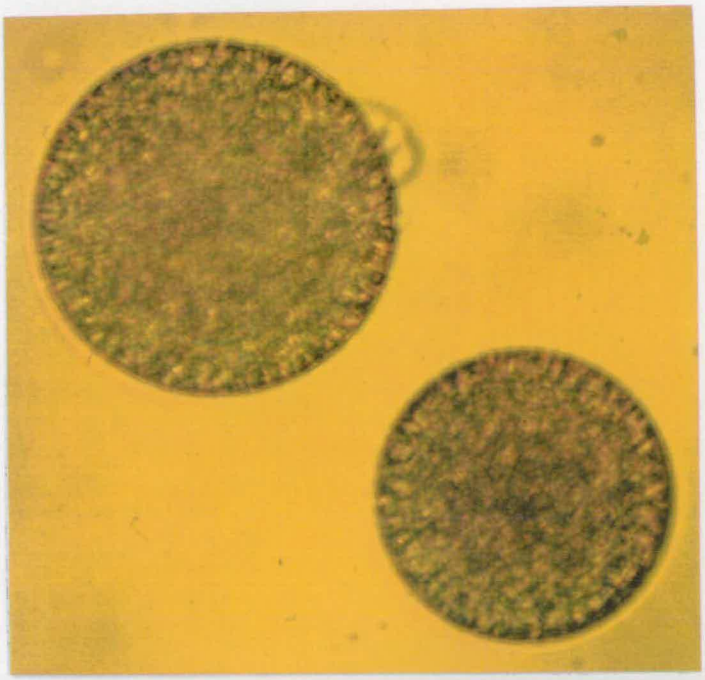

b

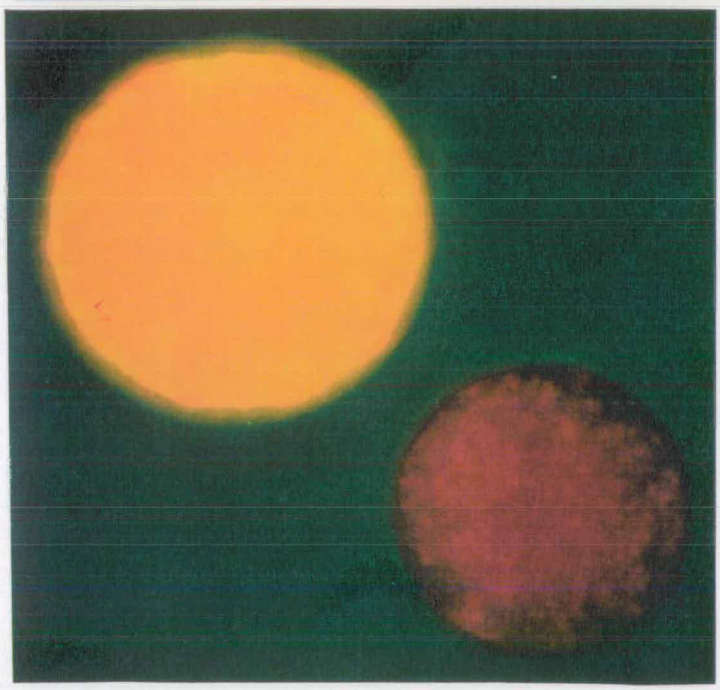

Figure 3-6-2. A *Fucus serratus* egg microinjected with calcium green.

a: Bright field micrograph of two *F. serratus* eggs. The upper one was microinjected with calcium green, and the lower one was untouched. Following microinjection eggs appear normal. Fertilisation and embryonic development is unimpaired.

b: The same eggs as in (**a**), with calcium green fluorescence visualised as described in Section *2. 14. 2.* The red colour of the lower egg is due to chlorophyll fluorescence. The fluorescence of the upper egg is due to calcium green.

a

b

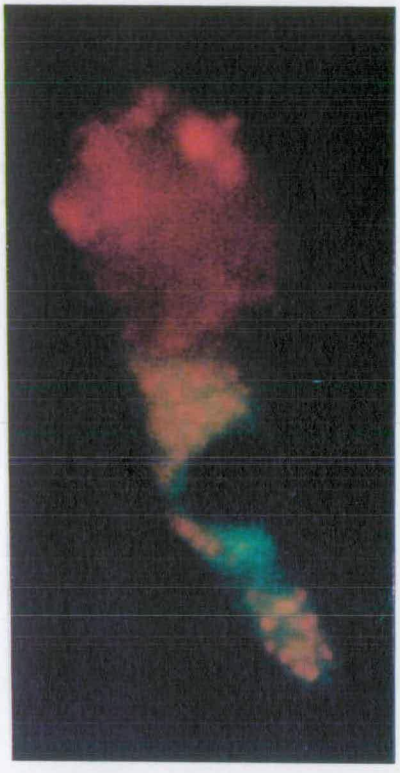

Figure 3-6-3. Persistence of calcium green fluorescence during *Fucus serratus* embryogenesis.

a: Bright field micrograph of a *F. serratus* 3-day embryo, injected with calcium green as an egg. Embryonic development is normal. The zygote was polarised by unilateral light as described in Section *2. 14. 1.* Light was directed from the top of the photograph.

b: The same zygote as in (**a**), with calcium green fluorescence visualised as described in Section *2. 14. 2.* Calcium green fluorescence is clearly visible in the rhizoid, mainly due to its form and relative lack of chloroplasts.

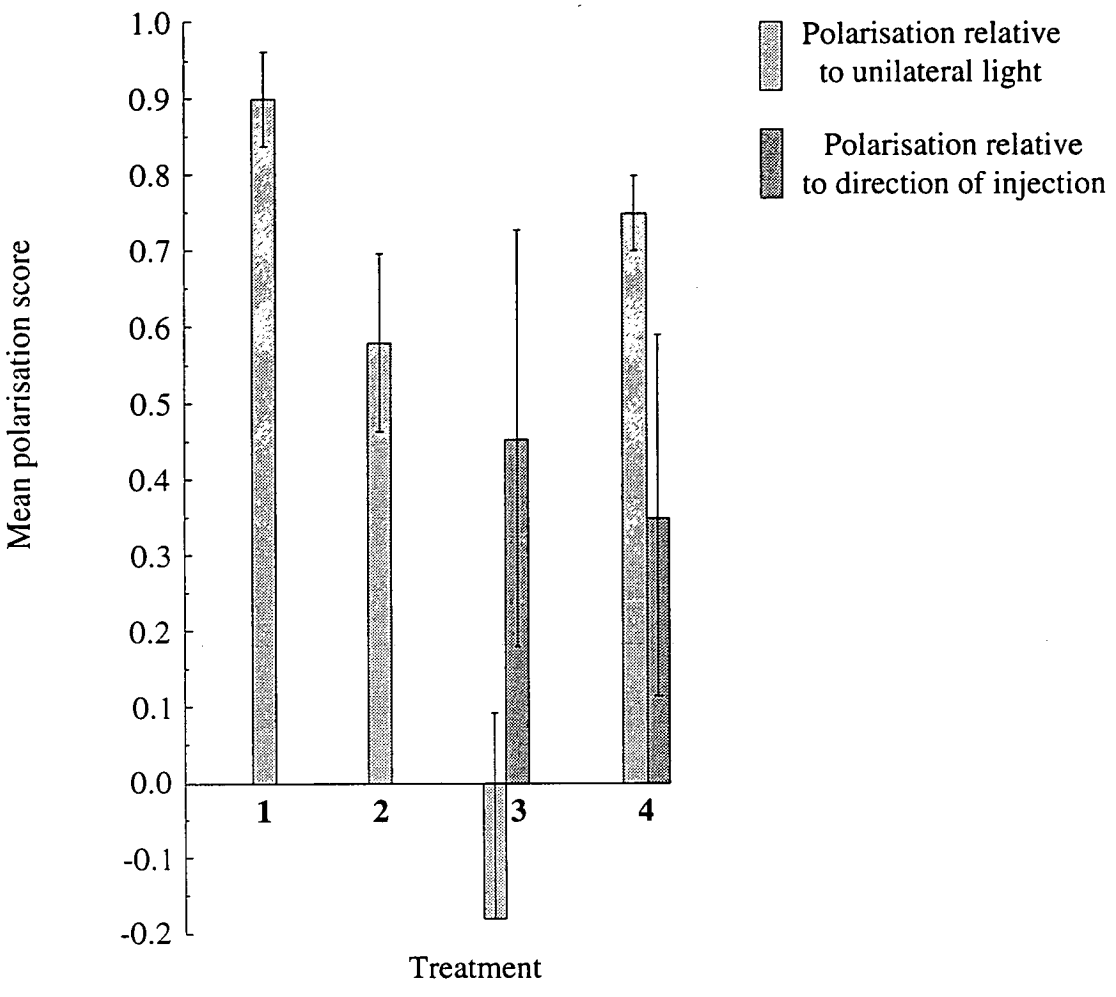

Figure 3-6-4. Polarisation scores of *Fucus serratus* embryos relative to unilateral light following microinjection with calcium green or calmodulin.

Polarisation was scored as described in Section *2. 14. 2.* Columns represent the mean polarisation score. Standard error bars are shown for each mean. Values of the standard error and the number of observations for each mean are given in the text.

Treatments were:

1: Eggs, microinjected with calcium green.
2: Photopolarised zygotes exposed to light under the microscope, from 13 h AF, and for the duration of an experiment (approximately 2 h).
3: Photopolarised zygotes, microinjected with calcium green.
4: Photopolarised zygotes, microinjected with calmodulin.

fertilised normally, but lysed during embryogenesis in 23 cases out of 28. The polarisation score of eggs which survived the treatment is not statstically valid.

3. 6. 2 Microinjections into photopolarised zygotes

Photopolarised zygotes were microinjected from approximately 13-15 h AF, several hours before axis fixation (Section *1. 2. 4*). During this time zygotes were exposed to intense light under the microscope, notably to blue light which was used to excite the fluorescent dye. Consequently, the photopolarisation score of zygotes is reduced to an average of 0.58 ± 0.117 ($n = 34$) (Figure 3-6-4). Microinjection with 1 μM calcium green caused rhizoid germination at the point opposite the site of microinjection. Consequently, the photopolarisation score in calcium green-microinjected zygotes was not significantly different from zero (-1.8 ± 0.275 ($n = 6$)) (Figure 3-6-4). Microinjections of calmodulin into photopolarised zygotes restored the score of photopolarisation to 0.75 ± 0.05 ($n = 6$), which is not significantly different from the photopolarisation score of photopolarised zygotes exposed only to light from the microscope for the duration of an experiment.

When polarisation is calculated relative to the vector of microinjection, no significant comparison can be drawn between polarisation in zygotes injected with calcium green and those injected with calmodulin (Figure 3-6-4).

Chapter 4

Discussion

4. 1 Ca^{2+} and calmodulin involvement in photopolarisation

4. 1. 1Calcium

As explained in Chapter **1**, the conventional model of *Fucus* polarisation centres on the formation of a dynamic Ca^{2+} gradient within the zygote. Essential to this hypothesis is a movement of Ca^{2+} from the medium to the zygote and *vice versa.* Hurst and Kropf (1991) challenged this view by culturing *P. fastigiata* zygotes in various ionic media. They found that cellular import of K^+, Na^+, Ca^{2+}, Mg^{2+}, Cl^- nor SO_4^{2-} were essential for polar axis formation. However, due to the design of their experiments, notably with respect to the timing of axis formation in *P. fastigiata*, the role of these ions in photopolarisation, especially Ca^{2+}, remained unclear (Section *1. 3. 3*). Conversely, in the experiments presented here, inhibition of polar axis formation was targeted to the time of photopolarisation and applied with the polarising stimulus. Moreover, only zygotes which had continued development in a normal way, by producing rhizoids, were scored. In this way, results reflect as closely as possible the processes of photopolarisation.

Depleting Ca^{2+} from the medium with 10 mM EGTA had no significant effect on axis orientation, indicating that zygotes photopolarised in the absence of extracellular free Ca^{2+}. This corroborates previous findings that Ca^{2+} circulation from the medium into the cell is not essential to photopolarisation (Hurst and Kropf, 1991). However, $LaCl_3$, a potent competitive inhibitor of Ca^{2+} uptake into cells (Dos Remedios, 1981 ;

Saunders and Hepler, 1983; Tlalka and Gabrys, 1993) reduced photopolarisation by 20% although 40% of zygotes were unaffected. Few zygotes survived 1 mM concentrations of $LaCl_3$. Electrophysiological data has shown that 5 mM $LaCl_3$ in normal sea water ($[Ca^{2+}] = 9$ mM) blocks Ca^{2+} entry into *Fucus* zygotes and that zygotes remain impermeable to La^{3+} (Brownlee and Wood, 1986 ; Taylor and Brownlee, 1993). Ca^{2+} import, as proposed by Jaffe's model (Jaffe *et al.*, 1974), was therefore essential for photopolarisation in certain *F. serratus* zygotes. La^{3+} also had an unforeseen and lasting effect on zygotes. Concentrations beyond 800 μM impeded zygotes' adhesion to the substratum, even though polar germination occurred normally. Exposure to La^{3+} appears to be impeding exocytosis of adhesive proteins at the rhizoid tip (Quatrano *et al.*, 1991 ; Battey and Blackbourn, 1993). As La^{3+} does not penetrate *Fucus* zygotes (Taylor and Brownlee, 1993), the manner in which this perturbation persists is unclear.

EGTA and $LaCl_3$ had contrasting effects on photopolarisation of *F. serratus* zygotes which must be reconciled to understand the role of extracellular Ca^{2+} in photopolarisation: La^{3+} directly inhibits Ca^{2+} entry into the cytosol, affecting 20% of zygotes, whereas EGTA indirectly blocks Ca^{2+} uptake by chelating extracellular free Ca^{2+}. Plant cells possess an important extracellular store of cell wall-bound Ca^{2+} (Poovaiah and Reddy, 1987) which is only removed by washing and culturing cells in EGTA solutions for several hours prior to experimentation (Saunders and Hepler, 1983 ; Lehtonen, 1984). Such a procedure was not applicable to photopolarising *F. serratus* zygotes. This cleansing procedure also shows that, although tightly bound to the cell wall, Ca^{2+} ions are not irrevocably fixed to the wall. Therefore, the pool of cell wall-bound Ca^{2+}, relatively unaffected by transient EGTA treatment, might have provided sufficient external free Ca^{2+} for normal photopolarisation, even under high EGTA

concentrations. As only minute perturbations in cytosolic [Ca^{2+}] are sufficient to initiate a polarisation response (Robinson and Jaffe, 1975 and 1976), it is possible that if enough Ca^{2+} escapes from the wall and is imported into the cell, polarisation might be initiated. This explanation must remain tentative because the binding dynamics of cell wall Ca^{2+} are largely unknown in plants generally and even more so in Fucoid algae, as are the kinetics of Ca^{2+} binding to EGTA and to Ca^{2+} import proteins *in vivo*. This idea, however, highlights the importance of Ca^{2+} import in photopolarisation, and the involvement of the cell wall as a potential extracellular Ca^{2+} store.

Transient exposure to various Ca^{2+} channel antagonists caused dose dependent inhibition of axis orientation in F. serratus zygotes. TMB-8, nifedipine, verapamil and bepridil, were effective within the concentration range observed in other plants and algae (Saunders and Hepler, 1983 ; Schramm, et al., 1983 ; Reiss and Herth, 1985 ; Lonergan, 1990 ; Heslop-Harrison and Heslop-Harrison, 1991). Bepridil inhibited photopolarisation in all zygotes. Although specificity for each individual inhibitor might reasonably be challenged, they are all inhibitors of cytosolic Ca^{2+} mobilisation and are chemically unrelated. Moreover, dissolution in ASW reduced the effect of both TMB-8 and nifedipine. High [Ca^{2+}] decreases sensitivity of Ca^{2+} channels to TMB-8 and to nifedipine, thereby reducing inhibition (Saunders and Hepler, 1983). Although the channel type specificity of Ca2+ channel blockers has not been ascertained in plant cells, this result suggests that TMB-8 and nifedipine specifically inhibited intracellular Ca^{2+} channels at the concentrations used. Controlled mobilisation of cytoplasmic Ca^{2+} from Ca^{2+} stores or from across the plasma membrane is therefore essential to photopolarisation.

Polarity in *Fucus* has been dominated by the concept of a polar gradient of cytoplasmic free Ca^{2+} (Jaffe *et al.*, 1974). It has been argued that microinjections of the Ca^{2+} chelator, BAPTA, which inhibited polarisation in *F. distichus*, did so by destroying a cytoplasmic Ca^{2+} gradient through increasing the mobility of Ca^{2+} in the cytosol (Speksnijder *et al.*, 1989). Using the Ca^{2+} sensitive dye calcium-green and confocal microscopy, a possible cytoplasmic Ca^{2+} gradient has been detected at the future rhizoid pole, and before rhizoid germination (Berger and Brownlee, 1993), although this data must be treated with caution (Section *1. 2. 5*). Given this background, the temptation to over interpret the experimental results obtained is strong, but must be resisted: No cytoplasmic Ca^{2+} gradient has been demonstrated, only the essential role of Ca^{2+} as a link between light perception and polar axis formation. Unlike the model (Jaffe *et al.*, 1974 ; Kropf, 1989), Ca^{2+} seems to originate from many sources, the extracellular medium, the cell wall, and intracellular Ca^{2+} stores, which may act in concert and complement each other. The emphasis is therefore displaced from a conception of Ca^{2+} movement into the polarising zygote, to one of Ca^{2+} mobilisation in the cytoplasm.

4. 1. 2 Calmodulin

W7 and TFP inhibited photopolarisation in a dose dependent manner, causing randomisation of the photopolar axis at 80-100 μM and 3 μM respectively. W7 and TFP are chemically unrelated and widely used as inhibitors of active calmodulin (Hidaka *et al.*, 1981 ; Saunders and Hepler, 1983 ; Poovaiah and Reddy, 1987 ; Hidaka and Ishikowa, 1992). Calmodulin is therefore essential to photopolarisation. However, since W7 and TFP also have secondary effects on cells, results must be muted with caution: W7 increases cytoplasmic $[Ca^{2+}]$ concentration, possibly by

inhibition of the putative calmodulin-dependent Ca^{2+}-ATPase of the plasmalemma and endoplasmic reticulum (Gilroy *et al.*, 1987*b*). TFP inhibits Ca^{2+} uptake by the endoplasmic reticulum and mitochondria in *Trypanosoma cruzi* (Vercesi *et al.*, 1991). *In vitro*, TFP inhibits myosin light chain kinase by interaction with the myosin phosphorylation site (Sobiezek, 1989).

Calmidazolium, unlike W7 and TFP, was ineffective against 35% of the zygotes. The mode of action of calmidazolium, however, is seen to be more and more complex. It inhibits Ca^{2+} uptake by the cytoplasmic reticulum and mitochondria in *T. cruzi* (Vercesi *et al.*, 1991) thereby increasing cytoplasmic $[Ca^{2+}]$. Conversely, calmidazolium binds to sarcoplasmic reticulum Ca^{2+}-ATPases in a non-competitive manner, inhibiting Ca^{2+} release (Fischer *et al.*, 1987). These ambivalent effects have been observed concurrently in gastric smooth muscle (Lucchesi and Scheid, 1988). *In vitro*, calmidazolium is also antagonistic towards erythrocyte Ca^{2+}-ATPases and other ion pumps such as the Na^{+}/K^{+} antiport (Gietzen, 1983). Results are therefore not as convincing as for W7 and TFP.

As explained in Chapter **1**, calmodulin localises to sites of cell growth in plants and yeasts (Haußer *et al.*, 1984 ; Sun *et al.*, 1992 ; Brockerhoff and Davis, 1992 ; Ohya and Botstein, 1994) where it controls, among other effects, F-actin localisation (Ohya and Botstein, 1994). F-actin is essential to polarity in *Fucus* (Brawley and Robinson, 1985) and is localised at the presumptive rhizoid pole during axis fixation of *F. distichus* zygotes (Kropf *et al.*, 1989). Results presented here indicate that calmodulin is essential for polar axis formation in photopolarising *F. serratus* zygotes. Given this parallel, a similar situation to that of budding yeast may exist in *Fucus* zygotes: Active calmodulin might polarise during axis formation and guide

the polar accumulation of F-actin at axis fixation. An asymmetric distribution of active calmodulin may therefore be a step between Ca^{2+} mobilisation during axis formation and F-actin redistribution at axis fixation.

4. 1. 3 Other inhibitors

Various other pharmacological inhibitors had no effect on axis orientation, showing that drug toxicity alone did not affect photopolarisation. It is, however, impossible to conclude on the involvement of the pathways which these compounds target during photopolarisation. These drugs act as positive controls and confirm that the effects of the Ca^{2+} channel and calmodulin inhibitors on polarity was due to antagonism, and not to toxicity and, as such, support the claim that the mobilisation of both intracellular free Ca^{2+} and of active calmodulin are key participants in photopolarisation.

4. 1. 4 How might these inhibitors be affecting zygotes?

Bepridil, W7 and TFP affected all zygotes and caused complete randomisation of the polar axis. A gradual response in terms of population, nevertheless means an all or none response for the individual zygote. The dose dependency of inhibition can be due to gradual reaching of inhibitory thresholds normally scattered throughout the population. Some zygotes may be more resistant to inhibitors than others because they possess more of the target molecule.

Inhibition dose dependency might also be due to complex dynamic interactions between the inhibitor and it's target molecule which is also in a constant state of biochemical flux. For example, the action of nifedipine upon Ca^{2+} channels is reduced in the presence of their normal ligand, Ca^{2+}, due to competition for binding sites and variations in relative affinity. Dose-

due to competition for binding sites and variations in relative affinity. Dose-dependency may also be consequential to a concentration dependent change in drug specificity. Verapamil inhibited photopolarisation in two zygote subpopulations, one group at lower concentrations and the other at higher concentrations. In this case, drug specificity may alter with increasing concentration resulting in a sudden inhibition of more pathways leading to an increased response throughout the population.

For $LaCl_3$, TMB-8, verapamil and calmidazolium, the zygote population was divided into inhibitor-sensitive and -insensitive groups. The variability between the zygotes' response to the different inhibitors may be explained by drug specificity. For example bepridil might block all Ca^{2+} channels, whereas the action of TMB-8 or verapamil may be more specific, inhibiting only one type of channel. However, specificity alone cannot be used to explain differences in response for only one inhibitor as exposure to one inhibitor will, in some zygotes, totally inhibit photopolarisation, while in others there will be no effect (photopolarisation is an all or none response). Insensitive zygotes are presumably using a different pathway from that which is blocked by the inhibitor to respond to the polarising stimulus. This alternative pathway may physically exist only in this subgroup, or, more realistically, be active only in this subgroup. Sensitive zygotes are perhaps at a stage in embryogenesis where the alternative is not possible. Only by targeting inhibition to a defined period of embryology could these individual differences be detected. A zygote's response to a given inhibitor is therefore dependent on the compound's specificity, its concentration, and the intracellular particularities and developmental stage of the individual zygote.

4. 2 Single cells and zygote populations: Individuality and conformism

Studies of Fucoid polarisation have generally dealt with the responses of the majority of a zygote population, and have therefore minimised, even discounted, individual variability relative to the global response. Notable exceptions are the research which demonstrated the epigenic nature of the polar axis (Jaffe, 1958) and the determination of the photosensitive period of a single zygote (Feucht and Bentrup, 1972). During the investigation described here (Sections *2. 2* and *3. 1*), individual zygotes sometimes segregated into inhibitor-responsive and -unresponsive groups, highlighting the individual heterogeneity within a zygote population.

4. 2. 1 Individuality conferred

Genetic differences are the most obvious causes of individuality between organisms. Zygotes, however, possess two genetic identities; that of the zygote residing in the nucleus, and that of the mother, maternal RNA stored in the cytoplasm during oogenesis (Slack, 1991). *F. serratus* eggs store both mRNP (Hetherington *et al.*, 1990) and mRNA (Masters *et al.*, 1992) which is translated during embryogenesis (Quatrano, 1968 ; Kropf *et al.*, 1989). Zygotes of *F. vesiculosus*, which compare well with those of *F. serratus* (Feucht and Bentrup, 1972), start transcription from 1-5 h AF, and translation from 8-12 h AF (Quatrano, 1968). Consequently, both zygotic and maternal genetic individuality are possible sources for heterogeneity within a zygote population.

Like for maternal mRNA, Fucoid eggs inherit different intracellular environments from different mother plants. These differences will result in varying intracellular biochemistries, and hence in developmental individuality. Perhaps this argument can be extended to include eggs produced between different oogonia, or even between the daughter cells of a

single oogonium. In this case smaller differences may be expected.

Finally, environmental factors might influence a zygote's individuality. Seasonality, forced gamete secretion and fertilisation in the laboratory may enhance differences between zygotes' maturity. Laboratory cultures, dominated by zygotes issued from a restricted number of mothers, cannot be representative of the wild population. Moreover, *Fucus* zygotes respond to a variety of stimuli. Integrating environmental information from distinct sources and using various signal transduction pathways could thereby enhance individual differences. These ideas are speculation, but stress that numerous genetic, cellular and environmental factors may confer heterogeneity to a zygote population, even though the experimental protocol strove to minimise these differences.

4 .2 .2 Individuality expressed

In ASW, photopolarisation reaches a maximum 75-85% during the experiments described in Section **2. 2.** In *F. serratus* PSP_{pop} begins at 6 h AF (Feucht and Bentrup, 1972). Photosensitivity of the population, not of a single zygote, gradually increases to reach a maximum between 10-13 h AF. Following a brief decline at 13-14 h AF, PSP_{pop} peaks again, before declining to 0 (Figure 1-2-4). PSP_{pop} therefore lasts approximately 10 h. Alternatively, PSP_{cell} is only 1 h (Feucht and Bentrup, 1972 ; Bentrup, *pers. comm.*, 1993). If PSP_{cell} falls outside the interval of applied stimulus in these experiments (10-13 h AF), the zygote concerned would exhibit random polarity. Thus the 75-85% photopolarisation baseline may be due to the disparity between PSP_{pop} and PSP_{cell}.

A particular stage in early embryonic development is related to a particular period in the cell cycle (Quatrano, 1968 ; Kropf and Quatrano, 1987). The cell cycle, however, is only broadly synchronised and varies

between zygotes. For instance rhizoid germination, a morphological marker of cell cycle progression, occurs over a four hour period in *F. serratus* (Quatrano, 1968). Variation in zygotes responses to both polarising light and to inhibitors may therefore be influenced by individual timing.

4. 3 Calmodulin extraction and gene cloning from *Fucus serratus*

4. 3. 1 Calmodulin extraction

Pure calmodulin was extracted from *F. serratus* sperm by salt fractionation followed by W7 affinity chromatography (Sections **2. 2** and **3. 2**). The protein migrated with an apparent molecular weight of approximately 16 kDa on SDS PAGE, corresponding with that of calmodulin. Band shift in the presence or absence of Ca^{2+}, characteristic of calmodulin (Watterson *et al.*, 1980 ; Brawley and Roberts, 1989), was not shown due to the requirement for sample economy. Yield was low, 0.15 $\mu g \cdot g^{-1}$, and may be explained by a combination of factors. First, sperm are specialised to carry a male pronucleus to the female and, as such, are constitutively low in certain proteins relative to other tissues. Second, the viscosity of the initial sperm homogenate may have hindered homogenous $(NH_4)_2\,SO_4$ mixing and dissolution during ammonium sulphate fractionation (Englard and Seifter, 1990). Heterogeneous $(NH_4)_2\,SO_4$ dissolution, resulting in localised concentrations beyond the isoelectric point of calmodulin at pH 7.0, might cause calmodulin precipitation and therefore loss of an unknown, and possibly substantial amount of calmodulin. This possibility is supported by the failure to replicate calmodulin extractions using the same batch of sperm. Finally, a concentration of 10 mM EGTA in the W7 affinity eluate (calmodulin sample) might impede accurate spectrophotometric readings at Abs_{280}.

A combination of ion exchange chromatography and W7 affinity chromatography produced no calmodulin although calmodulin had previously been identified in similar fractions eluted from ion exchange columns (Brawley and Roberts, 1989), using 8 h old *P. fastigiata* zygotes. The use of *F. serratus* zygotes or eggs as source tissues was impractical due to the viscosity of lysates which blocked ion exchange columns. Sperm homogenates, however, penetrated the DE52 matrix, as indicated by the bright orange colour of the homogenate, and sample viscosity did not obstruct flow through the ion exchange column. A putative calmodulin band is visible on SDS PAGE of the sperm lysate applied to the ion exchange column. This band eluted with 0.3M NaCl, but when applied to the W7 affinity column, was not retained. Either the calmodulin concentration of the W7 affinity column was too low to be detected by coomassie blue staining, in which case calmodulin extractions using this method were not practical for future experiments, or this putative band was not, in fact, calmodulin. Failure to obtain calmodulin was therefore attributed to a combination of two factors: Calmodulin may be present only at low levels in sperm, or negatively charged polysaccharides such as alginic acid and fucoidin, which inevitably contaminated the homogenates, may have prevented the ion exchange column from functioning efficiently. Weakly negative or less concentrated molecules, such as calmodulin, may have thereby been lost during the procedure.

The presence of high concentrations of polysaccharide in sperm homogenates was unavoidable due to the method of sperm collection, and may possibly have originated from receptacle secretions or from antheridial cell walls. The need to retain the integrity of proteins prevented the use of enzymatic digestion to eliminate contaminating polysaccharides.

To avoid the problem of low yield from calmodulin extractions, an alternative source of calmodulin was sought. Cloning the calmodulin cDNA or gene from *F. serratus* would enable transgenic expression of calmodulin in bacteria (Das, 1990), and the use of *F. serratus* calmodulin in further experiments. Alternatively, knowledge of the gene sequence would assist in identifying heterologies between *F. serratus* and other calmodulins. The most closely related calmodulin could then be selected for further experimentation with developing *F. serratus* zygotes.

4. 3. 2 Nucleic acid extraction from Fucus serratus

RNA was extracted from *Fucus serratus* eggs or zygotes using 7 different methods, 3 of which yielded intact RNA. The first method, that of repeated phenol extractions followed by LiCl precipitation, produced RNA contaminated by significant amounts of algal polysaccharides. The RNA yield was low and may have been due to progressive loss of RNA during the various phenol extractions. A variation of this method, based on tissue lysis in guanidine thiocyanate buffer to protect RNA from degradation, followed by repeated phenol extractions, ethanol precipitation and polysaccharide cleansing, also produced RNA. Again the yield was low and the RNA was contaminated by polysaccharide. Repeated phenol extractions and difficulty in re-dissolving the RNA/polysaccharide pellet following ethanol precipitation might also account for the loss of a significant proportion of the RNA. Finally, a third method involving lysis in a CTAB buffer, repeated chloroform extractions, polysaccharide cleansing and LiCl precipitation, yielded up to a thousand fold more RNA than the two preceding methods, with less polysaccharide contamination. CTAB in the extraction buffer chelates and "protects" nucleic acids (Murray and Thompson, 1980) and might also isolate RNA from contaminating polysaccharides in the

homogenate, thus facilitating polysaccharide cleansing. Moreover, unlike the guanidine method RNA was not precipitated until the last step of the purification process, thereby avoiding simultaneous polysaccharide/RNA precipitation.

The RNA yield for all the extraction methods was erratic even between replicate experiments using the same tissue, the same solutions, and performed on the same day. The reason for this unreliability is not clear. Moreover, contamination by algal polysaccharides was persistent.

DNA was readily extracted from *F. serratus* sperm, and showed no particular pattern of methylation. Restriction digests resulted in uniform smearing, without any particular pattern of bands, demonstrating that the DNA interacted positively with DNA modifying enzymes.

4. 3. 3 Amplification of a calmodulin DNA fragment from cDNA

In vitro amplification with fully degenerate oligonucleotide primers to a consensus calmodulin sequence produced no DNA fragment with *F. serratus* cDNA as template, and may be explained in several ways.

It is possible that the primers did not anneal to the *F. serratus* calmodulin cDNA sequence due to heterology. For primer annealing and correct recognition by thermostable DNA polymerase, sequence homology between the target DNA and the last three bases of the 3' portion of the PCR primer is essential (McPherson *et al.*, 1991). If the primer and target sequence mismatch in this region, primer annealing is not perfect and amplification is hindered. Consequently, a single base heterology at the 3' end of the primer may stop amplification. The final amino acid of the peptide portions of calmodulin from which the primers 236 V, 113 Y and Q 34 were derived, are heterologous between species screened (Figure 2-11-1). It may seem peculiar to have selected amino acid

sequences from which to derive PCR primers which exhibited heterology in such an important position, but this heterology was due to the fungal element of the consensus, and did not indicate heterology between plant species. Moreover, these were the only sites which encompassed a series of characteristics, including exclusion from the calmodulin EF-hands, minimal heterology over 15-20 bp, minimal codon use (minimal redundancy), 50-60% guanine/cytosine content, and the potential for a guanine or cytosine at the 3' terminus of the derived primer. Considering these advantages, it was deemed acceptable to discount 3' terminal amino-acid heterology of fungal sequences. Regarding plant species alone, 236 V is the only primer with 3' terminal base heterology to the consensus, and was a relic from previous work within the research group with *A. thaliana.*

It is also possible that no calmodulin message was present in the cDNA. Either no calmodulin mRNA was present in eggs or zygotes or the reverse transcription reaction did not function correctly. The former situation is extremely unlikely as calmodulin is a constitutive protein of many cells and is present in the sperm, eggs and zygotes of *F. distichus* (Brawley and Roberts, 1989). The protein may be present in the cytoplasm of the egg or young zygote through maternal inheritance, but maternally inherited calmodulin mRNA would also be expected to be present in the cytosol of eggs. Furthermore, "eggs" purified for biochemical or molecular extractions also contained oogonia at various stages of maturity. Given the importance of calmodulin in the cell cycle (Section *1. 5. 2*), maturing oogonia were expected to contain high quantities of calmodulin mRNA and zygotes, which commence transcription 1-5 h AF (Quatrano, 1968), were expected to contain calmodulin mRNA by 24 h AF. The issue could have been resolved by northern analysis of RNA extracted from *F. serratus* eggs or zygotes using a probe for calmodulin, but was not possible due to the

difficulties of RNA extraction, notably poor reliability and low yield. The latter situation may have arisen due to contamination of RNA samples by acidic polysaccharides, such as those secreted by the Fucales, which inhibits the activity of nucleic acid modifying enzymes (Aoki and Koshihara, 1972 ; Su and Gibor, 1988 ; Fang *et al.*, 1992). Was mRNA retrotranscription inhibited by polysaccharide contamination, no template would exist for *in vitro* amplification. Alternatively, if cDNA synthesis did occur, polysaccharides may have been carried to the PCR reactions in the cDNA solution, inhibiting thermostable DNA polymerase activity. As polysaccharide contamination of extracted RNA was substantial, these two possibilities are the most probable explanation for the failure of PCR using cDNA as template.

4. 3. 4 Amplification of a calmodulin DNA fragment from genomic DNA

Southern blot analysis of *F. serratus* genomic DNA (Section **2. 9**) demonstrated the presence of nucleotide sequences which hybridised, under high stringency conditions, to the calmodulin cDNA from *C. reinhardtii.* However, *in vitro* amplification using *F. serratus* genomic DNA as template was hampered by persistent artefacts, the most severe being the annealing of Q 34 to both ends of the template DNA which yielded the B517 DNA fragment. An alternative reverse primer could not be designed due to the poor conservation of the calmodulin carboxyl terminus, and by the abundance of amino acids coded for by at least four codons in that region. This Q 34 artefact was ubiquitous over a range of annealing temperatures. Its presence may have inhibited the amplification of the targeted fragment. It is interesting to note that PCR produced a fragment of the correct size from *C. reinhardtii* genomic DNA using primers A 657 and Q 34, yet nothing from *F. serratus* genomic DNA barring B517.

4. 4 Cloning and expression of the calmodulin cDNA from *Macrocystis pyrifera*

4. 4. 1 Calmodulin PCR fragment, B320

A calmodulin PCR fragment labelled B320 was amplified using primers A 657 and Q 34 and DNA extracted from a *M. pyrifera* cDNA library (Section **2. 12**) as template. Amplification using primers 236 V and Q 34 yielded no fragment. Furthermore, amplification with primers 113 Y and Q 34 produced no PCR product when targeted to library DNA even though the target sequence and the primer sequence were homologous (Figure 3-4-3), yet gave a fragment of the correct size (~220 bp) when these primers were used to re-amplify B320. The use of fully redundant oligonucleotides might explain, in part, the complexities observed.

4. 4. 2 cDNA clone 4.2a nucleotide sequence

Clone 4.2a was 1487 bp in length. The sequence comprises an open reading frame of 450 bp, with 75.11% nucleotide sequence homology with *A. thaliana* calmodulin in a complete sequence overlap (EMBL database identifier; em_pl:atcam2). Homology to the calmodulin nucleotide sequences of *H. vulgare* (EMBL database identifier; em_pl:hvcama) and of *C. reinhardtii* (EMBL database identifier; em_pl:crcam) was 86.00% and 62.72% respectively. The first base of the translational start codon (ATG) of the open reading frame was labelled +1 and all other bases were labelled relative to this position. The start codon was present within a translational start sequence, $^{5'}$AXX ATG CG (Grierson and Covey, 1988), commencing at base -3. The translational stop sequence, TAG, occurred at position +448 bp. A 3' non-translated sequence of 295 bases followed the stop codon and preceded a poly-A tail of 29 adenines at +745 bp. A putative polyadenylation signal, $^{5'}$ACT AAA (Grierson and Covey, 1988), is present 25 bp upstream of the poly-A tail (+720 bp).

Although the genetic code is redundant (Figure 4-4-1), codon selection within a gene is not random (Old and Primrose, 1989). Codon bias seems to be dependent on both the abundance of various tRNAs in the cytoplasm which affect the translation rate, and the conservation of the translated sequence in the event of codon/anticodon mispairing; a sort of mistranslational "buffer". The coding sequence of clone 4.2a presents striking preference for cytosine or guanine at the third position of the codon. 10 amino acids of the 17 which make up *M. pyrifera* calmodulin (arginine, asparagine, glutamic acid, histidine, isoleucine, lysine, phenylalanine and proline) are coded for by a single codon terminating by either guanine or cytosine, though at least one other possible codon exists for each residue (Figure 4-4-1). Only 7 out of the 148 amino acid codons making up *M. pyrifera* calmodulin finish with a thymine; 2 for alanine (+4 bp and +31 bp), 2 for aspartic acid (+7 bp and +73 bp), 1 for glycine (+397 bp) and 2 for threonine (+103 bp and +133 bp). No codon carries an adenine at position 3. Due to the absence of other *M. pyrifera* nucleotide sequences in the EMBL database (search of 14-11-94), it is impossible to state whether this particular codon bias is characteristic of the species. In *A. thaliana*, such codon bias does not exist: 90 codons out of the 150 coding for calmodulin in *M. pyrifera* show third base heterology to their corresponding codon in *A. thaliana*. Of these 90, 59 substitutions are adenine or thymine replaced by guanine or cytosine. Conversely, *C. reinhardtii* presents a guanine-cytosine bias at codon position 3 for genomic RNAs (Zimmer *et al.*, 1988). This bias is not found, however, in chloroplast mRNAs. Again, due to the lack of previous research, it is impossible to compare this observation with *M. pyrifera*.

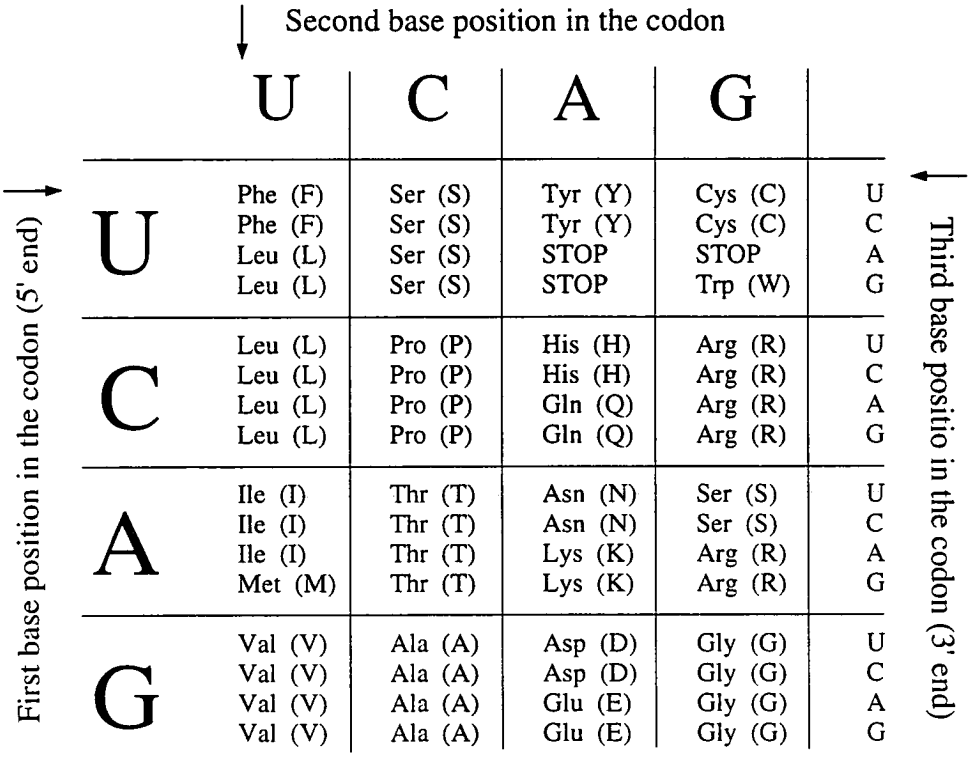

Figure 4-4-1. The genetic code.

RNA nucleotides are represented by their initials. Amino acids are represented both by their three-letter abbreviation and by the single letter code.

The 5' end of the cloned sequence starts with a *Xho* I site (-693 bp) linked to a region of 20 thymines which represents an inverted poly A tail. Clone 4.2a therefore carries a re-arrangement, possibly a cloning artefact which ligated two unrelated DNA strands. At the 5' terminus of the cDNA cloned into Uni-Zap XR, an *Eco* RI site is expected (Figure 2-12-1). In fact, two putative *Eco* RI sites are recognised upstream of the open reading frame, each possessing a single mutation relative to the normal *Eco* RI sequence ($^{5'}$GAA TT$_{\wedge}$C). The first, $^{5'}$GA***T*** TTC, is located at position -553 bp and the second, $^{5'}$G***T***A TTC, at position -85 bp (Figure 2-12-1). The leader sequence which precedes the coding sequence is generally 50-150 bp long (Grierson and Covey, 1988). Thus, the second transformed *Eco* RI site at -85 bp may represent the start of the leader sequence of the cloned calmodulin cDNA. Consequently, the re-arranged portion of clone 4.2a probably extends from position -693 bp to position -85 bp. A search of the EMBL database yielded no homologous sequence to the re-arrangement, the closest case being 41.9% homology to human RNA for a fetoprotein in a 31 amino-acid overlap. This absence of sequence identity is not surprising given the presence of the 2 transformed *Eco* RI sites which suggests the re-arrangement was, in fact, double.

By construction, a *Xho* I restriction site is fused to the poly-A tail of cDNA during the cDNA library cloning procedure (Figure 2-12-1). However, in clone 4.2a, a the poly A tail is linked to a transformed *Xho* I site, $^{5'}$CTC GA***C*** rather than $^{5'}$CTC GA$_{\wedge}$G (+773 bp). The nature of the mutation is significant in that a cytosine replaced a guanine, causing no change in hydrogen bonding within the site. This putative restriction site is linked to the *Eco* RI restriction site (+786 bp) by 7 nucleotide bases. Thus both ends of the calmodulin cDNA clone of *M. pyrifera* were re-arranged.

4. 4. 3 Macrocystis pyrifera calmodulin amino acid sequence

Translation of the open reading frame of clone 4.2a yielded a polypeptide with 92.62% homology to the plant and fungal calmodulin consensus sequence (Figure 2-11-1). As for other species, sequence heterologies are concentrated towards the carboxyl terminus of the protein (Davis *et al.*, 1986). The amino acid substitutions between *M. pyrifera* and the consensus preserve the polar or charged nature of the substituted residue in 10 cases out of 11. In the case where charge is altered by the substitution, an isoleucine (hydrophobic residue) replaces an arginine (positively charged residue) at amino acid position 88.

The calmodulin peptide sequence of *M. pyrifera* is 90.60% homologous to that of *A. thaliana*, and bears 93.29% homology with *H. vulgare*. *M. pyrifera* calmodulin presents 79.19% homology to that of *C. reinhardtii*, the only algal calmodulin present in the EMBL database. The protein lacks the characteristic N-terminus leader sequence and carboxyl terminus tail of *C. reinhardtii* (Zimmer *et al.*, 1988) suggesting that the calmodulin sequence of *C. reinhardtii* represents specific specialisation rather than an ancestral calmodulin as previously proposed (Schleicher *et al.*, 1983).

The presence of 3 methionine residues at positions 145, 146 and 147 of *M. pyrifera* calmodulin is unique among known calmodulin sequences. 46% of the solvent accessible surface area of the N and $COOH^-$ terminal lobes (residues 1-76 and residues 94-149) of bovine calmodulin are contributed by methionine side chains (O'Neil and DeGrado, 1990). Methionine is therefore particularly abundant on the surface of calmodulin generally. Moreover, unlike the other hydrophobic residues (alanine, isoleucine, leucine, phenylalanine, proline, tryptophan and valine), the side

chain of methionine is unbranched, providing high conformational flexibility. In turn, this flexibility is thought to enhance the sensitivity of methionine-rich binding sites to subtle variations in ligand surface conformation, while retaining a rigid backbone (O'Neil and DeGrado, 1990). It is possible that the methionine-rich portion of the carboxyl terminus of *M. pyrifera* calmodulin serves such a function.

4. 4. 4 Evolutionary conservation of Macrocystis pyrifera calmodulin

M. pyrifera calmodulin is highly homologous with other plant and fungal calmodulins, presenting less than 10% amino acid divergence from calmodulin of the dicotyledonous *A. thaliana*, or the monocotyledonous *H. vulgare*. These 3 species are the products of approximately 300 million years of independent evolution. It is therefore reasonable, albeit uncertain, to assume that calmodulin from *M. pyrifera* would also strongly resemble that of its close relative *F. serratus*. Although some amino acid substitutions have been shown to alter the activity of calmodulin (Davis, 1992*a* ; Lu *et al.*, 1993 ; Ohya and Botstein, 1994), it has also been observed that calmodulins from different species are interchangeable (Rasmussen and Means, 1989*b* ; Davis and Thorner, 1989). *M. pyrifera* calmodulin was therefore considered to present sufficient relationship with that of *F. serratus* to be microinjected into developing *F. serratus* zygotes in lieu of the native calmodulin.

4. 5 Expression of *Macrocystis pyrifera* calmodulin in bacteria

The *M. pyrifera* calmodulin coding sequence (clone 4.2a). was engineered into *E. coli* and recombinant protein expression induced by 4 M IPTG (Section **2. 13**). The protein was only present in lysates of transgenic bacteria which had been induced by IPTG. Calmodulin was soluble, and readily purified from bacterial lysates by W7 chromatography, though

approximately 70% of the calmodulin produced by bacteria was lost at this stage. Although the presence of EGTA in the elution buffer (Section *2. 2. 4*) impeded accurate spectroscopic measurements at Abs_{280}, SDS PAGE analysis identified the calmodulin containing fractions. Moreover, calmodulin was absent from any wash fractions indicating that the column was neither saturated no defective in affinity binding. Protein loss was therefore attributed to a suboptimal chromatographic process due to a low column length : section ratio (30 mm : 5 mm) (Wilson and Goulding, 1988).

Analysis by SDS PAGE demonstrated that the protein product of pB820-E behaved like a functional plant calmodulin, migrating at ~15 kDa in the presence of Ca^{2+}, with a electrophoretic band shift to ~18 kDa in the presence of EGTA (Watterson *et al.*, 1980). The protein was purified by W7 affinity chromatography, giving further evidence that it is calmodulin, and is functional. Purified calmodulin was concentrated to approximately 5 $\mu g \cdot \mu l^{-1}$. Phosphodiesterase assays will enable a comparison between the cyclic nucleotide phosphodiesterase activity of the recombinant *M. pyrifera* calmodulin (Cheung, 1970) with, for instance, bovine brain calmodulin or spinach calmodulin. These experiments are currently underway.

4. 6 Estimate of calmodulin concentration required for microinjection

Calmodulin microinjections into *F. serratus* eggs or zygotes were proposed to disrupt any polarised calmodulin localisations. Consequently, it was necessary to estimate the potential injected volume, and the concentration of calmodulin required in the injection microelectrode to cause a reasonable increase in intracellular calmodulin concentrations.

The average diameter (2r) of the *F. serratus* zygote is 60 μm.

Hence, the volume (Vz) of the *F. serratus* zygote is

$Vz = \frac{3}{4} \pi r^3 = \frac{3}{4} \pi (30 \cdot 10^{-6})^3 = \frac{3}{4} \pi 2.7 \cdot 10^{-14} = 63.6 \cdot 10^{-12}$ l = 63.6 pl

The maximum injectable volume, Vi_{max} = 10%Vz = 6.36 pl

The minimum injectable volume, Vi_{min} = 1%Vz = 0.64 pl

The calmodulin concentration of the purified samples is 5 $\mu g \cdot \mu l^{-1}$.

Hence the amounts of calmodulin injected, I_{max} and I_{min}, are,

I_{max} = 31.8 pg or, in moles, $I_{max} = 31.8 \cdot 10^{-12} / 18{,}000 = 572 \cdot 10^{-17}$ mol

I_{min} = 3.2 pg or, in moles, $I_{min} = 3.2 \cdot 10^{-12} / 18{,}000 = 57.6 \cdot 10^{-17}$ mol

The cytosolic calmodulin concentration in *F. serratus* zygotes was assumed to be 10^{-6} M, similar to that of other plant cells (Marmé and Dieter, 1983). Although previous calmodulin extractions (Sections **3. 2** and*4. 3. 1*) suggested a calmodulin concentration approximately 100 fold less in *F. serratus* than in plants generally, sperm, which might be constitutively lower in calmodulin, was used as source tissue. Consequently it is better to assume a greater calmodulin concentration in zygotes, which is, in moles,

$CaM = Vz \times 10^{-6} = 63.6 \cdot 10^{-12} \times 10^{-6} = 6.36 \cdot 10^{-17}$ mol

Thus, microinjection of the purified *M. pyrifera* calmodulin solution will increase the cytosolic calmodulin concentration by a factor of 10 to a factor of 100 (1-2 orders of magnitude).

4. 7 Calmodulin microinjections into *Fucus serratus* zygotes

Microinjection of calcium green into photopolarised zygotes disrupted photopolarisation (Figure 3-6-4). This effect, however, was countered by the simultaneous injection of calmodulin and calcium green into photopolarised zygotes which re-enforced photopolarisation. These experiments were performed under the assumption that calmodulin microinjections would disrupt any polarised calmodulin activity in photopolarised zygotes (Sections *1. 6. 2* and **4. 6**). Rather than swamping the proposed calmodulin localisations, microinjections of *M. pyrifera* calmodulin are instead enhancing photopolarisation (Section **3. 6**). This result can only be explained by the microinjected calmodulin being mobilised to the photopolar axis, thereby strengthening photopolarisation relative to the polarity caused by microinjection. Thus, localised calmodulin activity does indeed appear to be involved in photopolar axis formation. Moreover, it is polarisation of active calmodulin, rather than polarised activation of the protein which these experiments have uncovered. The evidence remains, however, circumstantial, and only direct visualisation of calmodulin by, for instance, phenothiazine fluorescence (Haußer *et al.*, 1984) or by immunolocalisation, will resolve the matter.

Given that polar accumulations of calmodulin are apparently involved in photopolar axis formation, the initial signal for calmodulin recruitment and the manner in which calmodulin is polarised remains a mystery. It is possible that a localised increase in Ca^{2+} may cause local activation of calmodulin which, in turn, causes calmodulin polarisation. This, however, is speculation.

4. 8 A model of photopolarisation in *Fucus serratus*

Current models of polarisation in Fucoid zygotes propose that a cytoplasmic Ca^{2+} gradient guides metabolic activity and cytoskeletal components (F-actin) to the presumptive rhizoid pole (Section *1. 3. 3*). The work presented here has shown that the mobilisation of cytoplasmic free Ca^{2+}, mainly from intracellular Ca^{2+} stores, and localisations of active calmodulin are essential components of photopolarisation in *F. serratus* zygotes (Sections **4. 1** and **4. 7**). These findings may be incorporated into a refined model of photopolarisation (Figure 4-8-1), based on the cortical epigenesis model (Figure 3-3-2).

During the period of photosensitivity, light causes a localised signal which results in a localised release of Ca^{2+} mainly from intracellular stores, although zygotes might also utilise Ca^{2+} from the surrounding medium (Figure 4-8-1_a). This mobilisation of cytoplasmic free Ca^{2+} might be self-enhancing by localised CICR. The increase in Ca^{2+}_{cyt} results in localised accumulation active calmodulin. As the rhizoid pole is the focus of cytoplasmic localisations, it is assumed that both Ca^{2+}_{cyt} and Ca^{2+}-CaM also localise at the presumptive rhizoid site, though this has not been demonstrated (Figure 4-8-1_b). Whether localised Ca^{2+} acts only as a trigger for calmodulin activation, or instead has another function, such as initiating trans-cellular currents and membrane protein segregation, is unclear. By comparison with yeast cell bud formation, Ca^{2+}-CaM polarisation then guides F-actin polymerisation at the incipient rhizoid (Figure 4-8-1_c). Cytoskeletal-cell wall bridges then stabilise and fix the polar axis. This scenario can explain the observed facts, but, it must be stressed, is only a model and an over simplification of the real processes involved during polar induction.

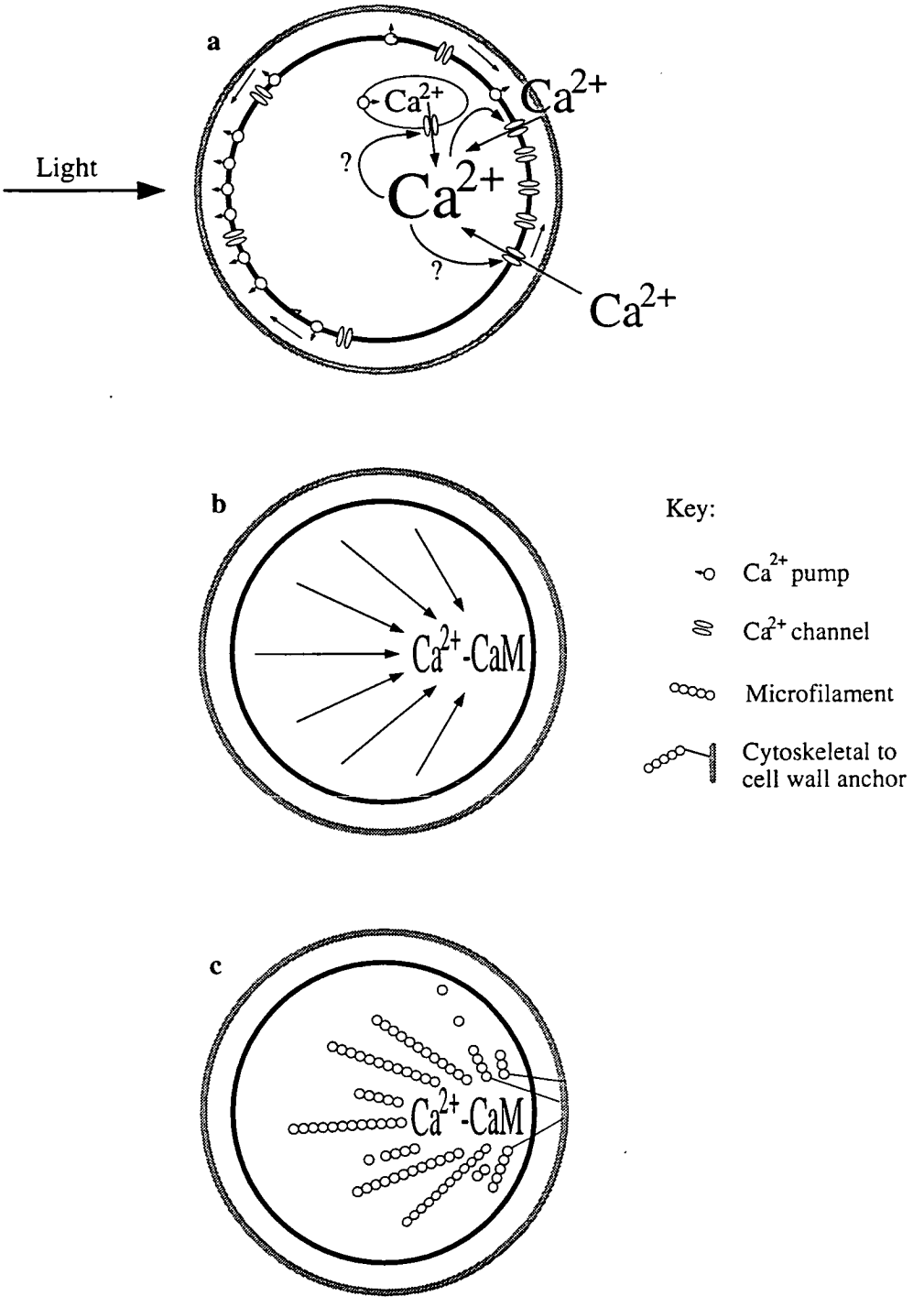

Figure 4-8-1. Model of photopolarisation involving intracellular Ca^{2+} mobilisation and localisation of Ca^{2+}-CaM.

The model presented refines the cortical epigenesis model (Figure 3-3-2). Details are given in the text.

4. 9 Future research

The experimental findings and the model of photopolarisation described highlight areas where further research is essential.

First, more work must be carried out regarding the role of Ca^{2+} in polarisation of plant cells. The dynamics of cytoplasmic Ca^{2+} in polarising cells should be visualised, and if this is not possible in the dense cytoplasm of the traditional *Fucus* zygote, a substitute must be found. Artificial Ca^{2+} gradients might be initiated in plant cells using caged compounds, and the effects on cell polarity monitored. More knowledge is required concerning the channels, pumps, and binding proteins which regulate Ca^{2+} mobilisation and concerning the events downstream of Ca^{2+} signalling. Moreover, the function of intracellular currents in polarisation needs to be clarified: are intracellular currents causes or consequences of polarity? Does lateral electrophoresis of membrane proteins really occur?

The movement and localisations of calmodulin are also targets for further study, both at the cellular and the molecular level. Calmodulin localisations may be visualised in polarising *Fucus* zygotes either by CTC fluorescence, or by immunolocalisation. The knowledge that the *M. pyrifera* calmodulin sequenceis homologoue to that of higher plants suggests that such experiments would be successful. The signals for calmodulin localisation and the molecules which might assist in calmodulin translocation also need to be identified. In this respect analysis of calmodulin mutants in yeast is useful, but such fine experiments must be also be adapted to plant cells. Targeted inhibition of selected portions of the calmodulin molecule using synthetic calmodulin-binding peptides might substitute for mutational studies in plant cells. Also, the use of antisense technology to produce calmodulin impoverished plants is worth considering.

Furthermore, the molecular interactions with calmodulin and components of the cytoskeleton, notably F-actin, should be investigated.

The periods of sensitivity to polarising cues in developing *Fucus* zygotes must be addressed anew. Particular attention should be given to the responsive periods of individual zygotes, as well as to zygote populations. Moreover, the intracellular events associated with perception and transduction of different polarising cues must be investigated. The use of widely varying stimuli, electromagnetic, electrical, mechanical and chemical would be beneficial. Intuitively, it seems that a point of convergence between the various stimuli would be found, but at what level in the signal transduction chain? Finally, a holistic approach should not be abandoned, and comparison between the mechanisms of polar initiation and maintenance in various plant systems should be almost permanent.

Chapter 5

Conclusion

The roles of Ca^{2+} and of calmodulin were investigated during photopolarisation in *F. serratus* zygotes. Transient application of various inhibitors of cytoplasmic Ca^{2+} mobilisation and of calmodulin activity to photopolarising zygotes demonstrated an essential role for both cytosolic free Ca^{2+} and for active calmodulin in photopolarisation. It was shown that although Ca^{2+} from the extracellular medium might be involved, intracellular Ca^{2+} stores were the main source for cytosolic Ca^{2+} mobilisation during polar axis formation. Comparison with bud formation in yeasts led to the hypothesis that calmodulin localisations were involved in polar axis selection in *F. serratus*. It was proposed that artificial increases in the cytoplasmic calmodulin concentration of photopolarising *F. serratus* zygotes would swamp any polarised signal, thus causing zygotes to polarise in random orientations *vis á vis* the applied light stimulus. Little, however, was known about calmodulin in the algae. The only algal calmodulin sequenced, that of *C. reinhardtii*, was substantially different from that of higher plants. More information regarding the calmodulin of *F. serratus* was therefore required.

Calmodulin purification from *F. serratus* tissues using a combination of ammonium sulphate precipitation and W7-affinity chromatography yielded approximately 0.15 μg calmodulin per gram of tissue, one hundred fold less than for plants generally. Moreover, the only practical tissue for protein extraction was sperm. To avoid the problem of low calmodulin yield, an alternative source of calmodulin was sought. Isolation of the calmodulin cDNA or gene from *F. serratus* would enable transgenic

calmodulin expression in bacteria. Also, knowledge of the gene sequence would assist in identifying heterologies between calmodulins from *F. serratus* and other plants. The most closely related calmodulin could then be selected for further experimentation with developing *F. serratus* zygotes. A homolog to the *C. reinhardtii* calmodulin cDNA clone was identified on Southern blots of *F. serratus*. However, due to persistent contamination of genetic material by algal polysaccharides, the use of fully redundant oligonucleotide primers for PCR and the limited range of possible primers, *in vitro* amplification of the *F. serratus* calmodulin nucleotide sequence resulted only in artefacts. As an alternative, the calmodulin cDNA was cloned from *M. pyrifera*, a close relative of *F. serratus*.

The *M. pyrifera* calmodulin cDNA clone displayed several remarkable features, notably over 75% coding sequence homology with *A. thaliana* and a strong codon bias favouring the presence of guanine or cytosine at the 3' base of each codon. The clone also carried a re-arrangement before the 5' non-coding region of the cDNA. At the amino acid level, *M. pyrifera* calmodulin lacks the characteristic extra amino acids at the N and carboxyl termini of *C. reinhardtii* calmodulin. However, it possesses a unique sequence of 3 methionines at the carboxyl terminus which may enhance binding between the calmodulin and certain target sequences. The cDNA coding sequence was engineered into *E. coli*, and recombinant *M. pyrifera* calmodulin expressed. The protein was purified by W7-affinity chromatography, and concentrated to 5 $\mu g \cdot \mu l^{-1}$ in an artificial cytoplasmic solution. At this concentration, and based on figures of calmodulin concentration in other plant cells, calmodulin microinjections into *F. serratus* zygotes was estimated to increase the intracellular calmodulin concentration by 1-2 orders of magnitude; sufficiently large to swamp any calmodulin localisations.

Calmodulin microinjections into photopolarised zygotes re-enforced the photopolar axis relative to zygotes injected with a control solution. This observation was interpreted as microinjected calmodulin being recruited to the polar axis, rather than diluting the signal as was expected. Active calmodulin therefore appeared to be both localised during photopolarisation, and translocated to the site of localisation according to the polarity induced by light. It was assumed that calmodulin would be localised at the presumptive rhizoid pole, and would guide microfilament assembly essential to axis fixation, somewhat like the process of budding in yeasts. Hence the cortical epigenesis model of polar formation in *F. serratus* zygotes must now incorporate both Ca^{2+} mobilisation from intracellular stores, and the localisation of calmodulin as essential components of polarity.

However, much more work still needs to be done. The role of Ca^{2+} must be pursued further, and calmodulin localisations must be visualised in polarising cells. Calmodulin itself must be scrutinised for localisation signals, and the mechanism of calmodulin translocation within cells studied. The signal transduction chains between several different polarising cues and axis formation need to be studied, as it is possible that several polarising mechanisms might work, in concert, during Fucoid embryogenesis. Moreover, accurate timing of polarisation events is essential to the success of any further study. Finally, the study of polarity cannot be restricted to one model system; several plant systems with different experimental qualities are required to explore this problem further, and meaningful comparisons made between them.

References

Alexandre, J. Lassales, J.P. and Kado, R.T. (1990)
Opening of Ca^{2+} channels in red beet root vacuole membrane by inositol 1,4,5,-triphosphate.
Nature, **343**; 567-570.

Allan E.F. and Trewavas, A.J. (1987)
The role of calcium in metabolic control.
in *Biochemistry of plants*, Vol. 12.
N.Y. Academic Press.

Allan, E. and Hepler, P.K. (1989)
Calmodulin and calcium binding proteins.
in *Biochemistry of plants*, Vol. 12.
N.Y. Academic Press.

Allbritton, N.L. Meyer, T. and Stryer, L. (1992)
Range of messenger action of calcium ion and inositol 1,4,5-triphosphate.
Science, **258**; 1812-1814.

Allen, R.D. Jacobsen, L. Joaquin, J. and Jaffe, L.F. (1972)
Ionic concentrations in developing *Pelvetia* eggs.
Dev. Biol. **27**; 538-545.

Allen, V.W. and Kropf, D.L. (1992)
Nuclear rotation and lineage specification in *Pelvetia* embryos.
Development, **115**; 873-883.

Aoki, Y. and Koshihara, H. (1972)
Inhibitory effects of acid polysaccharides from sea urchin embryos on RNA polymerase activity.
Biochem. Biophys. Acta, **272**; 33-43.

Babu, Y.S. Bugg, C.E. and Cook, W.J. (1988)
Structure of calmodulin refined at 2.2 Å resolution.
J. Mol. Biol. **204**; 191-204.

Battey, N.H. and Blackbourn, H.D. (1993)
The control of exocytosis in plant cells.
New Phytol. **125**; 307-338.

Bentrup, F.W. (1963)
Vergleichende Untersuchungen zur Polaritätsinduktion durch das Licht an der *Equisetum*-spore und der *Fucus*-zygote.
Planta, **59**; 472-491

Bentrup, F.W. (1964)
Zür Frange Eines Photoinaktivierungs-Effektes bei der Polaritätsinduktion in *Equisetum* Sporen und *Fucus* Zygoten.
Planta, **63**; 356-365.

Bentrup, F.W. and Jaffe, L.F. (1968)
Analyzing the "group effect": Rheotropic responses of developing *Fucus* eggs.
Protoplasma, **65**; 25-35

Bentrup, F. Sandan, T. and Jaffe, L. (1966)
Induction of polarity in *Fucus* eggs by potassium ion gradients.
Protoplasma, **64**; 254-266.

Berger, F. and Brownlee, C. (1993)
Ratio confocal imaging of free cytoplasmic calcium gradients in polarising and polarised *Fucus* zygotes.
Zygote, **1**; 9-15.

Berger, F. and Brownlee, C. (1994)
Photopolarization of the *Fucus sp.* zygote by blue light involves a plasma membrane redox chain.
Plant Physiol. **105**; 519-527.

Berger, F. Taylor, A. and Brownlee, C. (1994)
Cell fate determination by the cell wall in early *Fucus* development.
Science, **263**; 1421-1424.

Berkaloff, C. and Rousseau, B. (1979)
Ultrastructure of male gametogenesis in *Fucus serratus* (Phaeophyceae).
J. Phycol. **15**; 163-173.

Berridge, M.J. and Moreton, R.B. (1991)
Calcium waves and spirals.
Curr. Biol. **1**; 296-297.

Bjourson, A.J. and Cooper, J.E. (1992)
Band-stab PCR. A simple technique for the purification of individual PCR products.
Nucl. Acids Res. **20**; 4675.

Bolwell, G.P. Callow, J.A. Callow, M.E. and Evans, L.V. (1977)
Cross-fertilisation in fucoid seaweeds.
Nature, **268**; 626-627.

Bolwell, G.P. Callow, J.A. Callow, M.E. and Evans, L.V. (1979)
Fertilization in brown algae. II. Evidence for lectin sensitive complementary receptors involved in gamete recognition in *Fucus serratus*.
J. Cell. Sci. **36**; 19-30.

Bolwell, G.P. Callow, J.A. and Evans, L.V. (1980)
Fertilization in brown algae. III. Preliminary characterization of putative gamete receptors from eggs and sperm of *Fucus serratus*.
J. Cell. Sci. **43**; 209-224.

Brawley, S.H. (1987)
A sodium dependent fast lock to polyspermy occurs in eggs of Fucoid algae.
Dev. Biol. **124**; 390-397.

Brawley, S.H. (1990)
The polyspermy block in Fucoid algae.
in *Experimental Phycology*.

Brawley, S.H. (1991)
The fast block against polyspermy in Fucoid algae is an electrical block.
Dev. Biol. **144**; 94-106.

Brawley, S.H. and Bell, E. (1987)
Partial activation of *Fucus* eggs with calcium ionophores and low sodium sea water.
Dev. Biol. **122**; 217-226.

Brawley, S.H. and Quatrano, R.S. (1979)
Sulfation of fucoidin in *Fucus distichus* embryos. 4. Autoradiographic investigations of fucoidin sulfation secretion during differentiation and the effect of cytochalasin treatment.
Dev. Biol. **73**; 193-205.

Brawley, S.H. and Roberts, D.M. (1989)
Calmodulin binding proteins are developmentally regulated in gametes and embryos of Fucoid algae.
Dev. Biol. **131**; 313-320.

Brawley, S.H. and Robinson, K.R. (1985)
Cytochalasin treatment disrupts the endogenous currents associated with cell polarisation in Fucoid zygotes: Studies of the role of F-actin in embryogenesis.
J. Cell. Biol. **100**; 1173-1184.

Brawley, S.H. Wetherbee, R. and Quatrano, R.S. (1976*a*)
Fine structural studies of the gametes and embryo of *Fucus vesiculosus* L. (Phaeophyta). I. Fertilization and pronuclear fusion.
J. Cell. Sci. **20**; 233-254.

Brawley, S.H. Wetherbee, R. and Quatrano, R.S. (1976*b*)
Fine structural studies of the gametes and embryo of *Fucus vesiculosus* L. (Phaeophyta). II. The cytoplasm of the egg and young zygote.
J. Cell. Sci. **20**; 255-271.

Brawley, S.H. Wetherbee, R. and Quatrano, R.S. (1977)
Fine structural studies of the gametes and embryo of *Fucus vesiculosus* L. (Phaeophyta). III. Cytokinesis and the multicellular embryo.
J. Cell. Sci. **24**; 275-294.

Brockerhoff, S.E. and Davis, T.N. (1992)
Calmodulin concentrates at regions of cell growth in *Saccharomyces cerevisiae.*
J. Cell Biol. **118**; 619-629.

Brownlee, C. (1989)
Visualizing cytoplasmic calcium in polarizing zygotes and growing rhizoids of *Fucus serratus.*
Biol. Bull. **176** (S); 14-17.

Brownlee, C. and Pulsford, A. (1988)
Visualisation f th cytoplasmic Ca^{2+} gradient in *Fucus serratus* rhizoids: correlation with cell ultrastructure and polarity.
J. Cell. Sci. **91**; 249-256.

Brownlee, C. and Wood, J.W. (1986)
A gradient of cytoplasmic free calcium in growing rhizoid cells of *Fucus serratus.*
Nature, **320**; 624-626.

Burgoyne, R.D. and Cheek, T.R. (1991)
Locating intracellular calcium stores.
TIBS, **16**; 319-320.

Bush, D.S. (1993)
Regulation of cytosolic calcium in plants.
Plant Physiol. **103**; 7-13.

Callow, J.A. (1985)
Sexual recognition and fertilization in brown algae.
J. Cell. Sci. Suppl. **2**; 219-232.

Callow, J.A. Callow, M.E. and Evans, L.V. (1985)
Fertilization in *Fucus.*
in *Biology of fertilization*, **2**; 389-407.

Callow, M.E. Evans, L.V. Bolwell, G.P. and Callow, J.A. (1978)
Fertilization in brown algae. I. SEM and other observations on *Fucus serratus.*
J. Cell. Sci. **32**; 45-54.

Catt, J.W. Vithanage, H.I.M.V. Callow, J.A. Callow, M.E. and Evans, L.V. (1983).
Fertilization in brown algae. V. Further investigation of lectins as surface probes.
Exp. Cell Res. **147**; 127-133.

Chafouleas, J.G. Bolton, W.E. Hidaka, H. Boyd, III A.E. and Means, A.R. (1982)
Calmodulin and the cell cycle: Involvment in regulation of cell cycle progression.
Cell, **28**; 41-50.

Cheung, W.Y. (1970)
Cyclic 3',5'-nucleotide phosphodiesterase. Demonstration of an activator.
Biochem. Biophys. Res. Comm. **38**; 533-538.

Child, C.M. (1929)
The physiological gradients.
Protoplasma, **5**; 447-476.

Chirgwin, J.M. Przybyla, A.E. Mac Donald, R.J. and Rutter, W.J. (1979)
Isolation of biologically active ribonucleic acid from sources enriched in ribonuclease.
Biochemistry, **18**; 5294-5299.

Chomczynski, P. and Sacchi, N. (1987)
Single-step method of RNA isolation by acid guanidinium thiocyanate-phenol-chloroform extraction.
Analyt. Biochem. **162**; 156-159.

Chung, C.T. Niemala, S.L. and Miller, R.H. (1989)
One-step preparation of competent *Escherichia coli*: Transformation and storage of bacterial cells in the same solution.
Proc. Natl. Acad. Sci. USA. **86**; 2172-2175.

Cox, J.A. (1986)
Calcium-calmodulin interaction and cellular function.
J. Card. Pharma. **8** (Suppl. 8); S48-S51.

Créton, R. Zivkovic, D. Zwaan, G and Dohmen, R. (1993)
Polar ionic currents around embryos of *Lymnea stagnalis* during embryogenesis and gastrualtion.
Int. J. Dev. Biol. **37**; 425-431.

Cyr, R.J.
Calcium/calmodulin affects microtubule stability in lysed protoplasts.
J. Cell Sci. **100**; 311-317.

D'Arcy Wentworth Thompson (1917)
On Growth and Form.
Cambridge University Press.

Das, A. (1990)
Overproduction of proteins in *Escherichia coli*: Vectors, hosts and strategies.
Meth. Enzymol. **182**; 93-113.

Davis, T.N. (1992*a*)
Mutational analysis of calmodulin in *Saccharomyces cerevisiae.*
Cell Calcium, **13**; 435-444.

Davis, T.N. (1992*b*)
A temperature-sensitive calmodulin mutant loses viability during mitosis.
J. Cell Biol. **118**; 607-617.

Davis, T.N. and Thorner, J. (1989)
Vertebrate and yeast calmodulin, despite significant sequence divergence, are functionally interchangeable.
Proc. Natl. Acad. Sci. USA. **86**; 7909-7913.

Davis, T.N. Urdea, M.S. Masiarz, F.R. and Thorner, J. (1986)
Isolation of the yeast calmodulin gene: Calmodulin is an essential protein.
Cell, **47**; 423-431.

Delisle, S. (1991)
The four dimesions of calcium signalling in *Xenopus* oocytes.
Cell calcium, **12**; 217-227.

Dos Remedios, C.G. (1981)
Lanthanide ion probes of calcium-binding sites on cellular membranes.
Cell Calcium, **2**; 29-51.

du Buy, H.G. and Olson, R.A. (1937*a*)
The presence of growth regulators during the early development of *Fucus*.
Am. J. Bot. **24**; 609-611.

du Buy, H.G. and Olson, R.A. (1937*b*)
The role of growth substance in the polarity and morphogenesis of *Fucus*.
Am. J. Bot. **24**; 611-615.

Eliam, Y. and Chernichovsky, D. (1988)
Low concentrations of trifluoperazine arrest the cell division cycle of *Saccharomyces cerevisiae* at two specific stages.
J. Gen. Microbiol. **134**; 1063-1069.

Englard, S. and Seifter, S. (1990)
Precipitation techniques.
Meth. Enzymol. **182**; 285-300.

Evans, L.V. Callow, J.A. and Callow, M.E. (1982)
The biology and biochemistry of reproduction and early development in *Fucus*.
in *Progress in phycological research*, Vol. 1.
Round and Chapman.

Fallon, K.M. Shacklock, P.S. and Trewavas, A.J. (1993)
Detection *in vivo* of very rapid red light-induced calcium sensitive protein phosphorylation in etiolated wheat (*Triticum aestivum*) leaf protoplasts.
Plant Physiol. **101**; 1039-1045.

Fang, G. Hammar, S and Grumet, R. (1992)
A quick and inexpensive method for removing polysaccharides from plant genomic DNA.
BioTechniques, **13**; 52-54.

Farmer, J.B. and Williams, J.L. (1896)
On fertilisation and the segregation of the spore of *Fucus*.
Ann. Bot. **10**; 479-487.

Feinberg, A.P. and Vogelstein, B. (1982)
A technique for radiolabelling DNA restriction endonuclease fragments to high specific activity.
Analyt. Biochem. **132**; 6-13.

Feinberg, A.P. and Vogelstein, B. (1982)
Addenum. "A technique for radiolabelling DNA restriction endonuclease fragments to high specific activity."
Analyt. Biochem. **137**; 266-267.

Feucht, U. and Bentrup, F-W. (1972)
Über die photosensible Phase der Polaritätsinduktion dei *Equisetum* sporen und *Fucus* zygoten.
Z. Pflanzenphysiol. **66** S; 233-242

Fischer, T.H. Campbell, K.P. and White, G.C. (1987)
An investigation of functional similarities between the sarcoplasmic reticulum and platelet calcium-dependent adenosinetriphosphatases with the inhibitors quercentin and calmidazolium
Biochemistry, **26**; 8024-8030

Fulton, A.B. (1980)
Calcium ions, electrical currents and the choreography of (some) eukaryotic cells.
Cell, **22**; 5-6.

Gibbon, B.C. and Kropf, D.L. (1991)
pH gradients and cell polarity in *Pelvetia* embryos.
Protoplasma, **163**; 43-50.

Gibbon, B.C. and Kropf, D.L. (1993)
Intracellular pH and its regulation in *Pelvetia* zygotes.
Dev. Biol. **156**; 259-268.

Gibbon, B.C. and Kropf, D.L. (1994)
Cytosolic pH gradients associated with tip growth.
Science, **263**; 1419-1421.

Gietzen, K. (1983)
Comparaison of the calmodulin antagonists compound 48/80 and calmidazolium.
Biochem. J. **216**; 611-616

Gilroy, S. Bethke, P.C. and Jones, R.L. (1993)
Calcium homeostasis in plants.
J. Cell Sci. **106**; 453-462.

Gilroy, S. Blowers, D.T. and Trewavas, A.J. (1987*a*)
Calcium; a regulation system emerges in plant cells.
Development, **100**; 181-184.

Gilroy, S. Hughes, W.A. and Trewavas, A.J. (1987*b*)
Calmodulin antagonists increase the free cytosolic calcium levels in plant protoplasts *in vivo*.
FEBS. **212**; 133-137.

Goodner, B. and Quatrano, R.S. (1993*a*)
Fucus embryogenesis: a model to study the establishment of polarity.
Plant Cell, **5**; 1471-1481.

Goodner, B. and Quatrano, R.S. (1993*b*)
Conservation of proteins involved in polar axis formation - *Fucus* meets yeast.
J. Cell. Biochem. **17B**; 39.

Gopalakrishna, R. and Anderson, W.B. (1982)
Ca^{2+}-induced hydrophobic site on calmodulin: application for purification of calmodulin by phenyl-sepharose affinity chromatography.
Biochem. Biophys. Res. Comm. **104**; 830-836.

Grierson, D. and Covey, S.N. (1988)
Plant molecular biology. Second edition.
Chapman and Hall, New York.

Hahm, S.H. and Saunders, M.J. (1991)
Cytokinin increases intracellular Ca^{2+} in *Funaria*: Detection with Indo-1.
Cell calcium, **12**; 675-681.

Hartwig, J.H. Thelen, M. Rosen, A. Janmey, P.A. Nairn, A.C. and Aderem, A. (1992)
MARCKS is an actin filament crosslinking protein regulated by protein kinase C and calcium-calmodulin.
Nature, **365**; 618-622.

Haußer, I. Herth, W. and Reiss, H-D. (1984)
Calmodulin in tip growing plant cells, visualized by fluorescing calmodulin-binding phenothiazines.
Planta, **162**; 33-39.

Heizmann, C.W. and Hunziker, W. (1991)
Intracellular calcium binding proteins: More sites than insights.
TIBS. **16**; 98-103.

Hepler, P.K. (1990)
Does calcium regulate events through amplitude modulation?
Curr. Top. Plant Biochem. Physiol. **9**; 1-9.

Hepler, P.K. and Wayne, R.O. (1985)
Calcium and plant development.
Ann. Rev. Plant Physiol. **36**; 397-439.

Hepler, P.K. Zhang, D and Callahan, D.A. (1990)
Calcium and the regulation of mitosis.
in *Calcium and plant growth and development.*
Eds. Leonard, R.T. and Hepler, P.K.

Heslop-Harrison, J. and Heslop-Harrison, Y. (1992)
Germination of monocolpate angiosperm pollen: effect of inhibitory factors and the Ca^{2+} channel blocker, nifedipine.
Ann. Bot. **69**; 395-403.

Hetherington, A.M. Sommerville, J. Masters, A.K. and Mitchell, A.G. (1990)
Evidence which supports the presence of stored messenger ribonucleoprotein (mRNP) in the unfertilised eggs of *Fucus serratus.*
in *Mechanisms of fertilization.*
NATO ASI Series, Vol. H 45. (Ed. Dale)

Hidaka, H. and Ishikawa, T. (1992)
Molecular pharmacology of calmodulin pathways in the cell functions.
Cell Calcium, **13**; 465-472.

Hikada, H. Sasaki, Y. Tanaka, T. Endo, T. Ohno, S. Fujii, Y. and Nagata, T. (1981)
N-(6-Aminohexyl)-5-chloro-1-naphthalenesulfonamide, a calmodulin antagonist, inhibits cell proliferation.
Proc. Natl. Acad. Sci. USA. **78**; 4354-4357.

Holland, P. (1993)
Cloning genes using the polymerase chain reaction.
in *Essential developmental biology. A practical approach.*
Oxford University Press. (Eds. stern and Holland)

Hotary, K.B. and Robinson, K.R. (1992)
Evidence of a role for endogenous electrical fields in chick embryo development.
Development, **114**; 985-996.

Hurd, A.M. (1920)
Effect of unilateral monochromatic white light and group orientation on the polarity of germinating *Fucus* spores.
Bot. Gaz. **70**; 25-50.

Hurst, S.R. and Kropf, D.L. (1991)
Ionic requirements for the establishment of an embryonic axis in *Pelvetia* zygotes.
Planta, **185**; 27-33.

Iida, H. Sakaguchi, S. Yagawa, Y. and Anraku, Y. (1990)
Cell cycle control by Ca^{2+} in *Saccharomyces cerevisiae*.
J. Biol. Chem. **265**; 21216-21222.

Ikura, M. Barbato, G. Klee, C.B. and Bax, A. (1992)
Solution structure of calmodulin and its complex with a myosin light chain kinase fragment.
Cell Calcium, **13**; 391-400.

Ilmansee, K. and Mahowald, A. (1974)
Transplantation of posterior pole plasm in *Drosophila*. Induction of germ cells at the anterior pole of the egg.
Proc. Natl. Acad. Sci. USA. **71**; 1016-1020.

Jaffe, L.F. (1954)
Stimulation of the discharge of gametangia from a brown alga by a change from light to darkness.
Nature, **174**; 743.

Jaffe, L.F. (1955)
Do *Fucus* eggs interact through a CO_2-pH gradient?
Proc. Natl. Acad. Sci. USA. **41**; 267-270.

Jaffe, L.F. (1956)
Effect of polarized light on polarity of *Fucus*.
Science, **123**; 1081-1082

Jaffe, L.F. (1958)
Tropistic responses of zygotes of the Fucaceae to polarised light.
Exp. Cell. Res. **15**; 282-299.

Jaffe, L.F. (1966)
Electrical currents through the developing *Fucus* egg.
Proc. Natl. Acad. Sci. USA. **56**; 1102-1109.

Jaffe, L.F. (1968)
Localization in the developing *Fucus* egg and the general role of localizing currents.
Advan. Morphog. **7**; 295-328.

Jaffe, L.F. (1977)
Electrophoresis along cell membranes.
Nature, **265**; 600-602.

Jaffe, L.F. (1980)
Calcium explosions as triggers of development.
Ann. N. Y. Acad. Sci. **339**; 86-101.

Jaffe, L.F. (1983)
Sources of calcium in egg activation: A review and hypothesis.
Dev. Biol. **99**; 265-279.

Jaffe, L.F. (1991)
The path of calcium in cytosolic calcium oscillations: A unifying hypothesis.
Proc. Natl. Acad. Sci. USA. **88**; 9883-9887.

Jaffe, L.F. and Neuscheler, W. (1969)
On the mutual polarisation of nearby pairs of fucaceous eggs.
Dev. Biol. **19**; 549-565.

Jaffe, L.F. Robinson, K.R. and Nuccitelli, R. (1974)
Local cation entry and self electrophoresis as an intracellular localization mechanism.
Ann. N. Y. Acad. Sci. **238**; 372-389.

Jaffe, L.A. Weisenseel, M.H. and Jaffe, L.F. (1975)
Calcium accumulations within the growing tips of pollen tubes.
J. Cell. Biol. **67**; 488-492.

Jones, J.L. Callow, J.A. and Green, J.R. (1988)
Monoclonal antibodies to sperm surface antigens of the brown alga *Fucus serratus* exhibit region-, gamete-, species-, and genus-preferential binding.
Planta, **176**; 298-306.

Jones, J.L. Callow, J.A. and Green, J.R. (1990)
The molecular nature of *Fucus serratus* sperm surface antigens recognised by monoclonal antibodies FS1 and FS12.
Planta, **182**; 64-71.

Kasai, H. Li, Y.X. and Miyashita, Y. (1993)
Subcellular distribution of Ca^{2+} release channels underlying Ca^{2+} waves and oscillations in exocrine pancreas.
Cell, **74**; 669-677.

Keith, C.H. Ratan, R. Maxfield, F.R. Bajer, A. and Shelanski, M.L. (1985)
Local cytoplasmic calcium gradients in living mitotic cells.
Nature, **316**; 848-850.

Kiermayer, O. (1981)
Cytoplasmic basis of morphogenesis in *Micrasterias*.
Cell Biol. Mono. **8**; 147-189.

Klee, C.B. Crouch, T.H. and Richman, P.G. (1980)
Calmodulin.
Ann. Rev. Biochem. **49**; 489-515.

Kline, D. and Kline, J.T. (1992)
Repetative calcium transients and the role of calcium in exocytosis and cell cycle activation in the mouse egg.
Dev. Biol. **149**; 80-89.

Knapp, E. (1931)
Entwicklungsphysiologische Unterschungen an Fucacean Eiern. I. Zur Kenntnis der Polarität der Eier von *Cystoseira barbata.*
Planta, **14**; 731-751.

Kniepp, H. (1907)
Beiträge zur Keimungsphysiologie und -biologie von *Fucus*.
Jb. F. Wiss. Bot. **44**; 635.

Knight, M.R. Smith, S.M. and Trewavas, A.J. (1992)
Wind-induced plant motion immediately increases cytosolic calcium.
Proc. Natl. Acad. Sci. USA. **89**; 4967-4971.

Knight, M.R. Campbell, A.K. Smith, S.M. and Trewavas, A.J. (1991)
Transgenic plant aequorin reports the effects of touch and cold shock and elicitors on cytoplasmic calcium.
Nature, **352**; 524-526.

Knight, M.R. Read, N.D. Campbell, A.K. and Trewavas, A.J. (1993)
Imaging calcium dynamics in living plants using semi-synthetic recombinant aequorins.
J. Cell Biol. **121**; 83-90.

Koch, G.L.E. (1990)
The endoplasmic reticulum and calcium storage.
BioEssays, **12**; 527-531.

Kretsinger, R.H. (1992)
The linker of calmodulin - to helix or not to helix.
Cell Calcium, **13**; 363-378.

Kropf, D.L. (1989)
Calcium and early development in Fucoid algae.
Biol. Bull. **176** (S); 5-8.

Kropf, D.L. (1992)
Establishment and expression of cellular polarity in Fucoid zygotes.
Microbiol. Rev. **56**; 316-339.

Kropf, D.L. and Quatrano, R.S. (1987)
Localization of membrane associated calcium during development of Fucoid algae using chlorotetracycline.
Planta, **171**; 158-170.

Kropf, D.L. Berge, S.K. and Quatrano, R.S. (1989)
Actin localization during *Fucus* embryogenesis.
Plant Cell, **1**; 191-200.

Kropf, D.L. Kloareg, B. and Quatrano, R.S. (1988)
Cell wall is required for fixation of the embryonic axis in *Fucus* zygotes.
Science, **239**; 187-189.

Kropf, D.L. Maddock, A. and Gard, D.L. (1990)
Microtubule distribution and function in early *Pelvetia* development.
J. Cell. Sci. **97**; 545-552.

Kropf, D.L. Coffman, H.R. Kloareg, B. Glenn, P. and Allen, V.W. (1993)
Cell wall and rhizoid polarity in *Pelvetia* embryos.
Dev. Biol. **160**; 303-314.

Lee, K.S. and Tsien, R.W. (1983)
Mechanism of calcium channel blockade by verapamil, D600, diltiazem and nitrendipine in single dialysed heart cells.
Nature, **302**; 790-794

Lee, R.S. (1980)
Phycology.
Cambridge University Press.

Lehtonen, J. (1984)
The significance of Ca^{2+} in the morphogenesis of *Micrasterias* studied with EGTA, verapamil, $LaCl_3$ and calcium ionophore A 23187.
Plant Sci. Lett. **33**; 53-60

Levering, T. (1952)
Remarks on the submicroscopial structure of eggs and spermatozoids of *Fucus* and related genera.
Physiol. Plantarum, 5; 528-540.

Ley, A.C. and Quatrano, R.S. (1973)
Isolation and characterization of cell walls from developing *Fucus* embryos.
Biol. Bull. **145**; 446 (A).

Logemann, J. Schell, J. and Willmitzer, L. (1987)
Improved method for the isolation of RNA from plant tissues.
Analyt. Biochem. **163**; 16-20.

Lonergan, T.A. (1990)
Steps linking the photosynthetic light reactions to the biological clock require calcium.
Plant Physiol. **93**; 110-115

Lowrance, E.W. (1937)
Determination of polarity in *Fucus* eggs by temperature gradients.
Proc. Soc. Exp. Biol. Med. **36**; 590-591.

Lu, K.P. Osmani, S.A. Osmani, A.H. and Means, A.R. (1993)
Essential roles for calcium and calmodulin in G2/M progression in *Aspergillus nidulans*.
J. Cell Biol. **121**; 621-630.

Lucchesi, P.A. and Scheid, C.R. (1988)
Effects of the anti-calmodulin drugs calmidazolium and trifluoperazine on ^{45}Ca transport in plasmalemmal vesicles from gastric smooth muscle.
Cell Calcium, **9**; 87-94

Lund, E.J. (1923)
Electrical control of organic polarity in the eggs of *Fucus*.
Bot. Gaz. **76**; 288-231.

Lytton, J. and Nigam, S.K. (1992)
Intracellular calcium: molecules and pools.
Curr. Op. Cell. Biol. **4**; 220-226.

Mc Ainsh, M.R. Brownlee, C. and Hetherington, A.M. (1990)
Absisic acid induced elevation of guard cell cytosolic Ca^{2+} preceeds stomatal closure.
Nature, **343**; 186-188.

Mc Cully, M. (1968)
Histological studies on the genus *Fucus*. II. Histology of the reproductive tissues.
Protoplasma, **66**; 205-230.

Mc Lachlan, J. and Chen, L.C.M. (1972)
Formation of adventive embryos from rhizoidal filaments in sporelings of four species of *Fucus* (Phaeophyceae).
Can. J. Bot. **50**; 1841-1844.

McPherson, M.J. Jones, K.M. and Gurr, S.J. (1991)
PCR with highly degenerate primers.
in *PCR. A practical approach.*
Oxford University Press (Eds. McPherson, Quirke and Taylor)

Malagodi, M.H. and Chiou, C.Y. (1974)
Pharmacological evaluation of a mew Ca^{2+} antagonist, H-(*N,N*-diethylamino)-octyl-3,4,5-trimethoxybenzoate hydrochloride (TMB-8): studies in smooth muscle.
Eur. J. Pharmacol. **27**; 25-33.

Manalan, A.S. and Klee, C.B. (1984)
in *Advances in cyclic nucleotide and protein phosphorylation research.*
Vol. 18, pp. 229-294.
Eds. Greengard, P. and Robinson, G.A.
Raven Press, New York.

Manton, I. and Clarke, B. (1956)
Observations with the electron microscope on the internal structure of the spermatozoid of *Fucus*.
J. Exp. Bot. **7**; 416-432.

Marmé, D. and Dieter, P. (1983)
Role of Ca^{2+} and calmodulin in plants.
in *Calcium and cell function.* Vol. 4. pp. 263
N.Y. Academic Press.

Martin, B.R. (1987)
in *Metabolic regulation. A molecular approach.* ch 7, pp 105-117.
Blackwell Scientific Productions.

Masters, A.K. Shirras, A.D. and Hetherington, A.M. (1992)
Maternal mRNA and early development in *Fucus serratus*.
Plant J. **2**; 619-622.

Means, A.R. Bagchi, I.C. Vanberkum, M.F.A. and Rasmussen, C.D. (1991)
Calmodulin.
in *Cellular calcium. A practical approach.* ch. 9 pp. 205-247
Eds. Mc Cormack, J.G. and Cobbold, P.H.

Meindl, U. (1982)
Local accumulation of membrane-associated calcium according to cell pattern formation in *Micrasterias denticulata*, visualized by chlorotetracycline fluorescence.
Protoplasma, **110**; 143-146.

Moss, B. (1967)
The apical meristem of *Fucus*.
New Phytol. **66**; 67-74.

Müller, D.G. (1989)
The role of pheromones in sexual reproduction of brown algae.
in *Algae as experimental systems*, pp. 201-213
Alan R. Liss, Inc.

Müller, D.G. and Gassmann, G. (1978)
Identification of the sex attractant in the marine brown alga *Fucus vesiculosus*.
Naturwiss. **65**; 389-390.

Müller, D.G. and Gassmann, G. (1984)
Sexual reproduction and the role of sperm attraction in monoecious species of the brown algal order Fucales (*Fucus, Hesperophycus, Pelvetia* and *Pelvetiopsis*)
J. Plant. Physiol. **118**; 401-408.

Murray, M.G. and Thompson, W.F. (1980)
Rapid isolation of high molecular weight plant DNA.
Nucl. Acids. Res. **8**; 4321-4325.

Nelson, M. and McClelland, M. (1991)
Site-specific methylation: effect on DNA modificaton methyltransferases and restriction endonucleases.
Nucl. Acids Res. **19**; 2045-2075.

Neushul, M. (1971)
The species of *Macrocystis* with particular reference to those of North and South America.
in *The Biology of giant kelp beds (*Macrocystis*) in California.*
Ed. North, W.J.

North, W.J. (1971)
in *The Biology of giant kelp beds (*Macrocystis*) in California.*
Ed. North, W.J.

Novák, B. and Bentrup, F.W. (1973)
Orientation of *Fucus* egg polarity by electric a.c. and d.c. fields.
Biophysik, **9**; 253-260.

Novotny, A.M. and Foreman, M. (1974)
The relationship between changes in cell wall composition and the establishment of polarity in *Fucus* embryos.
Dev. Biol. **40**; 162-173.

Novotny, A.M. and Foreman, M. (1975)
The composition and development of cell walls of *Fucus* embryos.
Planta, **122**; 67-78.

Nuccitelli, R. (1978)
Oöplasmic segregation and secretion in the *Pelvetia* egg is accompanied by a membrane-generated electrical current.
Dev. Biol. **62**; 13-33.

Nuccitelli, R. and Jaffe, L.F. (1974)
Spontaneous current pulses through developing fucoid eggs.
Proc. Natl. Acad. Sci. USA. **71**; 4855-4859.

Nuccitelli, R. and Jaffe, L.F. (1975)
The pulse current pattern generated by developing fucoid eggs.
J. Cell. Biol. **64**; 636-643.

Ohya, Y. and Anraku, Y. (1992)
Yeast calmodulin: Structural and functional elements essential for the cell cycle.
Cell Calcium, **13**; 445-455.

Ohya, Y. and Botstein, D. (1994)
Diverse essential functions revealed by complementing yeast calmodulin mutants.
Science, **263**; 963-966.

Okayama, M. Kawaichi, M. Brownstein, F. Lee, T. Yokota, T. and Arai, K. (1987)
High-efficiency cloning of full length cDNA; constrction and screening of cDNA expression libraries for mammalian cells.
Meth. Enzymol. **154**; 3-28.

Old, R.W. and Primrose, S.B. (1989)
Principles of gene manipulation. An introduction to genetic engineering.
Blackwell Scientific Productions.

O'Neil, K.T and DeGrado, W.F. (1990)
How calmodulin binds its targets: Sequence independent recognition of amphiphilic α-helices.
TIBS. **15**; 59-64.

Oparka, K.J. Murphy, R. Derrick, P.M. Prior, D.A.M. and Smith, J.A.C (1991)
Modification of the pressure-probe technique permits controlled intracellular microinjection of fluorescent probes.
J. Cell Sci. **98**; 539-544.

Ostrove, S. (1990)
Affinity chromatography: General methods.
Meth. Enzymol. **182**; 357-371.

Parker, B.C. (1971)
The internal structure of *Macrocystis.*
in *The Biology of giant kelp beds (*Macrocystis*) in California.*
Ed. North, W.J.

Pollock, E.G. (1970)
Fertilisation in *Fucus.*
Planta, **92**; 85-99.

Poovaiah, B.W. and Reddy, A.S.N. (1987)
Calcium messenger system in plants
Crit. Rev. Plant Sci. **6**, 47-103

Preston, R.R. Kink, J.A. Hinrichsen, R.D. Saimi, Y. and Kung, C. (1991)
Calmodulin mutants and Ca^{2+}-dependent channels in *Paramecium.*
Annu. Rev. Physiol. **53**; 309-319.

Quatrano, R.S. (1968)
Rhizoid formation in *Fucus* zygotes: dependence on protein and ribonucleic acid syntheses.
Science, **162**; 468-470.

Quatrano, R.S. (1972)
An ultrastrucural study of the determined site of rhizoid formation in *Fucus* zygotes.
Exp. Cell. Res. **70**; 1-12.

Quatrano, R.S. (1973)
Separation of processes associated with differentiation of two celled *Fucus* embryos.
Dev. Biol. **30**; 209-213.

Quatrano, R.S. (1978)
Development of cell polarity.
Ann. Rev. Plant. Physiol. **29**; 487-510.

Quatrano, R.S. (1990)
Polar axis fixation and cytoplasmic localization in *Fucus*.
in *Genetics of pattern formation and growth control*, ch. 3, pp. 31-46.
Wiley-Liss.

Quatrano, R.S. Brian, L. Aldridge, J. and Schultz, T. (1991)
Polar axis fixation in *Fucus* zygotes: Components of the cytoskeleton and extracellular matrix.
Development, **1** (S); 11-16.

Rasmussen,C.D. and Means, A.R. (1989)*a*
Calmodulin, cell growth and gene expression.
TINS. **12**; 433-438.

Rasmussen, C.D. and Means, A.R. (1989)*b*
Calmodulin is required for cell cycle progression during G_1 and mitosis.
EMBO J. **8**; 73-82.

Rasmussen, C.D. Lu, K.P. Means, R.L. and Means, A.R. (1992)
Calmodulin and cell cycle control.
J. Physiol. **86**; 83-88.

Ratan, R.R. and Shelanski, M.L. (1986)
Calcium and the regulation of mitotic events.
TIBS. **11**; 456-459.

Read, N.D. Allan, W.T.G. Knight, H. Knight, M.R. Malhó, R. Russel, A. Sacklock, P.S. and Trewavas, A.J. (1992)
Imaging and measurement of cytosolic free calcium in plant and fungal cells.
J. Microscopy, **166**; 57-86.

Reed, E.A. and Whitaker, D.M. (1941)
Polarised plasmolysis of *Fucus* eggs with particular reference to ultraviolet light.
J. Cell. Comp. Physiol. **18**; 329-338.

Reiss, H-D. and Herth, W. (1985)
Nifedipine-sensitive calcium channels are involved in polar groeth of lily pollen tubes.
J. Cell Sci. **76**, 247-254

Roberts, D.M. and Harmon, A.C. (1992)
Calcium modulated proteins: Targets of intracellular calcium signals in higher plants.
Annu. Rev. Plant Physiol. Plant Mol. Biol. **43**; 375-414.

Roberts, S.K. Gillot, I. and Brownlee, C. (1994)
Cytoplasmic calcium and *Fucus* egg activation.
Development, **120**; 155-163.

Robinson, K.R. and Cone, R. (1979)
Polarization of Fucoid eggs by a calcium ionophore gradient.
Science, **207**; 77-78.

Robinson, K.R. and Jaffe, L.F. (1973)
Ion movements in a developing Fucoid egg.
Dev. Biol. **35**; 349-361.

Robinson, K.R. and Jaffe, L.F. (1975)
Polarizing Fucoid eggs drive a calcium current through themselves.
Science, **187**; 70-72.

Robinson, K.R. and Jaffe, L.F. (1976)
Calcium gradients and cell polarity.
J. Cell. Biol. **70**; 30(a); 110.

Robinson, K.R. Jaffe, L.F. and Brawley, S.H. (1981)
Electrophysiological properties of fucoid algal eggs during fertilization.
J. Cell. Biol. **19**; 179a.

Sambrook, J. Fritsch, E.F. and Maniatis, T. (1989)
Molecular cloning. A laboratory manual. (Second edition)
Cold Spring Harbour Laboratory Press.

Sarkar, G. Kapelner, S. and Sommer, S.S. (1990)
Formamide can dramatically improve the specificity of PCR.
Nucl. Acids Res. **18**; 7465.

Sasaki, Y and Hidaka, H. (1982)
Calmodulin and cell proliferation.
Biochem. Biophys. Res. Comm. **104**; 451-456.

Saunders, M.J. and Hepler, P.K. (1983)
Calcium antagonists and calmodulin inhibitors block cytokinin-induced bud formation in *Funaria*.
Dev. Biol. **99**; 41-49

Schleicher, M. Lukas, T.J. and Watterson, D.M. (1983)
Further characterisation of calmodulin from the monocoyledon barley (*Hordeum vulgare*).
Plant Physiol. **73**; 666-670.

Schramm, M. Thomas, G. Towart, R. and Franckowiak, G. (1983)
Novel dihydropyridines with positive inotropic action through activation of Ca^{2+} channels.
Nature, **303**, 535-537

Schroeder, J.I. and Thuleau, P. (1991)
Ca^{2+} channels in higher plant cells.
Plant Cell, **3**; 555-559.

Schröter, K. (1978)
Asymmetrical jelly secretion of zygotes of *Pelvetia* and *Fucus*: An early polarisation event.
Planta, **140**; 69-73.

Shacklock, P.S. Read, N.D. and Trewavas, A.J. (1992)
Cytosolic free calcium mediates red light-induced photomorphogenesis.
Nature, **358**; 753-755.

Slack, J.M.W. (1991)
From egg to embryo. Regional specification in early development.
Cambridge University Press.

Sobieszek, A. (1989)
Calmodulin antagonist action in smooth muscle myosin phosphorylation.
Biochem. J. **262**, 215-223

Southern, E.M. (1975)
Detection of specific sequences among DNA fragments separated by gel electrophoresis.
J. Mol. Biol. **98**; 503-517.

Speksnijder, J.E. Miller, A. Weisenseel, M.H. Chen, T.H. and Jaffe, L.F. (1989).
Calcium buffer injections block Fucoid egg dvelopment by facilitating calcium diffusion.
Proc. Natl. Acad. Sci. USA. **86**; 6607-6611.

Stafford, C.J. Green, J.R. and Callow, J.A. (1992)
Organisation of glycoproteins into plasma membrane domains on *Fucus serratus* eggs.
J. Cell. Sci. **101**; 437-448.

Starovasnik, M.A. Davis, T.N. and Klevit, R.E. (1993)
Similarities and differences between yeast and vertebrate calmodulin: an examination of the calcium-binding and structural properties of calmodulin from the yeast *Saccharomyces cerevisiae.*
Biochemistry, **32**; 3261-3270.

Stephen, D, Jones, C. and Schofield, J.P. (1990)
A rapid method for isolating high quality plasmid DNA suitable for DNA sequencing.
Nucl. Acids Res. **18**; 7463-7464.

Su, X. and Gibor, A. (1988)
A method for RNA isolation from marine macro-algae.
Analyt. Biochem. **174**; 650-657.

Sun, G-H. Ohya, Y. and Anraku, Y. (1992)
Yeast calmodulin localizes to sites of cell growth.
Protoplasma, **166**; 110-113.

Takeda, T. and Yamamoto, M. (1987)
Analysis and *in vivo* disruption of the gene coding for calmodulin in *Schizosaccharomyces pombe.*
Proc. Natl. Acad. Sci. USA. **84**; 3580-3584.

Taylor, A.R. and Brownlee, C. (1993)
Calcium and potassium currents in the *Fucus* egg.
Planta, **189**; 109-119.

Thuret, M.G. (1854)
Recherches sur la fécondation des fucacés suivies d'observations sur les anthéridies des algues.
Ann. Sci. Nat. **4**; 197-214.

Tlalka, M. and Gabrys, H. (1993)
Influence of calcium on blue light-induced chloroplast mouvement in *Lemna trisulca* L.
Planta, **189**; 491-498.

Torrey, J.G. and Galun, E. (1970)
Apolar embryos resulting from osmotic and chemical treatment.
Am. J. Bot. **57**; 111-119.

Trewavas, A.J. and Gilroy, S. (1991)
Signal transduction in plant cells.
TIG. **7**; 356-360.

Vercesi, A.E. Hoffmann, M.E. Bernardes, C.F. and Docampo, R. (1991)
Regulation of intracellular calcium homeostasis in *Trypanosoma cruzi.* Effects of Calmidazolium and trifluoperazine.
Cell Calcium, **12**; 361-369

Wagner, V.T. Brian, L. and Quatrano, R.S. (1992)
Role of a vitronectin-like molecule in embryo adhesion of the brown alga *Fucus.*
Proc. Natl. Acad. Sci. USA. **89**; 3644-3648.

Wasserman, W.J. and Smith, L.D. (1981)
Calmodulin triggers the resumption of meiosis in amphibian oocytes.
J. Cell Biol. **89**; 389-394.

Watterson, D.M. Iverson, D.B. and van Eldik, L.J. (1980)
Spinach calmodulin: Isolation, characterization and comparison with vertebrate calmodulins.
Biochemistry, **19**; 5762-5768.

Weisenberg, R.C. (1972)
Microtubule formation *in vitro* in solutions containing low calcium concentrations.
Science, **117**; 1104-1105.

Welch, M.D. Holtzman, D.A. and Drubin, D.G. (1994)
The yeast actin cytoskeleton.
Curr. Op. Cell Biol. **6**; 110-119.

Whitaker, D.M. (1931)
Some observations on the eggs of *Fucus* an upon their mutual influence in the determination of the developmental axis.
Biol. Bull. **61**; 294-308

Whitaker, D.M. (1936)
The effect of white light upon the rate of development of te rhizoid protuberance and the first cell division in *Fucus furcatus*.
Biol. Bull. **70**; 100-109.

Whitaker, D.M. (1937)
Determination of polarity by centrifuging eggs of *Fucus furcatus*.
Biol. Bull. **73**; 249-260.

Whitaker, D.M. (1938)
The effect of hydrogen ion concentrations upon the induction of polarity in *Fucus* eggs. III.
J. Gen. Physiol. **21**; 833-845.

Whitaker, D.M. (1940)
The effects of ultracentrifuging and pH on the development of *Fucus* eggs.
J. Cell. Comp. Physiol. **15**; 173-187.

Whitaker, D.M. and Berg, E.W. (1944)
The development of *Fucus* eggs in concentration gradients: a new method for establishing steep gradients across living cells.
Biol. Bull. **86**; 125-129.

Whitaker, D.M. and Lowrance, E.W. (1936)
On the period of suscepibility in the egg of *Fucus furcatus* when polarity is induced by brief exposure to directed white light.
J. Cell. Comp. Physiol. **7**; 417-424.

Williams, R.J.P. (1992)
Calcium and calmodulin.
Cell calcium, **13**; 355-362.

Wilson, K. and Goulding, K.H. (1988)
A biologist's guide to principles and techniques of practical biochemistry.
Edward Arnold, publisher.

Wolff, D.J. Ross, J.M. Thompson, P.N. Brostrom, M.A. and Brostrom, C.O. (1981)
Interaction of calmodulin with histones.
J. Biol. Chem. **256**; 1846-1860.

Zimmer, W.E. Schloss, J.A. Silflow, C.D. Youngblom, J. and Watterson, D.M. (1988)
Structural organization, DNA sequence, and expression of the calmodulin gene.
J. Biol. Chem. **263**; 19370-19383.

Zivkovic, D. and Dohmen, R. (1991)
Changes in transcellular currents associated with cytokinesis and polar lobe formation in embryos of *Bithinia tentaculata* (Mollusca).
Development, **112**; 451-459.